Investigations of Orthosomycin Biosynthesis

By

Emilianne Karyl McCranie

Dissertation

Submitted to the Faculty of the

Graduate School of Vanderbilt University

in partial fulfillment of the requirements

for the degree of

DOCTOR OF PHILOSOPHY

in

Chemistry

May 2016

Nashville, Tennessee

Approved:

Brian O. Bachmann, Ph.D.

Carmelo J. Rizzo, Ph.D.

Tina M. Iverson, Ph.D.

Lawrence J. Marnett, Ph.D.

To my loving parents who have supported me wholeheartedly and unconditionally and have believed in me when I did not believe in myself.

ACKNOWLEDGEMENTS

There are many people who have helped me reach this milestone. There is simply no way to acknowledge every family member, friend, mentor, and teacher who has helped me along the way. That would be a book unto itself. However, I would like to acknowledge some of the people who have made the largest impacts. My time at Vanderbilt University has been challenging but extremely rewarding. Without the support of my committee, the Department of Chemistry, Vanderbilt Institute of Chemical Biology, Organic Chemistry Teaching Assistant and Teaching Fellow positions, a grant from the Office of Naval Research, the D. Stanley and Ann T. Tarbell Endowment Fund, and the Arthur William Ingersoll Graduate Research Fellowship my research and this dissertation would not have been possible.

First, I would like to thank my parents. Throughout my life, they have been a source of encouragement and comfort. Even though pursuing my dreams meant moving away from the home I love so much, they let me know that they fully supported whatever I wanted to do. They always listened patiently when I called to complain and would be on their way at a moment's notice if I ever said that I needed them. I am beyond thankful that God blessed me with such wonderful parents. I would not be where I am today without the two of them. The least I can do is dedicate this work to them, and thank them from the bottom of my heart for being the strong foundation that has allowed me to become the person I am today.

I also must thank my wonderful husband. Dan always encourages me, supports me, and comforts me. He has been patient and understanding even though dating and being married to a graduate student could not have been easy. I am so thankful that my journey led me to Nashville and to him. He is a bright spot in every day. When I have tough days, it is wonderful to know that

I get to go home to him. Dan is my rock, and I cannot imagine my life without him. Not only did I gain a husband during my time at Vanderbilt, I also gained a family. I am blessed to have parents-in-law who are incredibly supportive and encouraging.

To the rest of my family and friends back in Dodge County, there are so many of you who have made an impact on my life and helped me reach this point. Since I have moved away from our little community, I have been able to see how special it really is. There is no other place in the world where I feel as loved and supported as I do there. There was a village responsible for raising this child, and I will never be able to thank everyone enough. However, I must thank a few extra special people. To Mama Jean and Papa Claude, the two of you always believed I could do whatever I wanted to do. I truly believe that my love of science began in your house watching the Discovery Channel and in your backyard tending to our menagerie of animals. I will always treasure our time together and will be forever thankful that I had such a wonderful "second set of parents."

I would be remiss if I did not thank the teachers who helped me along the way. From my kindergarten teacher, Mrs. Flossie, who rocked this crying child every morning of kindergarten, to Mrs. Marcie Jones, my high school teacher, tennis coach, and STAR teacher, I have been blessed with wonderful teachers. At Mercer University, there were so many professors who truly made a difference in my life and helped me to see the world in a new way. Once again, I cannot thank everyone, but I would like to especially thank Dr. Kevin Bucholtz. He encouraged me to participate in undergraduate research and eventually to pursue graduate studies in Chemistry. He opened my eyes to a whole new world of possibilities, and for that I am forever grateful.

Finally, I owe a great deal of gratitude to the people at Vanderbilt who have supported me along the way. Foremost I must thank my advisor, Dr. Brian Bachmann. I came to Vanderbilt knowing that I wanted to join Brian's lab. I thank him for allowing me to join the group and for mentoring me. Through his mentorship, I have become a better researcher, writer, and critical thinker. He has supported my career goals and has given me the space to pursue activities that will allow me to reach those goals. I will be forever grateful for his time and patience. I also must thank the other members of my dissertation committee, Dr. Tina Iverson, Dr. Carmelo Rizzo, and Dr. Lawrence Marnett for their insights and for giving their time and energy to help me pursue my Ph.D. Additionally, I would like to thank Dr. Iverson and Dr. Kathryn McCulloch for collaborating with us on the structural characterization of the orthosomycin-associated oxygenases. Without this collaboration, much of the oxygenase story would still be unknown.

I must also thank the people at Vanderbilt's Center for Teaching. The CFT was a great resource in preparing me to become a professor. I would especially like to thank Dr. Cynthia Brame who advised me on the BOLD Project. Cynthia helped to develop my philosophy of teaching and to understand what it really means to be a great teacher. I am thankful for the time and energy that she dedicated to the project and to me personally. I would also like to thank Dr. Michelle Sulikowski. As my teaching fellowship mentor and BOLD project mentor, Michelle worked closely with me to develop quality materials for the students. Michelle is an excellent teacher, and I am thankful that I had the privilege of working so closely with her for many years.

To the members of the Bachmann group, past and present, I would not have made it through graduate school without you. We were more than just coworkers, we became close

friends. I am grateful that the place I have spent the most time over the past five years was filled with wonderful and caring people who made even the worst of days better.

TABLE OF CONTENTS

Page

LIST OF FIGURES

Figure **Page**

LIST OF TABLES

Table **Page**

Chapter I

BIOACTIVE OLIGOSACCHARIDE NATURAL PRODUCTS

*This chapter was written by Emilianne K. McCranie and Brian O. Bachmann and was first published in Natural Product Reports **31,** 1026-1042 (2014).[111] Reproduced with permission from the Royal Society of Chemistry.*

Introduction

A large fraction of secondary metabolites may be considered oligomeric in nature, derived via sequences of condensation and modification of monomeric precursors that originate from various branches of primary and secondary metabolism. For instance, amino acids, isopentyl pyrophosphate, and malonates condense into polypeptide, polyisoprenoid, and polyketide secondary metabolites, respectively, or mixtures thereof. In many cases these classes provide core scaffolds that are further elaborated by oxidation, cyclization, and frequently glycosylation. Derivatization via glycosylation, which is typically effected via glycosyltransferase-mediated condensation of nucleoside diphosphate (NDP)-sugars onto aglycone scaffolds, is an essential determinant of bioactivity for many secondary metabolites.[1-4] Multiple glycosylation is not uncommon and indeed is a recurrent theme in many bioactive natural products.[5]

Given that poly-glycosylation is a common property of bioactive secondary metabolites, one would expect that oligomeric natural products derived predominantly from monomeric sugar precursors may also be common. Indeed, while oligosaccharide

natural products possessing a wide range of discerned biological activities and molecular targets are reported, they are not as well represented in nature's isolated pharmacopeia as other classes. This is perhaps surprising given the importance of oligosaccharide structural relatives found in primary metabolism which are important mediators of molecular recognition, particularly in cellular recognition, cancer, and the immunology of microbial pathogenesis.[6-9] The reasons for the oligosaccharide natural products' relative

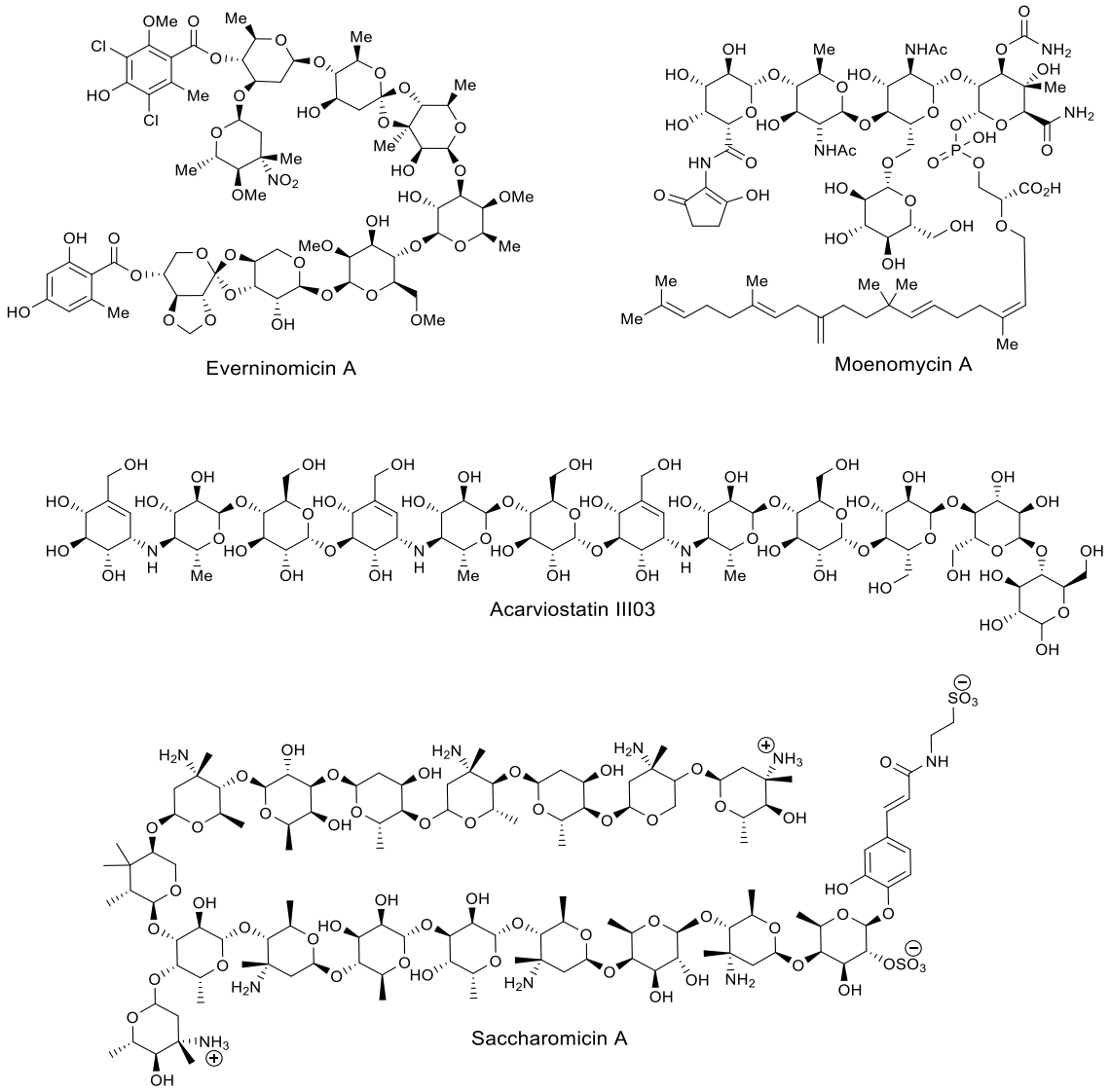

Figure 1-1. Representative members of the families of bioactive oligosaccharide natural products discussed in this chapter. Reproduced from *Nat Prod Rep* **31,** 1026-1042 (2014)[111] with permission from the Royal Society of Chemistry.

underrepresentation in secondary metabolic databases are unknown. Possibly these large, highly functionalized, polar metabolites may be expressed at lower levels, be more difficult to detect, isolate and identify, and be less stable than other classes of compounds.

The biosynthesis of oligomeric secondary metabolites has been primarily studied in the context of their appendage to polyketides, polypeptides, and polyisoprenoid scaffolds. However, the biochemistry of assembly of oligosaccharide secondary metabolites, either assembled on aglycones or into oligosaccharides, is only marginally understood at this time. Moreover, the inferred existence of secondary metabolic polysaccharides in genomically sequenced organisms is also less common. This may be a result of the scarcity of annotated and biochemically rationalized oligosaccharide secondary metabolite gene clusters.

Herein we collect and discuss the subset of oligosaccharide natural products (see Figure 1-1) reported to possess biological activity, with a focus on oligosaccharides larger than tetrasaccharides that have been biosynthetically characterized. Often these compounds comprise moderate and high molecular weight oligosaccharides that compete with binding sites of very large substrates, such as in the case of the moenomycins, or target large surface area macromolecular interfaces, as with the orthosomycin antibiotics. Understanding the biosynthesis of oligosaccharide natural products will aid in the identification of new members of this relatively underrepresented class of secondary metabolite via genomic analysis and potentially enable opportunities for rational reengineering of this compound class for improved pharmacological properties.

Orthosomycins

The orthosomycins were first coined as a class of antibiotics in 1979 although hygromycin B, produced by *S. hygroscopicus*, was isolated two decades earlier.[10,11] All orthosomycins contain a non-canonical orthoester linkage between sugar residues rather than the typical glycosidic linkage. The orthosomycins can be divided into two classes based on the number of orthoester linkages and sugar residues. Class I orthosomycins may be defined as hepta- and octasaccharides with two orthoester linkages and a dichloroisoeverninic acid ester. Avilamycins, everninomicins, flambamycin, and curamycin are all members of this class. Class II orthosomycins are pseudotrisaccharides with one orthoester linkage and an aminocyclitol. Hygromycin B and the destomycins are examples of this class. Class II orthosomycins will not be discussed in this review as they are more aptly classified with the aminoglycosides.[12]

Because little is known about the activity and biosynthesis of flambamycin and curamycin, this review will focus on the avilamycins and everninomicins. A complex of everninomicins, produced by *Micromonospora carbonacea*, was first described in 1964,[13] and in 1975 the structure of everninomicin D was reported.[14] To date, twelve everninomicins have been reported.[10,14-22] Figure 1-2 shows the variety of everninomicins isolated from *Micromonospora carbonacea.* All everninomicins, with the exception of Ever-2 which lacks the A ring nitrosugar, are octasaccharides containing dichloroisoeverninic acid. The majority of everninomicins also contain orsellinic acid at the opposite end of the saccharide chain. Everninomicins possess three unique oxidative features. The first is a methylenedioxy bridge attached to ring F. The second is its

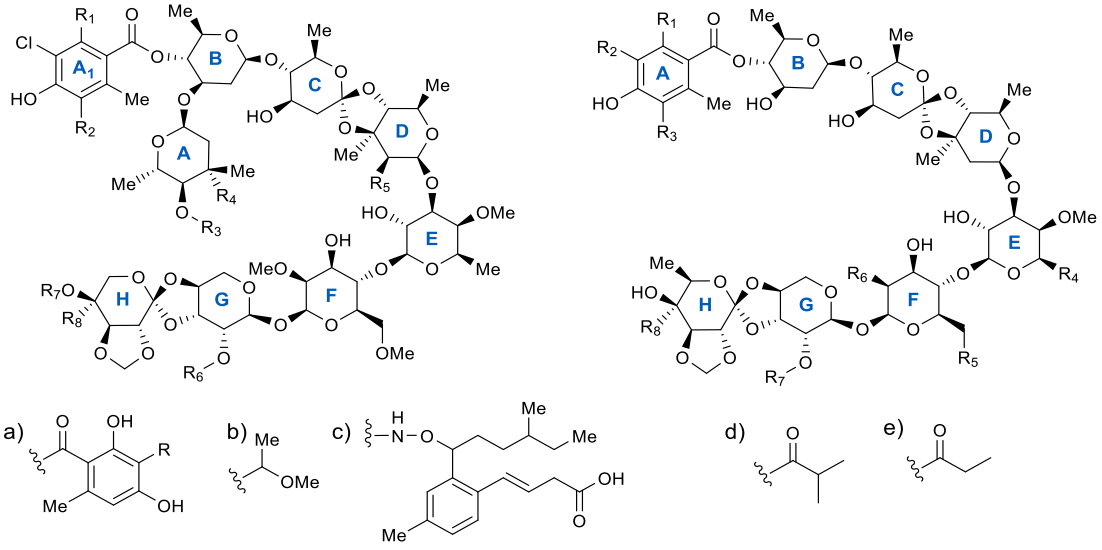

Everninomicins	R_1	R_2	R_3	R_4	R_5	R_6	R_7	R_8	( )
Everninomicin A	OMe	Cl	Me	NO_2	OH	H	a, R=H	H	CH_2
Everninomicin B	OMe	Cl	Me	NO_2	OH	Me	H	b	CH_2
Everninomicin C	OMe	Cl	Me	NO_2	H	Me	H	H	CH_2
Everninomicin D	OMe	Cl	Me	NO_2	H	Me	H	b	CH_2
SCH58769	OH	H	Me	NO_2	OH	H	a, R=H	H	CH_2
SCH58771	OMe	H	Me	NO_2	OH	H	a, R=H	H	CH_2
SCH58773	OMe	Cl	H	NO_2	OH	H	a, R=H	H	CH_2
SCH58775	OMe	Cl	Me	NO_2	OH	H	a, R=H	H	OCOH, H
Amino EverA	OMe	Cl	Me	NH_2	OH	H	a, R=H	H	CH_2
Ever-2 (No	OMe	Cl	-	-	H	Me	H	b	CH_2
13-384-1	OMe	Cl	Me	NO_2	H	Me	a, R=H	H	CH_2
13-384-5	OMe	Cl	Me	NH_2	H	Me	a, R=H	H	CH_2
SCH49088	OMe	Cl	Me	c	OH	H	a, R=H	H	CH_2
SCH58761	OMe	Cl	Me	NO_2	OH	H	a, R=Cl	H	CH_2

Avilamycins	R_1	R_2	R_3	R_4	R_5	R_6	R_7	R_8
Avilamycin A	OMe	Cl	Cl	Me	OMe	OMe	d	COMe
Avilamycin A'	OMe	Cl	Cl	Me	OMe	OMe	e	H
Avilamycin B	OMe	Cl	Cl	Me	OMe	OMe	COMe	COMe
Avilamycin C	OMe	Cl	Cl	Me	OMe	OMe	d	CH(OH)Me
Avilamycin D_1	OMe	Cl	Cl	Me	OMe	OMe	H	COMe
Avilamycin D_2	OMe	Cl	Cl	Me	OMe	OMe	COMe	CH(OH)Me
Avilamycin E	OMe	Cl	Cl	Me	OMe	OMe	H	CH(OH)Me
Avilamycin F	OH	H	Cl	Me	OMe	OMe	d	COMe
Avilamycin G	OMe	Cl	Cl	Me	OMe	OMe	COC_4H_9	COMe
Avilamycin H	OMe	Cl	H	Me	OMe	OMe	d	COMe
Avilamycin I	OMe	Cl	Cl	Me	OMe	OMe	e	COMe
Avilamycin J	OMe	Cl	Cl	Me	OH	OMe	d	COMe
Avilamycin K	OMe	Cl	Cl	CH_2OH	OMe	OMe	d	COMe
Avilamycin L	OMe	Cl	Cl	Me	OMe	OMe	d	CHO
Avilamycin M	OMe	Cl	Cl	H	OMe	OMe	d	COMe
Avilamycin N	OMe	Cl	Cl	Me	OMe	OH	d	COMe

Figure 1-2. Naturally occurring everninomicins and avilamycins. Reproduced from *Nat Prod Rep* **31,** 1026-1042 (2014)[111] with permission from the Royal Society of Chemistry.

namesake orthoester linkages located between rings C and D and rings G and H. Finally, L-evernitrose (ring A) is a nitrosugar unique to everninomicins. In contrast with the other polysaccharides discussed in this review, the everninomicins contain a large proportion of deoxy sugars. Rings A, B (D-olivose), and C (D-olivose), and sometimes ring D (D-evalose) are all 2,6-dideoxy sugars while ring E (4-*O*-methyl-D-fucose) is 6-deoxygenated. Ring F is 2,6-di-*O*-methyl-D-mannose, ring G is L-lyxose, and ring H is eurekanate.

Avilamycins, produced by *Streptomyces viridochromogenes* Tü57, are heptasaccharides similar to everninomicin but lacking the nitrosugar. At least sixteen avilamycins have been characterized to date (Figure 1-2).[10,23] Avilamycins have the same seven-sugar core as the everninomicins. All avilamycins contain dichloroisoeverninic acid but lack orsellinic acid at the eastern side of the molecule. The main points of differentiation among the avilamycins are the decorations of rings G and H. As in the everninomicins, the avilamycins also contain a methylenedioxy bridge and two orthoester linkages located between rings C and D and rings G and H.

Avilamycin antibiotics have found wide spread application as growth promoters in animal feed.[24] Interest in the everninomicin series of orthosomycins peaked in the early 2000s when Schering-Plough Corporation was developing everninomicin A (Ziracin) as an antimicrobial agent. Development of this product reached phase III clinical trials prior to withdrawal for unstated pharmacological complications.[25] However, investigation of the orthosomycins are still of interest as members of this class possess potent activity against clinically important strains such as methicillin-resistant staphylococci, vancomycin-resistant enterococci, and penicillin-resistant streptococci and may be especially useful

for treating infective endocarditis.[26-28]

Mode of Action

The orthosomycins act as bacterial translation inhibitors although by a different mechanism than antibiotics currently in clinical use. Early studies revealed that everninomicin is a potent inhibitor of prokaryote but not eukaryote protein synthesis, specifically targeting the 50S ribosomal subunit.[29, 30] ^{14}C-labeled everninomicin bound specifically to the *E. coli* and *S. aureus* 50S subunit. In competitive binding assays, known inhibitors of protein synthesis which also target the 50S subunit such as chloramphenicol, clindamycin, erythromycin, linezolid, and thiostrepton were unable to block binding of ^{14}C-labeled everninomicin. Only avilamycin and unlabelled everninomicin were able to block its binding suggesting that the orthosomycins target a unique site of the ribosome.[29]

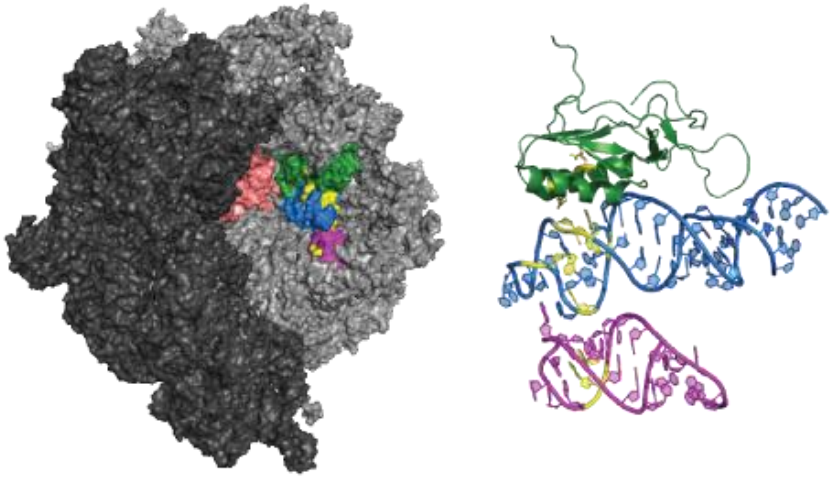

Figure 1-3. Ribosomal binding site of orthosomycin antibiotics. Small ribosomal subunit (PDB 2J00) is shown in dark grey and large subunit (PDB 2J01) is shown in lighter grey. The A and P sites are shown in salmon. Ribosomal protein L16 is shown in green (chain Q), helix 89 (chain A, residues 2454-2498) in blue, and helix 91 (chain A, residues 2520-2545) in magenta. Amino acid residues and nucleotides known to interact with everninomicin and avilamycin are highlighted in yellow. Reproduced from *Nat Prod Rep* **31,** 1026-1042 (2014)[111] with permission from the Royal Society of Chemistry.

Specifically, everninomicin appears to interact with ribosomal protein L16 and r23S RNA helices 89 and 91 (Figure 1-3). *Streptococcus pneumonia* strains with low levels of resistance to everninomicin were found to contain an isoleucine 52 to serine mutation in ribosomal protein L16.[31] Later studies confirmed this mutation as well as identifying two other L16 protein mutations which conferred everninomicin resistance. Mutation of arginines 56 and 51 to histidines resulted in everninomicin resistance in *E. faecium, E. faecalis*, and *S. aureus*.[32, 33]

In addition, an *Enterococcus faecium* strain was isolated which exhibited high-level resistance to everninomicin and avilamycin. The resistant strains contained a plasmid-borne rRNA methyltransferase called EmtA which methylates G2470 of 23S rRNA.[34] rRNA footprinting as well as mutational studies indicate that everninomicin interacts with several residues in helices 89 and 91 of 23S rRNA: A2468, A2469, A2476, A2478, A2482, A2534, G2535. [32, 35] Additionally, characterization of rRNA methyltransferases AviRa and AviRb revealed their role in methylation of G2535 and U2479 in 23S rRNA indicating that these residues are important for orthosomycin binding to the ribosome.[36, 37] Figure 1-3 highlights the amino acid residues and nucleotides that are known to interact with everninomicin and avilamycin.

More recently, Wilson and co-workers have shown that everninomicin prevents formation of the 70S initiation complex in an IF2-dependent manner. Moreover, it was demonstrated that orthosomycins do not inhibit translocation but are instead potent inhibitors of EF4-dependent back-translocation. Interestingly, mutations in protein L16 confer low-level everninomicin resistance while methylation or mutation of 23S rRNA

results in high-level resistance. These results indicate that everninomicin interacts directly with helices 89 and 91 but indirectly with ribosomal protein L16. Nevertheless, the orthosomycins have been shown to target a unique site on the large ribosomal subunit which is approximately 50 angstroms from the peptidyl-transferase center where many commonly used antibiotics are known to bind.[38]

During its development as an antimicrobial agent, the structure-activity relationship of everninomicin was investigated. Methylation or other capping of the hydroxyl group of the dichloroisoeverninic acid moiety significantly reduced activity against *S. aureus*; this suggests a crucial interaction between dichloroisoeverninic acid and the target. In addition permethylation of hydroxyls on rings C-G significantly reduces activity against *S. aure*us.[39, 40] Compound SCH58777, which is composed of rings F, G, H and orsellinic acid, had no antibacterial activity.[15] While everninomicin A was active against both Gram-negative and Gram-positive bacteria, both everninomicin D and everninomicin B were highly active against Gram-positive bacteria but inactive against Gram-negative strains.[10,26] The major difference between everninomicins A and D is the attachment of orsellinic acid to the eurekanate residue suggesting the second aromatic ring is important for conferring activity against Gram-negative strains. Additionally, reduction of the nitro group to the amino oxidation state abolished Gram-positive activity while substantially increasing Gram-negative activity.[41] Everninomicin 2 has activity similar to that of everninomicin A yet does not contain the nitrosugar indicating that while L-evernitrose can modulate activity it is not necessary for antibacterial activity.[10] Finally, hydrolysis of the orthoester between rings C and D resulted in a loss of activity while

reported inversion of the orthoester stereochemistry also reduced activity.[40]

Studies of the biosynthesis of avilamycin have also revealed clear structure-activity relationships. Inversion of the stereochemistry of C2 of ring F by disruption of *aviX12* resulted in the generation of a new analog with drastically reduced activity.[42] Desmethyl analogs created by disruption of five methyltransferases were isolated and tested for activity against a panel of streptococcus, enterococcus, and staphylococcus strains. Removal of any of the naturally occurring methyl groups significantly lowered the activity against enterococci species but did not drastically alter activity against streptococcus and staphylococcus strains. Although the removal of methyl groups did not inhibit antibacterial activity against streptococcus and staphylococcus strains, the polarity of the compounds was changed significantly. Physiochemical studies indicated that the desmethyl analogs had up to 10-fold higher water solubility.[43] These results underscore the potential for pharmacological improvements of the orthosomycins by creating new analogs.

Biosynthesis

The avilamycin A biosynthetic gene cluster from *Streptomyces viridochromogenes* Tü57 was first reported in 1997. Inactivation of two genes confirmed the role of this cluster in avilamycin biosynthesis.[44] This large cluster appears to contain 4 glycosyltransferases, 22 sugar synthesis and tailoring genes, 2 genes for orsellinic acid biosynthesis, 1 halogenase, 3 oxygenases, 5 genes involved in regulation and transport, and 2 genes responsible for avilamycin resistance (Figure 1-4).[45]

Four genes from the avilamycin cluster have been implicated in

dichloroisoeverninic acid biosynthesis. AviM is responsible for orsellinic acid synthesis while AviN may control the starter unit. Inactivation of *aviG4* resulted in loss of a methyl group from dichloroisoeverninic acid confirming it as an *O*-methyltransferase. Additionally, inactivation of the halogenase *aviH* resulted in an avilamycin analog lacking the two chlorine atoms of ring A.[45]

The exact function of the remaining three *O*-methyltransferases was determined by gene inactivation. AviG2 methylates the C6 oxygen of ring F, AviG5 is responsible for

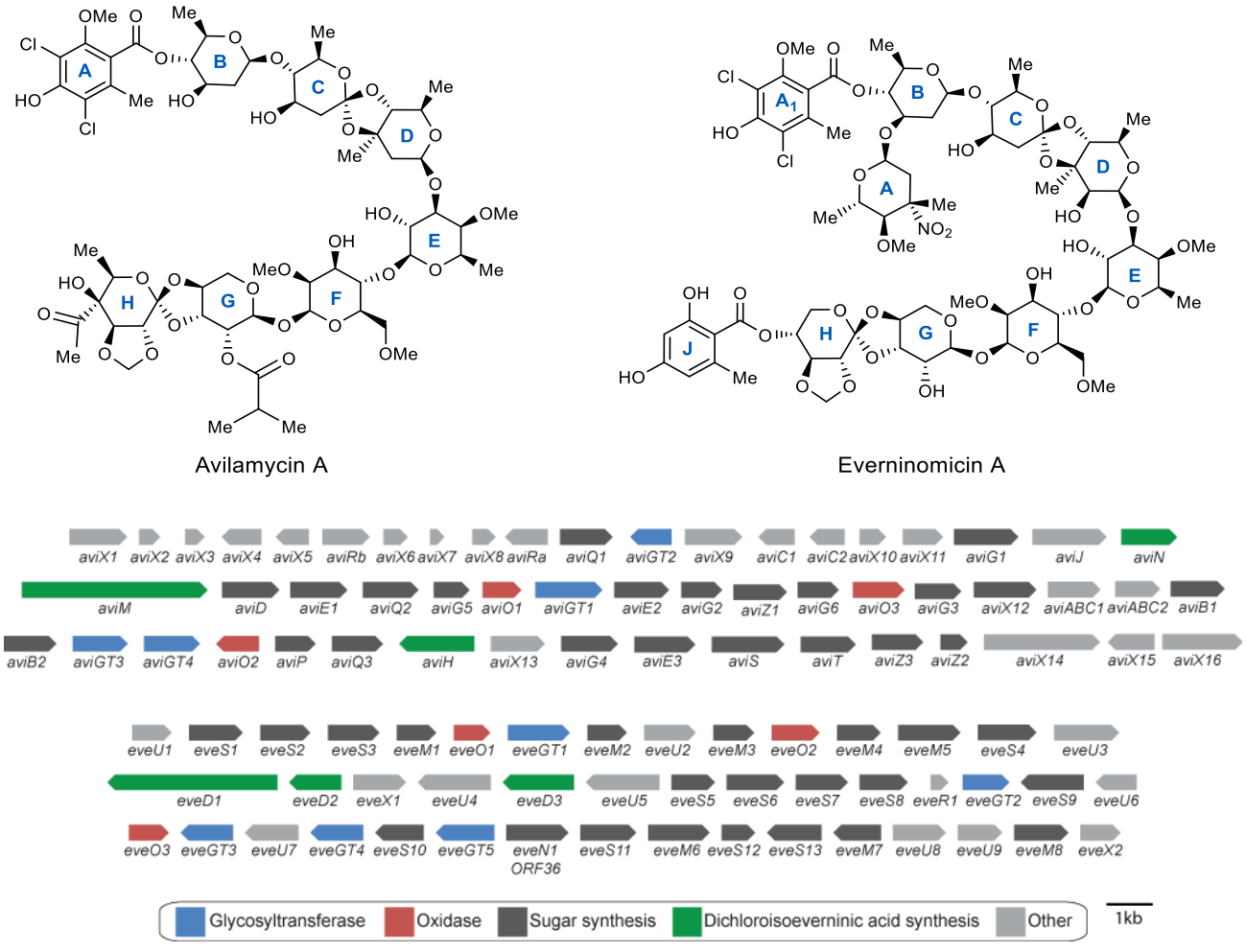

Figure 1-4. Orthosomycin biosynthesis. Structures of avilamycin A and everninomicin A. *Avi* gene cluster from *S. viridichromogenes* Tü57 and *eve* gene cluster from *M. carbonacea* var *africana*. Genes are color-coded according to putative functions. Reproduced from *Nat Prod Rep* **31,** 1026-1042 (2014)[111] with permission from the Royal Society of Chemistry.

O-methylation of ring E, and AviG6 methylates the C2 hydroxyl of ring F (Figure 1-5B). Bechthold and coworkers generated double and triple mutant combinations of these methyltransferases to produce an array of avilamycin analogs termed gavibamycins.[43]

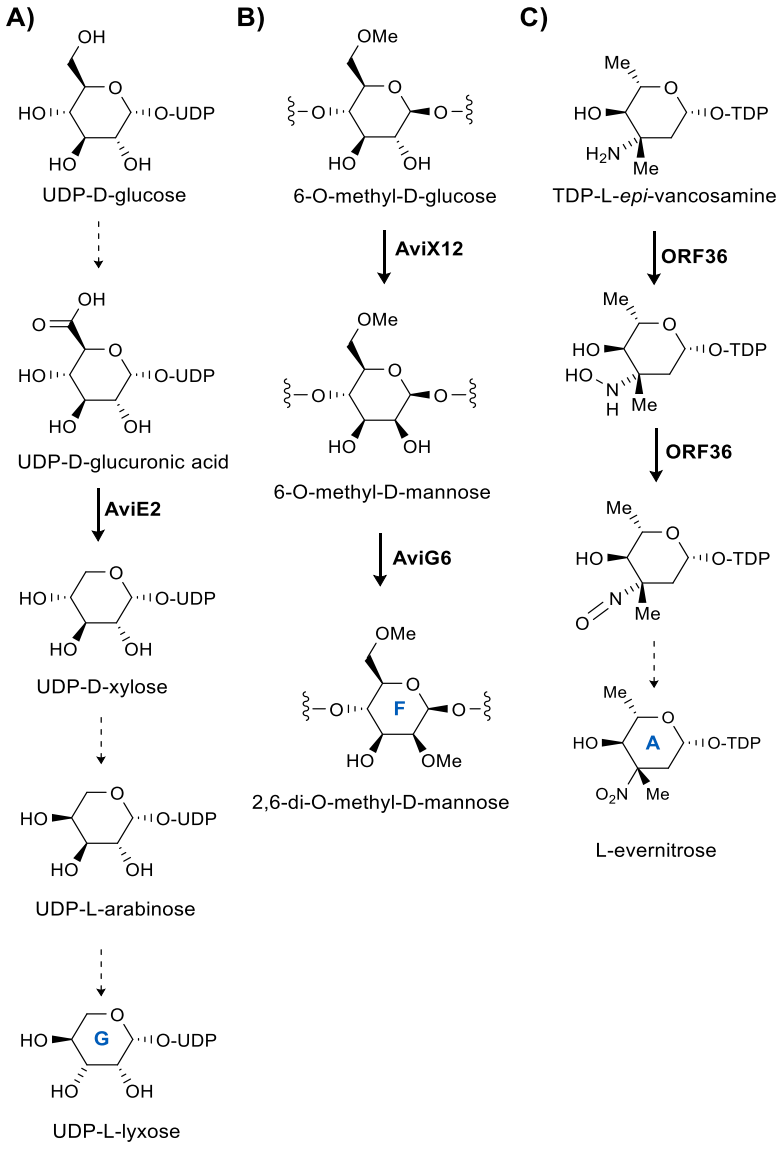

Figure 1-5. Orthosomycin biosynthesis. A) Proposed scheme for formation of ring G, L-lyxose. AviE2 has been shown to catalyse the decarboxylation of UDP-D-glucuronic acid to UDP-D-xylose. B) Scheme for formation of 2,6-di-O-methyl-D-mannose from 6-O-methyl-D-glucose. AviX12 catalyzes a unique radical epimerization. C) Formation of L-evernitrose from L-epi-vancosamine. ORF36 catalyzes the oxidation of the nitrogen from the amino to the nitroso oxidation state. It is likely spontaneous oxidation of the nitroso congener leads to the nitro form. Reproduced from *Nat Prod Rep* **31,** 1026-1042 (2014)[111] with permission from the Royal Society of Chemistry.

Disruption of the gene encoding the putative *C*-methyltransferase, AviG1, resulted in abolished avilamycin production. However, complementation of a *C*-methyltransferase *eryBIII* mutant with *aviG1* from the erythromycin pathway in *Saccharopolyspora erythraea* resulted in restored erythromycin production. This experiment confirmed the role of AviG1 as a *C*-methyltransferase likely involved in the synthesis of ring D.[46]

In vitro characterization of AviE2 revealed that it is a UDP-D-glucuronic acid decarboxylase involved in conversion of UDP-D-glucuronic acid to UDP-D-xylose. This results indicate that the pentose L-lyxose is originally derived from UDP-D-glucose. Two additional epimerization steps are necessary to convert D-xylose to L-lyxose (Figure 1-5A). The authors hypothesize that *aviQ1*, *aviQ2*, or *aviQ3* may encode the necessary chemistries for these epimerizations. This is the first description of a UDP-glucuronic acid decarboxylase involved in secondary metabolism.[47]

Inactivation of *aviX12* resulted in formation of an avilamycin analog containing D-glucose rather than D-mannose (ring F) which possess different stereochemistries at C2. Additionally the C2 hydroxyl was not methylated suggesting that epimerization precedes methylation of this position. As mentioned above, epimerization of the hydroxyl at C2 results in complete loss of antibiotic activity. Therefore, AviX12 is necessary for formation of an active avilamycin. However, this epimerization is notable as it takes place at an unactivated carbon (Figure 1-5B). Upon characterization of its [Fe-S] cluster, AviX12 was determined to be a member of the radical AdoMet family, and AviX12 appears to be the first reported member of the radical AdoMet family involved in epimerization of a sugar.[42]

Gene inactivation experiments suggest that AviO2 and AviB1 are involved in

eurekanate biosynthesis. Loss of *aviO2* and *aviB1* resulted in an avilamycin derivative proposed to have lost the acetyl residue at position C4 of ring H. It was hypothesized that AviB1 and AviB2 are part of an incomplete pyruvate decarboxylase complex that catalyzes the conversion of pyruvate to an acetyl carbanion which is subsequently attached to the saccharide chain through the action of AviO2.[48]

However, it has been previously proposed that AviO1, AviO2, and AviO3 were oxidases involved in orthoester and methylenedioxy bridge formation. Their original analysis of the avilamycin gene cluster found that these three genes had homology to non-heme iron, α-ketoglutarate dependent oxidases which are not likely involved in deoxysugar biosynthesis.[45] Inactivation of *aviO1* and *aviO3* resulted in abolished production although, as detailed above, inactivation of *aviO2* resulted in a putative de-acetylated avilamycin analog.[48] These results are curious in light of inspection of the everninomicin gene clusters from *M. carbonacea* var *africana*[49] (GenBank accession number AX195929) (Figure 1-4) and *M. carbonacea* var *aurantiaca* (GenBank accession numbers AX574200-2). Although everninomicin contains orsellinic acid attached to eurekanate rather than an acetyl group, its gene cluster still contains a close homolog of *aviO2.* Based on translated sequence similarities, putative functions for the genes have been proposed (see Figure 1-4). Additionally all known class I orthosomycins gene clusters contain three oxidases with striking homology to the three from the *avi* cluster. The class II orthosomycin hygromycin B gene cluster also contains a putative non-heme iron, α-ketoglutarate dependent oxidase, HygX. Based on this evidence, we hypothesize that the family of α-ketoglutarate dependent oxidases is responsible for orthoester and

methylenedioxy bridge formation.

Gene inactivation of *aviGT4* resulted in an avilamycin derivative which lacked the terminal eurekanate moiety. Interestingly, eurekanate is attached to the saccharide chain via an orthoester linkage in all orthosomycins. The lack of this linkage suggests that either AviGT4 alone is responsible for orthoester formation or, more likely, glycosylation precedes orthoester formation.[47]

The everninomicin gene cluster from *M. carbonacea* var *africana* ATCC39149 was reported in 2001. Insertional inactivation of *everJ*, *everF,* and *everW* resulted in abolished everninomicin production confirming the role of this gene cluster in everninomicin biosynthesis.[49] Although few biosynthetic studies of the everninomicin gene cluster have been reported, the nitrososynthase ORF36 from *M. carbonacea* var *africana* has been well characterized. Analysis of two everninomicin gene clusters and two avilamycin gene clusters accompanied by subtractive analysis identified a cassette of genes involved in L-evernitrose formation (Figure 1-4, genes N1-M7). Of particular interest is ORF36 (N1) a flavin-dependent monooxygenase that has been shown to oxidize the amino sugar L-TDP-*epi*-vancosamine to the nitroso form (Figure 1-5C).[50] Fermentation under aphotic conditions also results in accumulation of the nitroso compound indicating that full oxidation to the nitro may not be enzymatically catalyzed. A five-enzyme *in vitro* pathway was constructed to test the catalytic competence of ORF36. ORF36 was able to convert TDP-L-epi-vancosamine progenitors to the hydroxylamine oxidation state. $^{18}O_2$ labelling experiments revealed that molecular oxygen is incorporated into the hydroxylamine and nitroso products. Additionally, an X-ray crystal structure of ORF36 was solved revealing a

tetrameric enzyme with a fold similar to that of class D flavin-containing monooxygenases. The structure also revealed an unusually open active site which may explain their promiscuity.[51] Inactivation of *aviP*, a putative phosphatase, did not influence avilamycin production. However, inactivation of *aviD, aviO1, aviO3, aviE2, aviG1*, *everJ, everF,* and *everW* resulted in abolished orthosomycin production.

Moenomycins

First described in 1965, the moenomycins comprise a novel class of phosphoglycolipids natural products produced by at least four *Streptomyces* species.[52,53] The moenomycins were first isolated as a complex of antibiotics from *S. ghanaensis* with moenomycin A being the predominant congener and founding member.[52, 54] Moenomycin A can be divided into three structurally distinct regions: a pentasaccharide, a phosphoglycerate, and a C25 isoprenyl (moenocinyl) lipid tail. As shown in Figure 1-6, all moenomycins contain a core tetrasaccharide attached to a lipid chain through phosphoglycerate. Approximately half of structurally characterized moenomycins contain the D ring sugar residue forming the full pentasaccharide.[53] Other points of variability include rings C and E, which can be either N-acetyl glucosamine or the 6-deoxy derivative chinovosamine, and the C4 position of ring F. A new subfamily of the moenomycins termed nosokomycins have been isolated from *Streptomyces* sp. K04-0144. All nosokomycins lack the A ring common to other moenomycins and instead contain either a carboxylate or carbamate at this position.[55, 56] Two additional structurally characterized members include pholipomycin[57-60] and AC326-α[61] produced by *S. lividoclavatus* and the

unidentified *Actinomyces* sp. AC326 respectively. AC326-α is the only moenomycin that contains a diumycinol lipid tail rather than moenocinol.[61] At least 25 potential moenomycin family members have been reported although the structures of most have yet to be fully elucidated.[56, 58] A natural mixture of moenomycins (also known as bambermycins) marketed as Flavomycin® and Flavophospholipol have been used as animal growth promoters for at least forty years.[62-64] Despite their long use, no significant resistance to moenomycins has been described.[62, 65, 66]

The moenomycins are the only known direct inhibitors of peptidoglycan glycosyltransferases (PGTs) and are active against a range of Gram-positive bacteria with

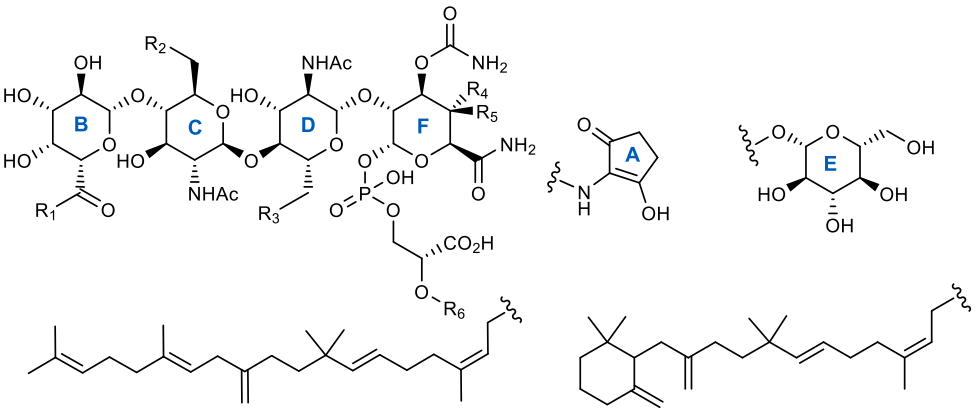

	R1	R2	R3	R4	R5	R6
Moenomycin A	a	H	b	OH	CH_3	c
Moenomycin A_{12}	a	H	b	H	OH	c
Moenomycin C_1	a	H	H	H	OH	c
Moenomycin C_3	a	H	H	OH	CH_3	c
Moenomycin C_4	a	H	OH	OH	CH_3	c
Compound 6	a	H	OH	H	OH	c
Compound 7	a	OH	b	OH	CH_3	c
Pholipomycin	a	OH	OH	OH	CH_3	c
AC326-α	a	OH	b	OH	CH_3	d
Nosokomycin A	OH	H	b	OH	CH_3	c
Nosokomycin B	NH_2	H	b	OH	CH_3	c
Nosokomycin C	OH	H	OH	OH	CH_3	c
Nosokomycin D	NH_2	H	OH	OH	CH_3	c

Figure 1-6. Naturally occurring moenomycins. Adapted from Ostash 2010.[53] Reproduced from *Nat Prod Rep* **31,** 1026-1042 (2014)[111] with permission from the Royal Society of Chemistry.

a potency of up to 1000-fold that of vancomycin.[53, 67, 68] Despite their novel mode of action and potency, the moenomycins have poor pharmacokinetic properties, including poor oral bioavailability and a long half-life, which have inhibited their clinical use.[69] However, interest in this class of antibiotics was renewed in the late 1990s and early 2000s, and significant efforts have been made to create moenomycin analogs with improved properties yet retained potency. An excellent review has been written recently on the moenomycin family of antibiotics including chemical and biological efforts to produce novel derivatives, and we direct readers to that article for a thorough history of the moenomycins.[53] In this review, we aim to highlight their unique mode of action, structural features contributing to their activity, and the biosynthetic pathway.

Mode of Action

Moenomycin was first determined to be an inhibitor of cell wall biosynthesis of *S. aureus* in 1968 by Huber and Nesemann.[70] Bacterial cell wall synthesis begins with the cytosolic synthesis of UDP-*N*-acetyl muramyl-pentapeptide which is subsequently transferred to a C55 undecaprenol phosphate carrier lipid by MraY to generate MurNAc-pentapeptide-pyrophosphoyl-undecaprenol or lipid I. *N*-acetylglucosamine is then transferred to lipid I by MurG to produce N-acetylglucosamine-β-1,3-MurNAc-pentapeptide-pyrophosphoryl-undecaprenol or lipid II. Transglycosylases, such as the bifunctional penicillin-binding proteins (PBPs) or the monofunctional MtgA, catalyze the polymerization of lipid II into peptidoglycan.[69, 71] Moenomycins exert their effects by inhibiting the transglycosylation step of cell wall biosynthesis leading to cell lysis and

death.[67]

Although moenomycin was originally thought to be a competitive inhibitor of lipid II,[69] more recent studies have shown the inability of lipid II to displace moenomycin in *E. coli* PBP1b indicating that moenomycin does not bind in the same area as lipid II. The authors proposed that moenomycin could be blocking elongation by binding in the polysaccharide binding site rather than the lipid II site.[72] Supporting this experiment, the structure of bifunctional PBP2 in complex with moenomycin reveals that it binds in an extended conformation that probably mimics the growing polysaccharide-chain substrate.[73] Subsequently, additional structures of moenomycin bound to various PGTs have been reported. Figure 1-7 illustrates two *S. aureus* monofunctional

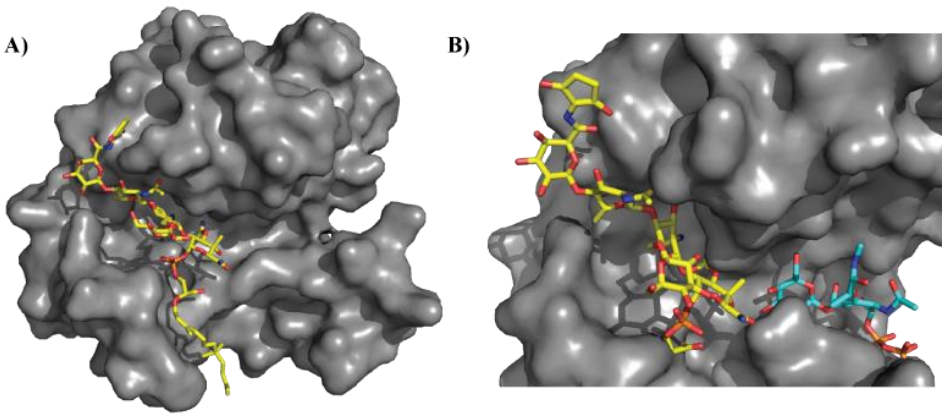

Figure 1-7. Site of moenomycin interaction with glycosyltransferases. A) Crystal structure of moenomycin (yellow) bound to *S. aureus* monofunctional transglycosylase (PDB 3HZS). Only 15 carbons of the lipid tail are ordered in this structure. B) Crystal structures of membrane-bound monofunctional glycosyltransferase with moenomycin (yellow; PDB 3VMR) and a lipid II analog (blue; PDB 3VMT). Note: 3VMR and 3VMT were aligned, and the surface of 3VMR was subsequently hidden for clarity. Moenomycin binds in the channel where the growing glycan chain normally binds thereby disrupting transglycosylation activity. Under normal biological conditions, lipid II would be transferred to the growing glycan chain forming a new β1-4 glycosidic linkage. Reproduced from *Nat Prod Rep* **31,** 1026-1042 (2014)[111] with permission from the Royal Society of Chemistry.

glycosyltransferase (MtgA) in complex with moenomycin. Moenomycin interacts with highly conserved residues in the active site of the glycosyltransferase providing the basis for its interaction across a broad range of PGTs.[74] Figure 1-7B depicts the binding of moenomycin and a lipid II analog to a *S. aureus* membrane-bound MGT.[75] As demonstrated in earlier experiments, moenomycin does not bind in the lipid II site but a separate portion of the active site where the extending saccharide likely binds. More recent studies have revealed that moenomycin A binds at the same site as lipid IV. The authors therefore suggest that moenomycin blocks the initiation step rather than elongation or termination. It is proposed that the phosphoglycerate and lipid portion of moenomycin mimics the diphospholipid leaving group of the donor substrate.[76]

Although natural moenomycins are not currently suitable for clinical use, multiple studies have been conducted to identify the minimal pharmacophore so that moenomycins may be designed with improved pharmacokinetic properties. Crystal structures of neryl-moenomycin A bound to the PGT domain of *Aquifex aeolicus* PBP1A revealed six conserved active site residues which appear to interact with the F ring and phosphoglycerate portions. Mutations of all six residues resulted in abolished or reduced enzyme activity. The authors propose that this may explain why resistance to moenomycin has not been observed. Although the majority of contacts involve interactions with the F ring and phosphoglycerate, there are a small number of interactions with the E ring and a single interaction with the C ring. Using heterologous expression, Walker and coworkers generated a moenomycin analog which maintained the key contacts. This DEF trisaccharide was found to inhibit *S. aureus* PBP2 more strongly

than moenomycin A.[77] Previously the minimal pharmacophore was thought to be the tetrasaccharide CDEF. [69] Together these results suggest that the minimal pharmacophore includes rings E and F, the phosphoglycerate, and either ring C or D.[77] Moenomycin derivatives that lack the D ring retain antibiotic activity. [73] Indeed crystal structures of bound moenomycin reveal that the D ring protrudes into the solvent, reinforcing the observation that the D ring is not necessary for activity. [77] In addition, both the carboxylate and the phosphoglycerate interact with important conserved active site residues and are necessary for activity.[78]

Because the lipid of moenomycin is thought to be responsible for the majority of its poor pharmacological properties, much effort has been devoted to identifying ways in which this portion can be modified. Although many studies have confirmed that the entire 25 carbon chain is not necessary for activity, the optimal length is still unknown.[68,72,76,77] A lipid chain with ten carbons is sufficient for *in vitro* enzyme inhibition activity but is not active *in vivo*.[68] In the crystal structure of *S. aureus* MTG in complex with moenomycin, fifteen carbons of the lipid chain are ordered and form hydrophobic interactions with four residues.[74] A 15 carbon analog possessed biological activity although the activity was reduced compared to the parent compound. [79] Since the length of the lipid tail is necessary for biological activity, it is hypothesized that the lipid portion interacts with the membrane and is involved in anchoring.[78] This theory is supported by the fact that the transmembrane portion of PBPs is necessary for moenomycin binding. [80]

In 2001, Kahne and coworkers reported three *E. coli imp* mutants that were resistant to moenomycin as well as vancomycin analogues and teicoplanin. Notably, the

mutants remained sensitive to β-lactams which inhibit the transpepdidation reaction as well as other antibiotics targeting other essential cellular functions which rules out a nonspecific mechanism of resistance such as altered permeability. The mutant strains all lacked expression of *yfgL*, a lipoprotein located on the inner surface of outer membrane. Although the role of YfgL in resistance is not known, the authors hypothesize that it affects regulation of lytic transglycosylases which when inappropriately activated may cause rapid cell death.[81] This marks the first reported study of moenomycin resistant mutant strains and provides insights into ways in which bacteria might acquire moenomycin resistance. Although PGT inhibition had long been hypothesized to be the bactericidal activity of moenomycin, only recently have moenomycin-resistant *S. aureus* mutants have been generated which resulted in a point mutation in the active site of PBP2 confirming the this mechanism of action.[82]

Though moenomycin A has yet to realize its full clinical potential, it is already used as a tool to discover new PGT inhibitors with better pharmacological properties. For example, a fluorescently labelled moenomycin analog based on the minimal pharmacophore has been synthesized and used in a screen to identify small molecules inhibitors of PGTs in displacement assays.[83] While non-carbohydrate bacterial transglycosylase inhibitors have been discovered, moenomycin remains the most potent inhibitor known to date. [84]

Biosynthesis

Although the total synthesis of moenomycin A has been reported,[85] the complexity of the molecule makes biosynthetic creation of analogs an attractive alternative. Walker

and coworkers have characterized the entire seventeen step moenomycin pathway.[79,86] The moenomycin biosynthetic genes from *S. ghanaensis* (ATCC14672) were identified using a whole-genome scanning approach. Surprisingly, the *moe* gene cluster is split into two separate clusters, a small 3 gene cassette involved in A ring biosynthesis and a larger 20 gene primary *moe* cluster involved in assembly of the phosphoglycolipid pentasaccharide (Figure 1-8). Despite moenomycin's large size, its gene cluster is surprisingly compact due to the use of isoprenoid and sugar-nucleotide building blocks from the host's primary metabolism.[86]

The large *moe* cluster 1 contains two prenyltransferases, five glycosyltransferases, seven sugar synthesis genes, and four transporters. It also contains two non-functional genes involved in A ring assembly, *moeA5* and *moeB5*. *MoeA4* is an aminolevulinate

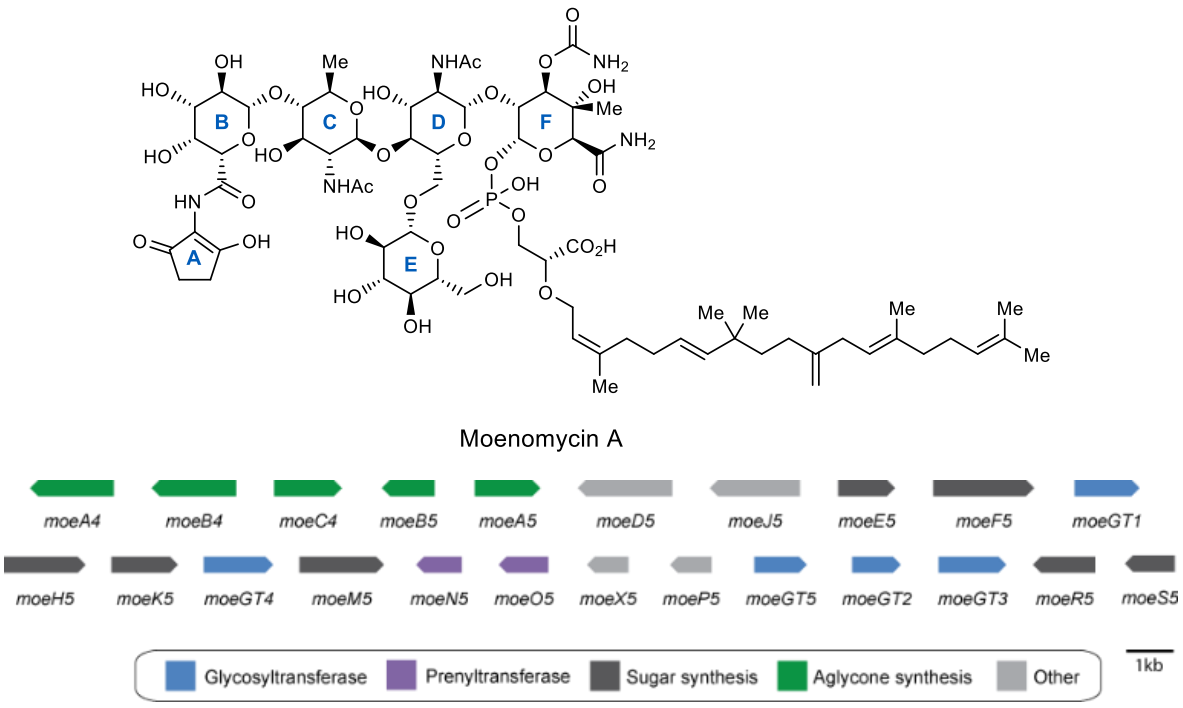

Figure 1-8. Moenomycin biosynthetic gene cluster from *Streptomyces ghanaensis*. Genes are color-coded according to function. Reproduced from *Nat Prod Rep* **31,** 1026-1042 (2014)[111] with permission from the Royal Society of Chemistry.

synthase, and *moeB4* is an aminolevulinate cyclase. Both of these genes as well as an amide synthetase *moeC4,* which attaches the A ring to moenomycin, are found in the smaller *moe* cluster 2. Therefore, *moe* cluster 2 is required for A ring assembly and attachment.[79, 86]

The entire moenomycin A biosynthetic pathway has been reconstituted in the heterologous host *S. lividans* and the function and timing of each gene was characterized (Figure 1-9). MoeO5 and MoeN5 are prenyltransferases that construct the lipid tail from primary metabolites. MoeO5 catalyzes the first step in the moenomycin biosynthetic pathway to form a C15 lipid-phosphoglycerate.[79] Interestingly, in addition to transferring the C15 lipid of farnesyl pyrophosphate to the 2-hydroxyl group of 3-phosphoglycerate, MoeO5 also catalyzes an unusual *trans*-to-c*i*s isomerization of the C2-C3 double bond. Recently, the crystal structure of MoeO5 in complex with the product lipid-phosphoglycerate has been solved providing insights into this unique isomerization.[87] Confirming the lipid-phosphoglycerate as an early intermediate in moenomycin biosynthesis, nosokophic acid (a C15 lipid-phosphoglycerate) was recently isolated from the culture broth of *Streptomyces* sp. K02-0144.[88] MoeN5 catalyzes transfer of the C10 lipid onto the C15 lipid tail after disaccharide assembly. [79]

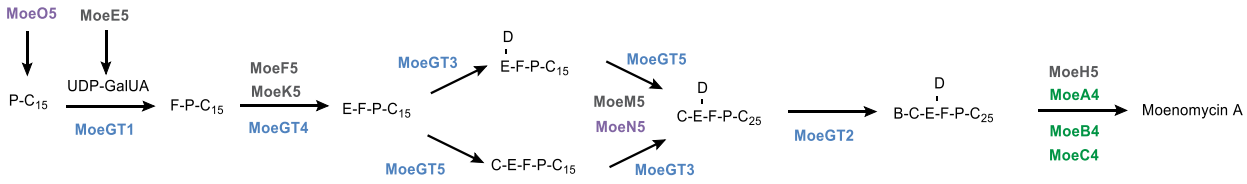

Figure 1-9. Experimentally determined order of moenomycin biosynthesis. P = phosphate; C_{15} = 15-carbon lipid chain; C_{25} = 25-carbon lipid chain; B-F indicate ring systems of moenomycin. Enzymes are color-coded to match the gene cluster in Figure 1-8. Reproduced from *Nat Prod Rep* **31,** 1026-1042 (2014)[111] with permission from the Royal Society of Chemistry.

Investigation of the five glycosyltransferases revealed the substrate and timing of each.[79] Interestingly, the glycosyltransferases of the moenomycin pathway are more closely related to those involved in primary metabolism than to other secondary metabolism glycosyltransferases.[86] MoeGT1 transfers the first sugar to the lipid phosphoglycerate. MoeGT4 transfers the next sugar to form the disaccharide. The authors suggest a branched pathway from the disaccharide with either MoeGT5 or MoeGT4 acting first followed by the remaining glycosyltransferase. Finally MoeGT2 attaches the B ring sugar to form the full pentasaccharide. [79]

Only three genes in the *moe* cluster are involved in the synthesis of NDP-sugars. MoeE5 has been shown to catalyze the epimerization of UDP-glucuronic acid to UDP-galacturonic acid (UDP-GalUA). UDP-GalUA is the natural substrate for MoeGT1; therefore epimerization occurs prior to glycosyl transfer. MoeR5 and MoeS5, a 4,6-dehydratase/ketoreductase pair, are responsible for the conversion of UDP-GlcNAc to its 6-deoxy version, UDP-chinovosamine.[79]

Four genes are involved in final tailoring of the sugar residues of moenomycin. MoeF5 is responsible for F ring carboxamidation while MoeH5 catalyzes amidation of the B ring. MoeK5 methylates ring F before epimerization of the C4 hydroxyl. The final sugar tailoring enzyme, MoeM5 is a carbamoyltransferase that installs the carbamate group on the F ring primarily during the trisaccharide stage.[79]

Because moenomycins are produced at low levels in heterologous hosts, recent studies have focused on improving moenomycin production. In particular, recent studies have shown that rational manipulation of the regulators and increased *moe* gene dosage

could be useful for improving moenomycin biosynthesis in heterologous hosts.[89] In addition, deletion of *wblA*$_{gh}$, encoding a homologue of the WhiB-family of proteins, blocked aerial mycelium sporulation and led to a 230% increase in moenomycin production.[90] Disruption of putative ABC transporters *moeX5* and *moeP5* resulted in reduced moenomycin production.[91] While much is known about the biosynthetic steps leading to production of moenomycin, less is known about its regulation and the regulation of natural product gene clusters in general.

Although the moenomycin cluster is already surprisingly compact, Walker and co-workers have shown that only seven genes (*moeE5, moeO5, moeGT1, moeF5, moeGT4, moeM5,* and either *moeGT3* or *moeGT5)* are required to make bioactive analogs. In addition, the biosynthetic pathway for moenomycin production appears to be highly malleable as only four gene disruptions (*moeGT1*, *moeF5*, *moeE5, moeO5*) resulted in abolished production of moenomycin analogs.[79] The mutability of the moenomycin gene cluster provides ample opportunity for creation of analogs.

Saccharomicins

In 1998, a new family of antibacterial polysaccharides were discovered and termed the saccharomicins. The saccharomicins are novel heptadecaglycoside antibiotics produced by the rare actinomycete *Saccharothrix espanaensis* LL-C19004 originally isolated from a soil sample in Spain.[92,93] To date, only two saccharomicins have been reported, saccharomicins A and B which differ only by the identity of the tenth sugar

residue (Figure 1-10). The saccharomicins are large oligosaccharides composed of seventeen 6-deoxy sugars and the aglycone *N*-(*m,p*-dihydroxycinnamoyl)taurine. The sugar residues can be separated into eight amino sugars and eight non-amino sugars. Half of the amino sugars are 4-*epi*-vancosamines and half are saccharosamines, a unique amino sugar found only in the saccharomicins. In addition there are four fucoses and a variant number of rhamnoses and digitoxoses adding to a total of four. Finally, the aglycone is linked to the sugar chain via a sulphated fucose residue.[92] While the absolute

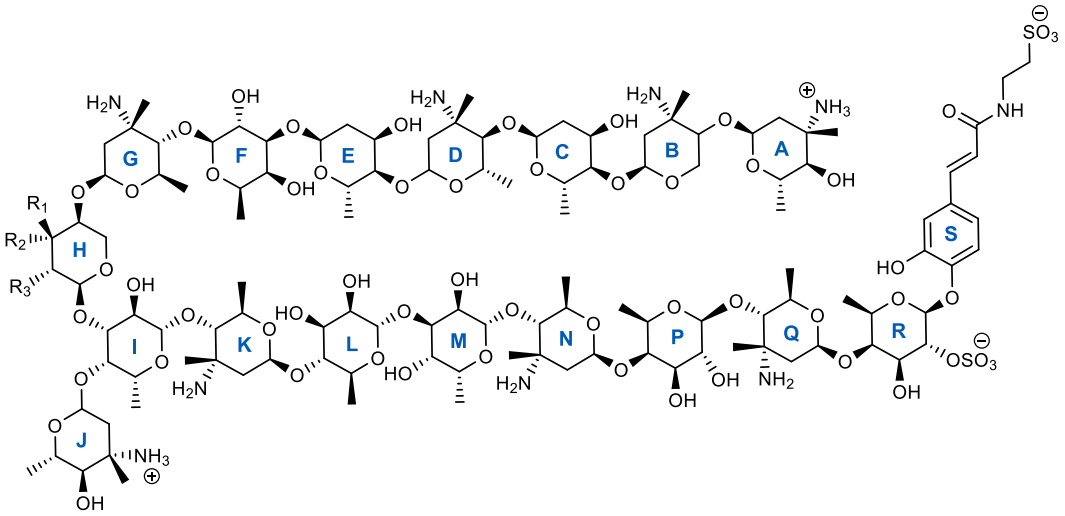

	R1	R2	R3
Saccharomicin A	H	OH	OH
Saccharomicin B	OH	H	H

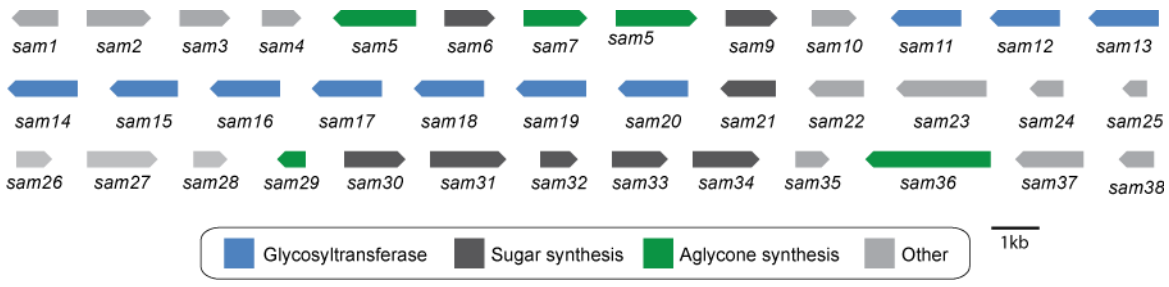

Figure 1-10. Naturally occurring saccharomicins and corresponding gene cluster from *Saccharothrix espanaensis* LL-C19004. Genes are color-coded according to putative function. Reproduced from *Nat Prod Rep* **31,** 1026-1042 (2014)[111] with permission from the Royal Society of Chemistry.

stereochemistry of all sugar residues has not been determined, synthetic efforts have determined that the sulphated fucose as well as the fucose-saccharosamine disaccharide units are all D-configuration.[94,95] In addition to the novel amino sugar saccharosamine, the saccharomicins also contain a unique β-β glycosidic linkage between the fucoses and saccharosamines allowing them to survive harsh acidic conditions.[92]

Both saccharomicins A and B possess activity against a panel of Gram-positive organisms including MRSA and VRE but are less potent against Gram-negative organisms. In addition, the saccharomicins had promising activity against all multiply-resistant staphylococci strains tested. These results provide evidence that the saccharomicins likely do not have cross-resistance with other families of antibiotics. Despite their promising antibacterial activities, the compounds exhibit toxic effects at high doses (LD_{50} = 16mg/kg) rendering them currently unsuitable for general use in the clinic.[92]

Mode of Action

While the precise mode of action has yet to be determined, various experiments have indicated that the primary target of the saccharomicins is associated with the bacterial cellular membrane. Initial experiments revealed that the saccharomicins completely inhibit DNA, RNA, and protein synthesis within ten minutes of treatment. Further experiments indicated that the saccharomicins caused cell death and lysis by disrupting the cell membrane. Adding the divalent cations Ca^{2+} or Mg^{2+} substantially decreased the activity against Gram-negative by up to sixteen-fold but had no effect on the activity against Gram-positive organisms. Other divalent cations such as Fe^{2+} or Cu^{2+}

had no effect on the saccharomicins' activity indicating that they are not general chelators but form interactions with the outer membrane-bound cations and self-promote their uptake like aminoglycosides and quinolones. Using an *E. coli imp* strain that has increased cell membrane permeability, the saccharomicins had an eight-fold higher activity compared to a regular *E. coli* strain. These results indicate that the poor activity against Gram-negative organisms is most likely due to the saccharomicins' inability to penetrate the outer membrane. In addition, there was extensive potassium leakage when the *E. coli imp* strain was treated with saccharomicins consistent with a sudden disruption of the cell membrane.[93]

Biosynthesis

In 2012, genomic analysis of the complete sequence of *S. espanaensis* DM44229^T revealed the presence of twenty-six biosynthetic gene clusters, including the cluster responsible for biosynthesis of the saccharomicins, designated the *sam* cluster. The gene cluster contains genes responsible for aglycone biosynthesis as well as ten glycosyltransferases and eight sugar synthesis genes. While saccharomicins contain seventeen sugar residues, only ten putative glycosyltransferases, *sam11-20,* are present in the cluster suggesting that some of the glycosyltransferases may work iteratively or be recruited from primary metabolism. In addition, there are only eight putative NDP-sugar biosynthesis genes that are responsible for formation of all seventeen sugars. *Sam6* is a putative glucose-1-phosphate nucleotidyltransferase. Two putative methyltransferases are found in the gene cluster. *Sam9* appears to be a SAM-dependent methyltransferase while *Sam34* has homology to NDP-hexose C-3 methyltransferases and is likely

responsible for adding the C-3 methyl group to form L-*epi*-vancosamine and/or the saccharosamine residues. *Sam21*, which has homology to NDP-4-keto-6-deoxyhexose-4-ketoreductases, *Sam30* a putative transaminase, *Sam31* a probable NDP-hexose 2,3-dehydratase, *Sam32,* which has homology to a dTDP-4-dehydrorhamnose 3,5-epimerase, and *Sam33*, a putative NDP-hexose 3-ketoreductase are responsible for the biosynthesis of the five types of sugars found in the saccharomicins. *Sam23* and *Sam24* encode putative transport proteins while *Sam1, 3, and 38* are most likely regulatory elements.[96]

Investigation of the biosynthesis of the aglycone portion of the saccharomicins was first reported in 2006 by Bechthold and coworkers who cloned and identified two genes from *S. espanaensis* which are involved in caffeic acid biosynthesis. Heterologous

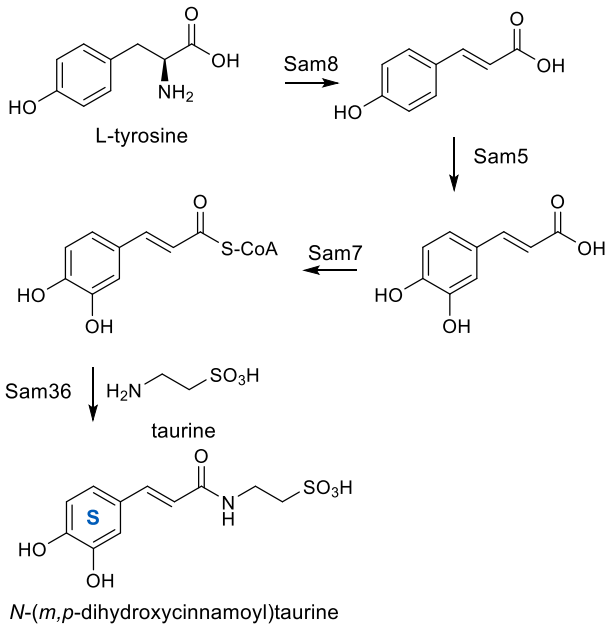

Figure 1-11. Biosynthesis of the saccharomicin aglycone beginning with L-tyrosine. Four enzymes have been shown to be sufficient to catalyze the formation of the saccharomicin aglycone. Reproduced from *Nat Prod Rep* **31,** 1026-1042 (2014)[111] with permission from the Royal Society of Chemistry.

expression of *sam8* and *sam5* led to production of *trans*-caffeic acid (Figure 1-11). Assays

identified Sam8 as a tyrosine ammonia-lyase and Sam5 as a 4-coumarate 3-hydroxylase, the first of both of these enzymes to be reported in an actinomycete.[97] Sam7 has similarity to acyl-CoA synthases indicating that it may be involved in the synthesis of caffeoyl-CoA which could be used to link taurine to form the aglycone, and Sam36 has homology to penicillin amidases and may be responsible for forming the amide bond between caffeic acid and taurine. The synthesis of taurine has yet to be described in bacteria; however, the authors speculate that *sam29* may encode a sulfinic acid decarboxylase.[96]

Although due to their toxicity the saccharomicins are not currently in clinical use, understanding the biosynthesis of the largest oligosaccharide antibiotic will further understanding of these bioactive oligosaccharides in general and may lead to potential new clinical candidates to treat the growing problem of antibacterial resistance.

Acarviostatins

In 2008, a class of novel pseudo-oligosaccharides termed the acarviostatins were reported from cultures of *S. coelicoflavus* ZG0656 (also known as *S. coelicoflavus* var. *nankaiensis*).[98] Six acarviostatins were originally identified and structurally characterized (Figure 1-12).[99, 100] Based on tandem mass spectrometry fragmentation patterns of the six aforementioned acarviostatins, a total of 80 acarviostatin analogs have been identified. Fragmentation as well as multiple reaction monitoring was necessary to identify all of the acarviostatins as many are positional isomers having the same m/z ratio.[101]

Although numerous acarviostatins have been identified, the majority can be

described by three variables on which a systematic naming system has been based. Each acarviostatin is composed of a pseudotrisaccharide core flanked by a variable number of D-glucose units. Acarviostatins can contain up to 5 pseudotrisaccharides which are denoted by Roman numerals. The middle digit of the acarviostatin name corresponds to the number of D-glucose units at the non-reducing end, and the last digit describes the number of D-glucose residues at the reducing end. For instance, acarviostatin II03 contains two pseudotrisaccharide units and three glucose residues at the reducing end.[99, 101]

The pseudotrisaccharide is composed of valienamine, 4-amino-4,6-dideoxy-D-glucose, and D-glucose. Valienamine and 4-amino-4,6-dideoxy-D-glucose form acarviosine which is the core structure of acarbose, a potent α-amylase inhibitor. Valienamine is a unique C_7N cyclitol also found in the antifungal validamycin A. Mode of action and biosynthesis of both acarviostatins and acarbose will be considered as acarbose is a building block of the acarviostatins.

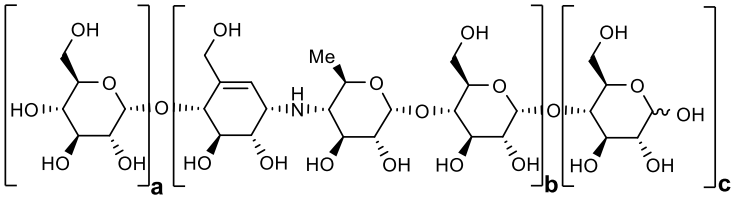

	a	b	c
Acarbose	0	1	1
Acarviostatin I03	0	1	3
Acarviostatin II03	0	2	3
Acarviostatin II13	1	2	3
Acarviostatin II23	2	2	3
Acarviostatin III03	0	3	3
Acarviostatin IV03	0	4	3

Figure 1- 12. Acarbose and the six original naturally-occurring acarviostatins. Reproduced from *Nat Prod Rep* **31,** 1026-1042 (2014)[111] with permission from the Royal Society of Chemistry.

Mode of Action

Human pancreatic α-amylase (HPA) is a major therapeutic target for the treatment of type II diabetes as it catalyzes the hydrolysis of α-D-(1,4)-glycosidic linkages found in starch. Acarbose, a drug successfully used for treatment of type II diabetes, was the first α-glucosidase inhibitor to be approved by the US Food and Drug Administration.[102, 103] Many of the acarviostatins, however, are more potent α-amylase inhibitors than acarbose. In fact, acarviostatin III03 is 260 times more potent than acarbose and is the most effective α-amylase inhibitor known to date.[99] Despite containing valienamine, validamycin A is not an inhibitor of α-amylase suggesting that the sugar residues attached to the aminocyclitol are necessary for inhibition.[102]

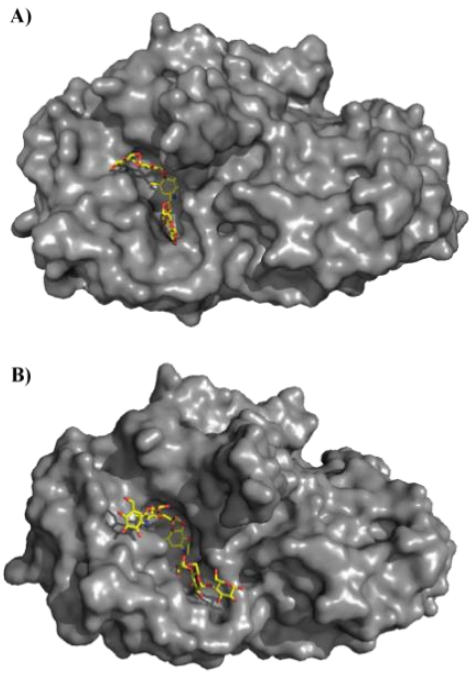

Figure 1-13. Human pancreatic amylase in complex (**a**) acarbose (pdb 1b2y) and (**b**) the hydrolysis product of acarviostatin iii03 (pdb 3olg). Both acarbose and the acarviostatins are competitive inhibitors of human pancreatic amylase by acting as transition-state analogs. Reproduced from *Nat Prod Rep* **31,** 1026-1042 (2014)[111] with permission from the Royal Society of Chemistry.

Recently, crystal structures of HPA in complex with a series of acarviostatins provided greater insights into their specific mode of action. Acarbose and acarviostatins all bind in the active site of HPA (Figure 1-13). Like acarbose, acarviostatin I03, which is only one glucose longer, undergoes a series of hydrolysis, condensation, and transglycosylation reactions resulting in a substantially rearranged product. However, crystal structures of HPA in complex with larger acarviostatins surprisingly revealed the same seven-ring hydrolysis product in each active site regardless of the original number of sugar residues (Figure 1-13B). The authors propose these larger acarviostatins undergo hydrolysis at either one or both ends to generate acarviostatin II01. These results indicate that an inhibitor containing seven sugar residues would provide the most efficient α-amylase inhibition while occupying the full active site.[103] In all cases, acarviosine inhibits the hydrolysis reaction by acting as a transition-state analog.[98,104] The nitrogen bond between valienamine and 4,6-dideoxyglucose cannot be cleaved rendering the acarviosine containing compounds competitive inhibitors of human pancreatic amylase.[103]

Biosynthesis

The biosynthesis of acarbose has been well researched and we point readers to two excellent reviews of the biosynthesis of acarbose as well as other aminocyclitol natural products.[105, 106] This review will briefly summarize the biosynthesis of acarbose while drawing parallels with the proposed acarviostatin biosynthetic pathway.

Reported in 2012, the genome sequence of *S. coelicoflavus* ZG0656 reveals the presence of a putative acarviostatin gene cluster. The gene cluster is approximately 40

kilobases and has significant similarity to two gene clusters known to be responsible for acarbose synthesis: *gac* from *S. glaucescens*[107] and *acb* from *Actinoplanes* sp. SE50/110[104]. This putative acarviostatin gene cluster is termed the *sct*-cluster and contains 16 genes that are proposed to encode enzymes for the synthesis of the pseudotrisaccharide core. In addition there are five α-glucosidic hydrolases and/or glycosyltransferases (*sctW, sctE1, sctE2, sctZ1, sctZ2*), two putative ATP-dependent transporter systems (*sctWXY* and *sctFGH*) and two putative regulators (*scrC1* and *scrC2*). Because the *sct* cluster is most similar to the acarbose *gac* cluster, the biosynthetic pathways are predicted to be highly similar (Figure 1-14). Therefore, the acarviostatin biosynthetic pathway that the authors

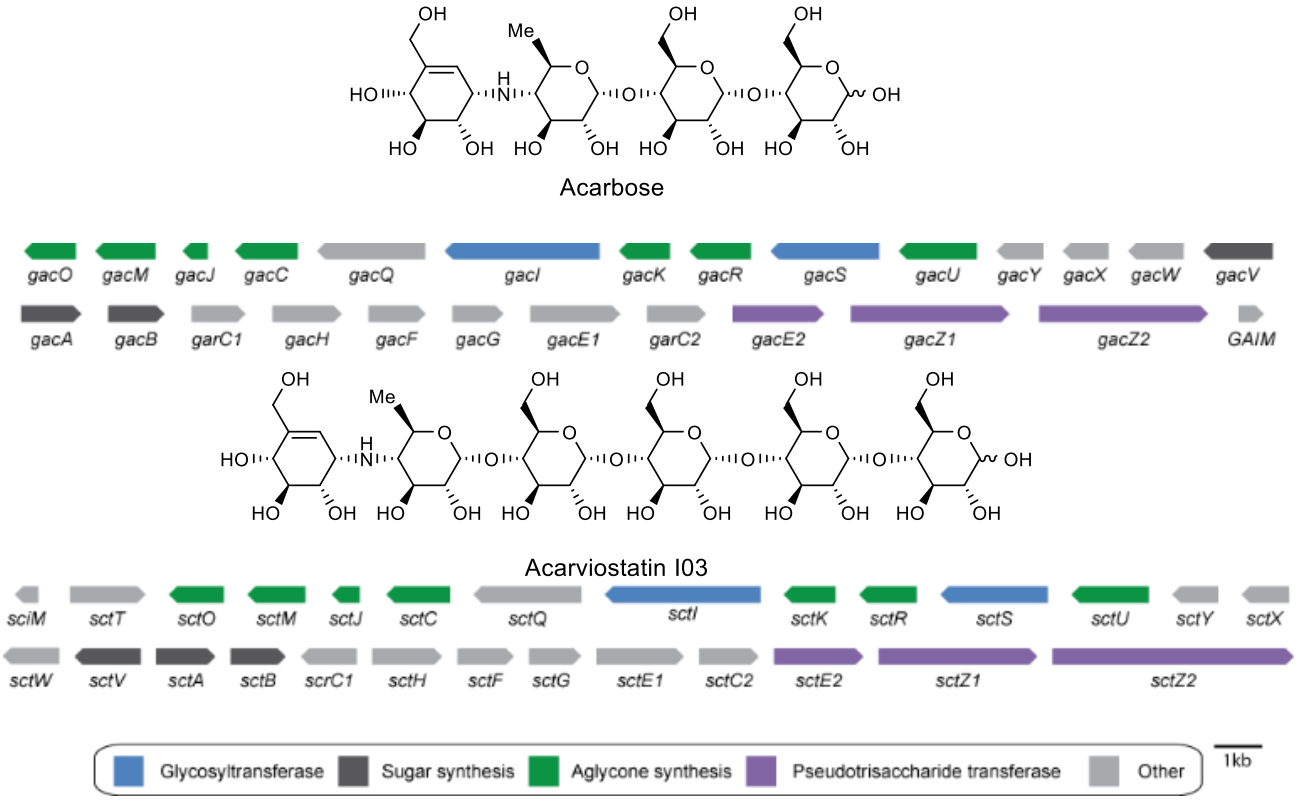

Figure 1-14. Acarbose biosynthetic gene cluster from *S. glaucescens* and putative acarviostatin biosynthetic gene cluster from *S. coelicoflavus* ZG0656. Genes are color-coded according to putative function. Reproduced from *Nat Prod Rep* **31,** 1026-1042 (2014)[111] with permission from the Royal Society of Chemistry.

proposed draws heavily from knowledge of acarbose biosynthesis.

Labelling studies have shown that valienamine of acarbose is derived from pentose phosphate pathway rather than the shikimate pathway.[108] Hence, the biosynthesis of acarbose as well as the acarviostatins is proposed to begin with cyclization of sedoheptulose 7-phosphate by GacC/SctC (gac corresponds to the acarbose enzymes; sct corresponds to the acarviostatin enzymes) to give 2-*epi*-5-*epi*-valiolone. GacJ/SctJ then epimerizes C-2 of 2-*epi*-5-*epi*-valiolone to give 5-*epi*-valiolone. The next step is presumably phosphorylation of C7 by GacM/SctM followed by GacO/SctO catalyzed dehydration and reduction to generate 1-*epi*-valienol-7-phosphate. GacU/SctU is proposed to catalyze a second phosphorylation to generate 1-*epi*-valienol-1,7-diphosphate which is

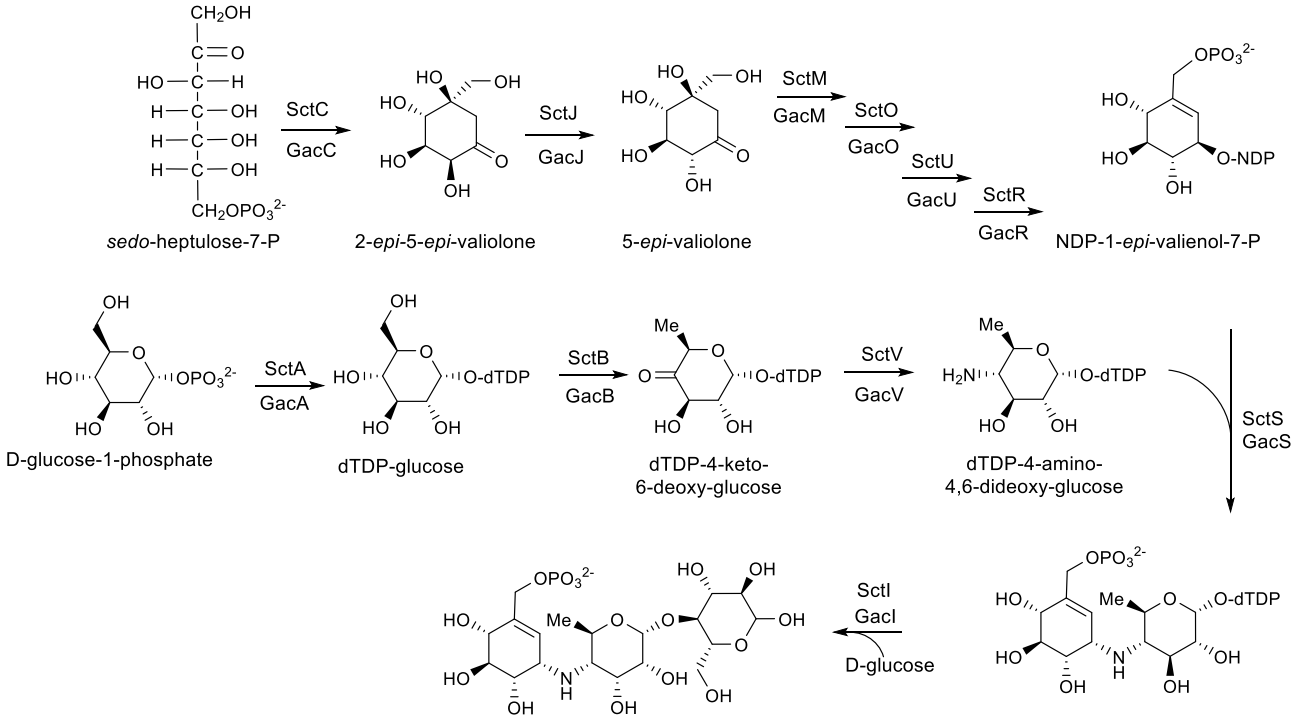

Figure 1-15. Proposed biosynthetic pathway to the acarviostatins beginning with *sedo*-heptulose-7-phosphate and D-glucose-1-phosphate. Sct genes correspond to those from the putative acarviostatin pathway while Gac genes are their corresponding homologs found in the acarbose gene cluster from *S. glaucescens.* Adapted from Guo 2012.[109] Reproduced from *Nat Prod Rep* **31,** 1026-1042 (2014)[111] with permission from the Royal Society of Chemistry.

subsequently converted to NDP-1-*epi*-valienol-7-phosphate by GacR/SctR (Figure 1-15).[107, 109]

A second pathway is presumed to produce dTDP-4-amino-4,6-dideoxy-glucose through the sequential action of GacA/SctA (dTDP-glucose synthase), GacB/SctB (4,6-dehydratase) and GacV/SctV(4-aminotransferase). The pathways then are proposed to converge via GacS/SctS to generate the pseudodisaccharide dTDP-acarviose-7-phosphate. The final step in formation of the pseudotrisaccharide core is proposed to be glycosylation by GacI/SctI (Figure 1-15).[109]

While these enzymes generate the pseudotrisaccharide core, glycosyl transferases and/or pseudotrisaccharide transferases are still necessary to complete the biosynthesis of the acarviostatins. SctE2 has moderate homology to AcbD of the *Actinoplanes* acarbose pathway. AcbD is an acarviose transferase which adds different maltooligosaccharides to acarviosine. [101, 110] Based on this homology, the authors speculate that SctE2 as well as SctZ1 and SctZ2 might be responsible for joining pseudotrisaccharide units as well as attaching additional glucose units to the reducing and non-reducing ends.[109] Further characterization of these genes is needed to definitively identify the gene(s) responsible for full construction of the acarviostatins.

The putative transporters SctWXY and SctFGH have homology to the ABC transporters in both acarbose gene clusters. It has been proposed that these transporters are involved in a recycling mechanism in which one secretes acarviostatin I00-7-phosphate out of the cell where hydrolases and transferases work to attach maltooligosaccharides to the acarviostatin core. The acarviostatins are then imported

back into the cell where SctQ and/or SctE1 hydrolyze the glucoses to regenerate acarviostatin I00-7-phosphate. The host may use this mechanism to transport hydrolyzed starch into the cell.[109] This recycling mechanism or 'carbophor' may also explain the vast assortment of acarviostatins that have been identified. The acarviostatins represent a unique biological activity for oligosaccharide natural products. Fully understanding the biosynthesis of these compounds can lead to new derivatives with improved efficacy that may aid in the fight against metabolic disorders, including diabetes.

Conclusions

With the recent expansion in 'genome mining' of natural products, understanding the distinguishing biosynthetic features of oligosaccharide secondary metabolites will likely enable the discovery of many more of this family of compounds. As evidenced by the examples above, many analogs of oligosaccharides can be generated by a single organism and conservative mutagenesis studies have been able to generate a variety of non-natural analogs with modulated biological properties. Moreover, with the improvement and widespread use of mass spectrometry to identify and characterize oligosaccharides, many family members can be rapidly identified. Finally, this class of natural products provides new insights into the biology of their targets by providing large molecule probes. Despite non-optimized pharmacological properties of native secondary metabolites, the gene clusters of oligosaccharides appear to be highly mutable allowing the generation of many analogs for structure-activity relationship studies.

Acknowledgements

This chapter was written by Emilianne K. McCranie and Brian O. Bachmann and was first published in *Natural Product Reports*.[111] Reproduced from reference 111 with permission from the Royal Society of Chemistry.

References

1. Thibodeaux, C.J., C. Melancon III, C.E, & Liu, H.W. Natural-product sugar biosynthesis and enzymatic glycodiversification. *Angew Chem Int Ed Engl.* **47**, 9814-9859 (2008).
2. Kren V. and Martinkova L. Glycosides in medicine: the role of glycosidic residue in biological activity. *Curr Med Chem* **8**, 1303-1328 (2001).
3. Thibodeaux, C.J., Melancon, C.E., and Liu, H.W. Unusual sugar biosynthesis and natural product glycodiversification. *Nature* **446**, 1008-1016 (2007).
4. Weymouth-Wilson, A.C. The role of carbohydrates in biologically active natural products. *Nat Prod Rep* **14**, 99-110 (1997).
5. Singh S., Phillips, G.N., Jr., and Thorson, J.S. The structural biology of enzymes involved in natural product glycosylation. *Nat Prod Rep* **29**, 1201-1237 (2012).
6. Rudd, P.M., Elliott, T., Cresswell, P., Wilson, I.A., and Dwek, R.A. Glycosylation and the immune system. *Science* **291**, 2370-2376 (2001).
7. Moremen, K.W., Tiemeyer, M., and Nairn, A.V. Vertebrate protein glycosylation: diversity, synthesis and function. *Nat Rev Mol Cell Biol **13***, 448-462 (2012).
8. Seeberger, P.H. and Werz, D.B. Synthesis and medical applications of oligosaccharides. *Nature* **446**, 1046-1051 (2007).
9. Varki, A. Biological roles of oligosaccharides: all of the theories are correct. *Glycobiology*, **3**, 97-130 (1997).
10. Wright, D.E. The orthosomycins, a new family of antibiotics. *Tetrahedron* **35**, 1207-1237 (1979).
11. Mann, R.L. and Bromer, W.W. The isolation of a second antibiotic from *Streptomyces hygroscopicus. J Am Chem Soc* **80**, 2714-2716 (1958).
12. Kudo, F. and Eguchi, T. *J.* Biosynthetic genes for aminoglycoside antibiotics. *J Antibiot* **62**, 471-481 (2009).
13. Weinstein, M. J., Luedemann, G. M., Oden, E. M. & Wagman, G. H. Everninomicin, a New Antibiotic Complex from *Micromonospora Carbonacea*. *Antimicrob Agents Chemother* **10**, 24-32 (1964).

14. Ganguly, A. K., Sarre, O. Z., Greeves, D. & Morton, J. Structure of Everninomicin D. *J Am Chem Soc* **97**, 1982-1985 (1975).
15. Chu, M., Mierzwa, R., Jenking, J., Chan, T., Das P., Pramanik, B.N., Patel, M. & Gullo, V. Isolation and Characterization of Novel Oligosaccharides Related to Ziracin. *J Nat Prod* **65**, 1588-1593 (2002).
16. Chen, G., Pramanik, B. N., Bartner, P. L., Saksena, A. K. & Gross, M. L. Multiple-Stage Mass Spectrometric Analysis of Complex Oligosaccharide Antibiotics (Everninomicins) in a Quadrupole Ion Trap. *J Am Soc Mass Spectrom* **13**, 1313-1321 (2002).
17. Herzog, H. L., Meseck, E., Delorenz, S., Murawski, A., Charney, W., & Rosselet, J.P. Chemistry of Antibiotics from Micromonospora. 3. Isolation and Characterization of Everninomicin D and B. *Appl Microbiol* **13**, 515-520 (1965).
18. Ganguly, A. K. & Szmulewicz, S. Letter: Structure of everninomicin C. *J Antibiot* **28**, 710-712 (1975).
19. Nakashio, S., Iwasawa, H., Dun, F. Y., Kanemitsu, K. & Shimada, J. Everninomicin, a new oligosaccharide antibiotic: its antimicrobial activity, post-antibiotic effect and synergistic bactericidal activity. *Drugs Exp Clin Res* **21**, 7-16 (1995).
20. Ganguly, A. K., McCormick, J. L., Saksena, A. K., Das, P. D. & Chan, T. Chemical Modifications and Structure Activity Studies of Ziracin and Related Everninomicin Antibiotics. *Bioorg Med Chem Lett* **9**, 1209-1214 (1999).
21. Ganguly, A. K. & Saksena, A. K. Structure of everninomicin B. *J Antibiot* **28**, 707-709 (1975).
22. Chu, M., Mierzwa, R., Patel, M., Jenkins, J., Das, P., Pramanik, B.N., & Chan, T. A novel everninomicin antibiotic active against multidrug-resistant bacteria. *Tetrahedron Lett* **41**, 6689-6693 (2000).
23. Mertz, J. L., Peloso, J.S., Barker, B.J., Babbitt, G.E., Occolowitz, J.L., Simson, V.L., & Kline, R.M. Isolation and Structural Identification of Nine Avilamycins. *J Antibiot* **34**, 877-887 (1986).
24. Jones, D. J., Mowrey, D. H., Anderson, D. B. & Wellenreiter, R. H. Effect of various levels of avilamycin on the performance of growing-finishing swine. *J Anim Sci* **65**, 881-885 (1987).
25. Shryock, T. R. Will Avilamycin Convert Ziracine into Zerocine. *Emerg Infect Dis* **7**, 488-489 (2001).
26. Foster, D. R. & Rybak, M. J. Pharmacologic and bacteriologic properties of SCH-27899 (Ziracin), an investigational antibiotic from the everninomicin family. *Pharmacotherapy* **19**, 1111-1117 (1999).
27. Souli, M., Thauvin-Eliopoulos, C. & Eliopoulos, G. M. In vivo activities of evernimicin (SCH 27899) against vancomycin-susceptible and vancomycin-resistant enterococci in experimental endocarditis. *Antimicob Agents Chemother* **44**, 2733-2739 (2000).
28. Boucher, H. W., Thauvin-Eliopoulos, C., Loebenberg, D. & Eliopoulos, G. M. In vivo activity of evernimicin (SCH 27899) against methicillin-resistant *Staphylococcus aureus* in experimental infective endocarditis. *Antimicrob Agents Chemother* **45**, 208-211 (2001).

29. McNicholas, P. M., Najarian, D.J., Mann, P.A., Hesk, D., Hare, R.S., Shaw, K.J., & Black, T.A. Evernimicin Binds Exclusively to the 50S Ribosomal Subunit and Inhibits Translation in Cell-Free Systems Derived from both Gram-Positive and Gram-Negative Bacteria. *Antimicrob Agents Chemother* **44**, 1121-1126 (2000).
30. Champney, W. S. T., C. L. Evernimicin (SCH27899) Inhibits both Translation and 50S Ribosomal Subunit Formation in *Staphylococcus aureus* Cells. *Antimicrob Agents Chemother* **44**, 1413-1417 (2000).
31. Adrian, P. V., Zhao, W., Black, T.A., Shaw, K.J., Hare, R.S., & Klugman, K.P. Mutations in ribosomal protein L16 conferring reduced susceptibility to evernimicin (SCH27899): implications for mechanism of action. *Antimicrob Agents Chemother* **44**, 732-738 (2000).
32. Zarazaga, M., Tenorio, C., Del Campo, R., Ruiz-Larrea, F. & Torres, C. Mutations in Ribosomal Protein L16 and in 23S rRNA in *Enterococcus* Strains for Which Evernimicin MICs Differ. *Antimicrob Agents Chemother* **46**, 3657-3659 (2002).
33. McNicholas, P. M., Mann, P.A., Najarian, D.J., Misesel, L., Hare, R.S., & Black, T.A. Effects of mutations in ribosomal protein L16 on susceptibility and accumulation of evernimicin. *Antimicrob Agents Chemother* **45**, 79-83 (2001).
34. Mann, P. A., Xiong, L., Mankin, A.S., Chau, A.S., Mendrick, C.A., Najarian, D.J., Cramer, C.A., Loebenberg, D., Coates, E., Murgolo, N.J., Aarestrup, F.M., Goering, R.V., Black, T.A., Hare, R.S., & McNicholas, P.M. EmtA, a rRNA methyltransferase conferring high-level evernimicin resistance. *Mol Microbiol* **41**, 1349-1356 (2001).
35. Belova, L., Tenson, T., Xiong, L., McNicholas, P. M. & Mankin, A. S. A novel site of antibiotic action in the ribosome: interaction of evernimicin with the large ribosomal subunit. *Proc Nat Acad Sci USA* **98**, 3726-3731 (2001).
36. Treede, I., Jackobsen, L., Kirkpekar, F., Vester, B., Weitnauer, G., Bechthold, A., & Douthwaite, S. The avilamycin resistance determinants AviRa and AviRb methylate 23S rRNA at the guanosine 2535 base and the uridine 2479 ribose. *Mol Microbiol* **49**, 309-318 (2003).
37. Mosbacher, T. G., Bechthold, A. & Schulz, G. E. Crystal structure of the avilamycin resistance-conferring methyltransferase AviRa from Streptomyces viridochromogenes. *J Mol Biol* **329**, 147-157 (2003).
38. Mikolajka, A., Liu, H., Chen, Y., Starosta, A.L., Marquez, V., Ivanova, M., Cooperman, B.S., & Wilson, D.N. Differential effects of thiopeptide and orthosomycin antibiotics on translational GTPases. *Chem Biol* **18**, 589-600 (2011).
39. Ganguly, A. K., McCormick, J. L., Saksena, A. K., Das, P. R. & Chan, T. M. Chemical modifications and structure activity studies of ziracin and related everninomicin antibiotics. *Bioorg Med Chem Lett* **9**, 1209-1214 (1999).
40. Ganguly, A. K. Ziracin, a novel oligosaccharide antibiotic. *J Antibiot* **53**, 1038-1044 (2000).
41. Waitz, J.A. & Horan, A.C. Assignee: Schering Corporation, Kenilworth, NJ. Micromonospora carbonacea var. africana. U.S. Patent Application Number 4,735,903, 1988.

42. Boll, R., Hofmann, C., Heitmann, B., Hauser, G., Glaser, S., Koslowski, T., Friedrich, T., & Bechthold, A. Tche active conformation of avilamycin A is conferred by AviX12, a radical AdoMet enzyme. *J Biol Chem* **281**, 14756-14763 (2006).
43. Weitnauer, G., Hauser, G., Hofmann, C., Linder, U., Boll, R., Pelz, K., Glaser, S.J., & Bechthold, A. Novel avilamycin derivatives with improved polarity generated by targeted gene disruption. *Chem Biol* **11**, 1403-1411 (2004).
44. Gaisser, S., Trefzer, A., Stockert, S., Kirschning, A. & Bechthold, A. Cloning of an avilamycin biosynthetic gene cluster from Streptomyces viridochromogenes Tu57. *J Bacteriol* **179**, 6271-6278 (1997).
45. Weitnauer, G., Muhlenweg, A., Trefzer, A., Hoffmeister, D., Sussmuth, R.D., Jung, G., Welzel, K., Vente, A., Girreser, U., & Bechthold, A. Biosynthesis of the orthosomycin antibiotic avilamycin A: deductions from the molecular analysis of the *avi* biosynthetic gene cluster of *Streptomyces viridochromogenes* Tu57 and production of new antibiotics. *Chem Biol* **8**, 569-581 (2001).
46. Weitnauer, G., Gaisser, S., Kellenberger, L., Leadlay, P. F. & Bechthold, A. Analysis of a C-methyltransferase gene (aviG1) involved in avilamycin biosynthesis in *Streptomyces* viridochromogenes Tu57 and complementation of a S*accharopolyspora erythraea eryBIII* mutant by *aviG1*. *Microbiology* **148**, 373-379 (2002).
47. Hofmann, C., Boll, R., Heitmann, B., Hauser, G., Durr, C., Frerich, A., Weitnauer, G., Glaser, S.J., & Bechthold, A.. Genes encoding enzymes responsible for biosynthesis of L-lyxose and attachment of eurekanate during avilamycin biosynthesis. *Chem Biol* **12**, 1137-1143 (2005).
48. Treede, I., Hause,r G., Muhlenewg, A., Hofmann, C., Schmidt, M., Weitnauer, G., Glaser, S., & Bechthold, A. Genes involved in formation and attachment of a two-carbon chain as a component of eurekanate, a branched-chain sugar moiety of avilamycin A. *App Env Microbiol* **71**, 400-406 (2005).
49. Hosted, T. J., Wang, T. X., Alexander, D. C. & Horan, A. C. Characterization of the biosynthetic gene cluster for the oligosaccharide antibiotic, Evernimicin, in *Micromonospora carbonacea* var. *africana* ATCC39149. *J Ind Microbiol Biotechnol* **27**, 386-392 (2001).
50. Hu, Y., Al-Mestarihi, A., Grimes, C. L., Kahne, D. & Bachmann, B. O. A unifying nitrososynthase involved in nitrosugar biosynthesis. *J Am Chem Soc* **130**, 15756-15757 (2008).
51. Vey, J. L. Al-Mestarihi, A., Hu, Y. Funk, M.A., Bachmann, B.O. & Iverson, T.M. Structure and mechanism of ORF36, an amino sugar oxidizing enzyme in everninomicin biosynthesis. *Biochemistry* **49**, 9306-9317 (2010).
52. Wallhausser, K. H., Nesemann, G., Prave, P. & Steigler, A. Moenomycin, a new antibiotic. I. Fermentation and isolation. *Antimicrob Agents Chemother* **5**, 734-736 (1965).
53. Ostash, B. & Walker, S. Moenomycin family antibiotics: chemical synthesis, biosynthesis, and biological activity. *Nat Prod Rep* **27**, 1594-1617 (2010).

54. Fehlhaber, H. W., Girg, M., Seibert, G., Hobert, K., Welzel, P., Vanheijenoort, Y. & Vanheijenoort, J. Moenomycin-A - a structural revision and new structure-activity relations. *Tetrahedron* **46**, 1557-1568 (1990).
55. Uchida, R., Iwatsuki, M., Kim, Y. P., Omura, S. & Tomoda, H. Nosokomycins, new antibiotics discovered in an in vivo-mimic infection model using silkworm larvae. II: Structure elucidation. *J Antibiot* **63**, 157-163 (2010).
56. Uchida, R., Iwatsuki, M., Kim, Y.P., Ohte, S., Omura, S. & Tomoda, H. Nosokomycins, new antibiotics discovered in an in vivo-mimic infection model using silkworm larvae. I: Fermentation, isolation and biological properties. *J Antibiot* **63**, 151-155 (2010).
57. Arai, M. Nakayama, R., Yoshia, K., Takeuchi, M., Teramoto, S. & Torikata, A. Pholipomycin, a new member of phosphoglycolipid antibiotics. II. Physico-chemical properties and comparison with other members of this family of antibiotics. *J Antibiot* **30**, 1055-1059 (1977).
58. Arai, M., Torikata, A., Enokita, R., Fukatsu, H., Nakayama, R. & Yoshida K. Pholipomycin, a new member of phosphoglycolipid antibiotics. I. Taxonomy of producing organism and fermentation and isolation of pholipomycin. *J Antibiot* **30**, 1049-1054 (1977).
59. Torikata, A., Yoshikawa, H., Katayama, T., Arai, M., Nakahara, M. & Kitano, N. Pholipomycin, a new member of phosphoglycolipid antibiotics. III. Biological properties. *J Antibiot* **30**, 1060-1063 (1977).
60. Takahashi, S., Serita, K., Arai, M., Seto, H., Furihata, K. & Otake, N. Structure of Pholipomycin. *Tetrahedron Lett* **24**, 499-502 (1983).
61. He, H., Shen, B., Korshalla, J., Siegel, M. M. & Carter, G. T. Isolation and structural elucidation of AC326-alpha, a new member of the moenomycin group. *J Antibiot* **53**, 191-195 (2000).
62. Pfaller, M. A. Flavophospholipol use in animals: positive implications for antimicrobial resistance based on its microbiologic properties. *Diag Microbiol Infect Dis* **56**, 115-121 (2006).
63. Eichhorn, P. & Aga, D. S. Characterization of moenomycin antibiotics from medicated chicken feed by ion-trap mass spectrometry with electrospray ionization. *Rap Comm Mass Spectrom* **19** (2005).
64. Zehl, M., Pittenauer, E., Rizzi, A. & Allmaier, G. Characterization of moenomycin antibiotic complex by multistage MALDI-IT/RTOF-MS and ESI-IT-MS. *J Am Soc Mass Spectrom* **17**, 1081-1090 (2006).
65. Butaye, P., Devriese, L. A. & Haesebrouck, F. Antimicrobial growth promoters used in animal feed: effects of less well known antibiotics on gram-positive bacteria. *Clin Microbiol Rev* **16**, 175-188 (2003).
66. Butaye, P., Devriese, L. A. & Haesebrouck, F. Differences in antibiotic resistance patterns of *Enterococcus faecalis* and *Enterococcus faecium* strains isolated from farm and pet animals. *Antimicrob Agents Chemother* **45**, 1374-1378 (2001).

67. Goldman, R. C., Baizman, E. R., Branstrom, A. A. & Longley, C. B. Differential antibacterial activity of moenomycin analogues on gram-positive bacteria. *Bioorg Med Chem Lett* **10**, 2251-2254 (2000).
68. Adachi, M., Zhang, Y., Leimkuhler, C., Sun, B., LaTour, J.V. & Kahne, D.E. Degradation and reconstruction of moenomycin A and derivatives: dissecting the function of the isoprenoid chain. *J Am Chem Soc* **128**, 14012-14013 (2006).
69. Goldman, R. C. & Gange, D. Inhibition of transglycosylation involved in bacterial peptidoglycan synthesis. *Curr Med Chem* **7**, 801-820 (2000).
70. Huber, G. & Nesemann, G. Moenomycin, an inhibitor of cell wall synthesis. *Biochem Biophys Res Comm* **30**, 7-13 (1968).
71. Baizman, E. R., Branstrom, A.A., Longley, C.B., Allanson, N., Sofia, M.J., Gange, D. & Goldman, R.C. Antibacterial activity of synthetic analogues based on the disaccharide structure of moenomycin, an inhibitor of bacterial transglycosylase. *Microbiology* **146**, *12*, 3129-3140 (2000).
72. Chen, L., Walker, D., Sun, B., Hu, Y., Walker, S. & Kahne, D. Vancomycin analogues active against vanA-resistant strains inhibit bacterial transglycosylase without binding substrate. *Proc Nat Acad Sci USA* **100**, 5658-5663 (2003).
73. Lovering, A. L., de Castro, L. H., Lim, D. & Strynadka, N. C. Structural insight into the transglycosylation step of bacterial cell-wall biosynthesis. *Science* **315**, 1402-1405 (2007).
74. Heaslet, H., Shaw, B., Mistry, A. & Miller, A. A. Characterization of the active site of S. aureus monofunctional glycosyltransferase (Mtg) by site-directed mutation and structural analysis of the protein complexed with moenomycin. *J Struct Biol* **167**, 129-135 (2009).
75. Huang, C. Y., Shih, H.Wj, Lin, L.Y. Tien, Y.W., Cheng, T.J., Cheng W.C., Wong, C.H. & Ma, C. Crystal structure of Staphylococcus aureus transglycosylase in complex with a lipid II analog and elucidation of peptidoglycan synthesis mechanism. *Proc Nat Acad Sci USA* **109**, 6496-6501 (2012).
76. Gampe, C. M., Tsukamoto, H., Wang, T. S., Walker, S. & Kahne, D. Modular synthesis of diphospholipid oligosaccharide fragments of the bacterial cell wall and their use to study the mechanism of moenomycin and other antibiotics. *Tetrahedron* **67**, 9771-9778 (2011).
77. Yuan, Y., Fuse, S. Ostash, B., Sliz, P., Kahne, D. Walker, S. Structural analysis of the contacts anchoring moenomycin to peptidoglycan glycosyltransferases and implications for antibiotic design. *ACS Chem Biol* **3**, 429-436 (2008).
78. Fuse, S., Tsukamoto, H., Yuan, Y., Wang, T.S., Zhang, Y., Bolla, M., Walker, S., Sliz, P. & Kahne, D. Functional and structural analysis of a key region of the cell wall inhibitor moenomycin. *ACS Chem Biol* **5**, 701-711 (2010).
79. Ostash, B., Doud, E.H., Lin, C. Ostash, I., Perlstein, D.L., Fuse, S., Wolpert, M., Kahne, D. & Walker, S. Complete characterization of the seventeen step moenomycin biosynthetic pathway. *Biochemistry* **48**, 8830-8841 (2009).

80. Cheng, T. J., Sung, M.T., Liao, H.Y., Chang, Y.F., Chen, C.W., Huang, C.Y., Chou, L.Y., Wu, Y.D., Chen, Y.H., Cheng, Y.S., Wong, C.H., Ma, C. & Cheng, W.C. Domain requirement of moenomycin binding to bifunctional transglycosylases and development of high-throughput discovery of antibiotics. *Proc Nat Acad Sci USA* **105**, 431-436 (2008).
81. Eggert, U. S., Ruiz, N., Falcone, B.V., Branstrom, A.A., Goldman, R.C., Silhavy, T.J. & Kahne D. Genetic basis for activity differences between vancomycin and glycolipid derivatives of vancomycin. *Science* **294**, 361-364 (2001).
82. Rebets, Y., Boll, R., Horbal, L., Fedorenko, V. & Bechthold, A. Production of avilamycin A is regulated by AviC1 and AviC2, two transcriptional activators. *J Antiobiot* **62**, 461-464 (2009).
83. Gampe, C. M., Tsukamoto, H., Doud, E. H., Walker, S. & Kahne, D. Tuning the Moenomycin Pharmacophore To Enable Discovery of Bacterial Cell Wall Synthesis Inhibitors. *J Am Chem Soc* **135**, 3776-3779 (2013).
84. Cheng, T. J. Wu, Y.T. Yang, S.T., Lo, K.H., Chen, S.K., Chen, Y.H., Huang, W.I., Yuan, C.H., Guo, C.W., Huang, L.Y., Chen, K.T., Shih, H.W., Cheng, Y.S., Cheng, W.C. & Wong, C.H. High-throughput identification of antibacterials against methicillin-resistant Staphylococcus aureus (MRSA) and the transglycosylase. *Bioorg Med Chem* **18**, 8512-8529 (2010).
85. Taylor, J. G., Li, X., Oberthur, M., Zhu, W. & Kahne, D. E. The total synthesis of moenomycin A. *J Am Chem Soc* **128**, 15084-15085 (2006).
86. Ostash, B., Saghatelian, A. & Walker, S. A streamlined metabolic pathway for the biosynthesis of moenomycin A. *Chem Biol* **14**, 257-267 (2007).
87. Ren, F., Ko, T.P., Feng, X., Huang, C.H., Chan, H.C., Hug, Y., Wang, K., Ma, Y., Liang, P.H., Wang, A.H., Oldfield, E. & Guo, R.T. Insights into the Mechanism of the Antibiotic-Synthesizing Enzyme MoeO5 from Crystal Structures of Different Complexes. *Ang Chem Int Ed Engl* **51**, *17*, 4157-4160 (2012).
88. Koyama, N., Tokura, Y., Takahashi, Y. & Tomoda, H. Discovery of nosokophic acid, a predicted intermediate of moenomycins, from nosokomycin-producing *Streptomyces* sp. K04-0144. *Bioorg Med Chem Lett* **23**, 860-863 (2013).
89. Makitrynskyy, R., Rebets, Y., Ostash, B., Zaburannyi, N., Rabyk, M., Walker, S. & Fedorenko, V. Genetic factors that influence moenomycin production in streptomycetes. *J Ind Microbiol Biotechnol* **37**, 559-566 (2010).
90. Rabyk, M., Ostash, B., Rebets, Y., Walker, S. & Fedorenko, V. *Streptomyces ghanaensis* pleiotropic regulatory gene wblA(gh) influences morphogenesis and moenomycin production. *Biotechnol Lett* **33**, 2481-2486 (2011).
91. Ostash, B., Doud, E. & Walker, S. ABC transporter genes from *Streptomyces ghanaensis* moenomycin biosynthetic gene cluster: roles in antibiotic production and export. *Arch Microbiol* **194**, 915-922 (2012).

92. Kong, F., Zhao, N., Siegel, M.M., Janota, K., Ashcroft, J.S., Koehn, F.E., Borders, D.B. & Carter, G.T. Saccharomicins, Novel Heptadecaglycoside Antibiotics Effective against Multidrug-Resistant Bacteria. *J Am Chem Soc* **120**, 13301-13311 (1998).
93. Singh, M. P., Petersen, P. J., Weiss, W. J., Kong, F. & Greenstein, M. Saccharomicins, novel heptadecaglycoside antibiotics produced by *Saccharothrix espanaensis*: antibacterial and mechanistic activities. *Antimicrob Agents Chemother* **44**, 2154-2159 (2000).
94. Pletcher, J. M. & McDonald, F. E. Synthesis of the saccharomicin fucose-aglycon conjugate and determination of absolute configuration. *Org Lett* **7**, 4749-4752 (2005).
95. Balthaser, B. R. & McDonald, F. E. Bronsted acid-promoted glycosylations of disaccharide glycal substructures of the saccharomicins. *Org Lett* **11**, 4850-4853 (2009).
96. Strobel, T. Al-Dilaimi, A. Blom, J., Gessner, A., Kalinowski, J., Luzhetska, M., Puhler, A., Szczepanowski, R., Bechthold, A. & Ruckert, C. Complete genome sequence of *Saccharothrix espanaensis* DSM 44229T and comparison to the other completely sequenced *Pseudonocardiaceae*. *BMC Genomics* **13**, 465 (2012).
97. Berner, M., Krug, D., Bihlmaier, C., Vente, A., Muller, R. & Bechthold, A. Genes and enzymes involved in caffeic acid biosynthesis in the actinomycete Saccharothrix espanaensis. *J Bacteriol* **188**, 2666-2673 (2006).
98. Geng, P., Bai, G., Shi, Q., Zhang, L., Gao, Z. & Zhang, Q. Taxonomy of the Streptomyces strain ZG0656 that produces acarviostatin alpha-amylase inhibitors and analysis of their effects on blood glucose levels in mammalian systems. *J Appl Microbiol* **106**, 525-533 (2009).
99. Geng, P. & Bai, G. Two novel aminooligosaccharides isolated from the culture of Streptomyces coelicoflavus ZG0656 as potent inhibitors of alpha-amylase. *Carbohyd Res* **343**, 470-476 (2008).
100. Geng, P., Qiu, F., Zhu, Y. & Bai, G. Four acarviosin-containing oligosaccharides identified from Streptomyces coelicoflavus ZG0656 are potent inhibitors of alpha-amylase. *Carbohyd Res* **343**, 882-892 (2008).
101. Geng, P., Meng, X., Bai, G. & Luo, G. Profiling of acarviostatin family secondary metabolites secreted by Streptomyces coelicoflavus ZG0656 using ultraperformance liquid chromatography coupled with electrospray ionization mass spectrometry. *Anal Chem* **80**, 7554-7561 (2008).
102. Mahmud, T. The C7N aminocyclitol family of natural products. *Nat Prod Rep* **20**, 137-166 (2003).
103. Qin, X., Ren, L., Yang, X., Bai, F., Wang, L., Geng, P., Bai, G. & Shen, Y. Structures of human pancreatic alpha-amylase in complex with acarviostatins: Implications for drug design against type II diabetes. *J Struct Biol* **174**, 196-202 (2011).
104. Wehmeier, U. F. & Piepersberg, W. Biotechnology and molecular biology of the alpha-glucosidase inhibitor acarbose. *Appl Microbiol Biotechnol* **63**, 613-625 (2004).

105. Flatt, P. M. & Mahmud, T. Biosynthesis of aminocyclitol-aminoglycoside antibiotics and related compounds. *Nat Prod Rep* **24**, 358-392 (2007).
106. Mahmud, T., Flatt, P. M. & Wu, X. Biosynthesis of unusual aminocyclitol-containing natural products. *J Nat Prod* **70**, 1384-1391 (2007).
107. Rockser, Y. & Wehmeier, U. F. The gac-gene cluster for the production of acarbose from Streptomyces glaucescens GLA.O: identification, isolation and characterization. *J Biotehchnol* **140**, 114-123 (2009).
108. Degwert, U., van Hulst, R., Pape, H., Herrold, R.E., Bale, J.M., Keller, P.J., Lee, J.P. & Floss, H.G. Studies on the biosynthesis of the alpha-glucosidase inhibitor acarbose: valienamine, a m-C7N unit not derived from the shikimate pathway. *J Antibiot* **40**, 855-861 (1987).
109. Guo, X., Geng, P., Bai, F., Bai, G., Sun, T., Li, X., Shi, L. & Zhong, Q. Draft genome sequence of Streptomyces coelicoflavus ZG0656 reveals the putative biosynthetic gene cluster of acarviostatin family alpha-amylase inhibitors. *Lett Appl Microbiol* **55**, 162-169 (2012).
110. Hemker, M., Stratmenn, A. Goeke, K., Schroder, W., Lenz, J., Piepersberg, W. & Pape, H. Identification, cloning, expression, and characterization of the extracellular acarbose-modifying glycosyltransferase, AcbD, from Actinoplanes sp. strain SE50. *J Bacteriol* **183**, 4484-4492 (2001).
111. McCranie, E. K. & Bachmann, B. O. Bioactive oligosaccharide natural products. *Nat Prod Rep* **31**, 1026-1042 (2014).

Dissertation statement

Orthosomycins are highly decorated oligosaccharides with potent activity against a variety of Gram-positive bacteria including methicillin-resistant staphylococci and vancomycin-resistant enterococci. One member of this family, everninomicin A (Ziracin™), advanced to phase III clinical trials before being discontinued due to undisclosed pharmacological complications. Despite their clinical importance, little is known about the biosynthesis of the orthosomycins or the structural features that contribute to their activity. The research in this dissertation focuses on a deeper understanding of orthosomycin biosynthesis towards the translational goal of developing an everninomicin with improved pharmacology and potent activity against dangerous human pathogens.

Prior to this work, the everninomicins produced by *Micromonospora carbonacea* var *aurantiaca* were unknown. We drastically increased production levels by altering production parameters, and this allowed us to identify the everninomicin congeners that are produced by *M. carbonacea* var *aurantiaca*. Additionally, we identified unusual everninomicin-rosaramicin conjugates that retained potency against *Staphylococcus aureus.* To investigate the biosynthesis of everninomicins, we developed methods for the genetic manipulation of *M. carbonacea* and for facile analysis of everninomicin analogs. These methods as well as characterization of everninomicins produced by this strain are presented in Chapter II.

Chapter III describes the first functional analysis of the everninomicin gene cluster from *M. carbonacea* var *aurantiaca.* We used translated sequence similarities to propose functions for each open reading frame in three orthosomycin gene clusters. Using the methods described in

Chapter II, we constructed three targeted gene replacements which resulted in loss of wild type everninomicin production and provided the first experimental confirmation of the everninomicin gene cluster in *M. carbonacea* var *aurantiaca.* We identified four everninomicin analogs from the targeted gene replacements, three of which had not been reported previously. Notably, everninomicin H, one of the new analogs generated from the replacement of the C-3 methyltransferase *evdM3,* retained activity against *S. aureus*. Unfortunately, the other analogs were not produced in sufficient quantities for biological testing. In addition to generating new everninomicin analogs, the gene replacements provided important information about the mutability of the everninomicin gene cluster and timing of everninomicin biosynthesis.

Chapter IV describes the identification of a family of non-heme iron, α-ketoglutarate dependent oxygenases responsible for formation of the unique oxidative features of the orthosomycins. We constructed targeted gene replacements of two of these oxygenases from the everninomicin gene cluster of *M. carbonacea* var *aurantiaca* which resulted in abolished everninomicin production and confirmed the role of these oxygenases in orthosomycin biosynthesis. Structural characterization of four of these oxygenases revealed a conserved fold common to α-ketoglutarate dependent oxygenases. Furthermore, we determined a crystal structure of hygromycin B bound to HygX, the oxygenase from the hygromycin B pathway of *Streptomyces hygroscopicus*. Inspection of this structure revealed that hygromycin B bound in a chemically productive orientation for orthoester linkage formation. While no suitable substrates were available for analysis, the fact that HygX was able to bind the fully elaborated hygromycin B in a chemically productive orientation strongly suggests that orthoester formation takes place

at the end of hygromycin B biosynthesis and that the substrate is the fully elaborated trisaccharide.

Together these results provide significant contributions to the understanding of orthosomycin biosynthesis. The methods developed and the knowledge acquired lay the groundwork for further explorations of orthosomycin biosynthesis in particular and oligosaccharide biosynthesis in general. The ability to generate new everninomicin analogs via biosynthetic manipulations will prove critical in understanding their structure-activity relationship and developing an everninomicin with an improved pharmacological profile and potent activity against dangerous bacterial infections.

CHAPTER II

METHODS FOR GENETIC MANIPULATION OF *MICROMONOSPORA CARBONACEA* VAR *AURANTIACA* AND FOR ANALYSIS OF EVERNINOMICINS

Introduction

The increasing prevalence of drug-resistant bacteria in the clinic has necessitated the need for new antibacterial agents. According to the 2013 report by the Centers for Disease Control and Prevention, antibiotic resistance infections resulted in more than 2,049,442 illnesses and 23,000 deaths. Methicillin-resistant *Staphylococcus aureus* (MRSA) and vancomycin-resistant enterococci (VRE) alone are responsible for approximately 100,000 infections and about half of the deaths each year.[1] With these dangerous infections raging in the clinic, there is a desperate need for new antibiotics. While modification of existing scaffolds is the simplest method for generating new antimicrobials, new scaffolds with novel targets are needed. Most current classes of antibiotics were discovered during the "golden era" of antibiotic research from the 1930s to the 1970s. However, from the early 1970s to 1999, only one new class of antibiotic was launched.[2] Although the situation has improved somewhat with the approval of five new classes of antibiotics since 2000, the statistics presented above show that there is still a desperate need for new classes of antibiotics with novel modes of actions that will not exhibit cross-resistance with those currently on the market.[2]

Re-examination of discarded compounds is one way to identify novel scaffolds with clinical potential. An excellent example of this is daptomycin, a lipopetide first identified by Eli

Lilly and Company in the 1980s. Due to its toxicity at high doses, research on the drug was halted. In 2003, daptomycin was reformulated and introduced by Cubist as a treatment for *S. aureus* infections.[3] Daptomycin is not the only example of an old compound to be renewed after reformulation and derivatization, three of the four other new classes of antibiotics introduced since 2000 – mutilins, oxazolidinones, and tiacumicins – were discovered more than two decades before their clinical introduction.[4] These precedents provide excellent motivation for looking for new antibiotics in the scientific archives.

We consider the everninomicins to be members of this group of under-explored antibiotics with great clinical potential. The everninomicins are a group of oligosaccharide natural products produced by *Micromonospora carbonacea* that display activity against a variety of Gram-positive organisms including MRSA and VRE.[5-9] A hallmark of the everninomicins is the presence of orthoester linkages between sugar residues. The everninomicins also contain a unique nitro sugar (evernitrose) and a methylenedioxy bridge. Prior to this work, fourteen everninomicin have been reported and are detailed in chapter I (Figure 1-2). These everninomicins differ in the decoration of sugar residues, presence of orsellinic acid, and oxidation state of evernitrose. The Schering-Plough Corporation studied the naturally-occurring everninomicins culminating with everninomicin A (Ziracin®) advancing to phase III clinical trials before being dismissed due to undisclosed pharmacological complications.[10-21]

The everninomicins act as bacterial translation inhibitors by targeting the ribosome although their target is distinct from other antibiotics currently in clinical use and no cross-resistance is observed. The everninomicins bind to a unique site on the 50S ribosomal subunit and prevent the formation of the 70S initiation complex in an IF2 dependent manner thereby

inhibiting bacterial translation. Everninomicins are also potent inhibitors of back-translocation by inhibiting the GTPase activity of EF-4.[22,23] Due to their activity against a variety of drug-resistant Gram-positive bacteria as well as their novel bacterial targets, the everninomicins have the potential to become clinically useful drugs.

To fully explore the potential of this class, we must be able to create analogs for structure-activity relationship studies. While total synthesis of everninomicin A has been accomplished, it required 134 steps rendering it impractical for generation of analogs.[24-26] Instead, we propose to use biosynthetic engineering to make new analogs and study its structure-activity relationship. In order to harness the biosynthetic machinery for generation of new analogs, we must first understand the way in which *M. carbonacea* manufactures everninomicins.

Micromonospora species are soil actinomycetes which were first established as a genus in 1923.[27] The first antibiotic activity from the *Micromonospora* genus was reported in 1942 with the first bioactive metabolite, micromonosporin, from this genus reported in 1947.[28,29] By 1963, several antibiotics including actinomycin, the microcins, and gentamicin had been discovered from *Micromonospora* species. After the discovery of the clinically relevant antibiotic gentamicin, increased interest in *Micromonospora* species revealed the prolific antibiotic-producing capability of this genus which had previously been overlooked.[27]

With the new interest in the *Micromonospora* genus, several new antibiotics were identified including the everninomicins from *M. carbonacea* var *africana* in 1964.[30] Of note, prior to this study, the everninomicins produced by *M. carbonacea* var *aurantiaca* had not been reported. Initial efforts to characterize the everninomicins produced by *M. carbonacea* var *aurantiaca* were impeded by low production levels. Modification of the patent-reported media

composition and culture conditions resulted in dramatic improvements in everninomicin titers and allowed for the detection of everninomicins produced by this variant. To identify the individual everninomicins of the complex, mass spectrometric fragmentation was employed. Oligosaccharides are particularly well suited to analysis by fragmentation as they can be sequenced by sequential loss of sugar residues. Both MS^2 and MS^n approaches can be applied to evaluate the composition of everninomicin congeners. Previously, the Schering group used MS^n analysis to analyze the structure of everninomicins produced by *M. carbonacea* var *africana*.[31,32] Likewise, fragmentation of avilamycins allowed for facile structure elucidation.[33] We employed MS^2 methods for determining the structures of the everninomicins produced by *M. carbonacea* var *aurantiaca*.

Despite the interest in everninomicins, a robust procedure for the genetic manipulation of *M. carbonacea* var *aurantiaca* was not available. Early work on understanding the biosynthesis of the everninomicins focused on insertional mutagenesis. The role of only a few genes was explored this way with all mutants having abolished production of everninomicin and no reported accumulation of analogs.[34] Later, the Schering group reported the development of an integrative vector although no biosynthetic endeavors were reported using it.[35] Although reports stated that *M. carbonacea* was transformed by intergeneric conjugation, the method is not described. As this project relied heavily on the genetic manipulation of *M. carboanca* var *aurantiaca*, a robust method for the genetic manipulation had to be developed.

As the classical protoplast conjugation methods for Streptomyces developed by Bierman and Mazodier did not produce *M. carbonacea* transformants, a modified protocol was developed.[36,37] For the conjugal transfer of DNA into actinomycetes, *Escherichia coli* is commonly

used as the donor bacterium. As many actinomycetes are methyl-restricting, DNA is passaged through a non-methylating strain, *E. coli* 12567, prior to transfer. Vectors containing *oriT* can then be mobilized into *M. carbonacea* var *aurantiaca* by *E. coli* 12567 containing the non-transmissible plasmid pUZ8002. We employed *E. coli* 12567/pUZ8002 as the donor strain but modified other parameters of the Bierman protocol including temperature, mode of selection, and preparation of recipient *M. carbonacea* strains.[36] Additionally, as no suitable vector was available for genetic complementation of gene replacements, we designed and implemented a new vector system for the successful transformation of *M. carbonacea.*

In this study, we have described the structures of the four major everninomicins produced by *M. carbonacea* var *aurantiaca*. Surprisingly, we also isolated two compounds that are conjugates of everninomicin and rosaramicin, another metabolite produced by *M. carbonacea*. Additionally, we developed a robust method for the genetic manipulation of *M. carbonacea* including a new vector system. The development of these tools will allow for investigation of the biosynthesis of the everninomicins and for the generation of new analogs with improved antibacterial activity and efficacy.

Methods

Bacterial culture conditions

E. coli strains were grown in LB broth. *M. carbonacea* var *aurantiaca* NRRL 2997 and replacement mutants were grown on TSB (Oxoid™ Tryptone Soy Broth) agar and in TSB liquid. Intergeneric conjugations were performed on solid AS1 media (0.1 % yeast extract, 0.5 % soluble starch, 0.02 % L-alanine, 0.02 % L-arginine, 0.05 % L-asparagine, 0.25 % NaCl, 1 % Na_2SO_4, 2 %

agarose at pH 7.5, supplemented with 10 mM $MgCl_2$). Apramycin (50 μg/ml), nalidixic acid (12.5 μg/ml), chloramphenicol (30 μg/ml), and kanamycin (50 μg/ml) were used as required for selection as described below.

Production of everninomicins from M. carbonacea var aurantiaca

Seed cultures were generated by inoculating a loop of mycelia from TSB agar into 100 mL of 2997 Germination Medium (0.3 % beef extract, 0.5 % tryptose, 0.1 % dextrose, 2.4 % soluble starch, 0.5 % yeast extract, and 0.1 % calcium carbonate) for 5 days at 30°C in a 500 mL Erlenmeyer flask with shaking. For everninomicin production, 25 mL of the seed culture was added to 500 mL Production Medium (0.5 % yeast extract, 0.1 % corn steep solids, 0.1 % calcium carbonate, 3 % glucose) in a 2 L baffled Fernbach flask and grown with shaking at 30 °C for 10 days. Diaion HP-20 resin (100 mL, previously pre-equilibrated with methanol and washed with water) was added to the fermentation cultures and incubated for 60 minutes with shaking. The combined resin and mycelia were collected by centrifugation at 3000 x g, extracted successively with 250 mL methanol and 250 mL acetone, and evaporated to dryness by rotary evaporation. The resulting crude extract was resuspended in 300 mL solvent grade methanol and filtered through a fritted glass funnel containing silica gel (9 x 2 cm) via vacuum filtration and concentrated to dryness. Extracts were resuspended at a final concentration of 200 mg/mL in HPLC grade methanol prior to analysis by LC/MS.

Isolation of everninomicin-rosaramicin conjugates

The first dimension of separation for crude extracts was size-exclusion chromatography using a Sephadex LH20 column in methanol. Fractions were analyzed by LC/MS, and the fractions

containing the everninomicins were combined and separated on a RP-HPLC using a linear gradient. Mobile phases were: (A) 99% water/1% acetonitrile with 10 mM ammonium acetate, pH = 8 and (B) 5 % water/95 % acetonitrile with 10 mM ammonium acetate, pH = 8.

Degradation of everninomicin-rosaramicin conjugate

Purified, full-length everninomicin-rosaramicin conjugate (concentration of 0.2 mg/mL in 90 % water/10 % DMSO) was incubated at 30 °C with shaking for 48 hours. Aliquots were taken at designated time points and subjected to LC/MS analysis.

Mass spectral analysis of everninomicins

Extracts were analyzed in both negative and positive ion modes using a TSQ Quantum Access Max triple stage quadrupole mass spectrometer (Thermo Scientific, Waltham, MA) equipped with a HESI electrospray ionization source. Injections of 20µl were separated on an Accucore C18 column (particle size: 2.6 µm, 150 x 4.6 mm, Thermo Scientific, Waltham, MA) or a Luna C18(2) column (particle size: 5 µm, 250 x 4.6 mm, Phenomenex, Torrance, CA) using a Finnigan Surveyor LC Pump Plus (Thermo Scientific, Waltham, MA). Mobile phases were: (A) 95% water/5% acetonitrile with 10mM ammonium acetate and (B) 5 % water/95 % acetonitrile with 10 mM ammonium acetate. Gradient conditions for the Accucore C18 column were: 0-1 min, 100 % A; 1-20 min, linear gradient to 100 % B; 20-26 min, 100 % B; 26-7 min, linear gradient to 100 % A; 27-30 min, 100 % A. Gradient conditions for the Luna C18 column were: 0-1 min, 100 % A; 1-30 min, linear gradient to 100 % B; 30-45 min, 100 % B; 45-47 min, linear gradient to 100 % A; 47-50 min, 100 % A. The flow rate was maintained at 1ml/min with 15 µl sent to an Accela PDA detector (Thermo Scientific) and 5 µl subjected to mass spectral analysis. Nitrogen was used for

both the auxiliary and sheath gas set to 10 psi and 54 psi respectively. For analysis in positive ion mode: capillary temperature 275 °C; spray voltage 4.5 kV; capillary offset 35V; tube lens voltage 133 V; skimmer offset 5 V. For analysis in negative ion mode: capillary temperature 275 °C; spray voltage 3.0 kV; capillary offset -35 V; tube lens voltage -132 V; skimmer offset 5 V. For fragmentation studies, a collision energy or 20, 30 35, or 40 V were used with a collision energy of 35 V producing the best results.

Bioactivity testing against S. aureus subsp. aureus Rosenbach

The antibacterial activity of purified everninomicins and conjugates was determined by the broth microdilution assay according to NCCLS guidelines using *Staphyloccocus aureus* subsp. *aureus Rosenbach* (ATCC 6538P) as the test organism.[38]

M. carbonacea var aurantiaca conjugation without membrane

M. carbonacea was grown on TSB agar (Oxoid™ Tryptone Soy Broth, 2 % agarose) for 7 days at 30 °C. Conjugal acceptor mycelia were prepared by inoculating a loop of mycelia into 10 mL of TSB medium in a 50 mL Falcon tube and incubating with shaking at 30 °C for 5 days. The culture was then centrifuged at 3000 x g for 10 minutes and the pellet resuspended in 2 mL fresh TSB. 150 µL aliquots were transferred into sterile 1.5 mL Eppendorf tubes and homogenized using a sterile plastic cell homogenizer. Donor *E. coli* ET12567/pUZ8002 cells containing the gene replacement were prepared by inoculating 1 % of a freshly prepared overnight LB culture into 10 mL LB medium in a 50 mL Falcon tube containing apramycin and kanamycin and grown to an OD_{600} of 0.4 at 37 °C with shaking. The culture was centrifuged at 3000 x g for 10 minutes, and the pellet was washed three times with 10 mL fresh LB. After the final wash, the pellet was

resuspended in 150 µL LB. 50 µL of donor E. coli was added to 150 µL of recipient *M. carbonacea*. The bacterial mixture was plated on AS1 agar (0.1 % yeast extract, 0.5 % soluble starch, 0.02 % L-alanine, 0.02 % L-arginine, 0.05 % L-asparagine, 0.25 % NaCl, 1 % Na_2SO_4, 2 % agarose at pH 7.5, supplemented with 10 mM $MgCl_2$). The plates were then incubated at 37 °C for 1-2 hours until thoroughly dried. After 16-20 hours of incubation at 30 °C, apramycin (50 µg/mL) and nalidixic acid (12.5 µg/mL) were spread on the plates. The plates were then incubated at 30 °C for an additional 6-9 days until colonies were clearly visible. Conjugation colonies were then picked using a sterile pipette tip onto a fresh TSB plate containing apramycin (50 µg/mL) and nalidixic acid (12.5 µg/mL). This process was repeated until pure *M. carbonacea* colonies were isolated.

M. carbonacea var aurantiaca conjugation with membrane

Donor and recipient cultures were prepared as above. Prior to plating, a sterile 0.4 µm membrane (EMD Millipore, Item No. HTTP04700) was attached to a sterile plastic washer using Dow Corning® 732 multipurpose sealant (100 % silicon rubber). After drying, each membrane-washer apparatus was placed on an AS1 agar plate. Then the mixture of bacteria was plated on top of the membrane. Each plate was incubated at 37 °C for 1-2 hours until completely dried. After 16 hours of incubation at 30 °C, apramycin (50 µg/mL) was added to the bacteria mixture on top of the washer to select for apramycin-resistant exconjugants. After 7-9 days of incubation at 30 °C, membranes were removed and pure colonies were streaked onto TSB plates containing apramycin.

Results

Improvements in everninomicin production parameters

Initially, production of everninomicins was extremely low rendering analysis of wild-type everninomicins difficult and analysis of metabolites from mutant strains, where production was even lower, impossible. To improve everninomicin titers, production parameters including media components, temperature, and time were modified. Original production parameters, which were extracted from a patent, were media components of 3% lactose, 0.5% yeast extract, 0.1% corn steep solids, and 0.1% calcium carbonate with an incubation temperature of 26 °C and a production time of 4 days.[39] As glucose is the precursor to most of the sugars of everninomicin, we hypothesized adding glucose would increase production levels. Indeed the addition of 2% glucose to the media increased everninomicin production slightly. Moreover, increasing the

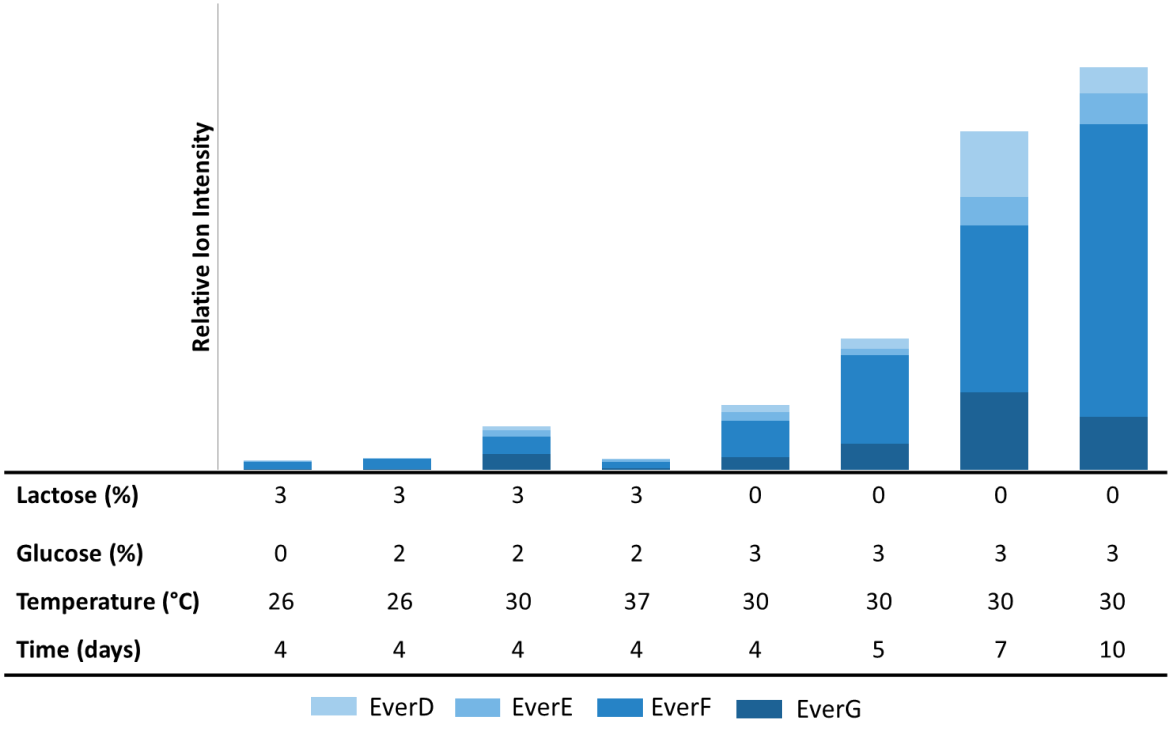

Figure 2-1. Improvements in Everninomicin production. Relative levels of each everninomicin (D-G) produced by each culture are shown in differing shades of blue.

temperature to 30 °C produced even greater everninomicin levels (35% and 133% improvements respectively, Figure 2-1). However, increasing the temperature to 37 °C had a negative impact on production. Adding additional glucose and removing the disaccharide lactose from the media resulted in another substantial (384%) improvement in everninomicin production. The final parameter that was modified was time. The length of time the culture spent in the production phase was directly correlated with everninomicin production levels with a length of 10 days producing the highest titers of everninomicin, an increase of over 3,000% (Figure 2-1).

Identification of everninomicins produced by M. carbonacea var aurantiaca

To characterize the everninomicins produced by *M. carbonacea* var *aurantiaca*, mass spectrometric fragmentation was employed. Using this method, we identified the major everninomicin analogs that were produced by *M. carbonacea* var *aurantiaca*, termed everninomicins D-G (**1-4**) (Figure 2-2). Each of these congeners differ in the oxidation state of the

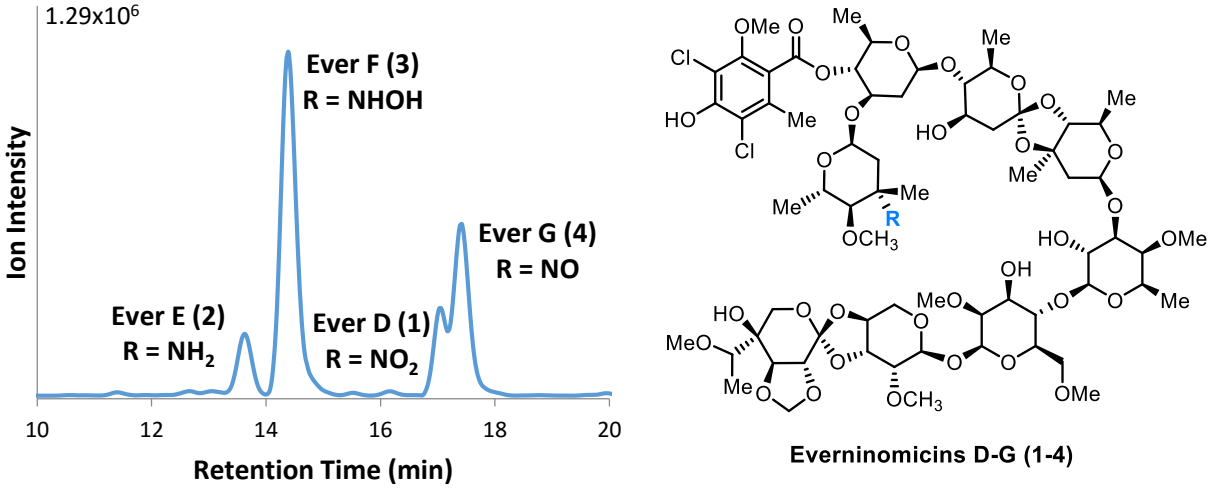

Figure 2-2. Everninomicins produced by *M. carbonacea* var *aurantiaca*. "R" is the oxidation state of the nitrogen which varies among the congeners. A) Extracted ion chromatogram from LC/MS analysis of everninomicins in negative mode: ever D, m/z = 1534.5 $[M-H]^-$; ever D, m/z = 1504.5, $[M-H]^-$; ever F, m/z = 1522.5 $[M-H]^-$; ever G, m/z = 1520.5 $[M-H]^-$. B) Structure of everninomicins D-G. See Figure B-1 for spectra of each everninomicin.

nitrogen providing a ladder of biosynthetic intermediates moving from the amino through the hydroxyl amino and nitroso stages to the fully oxidized nitro. Based on relative ion intensity, the hydroxyl amino oxidation state is the major everninomicin congener produced by *M. carbonacea* var *aurantiaca*.

The lability of the glycosidic linkages was exploited to generate a predictable fragmentation pattern where each transition represents the loss of a sugar residue. Of note, loss of the A ring to give a positively charged ion was used to diagnose the N-oxidation state. Fragmentation of everninomicin F (**3**), revealed that the highly labile orthoester linkage between rings C and D fragments first to give a pentasaccharide fragment (Figure 2-3). The sequential loss of sugar residues E-H then occurred in a predictable fashion. Additionally, fragments were

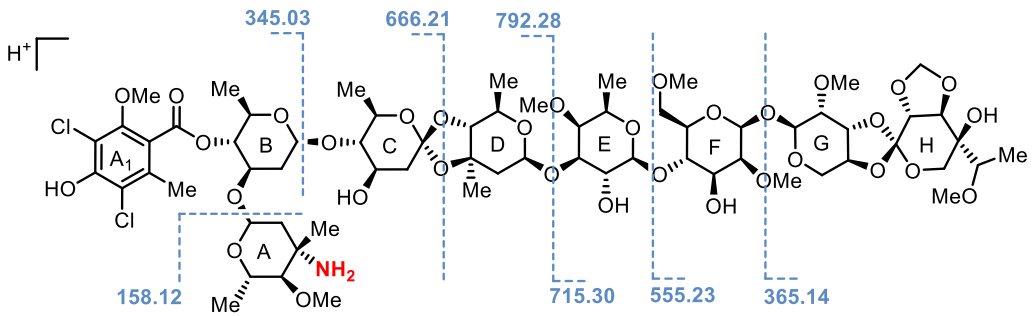

Figure 2-3. Mass spectrometric fragmentation pattern of everninomicins E (m/z = 1506.56691 [M+H$^+$]) and F (m/z = 1522.5 [M+H$^+$]). Dashed lines indicate positions of cleavage during fragmentation experiments. Fragmentation spectra are located in Figures B-2 and B-3.

observed for the A_1-(A)-B-C-D rings with loss of the A_1 and B residues as a unit and sequential loss of other residues. A similar fragmentation pattern was observed for everninomicin E (**2**) (Figure 2-3) although not as many fragments were identified due to lower ionization and/or production levels. This predictable fragmentation pattern allowed for the facile identification of wild type everninomicins and was essential for the characterization of metabolites produced by mutant strains.

Identification of a bifunctional antibiotic

A surprising discovery while evaluating the everninomicins produced by this variant is that everninomicin F reacts with another natural product, rosaramicin (**5**), also produced by *M. carbonacea.* Specifically, the hydroxylamino functionality of everninomicin F reacts with the aldehyde of rosaramicin to produce nitrone that tethers the two metabolites together (Figure 2-4A). Rosaramicin (also known as rosamicin) is a 16-membered macrolide antibiotic which has previously been characterized from *M. rosaria* and has activity against a variety of organisms including *S. aureus*, *Neisseria gonorrhoeae*, and *Chlamydia trachomatis*.[40-45] In addition to the full-length everninomicin-rosaramicin conjugate (**6**), a truncated version is also present in the crude extracts of wild type *M. carbonacea.* Structures of both the truncated and full-length conjugate were solved by NMR (spectra are located in Appendix A: Tables A-1 and A-2 and Figures A-1 – A-11). We have shown that the full-length everninomicin-rosaramicin conjugate degrades under normal culture conditions to an everninomicin-trisaccharide that remains tethered through the nitrone linkage to rosaramicin (**7**) (Figure 2-4B). When these two conjugates were tested against *S. aureus* subsp. *aureus Rosenbach* in a microdilution assay, both everninomicin-

A)

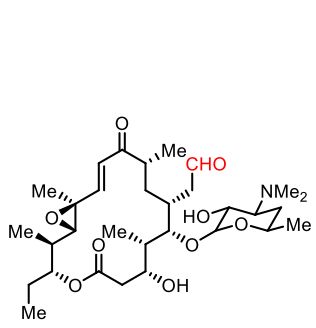

Rosaramicin (5)

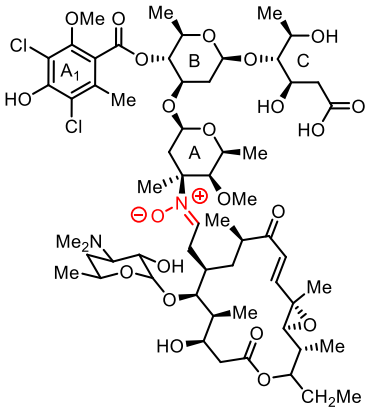

Truncated Everninomicin-Rosaramicin (7)

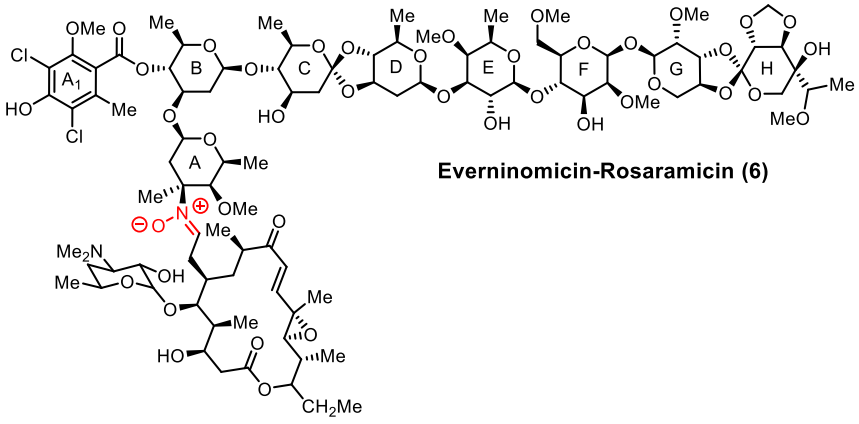

Everninomicin-Rosaramicin (6)

B)

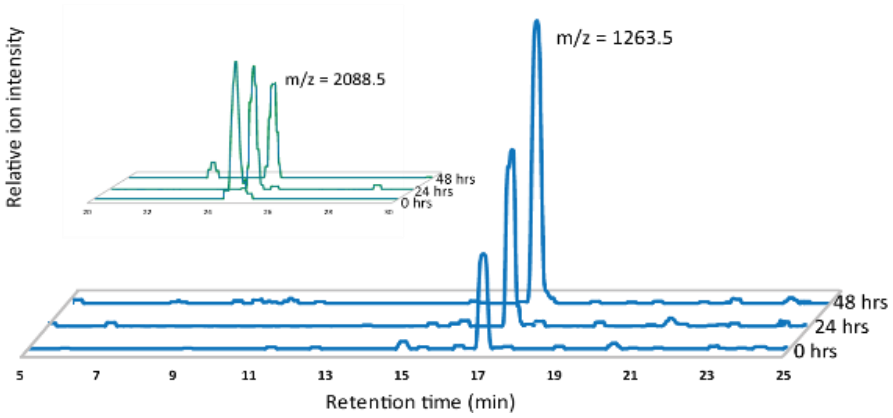

Figure 2-4. A) Structures of rosaramicin and new everninomicin-rosaramicin conjugates. B) Extracted ion chromatogram of the truncated conjugate (m/z = 1263.5 $[M+H]^+$) and full-length conjugate (m/z = 2088.5 $[M+H_2O]^+$) when pure full-length conjugate was incubated in water at 30 °C for 2 days.

-rosaramicin conjugates were found to have an MIC equal to that of everninomicin A (Figure 2-5, 1 µg/mL). The unexpected discovery of this everninomicin-rosaramicin conjugate provides an interesting study of a bifunctional antibiotic composed of members of two distinct classes of molecules.

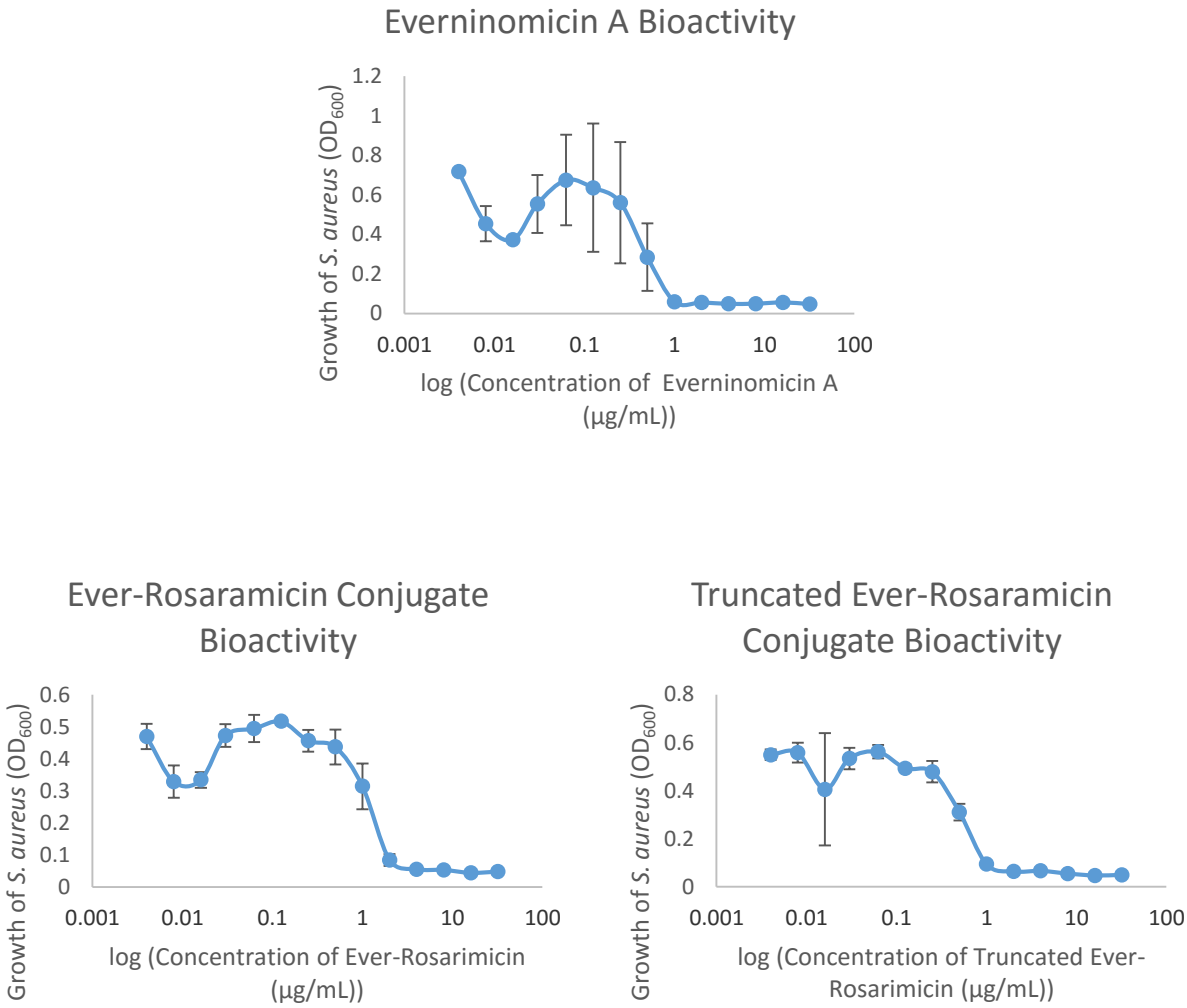

Figure 2-5. The minimal inhibitory concentration of each everninomicin analog was tested against *S. aureus* subsp. a*ureus Rosenbach*. (A) Activity of everninomicin A against *S. aureus* subsp. a*ureus Rosenbach* at various concentrations. (B) Activity of full-length everninomicin-rosaramicin conjugate against *S. aureus* subsp. a*ureus Rosenbach* at various concentrations. (C) Activity of truncated everninomicin-rosaramicin conjugate against *S. aureus* subsp. *aureus Rosenbach* at various concentrations.

Transformation of M. carbonacea var aurantiaca via conjugation

In order to interrogate the biosynthesis of the everninomicins and to create new analogs by alteration of the biosynthetic machinery, a robust procedure for genetic manipulation of *M. carbonacea* was required. Previous reports of transformation of *M. carbonacea* and other *Micromonospora* species relied on intergeneric conjugation although few details were reported. Unfortunately, classical methods for intergeneric conjugation did not produce efficient transformation results.[37,38] Therefore, an alternative method for the transformation of *M. carbonacea* by intergeneric conjugation was developed. Typically, nalidixic acid is used to remove the *E. coli* from the conjugation mixture. However, at concentrations that effectively remove *E. coli*, *M. carbonacea* cannot survive. Different concentrations of nalidixic acid were tested to find the best balance between killing of *E. coli* and survival of *M. carbonacea*. At 50 µg/mL, *M. carbonacea* was not viable. A nalidixic acid concentration of 25 µg/mL, stunted the growth of *E. coli* but also stunted the growth of *M. carbonacea*. Lowering the concentration of nalidixic acid to 12.5 µg/mL still stunted *E. coli* growth but allowed for substantially more *M. carbonacea* growth (Figure 2-6). Subsequent transformations were conducted with 12.5 µg/mL nalidixic acid.

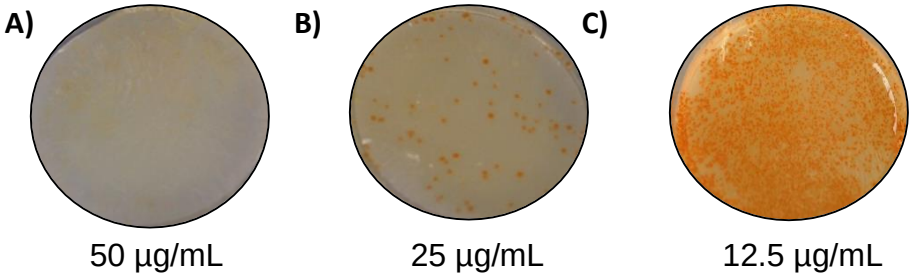

Figure 2-6. Transformation of *M. carbonacea* with pSET152 and selection with different nalidixic acid concentrations: A) 50 µg/mL; B) 25 µg/mL; and C) 12.5 µg/mL. The best *M. carbonacea* growth was seen at 12.5 µg/mL of nalidixic acid.

To further improve conjugation efficiencies, excess *E. coli* were gently washed from the conjugation plates after 16 hours of incubation immediately before application of antibiotics. As conjugation requires physical interaction between the donor and recipient organisms, *M. carbonacea* cultures were mechanically homogenized to create a greater surface area for conjugation between the donor *E. coli* and the recipient *M. carbonacea*. Additionally, since conjugation between bacteria happens most efficiently on solid surfaces rather than in liquid, thoroughly drying the plates at 37 °C after initial plating of the bacteria resulted in higher conjugation efficiencies. Finally, conjugation efficiencies were evaluated at both 30 °C and 37 °C with incubation at 30 °C yielding the greatest number of colonies in contrast to the results reported by Bierman and coworkers.[37]

Although the above modifications to the conjugation procedure yielded sufficient conjugation efficiencies, a nalidixic acid-free method for the removal of *E. coli* was developed allowing easier and faster isolation of pure *M. carbonacea* exconjugants. The conjugation mixture of the donor and recipient bacteria was plated on a 0.4 µm membrane surrounded by a sterile plastic washer on AS1 agar (Figure 2-7A). Prior to plating, the membrane was attached to the washer by silicon glue. The washer contains the bacterial mixture while the membrane allows selective penetration of *M. carbonacea* but not the *E. coli* to the agar beneath. After 9 days the

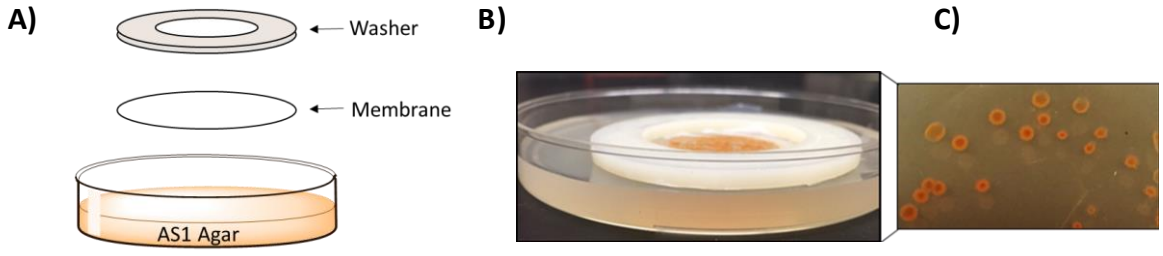

Figure 2-7. A) Diagram of washer/membrane assembly B) The washer/membrane assembly with conjugation mixture plate in the center. C) After 9 days the washer/membrane assembly was removed revealing pure colonies of apramycin-resistant exconjugants.

washer/membrane assembly was removed to reveal pure colonies of apramycin-resistant exconjugants on the agar (Figure 2-7B).

Development of a genetic complementation system

As no suitable genetic complementation plasmid was available, a new vector, pSET152ermE, was created by modifying pSET152, a commonly used integrative vector for use in actinomycetes (Figure 2-8). The modified vector was designed and then ordered from Mutagenex. Requirements for a genetic complementation plasmid included an appropriate resistance marker, a constitutively active promoter for expression of the gene of interest, an origin of transfer site (*oriT)* for conjugation into an actinomycete, and an integrase for stable incorporation into the host chromosome. pSET152 already contained an integrase and *oriT* but lacked the appropriate resistance marker and promoter. pSET152 was first modified by replacing

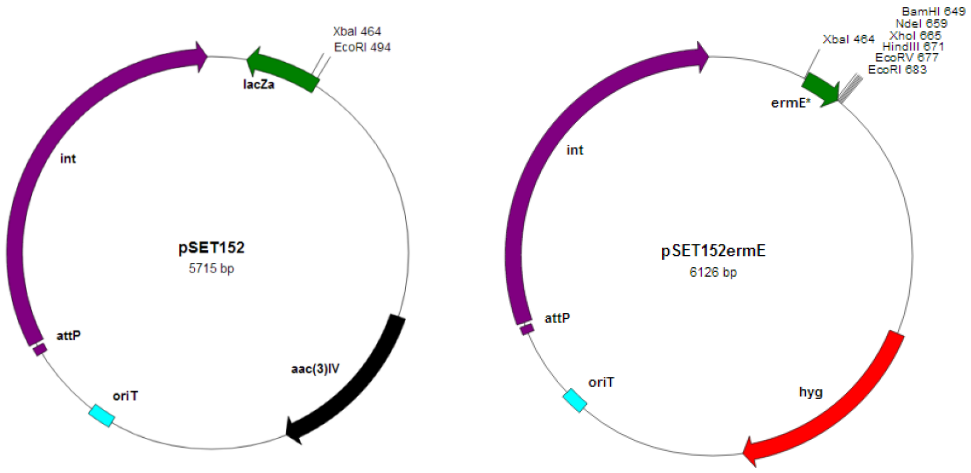

Figure 2-8. Maps of pSET152 and pSET152ermE. *aac(3)IV* is the apramycin resistance marker; *hyg* is the hygromycin resistance marker *hph*; oriT is the origin of transfer; *int* is the phage ϕC31 integrase; attP is the phage ϕC31 attachment site; *ermE** encodes a constitutively active promoter directly upstream of the multiple cloning site.

the apramycin resistance element (*aac(3)IV*) with a hygromycin B phosphotransfersase, *hph*, conferring resistance to hygromycin B. Additionally, *ermE**, which encodes a constitutively active promoter, in combination with a downstream multiple cloning site was cloned into the XbaI and EcoRI sites of pSET152. The newly created pSET152ermE was readily transformed into wild type *M. carbonacea* via conjugation. Successful transformation was confirmed by PCR amplification of the hygromycin resistance gene.

Discussion

Here we present methods for analysis of everninomicins and for genetic manipulation of *M. carbonacea*. Due to low production levels, initial experiments focused on improving everninomicin titers. Methodically varying the previously reported production parameters, resulted in more than a 3,000 % increase in everninomicin levels. This increase was not only necessary for identification of wild type everninomicins but also for characterization of everninomicin analogs and shunt metabolites produced by mutant strains. As the everninomicins produced by *M. carbonacea* had not previously been reported, we provided the first characterization of everninomicins produced by this variant. To easily identify the various everninomicin congeners, we developed a mass spectrometric fragmentation method. Proper tuning of the collision energies resulted in sequential loss of sugar residues providing a predictable pattern. Careful analysis of the fragmentation pattern allows for identification of modified sugars residues and permits faster characterization.

We identified four everninomicins that differ only in the N-oxidation state of the A ring. These data provide interesting insights into the biosynthesis of everninomicin. Previous work in

our lab by Al-Mestarihi and coworkers showed that ORF36, the nitrososynthase from the *africana* variant, catalyzes the oxidation TDP-L-*epi*-vancosamine to the corresponding nitroso sugar.[46] This *in vitro* work demonstrated that the nitrososynthase acts on the monosaccharide. Combined with the data from everninomicins identified in the *aurantiaca* variant, this suggests that the evernitrose glycosyltransferase has substrate flexibility and can accept different N-oxidation states. Knowledge of this promiscuity will prove useful for future biosynthetic engineering efforts.

A serendipitous finding while evaluating the everninomicins produced by *M. carbonacea* var *aurantiaca* was the discovery of two everninomicin-rosaramicin conjugates that have never before been reported. The potent activity the full-length conjugate displays against *S. aureus* makes it an interesting candidate for further studies. Like other macrolides, rosaramicin has been shown to target the large ribosomal subunit.[47,48] Other 16-membered macrolides, such as tylosin, carbomycin A, and spiramycin, inhibit protein synthesis by binding in the peptide exit tunnel.[49] Everninomicin also binds to the large ribosomal subunit although it targets a site approximately 50 Å from the peptidyl transferase center.[23] An intriguing hypothesis is that the potent bioactivity could be attributed to tandem targeting of two separate sites on the ribosome. This tandem targeting could result in a slower emergence of resistance. Future work will focus on understanding the mode of action of this unique conjugate and its spectrum of activity.

Finally, we developed a modified protocol for genetic manipulation of *M. carbonacea* as typical conjugation methods were unsuccessful in producing transformants. Modifications to the preparation of recipient bacterium, method of exconjugant isolation, and incubation temperature resulted in much higher conjugation efficiencies. Development of the membrane-

washer assembly now allows for quick isolation of exconjugants. Previously, low concentrations of nalidixic acid were used to stunt the growth of the donor *E. coli*. Isolation of colonies using these conditions was tedious and required multiple steps to obtain pure *M. carbonacea* colonies with *E. coli* frequently overtaking the slower-growing *M. carbonacea* colonies. The 0.4 µm membrane allows the mycelia of *M. carbonacea* to penetrate beneath to the agar while the larger *E. coli* are trapped on top of membrane. Removal of the membrane after the appropriate incubation time reveals colonies which do not have to be further separated from *E. coli.* The washer-membrane assembly greatly simplifies the isolation procedure and reduces the time it takes to obtain pure exconjugants.

As no suitable vector was available for genetic complementation of gene replacement mutants, we designed a new plasmid which was successfully transformed into *M. carbonacea*. This plasmid, pSET152ermE, will be used primarily for genetic complementation experiments. However, it also provides the necessary tools for heterologous expression of enzymes from other biosynthetic pathways to produce novel everninomicin analogs. Additionally, pSET152ermE is not restricted to use in only *M. carbonacea*. Recent work in our lab has shown that pSET152ermE can be successfully transformed into *Nocardiopsis* FU40, an unrelated soil actinomycete. As a result, other researchers will be able to use this new vector system for genetic complementation and/or heterologous expression in other actinomycetes.

Conclusions

The new methods presented here provide the groundwork for biosynthetic engineering of the everninomicin pathway in *M. carbonacea*. Identification of everninomicins, including the

unexpected everninomicin-rosaramicin conjugates, produced by the *aurantiaca* variant provided a starting point for assessing mutant strains. The mass spectrometric fragmentation method developed proved essential for characterizing metabolites produced by both wild type and mutant strains. Finally, development of a method for the genetic manipulation of *M. carbonacea* was crucial for the generation of gene replacements to investigate the biosynthesis of everninomicin.

Acknowledgements

This work was contributed to by Emilianne K. McCranie, Kasia Derewacz, Jeffrey Spraggins, and Brian O. Bachmann. E.K.M. performed experiments leading to improvements in everninomicin production, identified wild type everninomicins, performed bioactivity assays, and developed conjugation methods. K.D. isolated and solved the structures of the everninomicin-rosaramicin conjugates. J.S. performed FT-ICR mass spectral analysis of everninomicin E. B.O.B supervised all experiments and analysis of data. We thank Kasia Derewacz for discussions that brought about the new membrane method of isolation.

References

1. Antibiotic Resistant Threats in the United States, 2013. (U.S. Department of Health and Human Services: Centers for Disease Control and Prevention, 2014).
2. Butler, M. S., Blaskovich, M. A. & Cooper, M. A. Antibiotics in the clinical pipeline in 2013. *J Antibiot* **66**, 571-591 (2013).
3. Taubes, G. The Bacteria Fight Back. *Science* **321**, 356-361 (2008).
4. Fischbach, M. A. & Walsh, C. T. Antibiotics for emerging pathogens. *Science* **325**, 1089-1093 (2009).

5. Weinstein, M. J., Wagman, G.H., Oden, E.M., Luedemann, G.M., Sloane, P., Murawski, A. & Marquez, J.. Purification and biological studies of everninomicin B. *Antimicrob Agents Chemother* **5**, 821-827 (1965).
6. Ganguly, A. K., McCormick, J. L., Saksena, A. K., Das, P. D. & Chan, T. Chemical Modifications and Structure Activity Studies of Ziracin and Related Everninomicin Antibiotics. *Bioorg Med Chem Lett* **9**, 1209-1214 (1999).
7. Marshall, S. A., Jones, R. N. & Erwin, M. E. Antimicrobial activity of SCH27899 (Ziracin), a novel everninomicin derivative, tested against Streptococcus spp.: disk diffusion/etest method evaluations and quality control guidelines. The Quality Control Study Group. *Diag Microbiol Inf Dis* **33**, 19-25 (1999).
8. Ganguly, A. K. Ziracin, a novel oligosaccharide antibiotic. *J Antiobiot* **53**, 1038-1044 (2000).
9. Souli, M., Thauvin-Eliopoulos, C. & Eliopoulos, G. M. In vivo activities of evernimicin (SCH 27899) against vancomycin-susceptible and vancomycin-resistant enterococci in experimental endocarditis. *Antimicrob Agents Chemother* **44**, 2733-2739 (2000).
10. Sanders, W. E. & Sanders, C. C. Microbiological characterization of everninomicin-B and everninomicin-D. *Antimicrob Agents Chemother* **6**, 232-238 (1974).
11. Ganguly, A. K., Sarre, O. Z., Greeves, D. & Morton, J. Structure of Everninomicin D. *J Am Chem Soc* **97**, 1982-1985 (1975).
12. Ganguly, A. K. & Szmulewicz, S. Structure of everninomicin C. *J Antibiot* **28**, 710-712 (1975).
13. Ganguly, A. K., Szmulewicz, S., Sarre, O. Z. & Girijavallabhan, V. M. Structure of everninomicin-2. *J Chem Soc Chem Comm* 609-611 (1976).
14. Ganguly, A. K., Kabasakalina, P., Morton, J., Sarre, O., Westcott, A., Kalliney, S., Mangiaracina, P. & Papaphilippou, A. Electrochemical modification of everninomicin D. *J Chem Soc Chem Comm* 56-58 (1980).
15. Ganguly, A. K., Pramanik, B., Chan, T. M., Sarre, O., Liu, Y.T., Morton, J. & Girijavalabhan, V. The Structure of New Oligosaccharide Antibiotics, 13-384 Component-1 and Component-5. *Heterocycles* **28**, 83-88 (1989).
16. Cormican, M. G., Marshall, S. A. & Jones, R. N. Preliminary interpretive criteria for disk diffusion susceptibility testing of SCH 27899, a compound in the everninomicin class of antimicrobial agents. *Diag Microbiol Inf Dis* **23**, 157-160 (1995).
17. Urban, C., Mariano, N., Mosinka-Snipas, K., Wadee, C., Charhour, T. & Rahal, J.J. Comparative in-vitro activity of SCH 27899, a novel everninomicin, and vancomycin. *J Antimicrob Chemother* **37**, 361-364 (1996).
18. Bartner, P., Pramanik, B.N., Saksena, A.K., Liu, Y.H., Das, P.R., Sarre, O. & Ganguly, A.K. Structure elucidation of Everninomicin-6, a new oligosaccharide antibiotic, by chemical degradation and FAB-MS methods. *J Am Soc Mass Spectrom* **8**, 1134-1140 (1997).

19. Ganguly, A. K., McCormick, J. L., Chan, T.-M., Saksena, A. K. & Das, P. R. Determination of the absolute stereochemistry at the C16 orthoester of everninomicin antibiotics; a novel acid-catalyzed isomerization of orthoesters. *Tetrahedron Lett* **38**, 7989-7992, (1997).
20. Dever, L. L., Torigian, C. V. & Barbour, A. G. In vitro activities of the everninomicin SCH 27899 and other newer antimicrobial agents against Borrelia burgdorferi. *Antimicrob Agents Chemother* **43**, 1773-1775 (1999).
21. Foster, D. R. & Rybak, M. J. Pharmacologic and bacteriologic properties of SCH-27899 (Ziracin), an investigational antibiotic from the everninomicin family. *Pharmacotherapy* **19**, 1111-1117 (1999).
22. Wilson, D. N. The A-Z of bacterial translation inhibitors. *Critic Rev Biochem Mol Biol* **44**, 393-43 (2009).
23. Mikolajka, A., Liu, H., Chen, Y. Starsota, A.L., Marquez, V., Ivanova, M., Cooperman, B.S. & Wilson, D.N. Differential effects of thiopeptide and orthosomycin antibiotics on translational GTPases. *Chem Biol* **18**, 589-600 (2011).
24. Nicolaou, K. C., Fylaktakidou, K.C., Mitchell H.J., van Delft, F.L., Rodriguez, R.M., Conley, S.R. & Jin, Z. Total synthesis of everninomicin 13,384-1--Part 4: explorations of methodology; stereocontrolled synthesis of 1,1'-disaccharides, 1,2-seleno migrations in carbohydrates, and solution- and solid-phase synthesis of 2-deoxy glycosides and orthoesters. *Chemistry* **6**, 3166-3185 (2000).
25. Nicolaou, K. C., Mitchell, H. J., Fylaktakidou, K. C., Rodriguez, R. M. & Suzuki, H. Total synthesis of everninomicin 13,384-1--Part 2: synthesis of the FGHA2 fragment. *Chemistry* **6**, 3116-3148 (2000).
26. Nicolaou, K. C., Mitchell, H.J., Rodriguez, R.M., Fylaktakidou, K.C., Suzuki, H. & Conley, S.R. Total synthesis of everninomicin 13,384-1--Part 3: synthesis of the DE fragment and completion of the total synthesis. *Chemistry* **6**, 3149-3165 (2000).
27. Wagman, G. H. & Weinstein, M. J. Antibiotics from Micromonospora. *Ann Rev Microbiol* **34**, 537-557 (1980).
28. Welsch, M. Bacteriostatic and Bacteriolytic Properties of Actinomycetes. *J Bacteriol* **44**, 571-588 (1942).
29. Waksman, S. A., Geiger, W. B. & Bugie, E. Micromonosporin, an Antibiotic Substance from a Little-known Group of Microorganisms. *J Bacteriol* **53**, 355-357 (1947).
30. Weinstein, M. J., Luedemann, G. M., Oden, E. M. & Wagman, G. H. Everninomicin, a New Antibiotic Complex from Micromonospora Carbonacea. *Antimicrob Agents Chemother* **10**, 24-32 (1964).
31. Chen, G., Pramanik, B. N., Bartner, P. L., Saksena, A. K. & Gross, M. L. Multiple-Stage Mass Spectrometric Analysis of Complex Oligosaccharide Antibiotics (Everninomicins) in a Quadrupole Ion Trap. *J Am Soc Mass Spectrom* **13**, 1313-1321 (2002).

32. Ganguly, A. K., Chen, G.D., Pramanik, B.N., Daaro, I., Luk, E., Bartner, P.L., Saksena, A.K. & Girijavallabhan, V.M. Negative ion multiple-stage mass spectrometric analysis of complex oligosaccharides (everninomicins) in a quadrupole ion trap: Implications for charge-remote fragmentation. *Arkivoc*, 31-44 (2003).
33. Eichhorn, P., Perez, S., Bechtholt, A. & Aga, D. S. Fragmentation studies on the antibiotic avilamycin A using ion trap mass spectrometry. *J Mass Spectrom* **39**, 1541-1553 (2004).
34. Hosted, T. J., Wang, T. X., Alexander, D. C. & Horan, A. C. Characterization of the biosynthetic gene cluster for the oligosaccharide antibiotic, Evernimicin, in *Micromonospora carbonacea* var. *africana* ATCC39149. *J Ind Microbiol Biotechnol* **27**, 386-392 (2001).
35. Alexander, D. C., Devlin, D. J., Hewitt, D. D., Horan, A. C. & Hosted, T. J. Development of the Micromonospora carbonacea var. africana ATCC 39149 bacteriophage pMLP1 integrase for site-specific integration in Micromonospora spp. *Microbiology* **149**, 2443-2453 (2003).
36. Bierman, M., Logan, R., Obrien, K., Seno, E.T., Rao, R.N. & Schoner, B.E. Plasmid Cloning Vectors for the Conjugal Transfer of DNA from *Escherichia coli* to *Streptomyces* Spp. *Gene* **116**, 43-49 (1992).
37. Mazodier, P., Petter, R. & Thompson, C. Intergeneric Conjugation between *Escherichia coli* and *Streptomyces* species. *J Bacteriol* **171**, 3583-3585 (1989).
38. CLSI. *Methods for Dilution Antimicrobial Susceptibility Tests for Bacteria that Grow Aerobically; Approved Standard - Ninth Edition.*, Vol. CLSI document M07-A9 (Clinical and Laboratory Standards Institute, 2012).
39. Luedemann, G. M., Ridge, G., Weinstein, M.J. Everninomicin Antibiotics and Method for the Manufacture Thereof. USA patent 3,499,078 (1970).
40. Smith, J. A., Skidmore, A. G. & Salit, I. E. Rosaramicin: in-vitro activity against common bacterial isolates. *J Antimicrob Chemother* **7**, 505-513 (1981).
41. Lin, C. C., Chung, M., Gural, R., Schuessler, D., Kim, H.K., Radwanski, E., Marco, A., Digiore, C. & Symchowicz, S. Pharmacokinetics and metabolism of rosaramicin in humans. *Antimicrob Agents Chemother* **26**, 522-526 (1984).
42. Funaishi, K., Kawamura, K., Satoh, F., Hiramatsu, M., Hagiwara, M. & Okanish, M. New analogues of rosaramicin isolated from a Micromonospora strain. I. Taxonomy, fermentation, isolation and physico-chemical and biological properties. *J Antibiot* **43**, 938-947 (1990).
43. Nakajima, S., Kojiri, K., Morishima, H. & Okanishi, M. New analogs of rosaramicin isolated from a Micromonospora strain. II. Structure determination. *J Antibiot* **43**, 1006-1009 (1990).
44. Iizaka, Y., Higashi, N., Ishida, M., Oiwa, R., Ichikawa, Y., Takeda, M., Anzai, Y. & Kato, F. Function of cytochrome P450 enzymes RosC and RosD in the biosynthesis of rosamicin macrolide antibiotic produced by Micromonospora rosaria. *Antimicrob Agents Chemother* **57**, 1529-1531 (2013).

45. Huong, N. L., Hoang, N.H., Shrestha, A., Sohng, J.K., Yoon, Y.J. & Park, J.W. Biotransformation of rosamicin antibiotic into 10,11-dihydrorosamicin with enhanced in vitro antibacterial activity against MRSA. *J Microbiol Biotechnol* **24**, 44-47 (2014).
46. Vey, J. L., Al-Mestarihi, A., Hu, Y., Funk, M.A., Bachmann, B.O. & Iverson, T.M. Structure and mechanism of ORF36, an amino sugar oxidizing enzyme in everninomicin biosynthesis. *Biochemistry* **49**, 9306-9317 (2010).
47. Siegrist, S., Lagouardat, J., Moreau, N. & LeGoffic, F. Mechanism of action of a 16-membered macrolide: Binding of rosaramicin to the *Escherichia coli* ribosome and its subunits. *Eur J Biochem* **115**(2), 323-327 (1981).
48. Siegrist, S., Velitchkovitch, S., Le Goffic, F. & Moreau, N. Mechanism of action of a 16-membered macrolide: Characteristics of dihydrorosaramicin binding to *Escherichia coli* ribosome and the effecs of some competitors. *J Antibiot* **35**(7), 866-874 (1982).
49. Hansen, J. L., Ippolito, J.A., Ban, N., Nissen, P., Moore, P.B. & Steitz, T.A. The Structures of Four Macrolide Antibiotics Bound to the Large Ribosomal Subunit. *Mol Cell* **10**, 117-128 (2002).

CHAPTER III

FUNCTIONAL ANALYSIS OF THE EVERNINOMICIN PATHWAY IN *MICROMONOSPORA CARBONACEA* VAR *AURANTIACA*

Introduction

Natural products are valuable sources of pharmaceutical compounds. From 1981-2010, 50% of small-molecule approved drugs were natural products (6%), natural product derivatives (28%), or were inspired by natural products (16%).[1] Notably, of the small-molecule antibacterials that were approved in the same time period, 74.5% were either natural products (9.8%) or natural product derivatives (64.7%).[1] As evidenced by these data, natural products provide useful leads and scaffolds for developing new antibacterials although derivatization is often needed to cultivate their full clinical potential.

The everninomicins are a family of bacterial natural products with excellent clinical potential. The everninomicins have potent activity against a variety of harmful pathogens including methicillin-resistant *Staphylococcus aureus,* vancomycin-resistant enterococci, and *Clostridium difficile*.[2] From the variety of natural everninomicin analogs produced by *Micromonospora carbonacea* as well as non-natural chemical modifications to major analogs, some information about the structure-activity relationships of everninomicins is known. Specifically, capping of the hydroxyl groups significantly reduces activity,[3,4] reduction of the nitro to the amino abolishes Gram-positive activity and increases Gram-negative activity,[3,5] and hydrolysis of the orthoester linkage between rings C and D results in complete loss of activity.[4]

However, to develop a pharmacologically suitable drug, more analogs are needed to fully explore the structure-activity relationships of the everninomicins.

Chemical synthesis can be a useful tool for developing natural product derivatives. However, due to everninomicin's size and complexity, chemical synthesis of derivatives is not practical. In 1999, K.C. Nicolaou's group published the first total synthesis of everninomicin which required 134 steps.[6-8] An alternative to chemical synthesis of analogs is to alter the biosynthetic pathway responsible for production of everninomicins. By deleting, adding, or modifying enzymes in the pathway, new analogs can be created.

Creating new analogs by modification of the biosynthetic pathway requires a knowledge of the arrangement and encoded functions of genes in the gene cluster. Here we used translated sequence similarities to deduce the function of each enzyme in the everninomicin biosynthetic pathway from *M. carbonacea* var *aurantiaca*. Additionally, two additional orthosomycin gene clusters, *eve* and *ava*, were annotated to provide a fuller picture of orthosomycin biosynthesis. Targeted gene replacement of 3 genes from the everninomicin pathway in *M. carbonacea* var *aurantiaca* provided the first functional assessment of this gene cluster and resulted in the accumulation of 5 new everninomicin analogs. By providing critical information about the mutability of the gene cluster as well as tolerance of the biosynthetic enzymes for non-natural substrates, the work presented here lays the groundwork for construction of novel everninomicin analogs with improved efficacy and pharmacological properties through manipulation of the biosynthetic pathway.

Methods

Annotation of the Evd, Eve, and Ava Gene Clusters

Using antiSMASH (antismash.secondarymetabolites.org), open reading frames (ORFs) were identified from GenBank nucleotide sequences. Each ORF was analyzed using Translated BLAST (BlastX). Based on the function of homologous proteins, gene names were assigned and functions were proposed.

Bacterial culture conditions

E. coli strains were grown in LB broth. *M. carbonacea* var *aurantiaca* NRRL 2997 and replacement mutants were grown on TSB (Oxoid™ Tryptone Soy Broth) agar and in TSB liquid. Intergeneric conjugations were performed on solid AS1 media (0.1% yeast extract, 0.5% soluble starch, 0.02% L-alanine, 0.02% L-arginine, 0.05% L-asparagine, 0.25% NaCl, 1% Na_2SO_4, 2% agarose at pH 7.5, supplemented with 10 mM $MgCl_2$). Apramycin (50 μg/ml), nalidixic acid (12.5 μg/ml), chloramphenicol (30 μg/ml), and kanamycin (50 μg/ml) were used when required for selection as described below.

Construction of gene replacements

The genes *evdM2, evdM3,* and *evdN1* were individually deleted on cosmids CA or CG using a two-step PCR-targeted gene replacement strategy. The first step was replacement of the gene(s) of interest in *E. coli*. λ Red competent cells were prepared by inoculating 1% of a fresh overnight culture of *E. coli* BW25113/pIJ790 containing cosmid CA (containing the evd gene cluster) into 10 mL of LB medium containing 20 mM MgSO4, 50 μg/mL kanamycin, 30 μg/mL chloramphenicol, and 10 mM L-arabinose. The culture was grown at 30 °C with shaking to an

OD_{600} of 0.6. The cells were recovered by centrifugation at 3,000 × g for 10 min at 4 °C. The pellet was washed three times with 10 mL ice-cold 10% glycerol. The washed pellet was then resuspended in 100 µL of ice-cold 10% glycerol and kept on ice until transformation.

The gene replacement cassette containing the apramycin resistance marker (*aac*(*3*)*IV*), *oriT,* and FRT regions was amplified by PCR using the primers listed in table 3-1. PCR products were then directly transformed via electroporation into the arabinose-induced strain *E. coli* BW25113/pIJ790 containing cosmid CA in which gene replacement of *evdN1*, *evdM3*, or *evdM2* was enabled via λ Red-mediated homologous recombination. Transformed *E. coli* were plated on LB containing apramycin and incubated overnight at 37 °C to promote loss of pIJ790. Colonies were inoculated into LB containing apramycin and kanamycin and grown overnight at 37 °C with shaking. The resultant cosmid was isolated, confirmed by sequencing, and then transformed by electroporation into the non-methylating *E. coli* strain ET12567 containing plasmid pUZ8002, which contains genes necessary for conjugal transfer of the cosmid. This strain was maintained at 37 °C in liquid LB medium containing 50 µg/mL kanamycin, 50 µg/mL apramycin, and 30 µg/mL chloramphenicol.

The second step of the PCR-targeted Streptomyces gene-replacement strategy was replacement of the gene(s) of interest in the everninomicin-producing organism. Transformation of *M. carbonacea* var *aurantiaca* was accomplished using the methods described in Chapter I. Two rounds of homologous recombination were necessary to generate in-frame double crossovers. After 7-9 d of incubation at 30 °C, exconjugants were streaked onto solid TSB medium containing either apramycin or kanamycin to identify double-crossover mutants. Double crossovers were confirmed by PCR amplification of the kanamycin and apramycin resistance

genes using the primers AprUp and AprDn for amplifying the apramycin resistance gene and NeoUp and NeoDn for amplifying the kanamycin resistance gene (sequences can be found in Table 3-1).

Double-crossover mutants in *M. carbonacea* were confirmed by Southern hybridization. Gene specific probes were designed upstream of the genes of interest (primer sequences can be found in table 3-1). The evdM2 probe (782 bp) was amplified using primers EvdM2-Southern-For and EvdM2-Southern-Rev. The evdM3 probe (574 bp) was amplified using primers EvdM3-

Primer Name	Purpose	Sequence (5'-3')
RED-N1-For	Δ*evdN1*::*aac(3)IV*	ATGGTCGACCTGCTGACCGGCGTACTCCCGCAGATCCGG ATTCCGGGGATCCGTCGACC
RED-N1-Rev	Δ*evdN1*::*aac(3)IV*	ATTCCGGCAGGTAGTCCCACACTCGGATGGTCATGTTCA TGTAGGCTGGAGCTGCTTC
RED-M2-For	Δ*evdM2*::*aac(3)IV*	GACACCGCCGGTCCACCGTGGGCAGGAGCCCCGGCGGT GATTCCGGGGATCCGTCGACC
RED-M2-Rev	Δ*evdM2*::*aac(3)IV*	CCACGCTCTCGTCATACGCTGATGCGGTCCGACTCACGT TGTAGGCTGGAGCTGCTTC
RED-M3-For	Δ*evdM3*::*aac(3)IV*	CGCCCGGAAACCCCACACGAAGGAGACCGCTACGTGAG TATTCCGGGGATCCGTCGACC
RED-M3-Rev	Δ*evdM3*::*aac(3)IV*	CCGCCGCGGCGAGCAGCCGCTGGACGAGCGAGCCGGT CATGTAGGCTGGAGCTGCTTC
EvdM2-Southern-For	EvdM2 Southern Probe	CGTTCGGGTAGTCGTAGACC
EvdM2-Southern-Rev	EvdM2 Southern Probe	ACTAGGGTTTCCCCCACAAC
EvdM3-Southern-For	EvdM3 Southern Probe	TACGCGCACTTCATCGATCT
EvdM3-Southern-Rev	EvdM3 Southern Probe	GATACGTGTCCAGGGAGCTG
EvdN1-Southern-For	EvdN1 Southern Probe	ACGACGAGCACTTCTTCCTG
EvdN1-Southern-Rev	EvdN1 Southern Probe	GAAGACCGAGTCCAGGTACG
Apr-Southern-For	Apramycin Southern Probe	ACCGACTGGACCTTCCTTCT
Apr-Southern-Rev	Apramycin Southern Probe	TCGCTATAATGACCCCGAAG
EvdM2-GC-For	pSET152ermE*-evdM2	CATATGGTGATCGGCTTGCTGGGC
EvdM2-GC-Rev	pSET152ermE*-evdM2	AGTACTGTAGCGGTCTCCTTCGTGTG
EvdN1-GC-For	pSET152ermE*-evdN1	CATATGAGCGAATTCATGGTCGACCTG
EvdN1-GC-Rev	pSET152ermE*-evdN1	GATATCCACTCGGATGGTCATGTTCA
EvdM3-GC-For	pSET152ermE*-evdM3	CATATGGTGAGTCGGACCGCATCA
EvdM3-GC-Rev	pSET152ermE*-evdM3	GATATCTCACGACCCCACCCGCGA
HygBCheck-For	Confirm GC vectors	GATTCGGATGATTCCTACGC
HygBCheck-Rev	Confirm GC vectors	GAAGGCGTTGAGATGCAGTT
Apr-For	Confirm gene replacements	ATTCCGGGGATCCGTCGACC
Apr-Rev	Confirm gene replacements	TGTAGGCTGGAGCTGCTTC
Neo-For	Confirm gene replacements	TGAATGAACTGCAGGACGAG
Neo-Rev	Confirm gene replacements	AATATCACGGGTAGCCAA

Table 3-1. Sequences of primers.

Southern-For and EvdM3-Southern-Rev. The evdN1 probe (700 bp) was amplified using primers EvdN1-Southern-For and EvdN1-Southern-Rev. An 884 bp probe specific to the apramycin resistance gene was also designed and amplified using primers Apr-Southern-For and Apr Southern-Rev. All probes were labeled with digoxigenin using the DIG High Prime DNA Labeling and Detection Starter Kit II (Roche, Cat No: 11585614910). Hybridization and detection were performed using the aforementioned DIG Starter Kit.

Complementation of gene replacement mutants

To generate a suitable complementation plasmid for use in *M. carbonacea var aurantiaca*, a pSET152 derivative was designed and constructed by Mutagenex with aid from the Iverson lab.

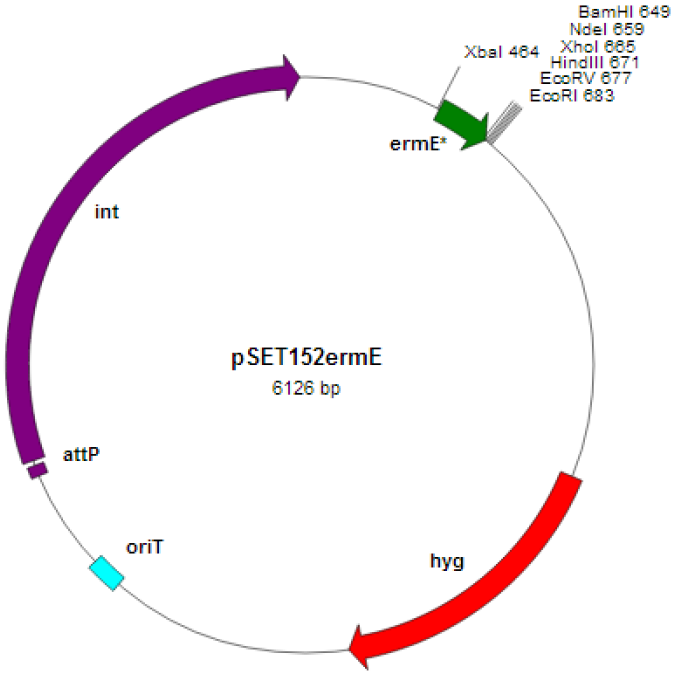

Figure 3-1. Map of pSET152ermE, the genetic complementation plasmid. Plasmid map was generated using Savvy (Scalable Vector Graphics & Plasmid Map Copyright© 2001, Malay K Basu) at http://www.bioinformatics.org/savvy/. Hyg is the hygromycin resistance marker hph; oriT is the origin of transfer; int is the phage ϕC31 integrase; attP is the phage ϕC31 attachment site; ermE* is the constitutively active promoter directly upstream of the multiple cloning site.

Starting with pSET152, the constitutive promoter ermE* was inserted upstream of the multiple cloning site. Next, the apramycin resistance gene (*aac(3)IV*) was replaced with the hygromycin B resistance marker *hyg* to generate the new complementation plasmid, pSET152ermE (map in Figure 3-1). For complementation of *ΔevdM2::aac(3)IV*, *ΔevdM3::aac(3)IV,* and *ΔevdN1::aac(3)IV*, *evdM2, evdM3*, and *evdN1* were amplified by PCR using the primers listed in table 3-1. The PCR products were subsequently cloned into the NdeI and EcoRV sites of pSET152ermE to generate complementation plasmids for each mutant strain.

Each of the complementation plasmids above were transformed into the conjugal *E. coli* strain ET12567/pUZ8002. Conjugation between the donor *E. coli* and recipient *M. carbonacea* was performed in the same manner as described previously except that apramycin and hygromycin were added after 16 hours of incubation to select for mutants that contained the gene replacement as well as the genetic complementation plasmid. Crude extracts of the complemented strains were prepared and analyzed by HPLC/MS as described below.

Analysis of Metabolites from M. carbonacea var aurantiaca Mutants

Seed cultures were generated by inoculating a loop of mycelia from TSB agar into 100 mL of 2997 Germination Medium (0.3 % beef extract, 0.5 % tryptose, 0.1 % dextrose, 2.4 % soluble starch, 0.5 % yeast extract, 0.1 % calcium carbonate, 50 µg/ml apramycin) for 5 days at 30 °C in a 500 mL Erlenmeyer flask with shaking. For production, 25 mL of the seed culture was added to 500 mL apramycin-free Production Medium (0.5 % yeast extract, 0.1 % corn steep solids, 0.1 % calcium carbonate, 3 % glucose) in a 2 L baffled Fernbach flask and grown with shaking at 30 °C for 10 days. Diaion HP-20 resin (100 mL, previously pre-equilibrated with methanol and washed

with water) was added to the fermentation cultures and incubated for 60 minutes with shaking. The combined resin and mycelia were collected by centrifugation at 3000 x g, extracted successively with 250 mL methanol and 250 mL acetone, and evaporated to dryness by rotary evaporation. The resulting crude extract was resuspended in 300 mL solvent grade methanol and filtered through a fritted glass funnel containing silica gel (9 x 2 cm) *via* vacuum filtration and concentrated to dryness. Extracts were resuspended at a final concentration of 200 mg/mL in HPLC grade methanol prior to analysis by LC/MS. Mass spectral analysis of crude extracts was accomplished using the methods described in Chapter II.

Isolation of Everninomicin H

The first dimension of separation for crude extracts was size-exclusion chromatography using a Sephadex LH20 column in methanol. Fractions were analyzed by LC/MS, and the fractions containing everninomicin H were combined and separated using reverse phase HPLC using a linear gradient. Mobile phases were: (A) 99 % water/1 % acetonitrile with 10 mM ammonium acetate, pH = 8 and (B) 5 % water/95 % acetonitrile with 10 mM ammonium acetate, pH = 8.

Structural Analysis of Everninomicin Analogs

The structure of Ever-2 was confirmed using the TSQ Quantum Access Max triple stage quadrupole mass spectrometer and parameters described in Chapter II. Collision energies of 20 V – 40 V with a skimmer offset of 5 V were employed in positive mode to fragment Ever-2. The structure of everninomicin H was determined by NMR analysis. Structures of everninomicins H, J, and K were determined using a 15T Bruker FTICR.

Bioactivity Testing

The antibacterial activities of the everninomicins were determined by the broth microdilution assay according to NCCLS guidelines using *Staphylococcus aureus* subsp. *aureus* Rosenbach (ATCC 6538P) as the test organism.[9]

Results

Deduced Functions of the ORFs of Evd, Eve, and Ava Gene Clusters

Five orthosomycin gene clusters are available in GenBank: *ava* (avilamycin biosynthesis from *Streptomyces mobaraensis*), *avi* (avilamycin biosynthesis from *S. viridochromogenes Tü57*), *evd* (everninomicin biosynthesis from *Micromonospora carbonacea* var *aurantiaca*), *eve* (everninomicin biosynthesis from *M. carbonacea* var *africana*), and *hyg* (hygromycin B biosynthesis from *S. hygroscopicus*). However, only two of these clusters, *avi* and *hyg*, include functional annotation. Therefore, we used translated sequence similarities and comparative genomics to propose functions for the *ava, evd*, and *eve* gene clusters. Figures 3-2, 3-3, and 3-4 depict the arrangement and deduced functions of the *evd, eve*, and *ava* gene clusters respectively.

<u>*Genes putatively involved in deoxysugar biosynthesis*</u>. Each cluster contains a putative glucose-1-phophate thymidyltransferase (EvdS4, EveS1, and AvaS2) responsible for formation of dTDP-glucose, a proposed precursor for all sugar residues. After formation of dTDP-glucose, a variety of enzymes are necessary to produce the deoxy- and dideoxysugars of the orthosomycins. In each of the everninomicin clusters, there are two putative 4,6 dehydratases (EvdS5, Evd10,

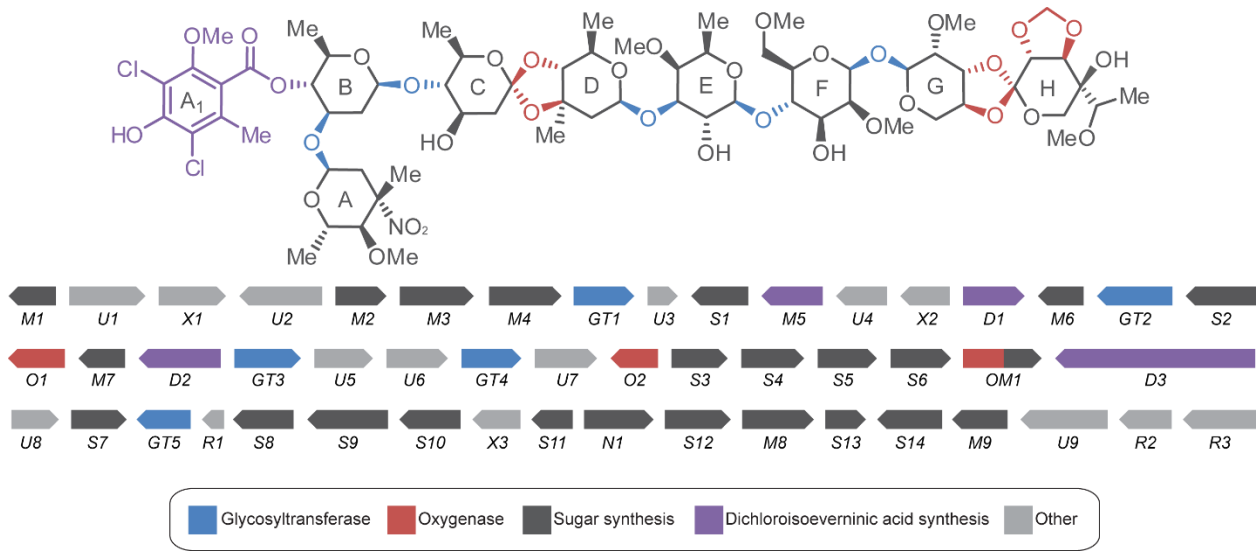

GenBank Accession #	Start/Stop (bp)	Gene	Size (aa)	Proposed function	Protein Homolog	Identity (%)	Gen Bank Accession #
AX574200	753-1	EvdM1	250	O-methyltransferase	ApoM1 (*Nocardiopsis* sp. FU40)	71	AEP40941
	1533-2861	EvdU1	442	Unknown	MCAG_03643 (*Micromonospora* sp. ATCC 39149)	76	ZP_04607386
	2898-4055	EvdX1	385	RNA methyltransferase	MCAG_03646 (*Micromonospora* sp. ATCC 39149)	70	ZP_04607389
	5529-4060	EvdU2	489	Unknown	MCAG_03647 (*Micromonospora* sp. ATCC 39149)	77	ZP_04607390
	6174-6998	EvdM2	274	O-methyltransferase	MCAG_03640 (*Micromonospora* sp. ATCC 39149)	79	ZP_04607383
	7040-8284	EvdM3	429	C-methyltransferase	MCAG_03641 (*Micromonospora* sp. ATCC 39149)	72	ZP_04607384
	8281-9465	EvdM4	423	O-methyltransferase	StfMIII O-methyltransferase (*Streptomyces steffisburgensis*)	100	CAJ43240
	9472-10491	EvdGT1	339	Glycosyltransferase	MCAG_03659 (*Micromonospora* sp. ATCC 39149)	57	ZP_0460742
	10595-11020	EvdU3	137	Unknown	AviX10 (*Streptomyces viridochromogenes* Tue57)	80	AAK83174
	12020-11076	EvdS1	314	4-ketoreductase	ApoH3 (*Nocardiopsis* sp. FU40)	63	AEP40908
	13056-12061	EvdM5	342	O-methyltransferase	MCAG_03673 (*Micromonospora* sp. ATCC 39149)	58	ZP_04607416
	13912-13082	EvdU4	276	Unknown	MCAG_03672 (*Micromonospora* sp. ATCC 39149)	69	ZP_04607415
	14812-14015	EvdX2	265	RNA methyltransferase	VAB18032_26045 (*Verrucosispora maris*)	57	YP_004406907
	15102-16211	EvdD1	344	Acyltransferase	MCAG_03645 (*Micromonospora* sp. ATCC 39149)	75	ZP_04607388
	17045-16377	EvdM6	240	O-methyltransferase	MCAG_03636 (*Micromonospora* sp. ATCC 39149)	67	ZP_04607379
	18415-17099	EvdGT2	438	Glycosyltransferase	ApoGT3 (*Nocardiopsis* sp. FU40)	76	AEP40907
	19900-18683	EvdS2	405	Epimerase	MCAG_03642 (*Micromonospora* sp. ATCC 39149)	74	ZP_04607385
	20858-19917	EvdO1	313	Orthoester synthase	AviO3 (*Streptomyces viridochromogenes*)	73	AAK83187
	21589-20858	EvdM7	243	O-methyltransferase	Mtf (*Catenuloplanes nepalensis*)	82	ACL80144
	23031-21586	EvdD2	481	Halogenase	MCAG_03648 (*Micromonospora* sp. ATCC 39149)	78	ZP_04607391
	23372-24487	EvdGT3	380	Glycosyltransferase	MCAG_03663 (*Micromonospora* sp. ATCC 39149)	61	ZP_04607406
	24565-25542	EvdU5	325	Pyruvate dehydrogenase	Dhg (*Catenuloplanes nepalensis*)	89	ACL80142
	25547-26509	EvdU6	344	Pyruvate dehydrogenase	AviB2 (*Streptomyces viridochromogenes*)	77	AAK83191
	26515-27570	EvdGT4	337	Glycosyltransferase	AviGT3 (*Streptomyces viridochromogenes*)	75	AAK83192
	27567-28619	EvdU7	350	Unknown	MCAG_03660 (*Micromonospora* sp. ATCC 39149)	64	ZP_04607403
	29397-28639	EvdO2	252	Orthoester synthase	MCAG_03658 (*Micromonospora* sp. ATCC 39149)	71	ZP_04607401
	29752-30681	EvdS3	309	Epimerase/dehydratase	UUA_15808 (*Rhodanobacter thiooxydans)*	42	ZP_10205860
	30879-31946	EvdS4	355	Glucose-1-phosphate thymidyltransferase	MCAG_03630 (*Micromonospora* sp. ATCC 39149)	79	ZP_04607373
	31946-32935	EvdS5	329	4,6-dehydratase	MCAG_03631 (*Micromonospora* sp. ATCC 39149)	78	ZP_04607374
	32990-34018	EvdS6	342	4-epimerase	AviQ2 (*Streptomyces viridochromogenes*)	82	AAK83170
	34073-35425	EvdOM1	450	Oxidase/methyltransferase	MCAG_03633 (*Micromonospora* sp. ATCC 39149)	77	ZP_04607376
	39383-35580	EvdD3	1267	Polyketide synthase	AviM (*Streptomyces viridochromogenes*)	65	AAK83194
	39773-40612	EvdU8	249	Unknown	MCAG_03657 (*Micromonospora* sp. ATCC 39149)	64	ZP_04607400
	40609-41532	EvdS7	307	4-ketoreductase	MCAG_03656 (*Micromonospora* sp. ATCC 39149)	66	ZP_04607399
	42326-41511	EvdGT5	295	Glycosyltransferase	MCAG_03655 (*Micromonospora* sp. ATCC 39149)	80	ZP_04607398

Figure 3-2. Depiction and deduced functional assignment of ORFs from the *evd* gene cluster of *M. carbonacea* var *aurantiaca. Table continued on next page.*

GenBank Accession #	Start/Stop (bp)	Gene	Size (aa)	Proposed function	Protein Homolog	Identity (%)	Gen Bank Accession #
AX574200	42708-42460	EvdR1	82	Regulator	MCAG_03654 (*Micromonospora* sp. ATCC 39149)	82	ZP_04607397
	44533-43532	EvdS8	341	3-ketoreductase	MCAG_03652 (*Micromonospora* sp. ATCC 39149)	68	ZP_04607395
	45966-44554	EvdS9	470	2,3-dehydratase	MCAG_03651 (*Micromonospora* sp. ATCC 39149)	70	ZP_04607394
	46910-45963	EvdS10	346	4,6-dehydratase	MCAG_03650 (*Micromonospora* sp. ATCC 39149)	76	ZP_04607392
	47878-47207	EvdX3	254	RNA Methyltransferase	MCAG_03674 (*Micromonospora* sp. ATCC 39149)	71	ZP_04607417
AX574200/1	48183-48070	EvdS11	209	UDP-glucose 4-epimerase	MCAG_03662 (*Micromonospora* sp. ATCC 39149)	74	ZP_04607405
AX574202	1-1203	EvdN1	400	Nitrososynthase	ORF36 (*Micromonospora* sp. ATCC 39149)	80	ACF94630
	1200-2327	EvdS12	375	3-aminotransferase	MCAG_03665 (*Micromonospora* sp. ATCC 39149)	79	ZP_04607408
	2357-36-7	EvdM8	416	C-methyltransferase	MCAG_03666 (*Micromonospora* sp. ATCC 39149)	81	ZP_04607409
	3616-4239	EvdS13	207	3,5-epimerase	MCAG_03667 (*Micromonospora* sp. ATCC 39149)	74	ZP_04607410
	5169-4060	EvdS14	369	4-ketoreductase	StaK (*Streptomyces* sp. TP-A0274)	58	BAC55215
	6086-5166	EvdM9	306	O-methyltransferase	MCAG_03669 (*Micromonospora* sp. ATCC 39149)	71	ZP_04607412
	7811-6261	EvdU9	517	Unknown	MCAG_00021 (*Micromonospora* sp. ATCC 39149)	66	ZP_04603764
	8746-7889	EvdR2	286	Regulator	Amir_6179 (*Actinosynnema mirum*)	61	YP_003103832
	10035-8764	EvdR3	423	Regulator	AMED_3740 (*Amycolatopsis mediterranei*)	63	YP_003765921

Figure 3-2 *continued*.

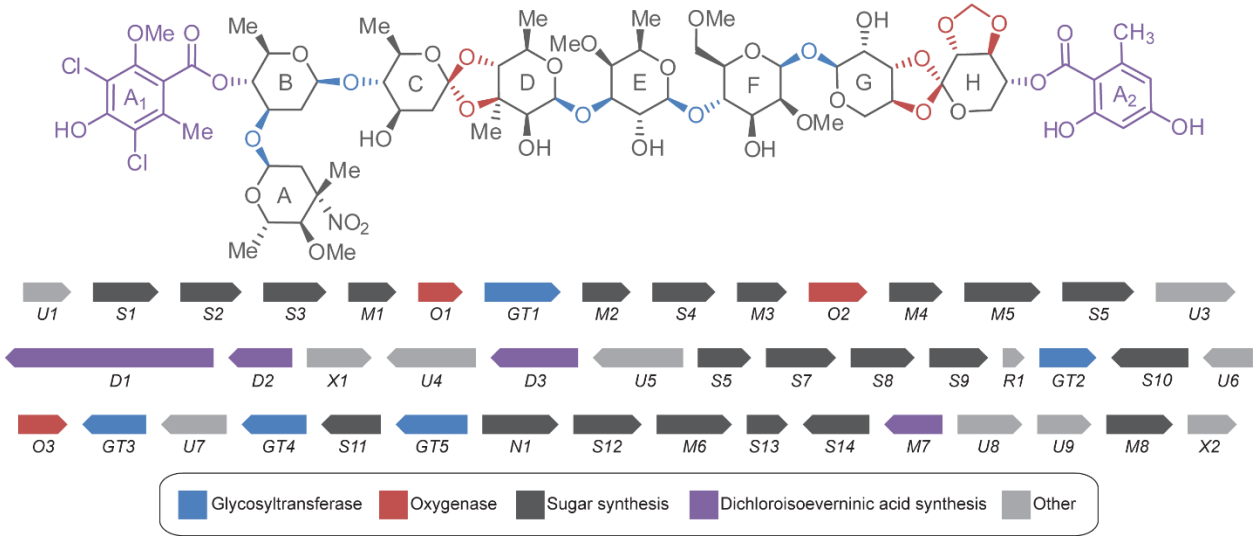

GenBank Accession #	Start/Stop (bp)	Gene	Size (#aa)	Proposed function	Protein Homolog	Identity (%)	Gen Bank Accession #
AX574198	1-747	*EveU1*	248	Unknown	AMIS_53450 (*Actinoplanes missouriensis*)	58	YP_005465081
	895-1962	*EveS1*	355	Glucose-1-phosphate thymidyltransferase	StaA (*Streptomyces sp. TP-A0274*)	70	BAC55207
	1962-2951	*EveS2*	329	4,6-dehydratase	AviE1 (*Streptomyces viridochromogenes*)	76	AAK83196
	3054-4082	*EveS3*	342	4-epimerase	AviQ2 (*Streptomyces viridochromogenes*)	81	AAK83179
	4137-4874	*EveM1*	245	Methyltransferase	AviG5 (*Streptomyces viridochromogenes*)	59	AAK83180
	4871-5545	*EveO1*	224	Oxidase (MDB)	AviO1 (*Streptomyces viridochromogenes*)	66	AAK83181
	5598-6869	*EveGT1*	423	Glycosyltransferase	AviGT1 (*Streptomyces viridochromogenes*)	70	AAK83182
	6946-7689	*EveM2*	247	Methyltransferase	AviG2 (*Streptomyces viridochromogenes*)	59	AAK83184
	7735-8763	*EveS4*	342	Ketoreductase	AviZ1 (*Streptomyces viridochromogenes*)	59	AAK83185
	8753-9526	*EveM3*	257	Methyltransferase	AviG6 (*Streptomyces viridochromogenes*)	74	AAK83186
	9523-10467	*EveO2*	314	Orthoester synthase	AviO3 (*Streptomyces viridochromogenes*)	75	AAK83187
	10464-11312	*EveM4*	282	Methyltransferase	AviG3 (*Streptomyces viridochromogenes*)	75	AAK83188
	11314-12594	*EveM5*	426	C-methyltransferase	OSCI_3520020 (*Oscillatoria sp. PCC 6506*)	50	ZP_07112622
	12627-13820	*EveS5*	397	Epimerase	AviX12 (*Streptomyces viridochromogenes*)	79	AAK83189
	13867-15204	*EveU3*	445	Unknown	Tcp34 (*Actinoplanes teichomyceticus*)	57	CAE53375

Figure 3-3. Depiction and deduced functional assignment of ORFs from the *eve* gene cluster of *M. carbonacea* var *africana. Table continued on next page.*

GenBank Accession #	Start/Stop (bp)	Gene	Size (#aa)	Proposed function	Protein Homolog	Identity (%)	Gen Bank Accession #
AX574199	3770-6	*EveD1*	1254	Polyketide synthase	AviM (*Streptomyces viridochromogenes*)	68	AAK83194
	4893-3859	*EveD2*	344	Acyltransferase	AviN (*Streptomyces viridochromogenes*)	66	AAK83178
	5247-6308	*EveX1*	353	RNA methyltransferase	Kfla_1517 (*Kribbella flavida*)	50	YP_003379414
	7815-6313	*EveU4*	500	Unknown	Sros_0818 (*Streptosporangium roseum*)	56	YP_003336575
	9421-7943	*EveD3*	492	Halogenase	Halogenase (*Catenuloplanes nepalensis*)	67	ACL80143
	11111-9579	*EveU5*	510	Transporter	Putative exporter (*Streptomyces auratus*)	53	ZP_10547180
	11767-12615	*EveS6*	282	4,6-dehydratase	PimJ (*Streptomyces natalensis*)	67	CAC20923
	12612-14066	*EveS7*	384	2,3-dehydratase	PokS3 (*Streptomyces diastatochromogenes*)	53	ACN64829
	14071-15105	*EveS8*	344	3-ketoreductase	SaqT (*Micromonospora sp. Tu 6368*)	55	ACP19378
	15140-16075	*EveS9*	311	4-ketoreductase	PokS6 (*Streptomyces diastatochromogenes*)	46	ACN64824
	17064-17312	*EveR1*	82	Regulator	AviC2 (*Streptomyces viridochromogenes*)	68	AAK83173
	17463-18377	*EveGT2*	304	Glycosyltransferase	AviGT2 (*Streptomyces viridochromogenes*)	72	AAK83170
	19301-18030	*EveS10*	423	Epimerase	ChaS4 (*Streptomyces chartreusis*)	44	CAH10166
	20061-19309	*EveU6*	250	Unknown	SCAB_21471 (*Streptomyces scabiei 87.22*)	44	YP_003487825
	20262-21023	*EveO3*	253	Orthoester synthase	CfE428DRAFT_0630 (*Chthoniobacter flavus*)	48	ZP_03127466
	22144-21122	*EveGT3*	340	Glycosyltransferase	AviGT4 (*Streptomyces viridochromogenes*)	66	2IV3_A
	23214-22159	*EveU7*	351	Unknown	SCAB_21441 (*Streptomyces scabiei 87.22*)	51	YP_003487822
	24252-23211	*EveGT4*	347	Glycosyltransferase	AviGT3 (*Streptomyces viridochromogenes*)	72	AAK83192
	25189-24251	*EveS11*	312	4-epimerase	AviQ1 (*Streptomyces viridochromogenes*)	56	AAK83169
	26343-25174	*EveGT5*	389	Glycosyltransferase	SaqGT5 (*Micromonospora sp. Tu 6368*)	47	ACP19370
	26599-27864	*EveN1*	421	Nitrososynthase	KijD3 (*Actinomadura kijaniata*)	65	3M9V_A
	27875-28996	*EveS12*	373	3-aminotransferase	KijD2 (*Actinomadura kijaniata*)	75	ACB46490
	29105-30355	*EveM6*	416	3-C-methyltransferase	KijD1 (*Actinomadura kijaniata*)	71	ACB46489
	30363-30965	*EveS13*	200	3,5-epimerase	StaE (*Streptomyces sp. TP-A0274*)	64	BAC55217
	32002-30923	*EveS14*	359	4-ketoreductase	StaK (*Streptomyces sp. TP-A0274*)	58	BAC55215
	32933-32004	*EveM7*	309	Methyltransferase	DacS7 (*Dactylosporangium sp. SC14051*)	64	AFU65919
	33190-34254	*EveU8*	354	Unknown	ANT_24670 (*Anaerolinea thermophila UNI-1*)	44	YP_004175093
	34375-35229	*EveU9*	284	Unknown	Rleg_3584 (*Rhizobium leguminosarum*)	50	YP_002977369
	35226-36314	*EveM8*	362	O-methyltransferase	KanP (*Streptomyces kanamyceticus*)	49	CAF60515
	36361-37116	*EveX2*	251	RNA methyltransferase	AviRa (*Streptomyces viridochromogenes*)	56	1O9G_A

Figure 3-3 *continued*.

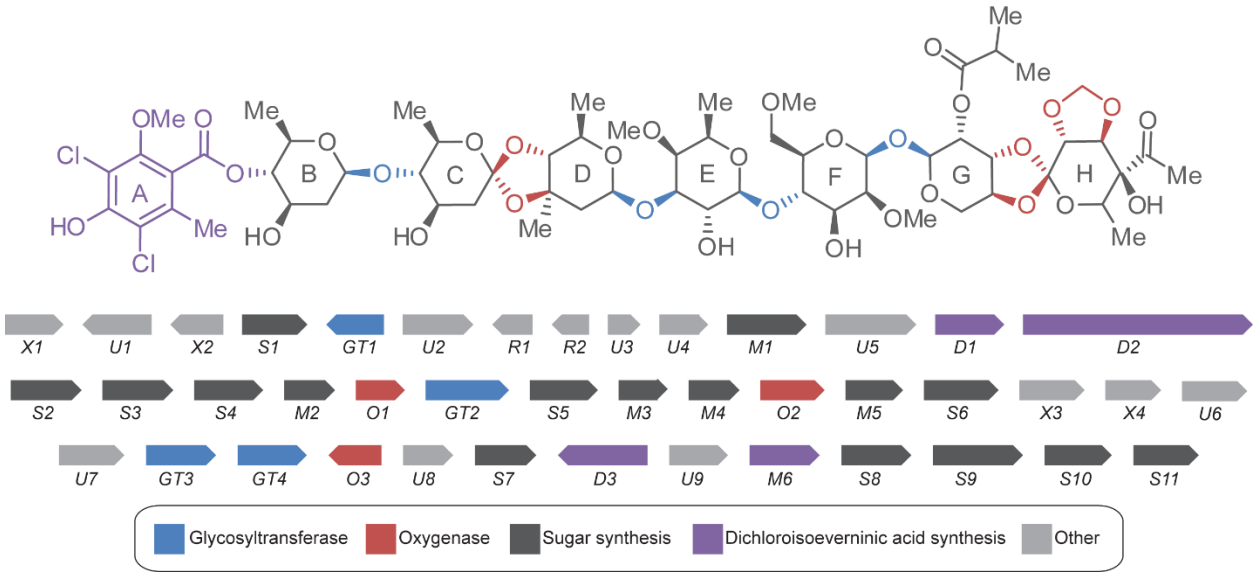

Figure 3-4. Depiction and deduced functional assignment of ORFs from the *ava* gene cluster of *S. mobaraensis. Table of assignments is found on the next page.*

GenBank Accession #	Start/Stop (bp)	Gene	Size (#aa)	Proposed function	Protein Homolog	Identity (%)	GenBank Accession #
AX574197	1-858	*AvaX1*	285	RNA methyltransferase	AviRb (*Streptomyces viridochromogenes*)	90	Q9F5K6
	1847-816	*AvaU1*	343	Unknown	MCAG_03660 (*Micromonospora* sp. ATCC39149)	64	ZP_04607403
	2721-1969	*AvaX2*	250	RNA methyltransferase	AviRa (*Streptomyces viridochromogenes*)	86	Q9F5K5.2
	2966-3934	*AvaS1*	322	4-epimerase	AviQ1 (*Streptomyces viridochromogenes*)	86	AAK83169
	4822-3986	*AvaGT1*	278	Glycosyltransferase	AviGT2 (*Streptomyces viridochromogenes*)	88	AAK83170
	5044-6114	*AvaU2*	356	Unknown	AviX9 (*Streptomyces viridochromogenes*)	87	AAK83171
	6641-6111	*AvaR1*	176	Regulator	AviC1 (*Streptomyces viridochromogenes*)	70	AAK83172
	7412-6936	*AvaR2*	158	Regulator	AviC2 (*Streptomyces viridochromogenes*)	89	AAK83173
	7639-8049	*AvaU3*	136	Unknown	AviX10 (*Streptomyces viridochromogenes*)	93	AAK83174
	8046-8741	*AvaU4*	231	Unknown	AviX11 (*Streptomyces viridochromogenes*)	91	AAK83175
	8738-9961	*AvaM1*	407	C-methyltransferase	AviG1 (*Streptomyces viridochromogenes*)	91	AAK83176
	9975-11390	*AvaU5*	471	Unknown	AviJ (*Streptomyces viridochromogenes*)	85	AAK83177
	11546-12580	*AvaD1*	344	Acyltransferase	AviN (*Streptomyces viridochromogenes*)	85	AAK83178
	12577-16431	*AvaD2*	1284	Polyketide synthase	AviM (*Streptomyces viridochromogenes*)	86	AAK83194
	16614-17690	*AvaS2*	358	Glucose-1-phosphate thymidyltransferase	AviD (*Streptomyces viridochromogenes*)	89	AAK83195
	17687-18763	*AvaS3*	358	4,6-dehydratase	AviE1 (*Streptomyces viridochromogenes*)	91	AAK83196
	18842-19870	*AvaS4*	342	4-epimerase	AviQ2 (*Streptomyces viridochromogenes*)	94	AAK83179
	19960-20676	*AvaM2*	238	Methyltransferase	AviG5 (*Streptomyces viridochromogenes*)	82	AAK83180
	20711-21394	*AvaO1*	227	Oxidase (MDB)	AviO1 (*Streptomyces viridochromogenes*)	93	AAK83181
	21451-22734	*AvaGT2*	427	Glycosyltransferase	AviGT1 (*Streptomyces viridochromogenes*)	91	AAK83182
	22731-23744	*AvaS5*	337	4,6-dehydratase	AviE2 (*Streptomyces viridochromogenes*)	90	AAK83183
	23777-24469	*AvaM3*	230	Methyltransferase	AviG2 (*Streptomyces viridochromogenes*)	90	AAK83184
	24512-25228	*AvaM4*	238	Methyltransferase	AviG6 (*Streptomyces viridochromogenes*)	91	AAK83186
	25239-26183	*AvaO2*	314	Orthoester synthase	AviO3 (*Streptomyces viridochromogenes*)	89	AAK83187
	26177-27013	*AvaM5*	278	Methyltransferase	AviG3 (*Streptomyces viridochromogenes*)	87	AAK83188
	27037-28200	*AvaS6*	378	Epimerase	AviX12 (*Streptomyces viridochromogenes*)	96	AAK83189
	28197-29168	*AvaX3*	323	ABC transporter	AviABC1 (*Streptomyces viridochromogenes*)	89	AAG32068
	29165-29962	*AvaX4*	265	ABC transporter	AviABC2 (*Streptomyces viridochromogenes*)	95	AAG32069
	30003-30980	*AvaU6*	325	Pyruvate dehydrogenase	AviB1 (*Streptomyces viridochromogenes*)	89	AAK83190
	30980-31942	*AvaU7*	320	Pyruvate dehydrogenase	AviB2 (*Streptomyces viridochromogenes*)	95	AAK83191
	31939-32988	*AvaGT3*	349	Glycosyltransferase	AviGT3 (*Streptomyces viridochromogenes*)	89	AAK83192
	32985-34013	*AvaGT4*	342	Glycosyltransferase	AviGT4 (*Streptomyces viridochromogenes*)	90	2IV3_A
	34813-34061	*AvaO3*	250	Orthoester synthase	MCAG_03658 (*Micromonospora* sp. ATCC39149)	69	ZP_04607401
	35036-35737	*AvaU8*	233	Unknown	MCAG_03657 (*Micromonospora* sp. ATCC39149)	62	ZP_04607400
	35773-36678	*AvaS7*	301	4-epimerase	MCAG_03656 (*Micromonospora* sp. ATCC39149)	61	ZP_04607399
	38237-36855	*AvaD3*	460	Halogenase	MCAG_03648 (*Micromonospora* sp. ATCC39149)	76	ZP_04607391
	38513-39367	*AvaU9*	284	Unknown	MCAG_03672 (*Micromonospora* sp. ATCC39149)	72	ZP_04607415
	39369-40415	*AvaM6*	348	O-methyltransferase	MCAG_03673 (*Micromonospora* sp. ATCC39149)	59	ZP_04607416
	40636-41682	*AvaS8*	348	4,6-dehydratase	MCAG_03650 (*Micromonospora* sp. ATCC39149)	74	ZP_04607392
	41676-43076	*AvaS9*	466	2,3-dehydratase	MCAG_03651 (*Micromonospora* sp. ATCC39149)	67	ZP_04607394
	43081-44091	*AvaS10*	336	Ketoreductase	MCAG_03652 (*Micromonospora* sp. ATCC39149)	60	ZP_04607395
	44081-45055	*AvaS11*	324	4-ketoreductase	MCAG_03653 (*Micromonospora* sp. ATCC39149)	53	ZP_04607396

Figure 3-4 *continued.*

EveS2, and EveS6) and one 2,3-dehydratase (EvdS9 and EveS7). In the avilamycin cluster, there are three putative 4,6-dehydratases (AvaS3, AvaS5, and AvaS8) and one 2,3-dehydratase (AvaS9). These dehydratases in the *ava* pathway correspond to the number and type of dehydratases proposed for the *avi* cluster.[10] Each everninomicin cluster contains 5 putative epimerases (EvdS2, EvdS3, EvdS6, EvdS11, EvdS13, EveS3, EveS5, EveS10, EveS11, and EveS13). The *ava* cluster only contains 4 putative epimerases (AvaS1, AvaS4, AvaS6, and AvaS7) as it lacks the epimerase needed for formation of evernitrose. Based on homology to AviX12 in the avilamycin pathway, we were able to assign functions of EvdS2 (71 % identity), EveS5 (79 % identity), and AvaS6 (96 % identity) as epimerases which act on the C-2 position of ring F.[11] Additionally, in each of the everninomicin clusters, there are four genes that encode putative ketoreductases (*evdS1, evdS7, evdS8, evdS14, eveS4, eveS8, eveS9,* and *eveS14*). However, only two genes encoding putative ketoreductases were found in the *ava* cluster (*avaS10* and *avaS11*). This is in contrast to the *avi* cluster which putatively encodes 4 ketoreductases.[10]

Genes putatively involved in dichloroisoeverninic acid biosynthesis. For formation of the dichloroisoeverninic acid moiety, a polyketide synthase, an acyltransferase, a halogenase, and an O-methyl transferase are necessary. Based on translated sequence similarities, *evdD3*, *eveD1,* and *avaD2* encode polyketide transferases. EvdD1, EveD2, and AvaD1 are putative acyltransferases. Notably, in the *eve, ava,* and *avi* gene clusters, the acyltransferase directly precedes the polyketide synthase, while in the *evd* gene cluster they are separated by 16 genes. EvdD2, EveD3, and AvaD3 are putative halogenases with homology to AviH (78, 72, and 92 % identities respectively), which has been shown to chlorinate isoeverninic acid.[10] Finally, *evdM5,*

eveM8, and *avaM6* encode putative aromatic O-methyltransferases. These genes have high homology to *aviG4* (60, 61, and 87 % identities respectively), which has been shown to methylate the *ortho* position of dichloroisoeverninic acid.[10]

Genes putatively involved in evernitrose biosynthesis. Unlike the other sugar residues, the genes responsible for evernitrose formation are clustered together at the end of the everninomicin gene clusters. Notably, no homologs of these genes are found in the pathways for avilamycin production which does not contain evernitrose. Previous work has shown that EveN1 (also known as ORF36) is responsible for oxidation of the amine to the nitroso.[12,13] Consequently, the homolog in the *evd* cluster *evdN1* is also proposed to be a nitrososynthase. *EvdM8* and *eveM6* appear to encode C-3-methyltransferases (both have 71 % identity to *kijD1*). Based on sequence similarity to the O-methyltransferase from the rubradirin pathway, RubN7, *EvdM9* (61 % identity) and *eveM7* (61 % identity) encode O-methyltransferases responsible for methylating the C-3-OH of evernitrose. Other enzymes proposed to be involved in evernitrose biosynthesis include the 3-aminotransferase (EvdS12 and EveS12), a 3,5-epimerase (EvdS13 and Eve S13), and a 4-ketoreductase (EvdS14 and EveS14).

Genes putatively involved in assembly of oligosaccharide chain. Interestingly, the number of glycosyltransferases in each cluster does not correspond directly to the number of glycosidic linkages. Each everninomicin and avilamycin contain two more glycosidic linkages than the number of glycosyltransferases. In each of the everninomicin pathways, we identified 5 putative glycosyltransferases (EvdGT1, EvdGT2, EvdGT3, EvdGT4, EvdGT5, EveGT1, EveGT2, EveGT3,

EveGT4, and EveGT5). There were four putative glycosyltransferases in the *ava* cluster (AvaGT1, AvaGT2, AvaGT3, and AvaGT4) corresponding to four proposed glycosyltransferases in the *avi* cluster.[10] Based on homology to AviGT4, a glycosyltransferase characterized from the avilamycin pathway, EvdGT1, EveGT3, and AvaGT4 are responsible for glycosidic attachment of ring H.[14] The fact the number of glycosyltransferase does not correlated directly with the number of sugar linkages suggests that some glycosyltransferases act iteratively or that another type of enzyme is responsible for both glycosidic linkage and orthoester linkage formation. A conserved family of oxygenases has been identified in each pathway (*EvdO1, EvdO2, EvdMO1, EveO1, EveO2, EveO3, AvaO1, AvaO2,* and *AvaO3*). Their role in the formation of the orthoester linkages and methylenedioxy bridges of the orthosomycins will be discussed in detail in Chapter IV.

<u>*Genes putatively involved in tailoring.*</u> The orthosomycins are highly decorated oligosaccharides that require a large number of tailoring enzymes. The *evd* cluster putatively encodes 8 *O*-methyltransferases (*evdM1, evdM2, evdM4, evdM5, evdM6, evdM7, evdM9*, and *evdMO1*) and 2 *C*-methyltransferases (*evdM3* and *evdM8*). Notably, *evdMO1* appears to be a fusion of an *O*-methyltransferase and an oxygenase. The *eve* cluster putatively encodes 6 *O*-methyltransferases (*eveM1, eveM2, eveM3, eveM4, eveM7,* and *eveM8*) and 2 *C*-methyltransferases (*eveM5* and *eveM6*). Generation of fully decorated everninomicin requires 9 methylation events. The *evd* cluster contains one additional methyltransferase which could be responsible for alternative everninomicin analogs. Notably, the *evd* cluster and *eve* cluster have been shown to produce different everninomicin analogs, and this explains the variation in the number of methyltransferases found in each cluster. The *ava* cluster putatively encodes 5 *O*-

methyltransferases (*avaM2, avaM3, avaM4, avaM5,* and *avaM6*) and 1 *C*-methyltransferase (*avaM1*). This corresponds to number and types of methyltransferases predicted in the *avi* gene cluster.[10] Each avilamycin gene cluster appears to contain one extra methyltransferase than the number of required methylation events for formation of avilamycin A.

Based on phylogenetic analysis of methyltransferases from the four class I orthosomycin gene clusters, *evd, eve, ava,* and *avi*, we were able to extrapolate the studies of the *avi* cluster to putatively assign the function of seven classes of methyltransferases (Figure 3-5). For the sake of

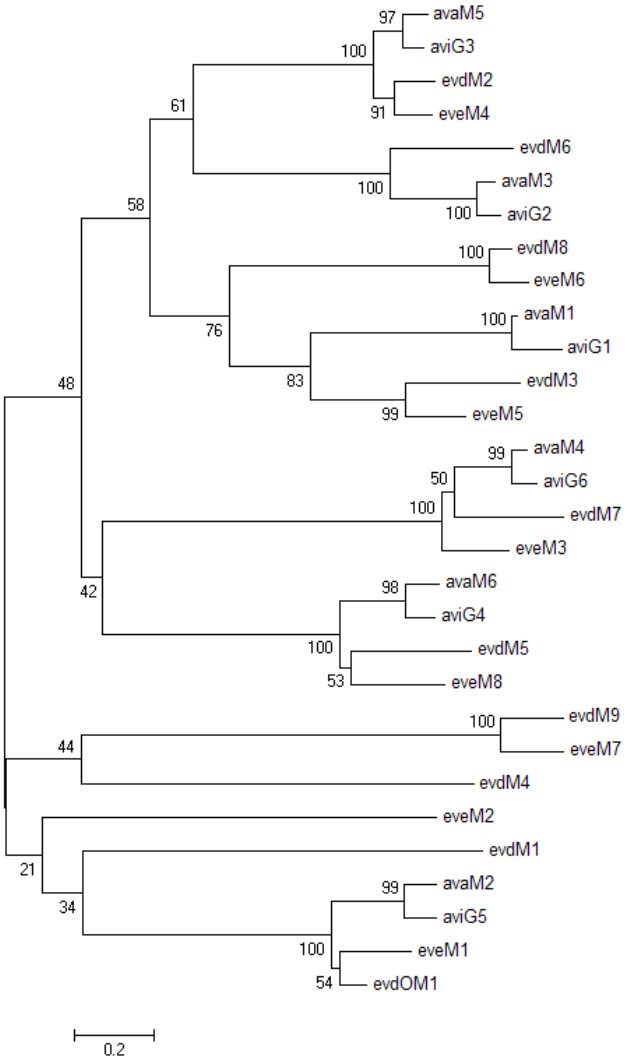

Figure 3-5. Phylogenetic analysis of methyltransferases from four class I orthosomycin gene clusters, *evd, eve, ava,* and *avi*.

simplicity, this section will focus on the putative function of the methyltransferases from the *evd* cluster. *EvdM3* is homologous to *aviG1* (45 % identity) from the avilamycin pathway which encodes a *C*-methyltransferase responsible for methylating the C-3 of the D ring.[15] As discussed previously, e*vdM5* is homologous to *aviG4* and is proposed to methylate the hydroxyl of dichloroisoeverninic acid. *EvdM6* is homologous (57 % identity) to *aviG2* which has been shown to methylate the C-6 hydroxyl of the F ring.[16] EvdM7 shares 66 % sequence identity with AviG6 which has been shown to methylate the C-2 hydroxyl of the F ring.[16] As discussed above, *evdM8* and *evdM9* are responsible for methylation of evernitrose. Finally, *evdMO1* encodes a C-terminal *O*-methyltransferase with homology to *aviG5,* the product of which has been shown to methylate the C-4 hydroxyl of the E ring of avilamycin.[16]

Genes putatively involved in regulation and resistance. Resistance genes are commonly clustered with biosynthetic genes for bacterial secondary metabolites. Indeed, in the orthosomycin pathways, there are several genes that appear to be involved in resistance. In the *evd* pathway, *evdX1, evdX2,* and *evdX2* appear to encode RNA methyltransferases. In the *eve* pathway, *evdX1* and *eveX2* appear to encode RNA methyltransferases. In the *ava* pathway, *avaX1* and *avaX2* have homology to *aviRb* and *aviRa* respectively. AviRa and AviRb have been shown to methylate 23S rRNA and confer resistance to avilamycin.[17] Additionally, the *ava* pathway encodes two putative ABC transporters, AvaX3 and AvaX4.

The *evd* cluster putatively encodes 3 regulators, EvdR1, EvdR2, and EvdR3. Interestingly, the *eve* cluster only appears to encode one regulator, EveR1. The *ava* cluster putatively encodes two regulators, AvaR1 and AvaR2, which have homology to AviC1 and AviC2 in the avilamycin

pathway. AviC1 and AviC2 have been shown to be transcriptional activators of the avilamycin pathway in *S. viridochromogenes Tü57.*[18]

Genes of unknown function. There are 9 putative open reading frames in each of the orthosomycin gene clusters discussed here (*evd, eve,* and *evd*) that encode genes of unknown function. Of note, each cluster contains a pair of genes that have homology to pyruvate dehydrogenases (*evdU5, evdU6, eveU8, eveU9, avaU6,* and *avaU7*). Their homologs in the avilamycin pathway, AviB1 and AviB2 are proposed to be responsible for the attachment of the acetyl group on the H ring.[19] However, the function of this group of enzymes needs to be researched further.

Construction of gene replacement mutants

For the first time, the *evd* cluster was experimentally verified to be responsible for biosynthesis of everninomicin by construction of gene replacements in *M. carbonacea* var *aurantiaca*. Targeted gene replacements of *evdN1, evdM3,* and *evdM2* were accomplished using a two-step PCR targeting strategy (Figure 3-6).[20-22] The gene replacements were first prepared on a cosmid in *E. coli* using λ-Red recombination. The cassette, encoding apramycin resistance and an origin of transfer, was designed with 39 base pair extensions that have homology to regions flanking the target gene. Induction of the three genes of the λ-Red recombination system (*gam, bet,* and *exo*) stimulated homologous recombination between the PCR-generated linear cassette and the cosmid containing the gene of interest in *E. coli* to generate the desired gene

replacement. Gene replacements were confirmed by PCR amplification of the cassette and sequencing.

Due to the methylation sensitivity of actinomycetes, the cosmid was then transformed via electroporation into ET12567, a non-methylating strain of *E. coli* containing plasmid pUZ8002 which is responsible for transmission of the cosmid during conjugation.[23] The de-methylated cosmid was subsequently transformed into *M. carbonacea* var *aurantiaca* by conjugation with a donor *E. coli* strain harboring a cosmid with the desired gene replacement. As discussed in Chapter II, a novel method for isolating exconjugants was developed. This method used a 0.4 µm membrane that the mycelia of *M. carbonacea* could penetrate while the donor *E. coli* remained trapped beneath.[24]

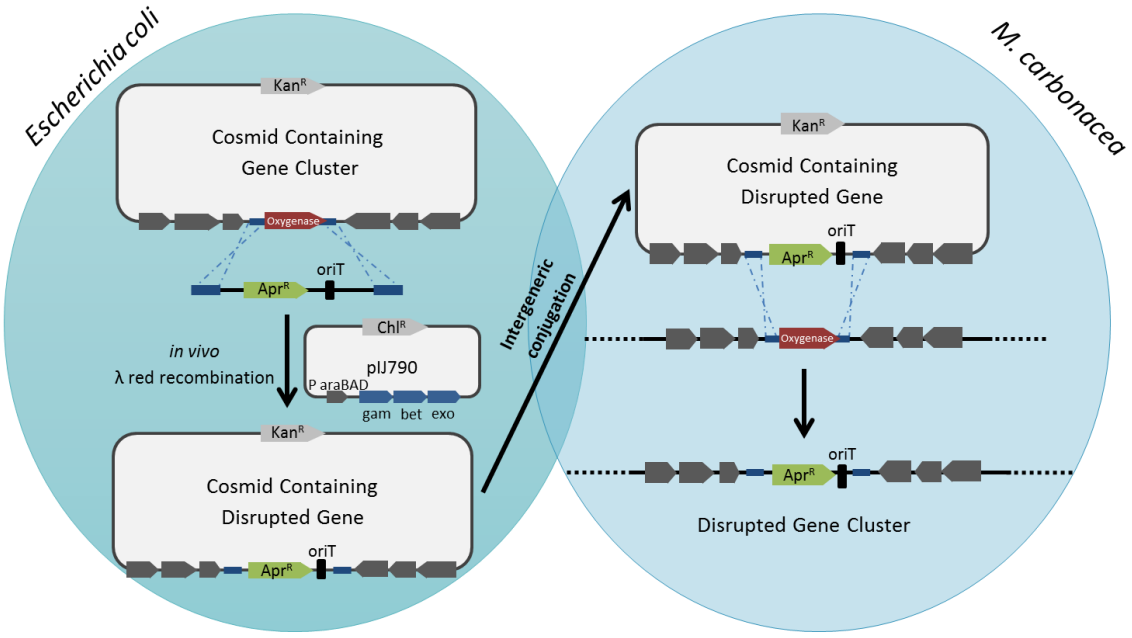

Figure 3-6. Scheme for two-step targeted gene disruptions.

Upon transformation of the cosmid into *M. carbonacea*, two rounds of homologous recombination must take place to generate a double crossover mutant (Figure 3-7). The first recombination event yields a single crossover where the entire cosmid is incorporated into the gene cluster. The insertion of such a large amount of DNA in a gene cluster can lead to polar effects and disruption of the entire gene cluster. Therefore, a double crossover generated by a second round of recombination was desirable. To select for double crossover mutants, exconjugants that were apramycin resistant and kanamycin sensitive were chosen for further analysis. These mutant strains were then analyzed via PCR amplification of the apramycin and kanamycin resistance genes to verify the double-crossover. Using this method of verification, *evdN1, evdM1,* and *evdM2* appeared to have been successfully disrupted in *M. carbonacea* var *aurantiaca*. However, as PCR cannot verify the genomic position of the crossover, we employed Southern blot analysis to confirm the replacement mutants (Figure 3-8). Digoxigenin (DIG)-labeled probes were designed upstream of each putative gene replacement. Genomic DNA from wildtype *M. carbonacea* and each mutant stain was isolated and digested with appropriate restriction endonucleases to give predictably sized fragments. Blots were analyzed for specific

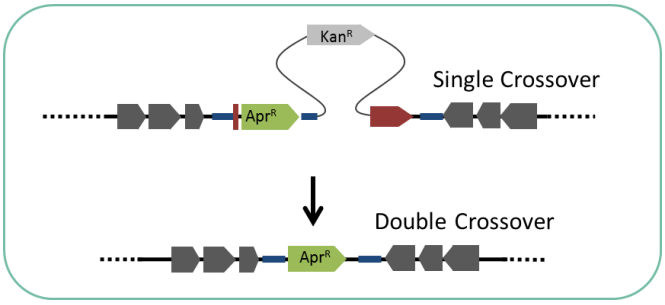

Figure 3-7. Depiction of a single crossover versus a double crossover replacement.

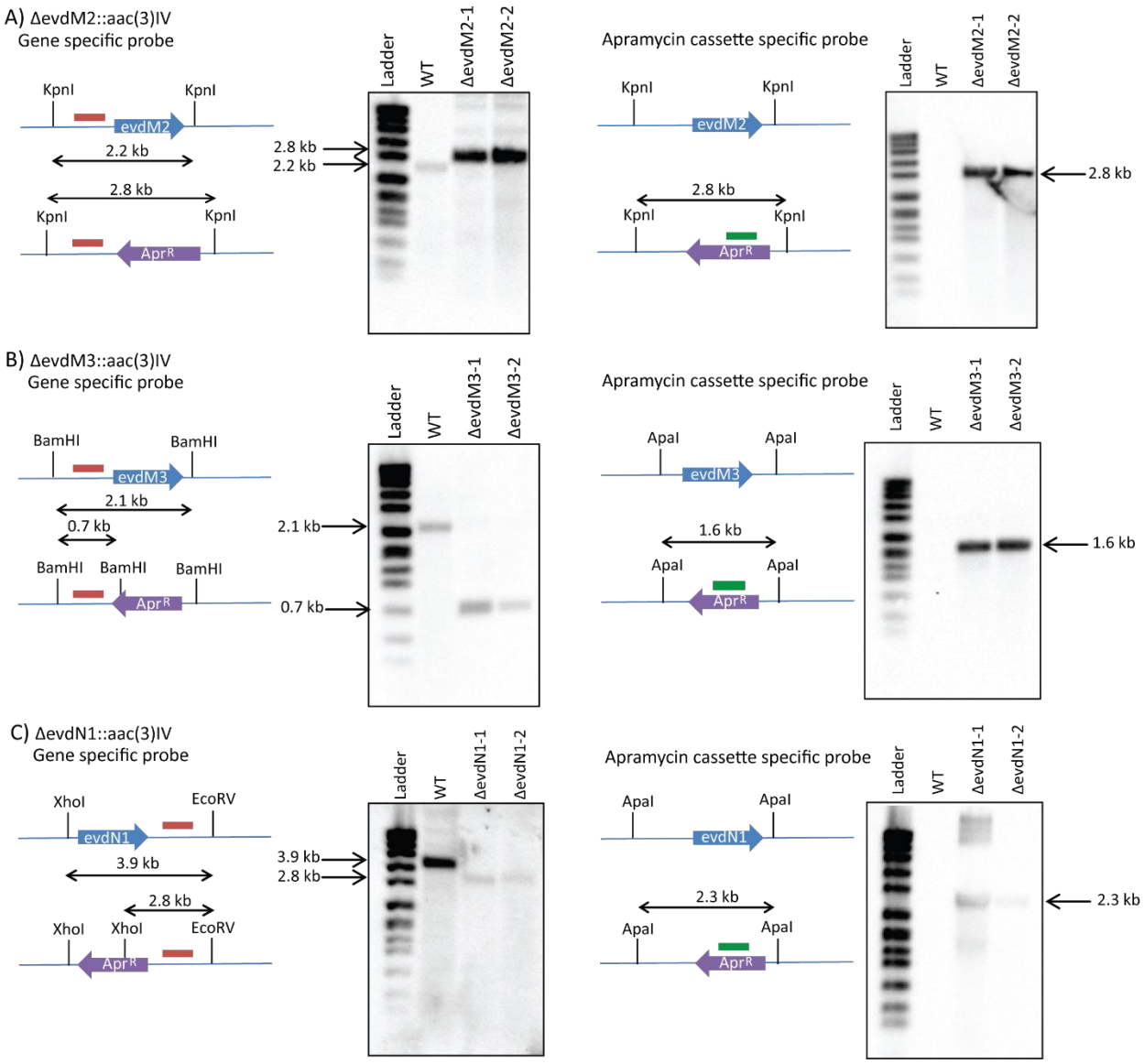

Figure 3-8. Southern hybridization of targeted replacement mutants verifying a double crossover event. All blots show predicted shifts were observed experimentally, thus confirming the double crossovers. (A) Southern blot analysis of *ΔevdM2::aac(3)IV*. Diagrams depict the relative shifts expected for replacement of *evdM2* with the apramycin cassette. (B) Southern blot analysis of *ΔevdM3::aac(3)IV*. Diagrams depict the relative shifts expected for replacement of *evdM3* with the apramycin cassette. (C) Southern blot analysis of *ΔevdN1::aac(3)IV*. Diagrams depict the relative shifts for replacement of *evdN1* with the apramycin cassette. Ladder is DNA molecular weight marker VII, DIG-labeled (product no. 11669940910; Roche Life Sciences). WT is wild-type *M. carbonacea* var *aurantiaca.* ApaI, KpnI, BamHI, XhoI, and EcoRV are restriction.

shift of probe-labeled fragments for wildtype *M. carbonacea* and each mutant strain. Gene replacements were confirmed for *evdN1, evdM3* and *evdM2* as predictable band shifts were observed (Figure 3-8).

To assess the effect of the three gene replacements on everninomicin production, tandem liquid chromatography mass spectral (LC/MS) analysis of the crude extracts of mutant strains was employed. Analysis of LC/MS data revealed abolished production of everninomicins D-G in all three gene replacement strains (Figures 3-9, 3-10, and 3-13). These results provided the first experimental confirmation of the everninomicin gene cluster in *M. carbonacea* var *aurantiaca*.

Role of evdN1 in everninomicin biosynthesis

The nitrososynthase, ORF36, of the *M. carbonacea* var *africana* everninomicin gene cluster was previously characterized *in vitro*. Biochemical characterization revealed that ORF36 catalyzes the double oxidation of the amino sugar of everninomicin E to the corresponding nitroso sugar of everninomicin G.[12] In order to characterize the nitrososynthase *in vivo*, we replaced *evdN1* with the apramycin cassette to generate Δ*evdN1*::*aac(3)IV.* Analysis of extracts of this mutant revealed loss of production of full length everninomicins D-G (**1-4)**, but accumulation of everninomicin-2 **(5),** which lacks the nitrosugar (Figure 3-9). Of note, the everninomicin-rosaramicin conjugates were no longer formed due to loss of the hydroxylamino functionality. The structure of Ever-2 was confirmed by mass spectrometric fragmentation (Figure 3-9). Genetic complementation did not result in restored production of wild type everninomicins indicating that, although the replacement was precise, polar effects caused loss of activity of downstream genes. Examination of the everninomicin gene cluster revealed that

the genes for biosynthesis of the nitrosugar cluster in one operon with *evdN1* at the beginning of the operon. Because of polar effects from the gene replacement of the nitrososynthase, we observed complete functional loss of the nitro sugar operon and therefore the A-ring.

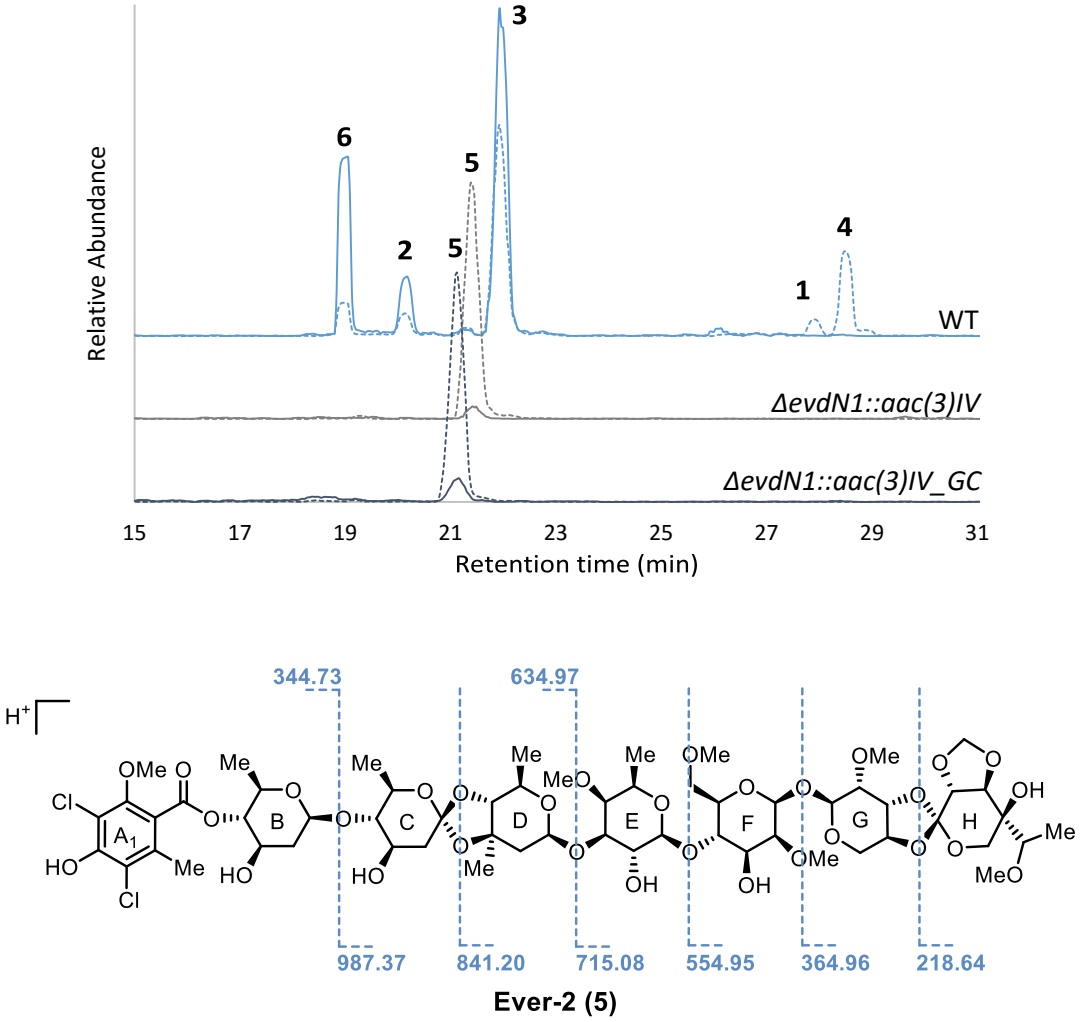

Figure 3-9. LC/MS analysis of wild type *M. carbonacea* var *aurantiaca*, gene replacement of *evdN1* (*ΔevdN1::aac(3)IV*), and genetic complementation of *evdN1* gene replacement (*ΔevdN1::aac(3)IV_GC*). The chromatogram shows summed ion intensities in negative mode and positive mode for everninomicins D–G and the truncated everninomicin-rosaramicin conjugate. Negative mode (dotted lines): ever D (**1**), m/z = 1,534.5 $[M-H]^-$; ever E (**2**), m/z = 1,504.5 $[M-H]^-$; ever F (**3**), m/z = 1,520.5 $[M-H]^-$; and ever G (**4**), m/z = 1,518.5 $[M-H]^-$; conjugate (**6**) 1261.5 $[M-H]^-$; ever-2 (**5**), m/z = 1347.5 $[M-H]^-$. Positive mode (solid lines): ever D, m/z = 1,536.5 $[M+H]^+$; ever E, m/z = 1,506.5 $[M+H]^+$; ever F, m/z = 1,522.5 $[M+H]^+$; and ever G, m/z = 1,520.5 $[M+H]^+$; conjugate 1261.5 $[M+H]^+$; ever-2 (**5**), m/z = 1349.5 $[M+H]^+$.

Role of evdM3 in everninomicin biosynthesis

As stated previously, *evdM3* was proposed to encode a *C*-3methyltransferase with homology to AviG1 from the avilamycin pathway in *S. viridochromogenes Tü57.* Previous *in vitro* work with AviG1 has shown that it is a C-methyltransferase that can complement the activity of EryBIII, a *C*-3-methyltransferase involved in L-mycarose biosynthesis in the erythromycin pathway.[15,25] When AviG1 was deleted in the avilamycin producer, *S. viridochromogenes* the Bechthold group reported abolished production of all avilamycins.[15] However, when *evdM3* was

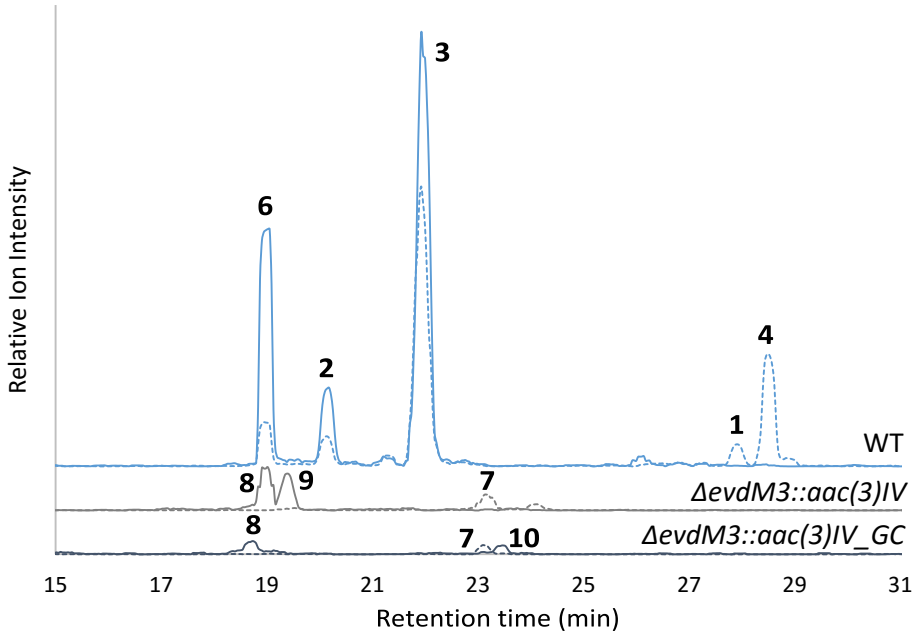

Figure 3-10. LC/MS analysis of wild type *M. carbonacea* var *aurantiaca*, gene replacement of *evdM3* (*ΔevdM3::aac(3)IV*), and genetic complementation of *evdM3* gene replacement (*Δevd3::aac(3)IV_GC*). The chromatogram shows summed ion intensities in negative mode and positive mode for everninomicins D–G and the truncated everninomicin-rosaramicin conjugate. Negative mode (dotted lines): ever D (**1**), m/z = 1,534.5 $[M-H]^-$; ever E (**2**), m/z = 1,504.5 $[M-H]^-$; ever F (**3**), m/z = 1,520.5 $[M-H]^-$; and ever G (**4**), m/z = 1,518.5 $[M-H]^-$; conjugate (**6**) 1261.5 $[M-H]^-$; ever H (**7**), m/z = 1521.5 $[M-H]^-$. Positive mode (solid lines): ever D, m/z = 1,536.5 $[M+H]^+$; ever E, m/z = 1,506.5 $[M+H]^+$; ever F, m/z = 1,522.5 $[M+H]^+$; and ever G, m/z = 1,520.5 $[M+H]^+$; conjugate 1261.5 $[M+H]^+$; ever J (**8**), m/z = 1494.5 $[M+H]^+$; ever K (**9**), m/z= 1508.5 $[M+H]^+$; ever L (**10**), m/z = 1555.5 $[M+H_2O]^+$. Spectra are be located in Figures B-4 – B-8.

inactivated in *M. carbonacea*, three new metabolites accumulated, which we termed everninomicins H, J, and K (Figure 3-10).

Everninomicin H **(7)** is the major metabolite in this mutant strain and its structure was determined by NMR spectroscopy (Table A-3 and Figures A-12-A17) and confirmed by mass

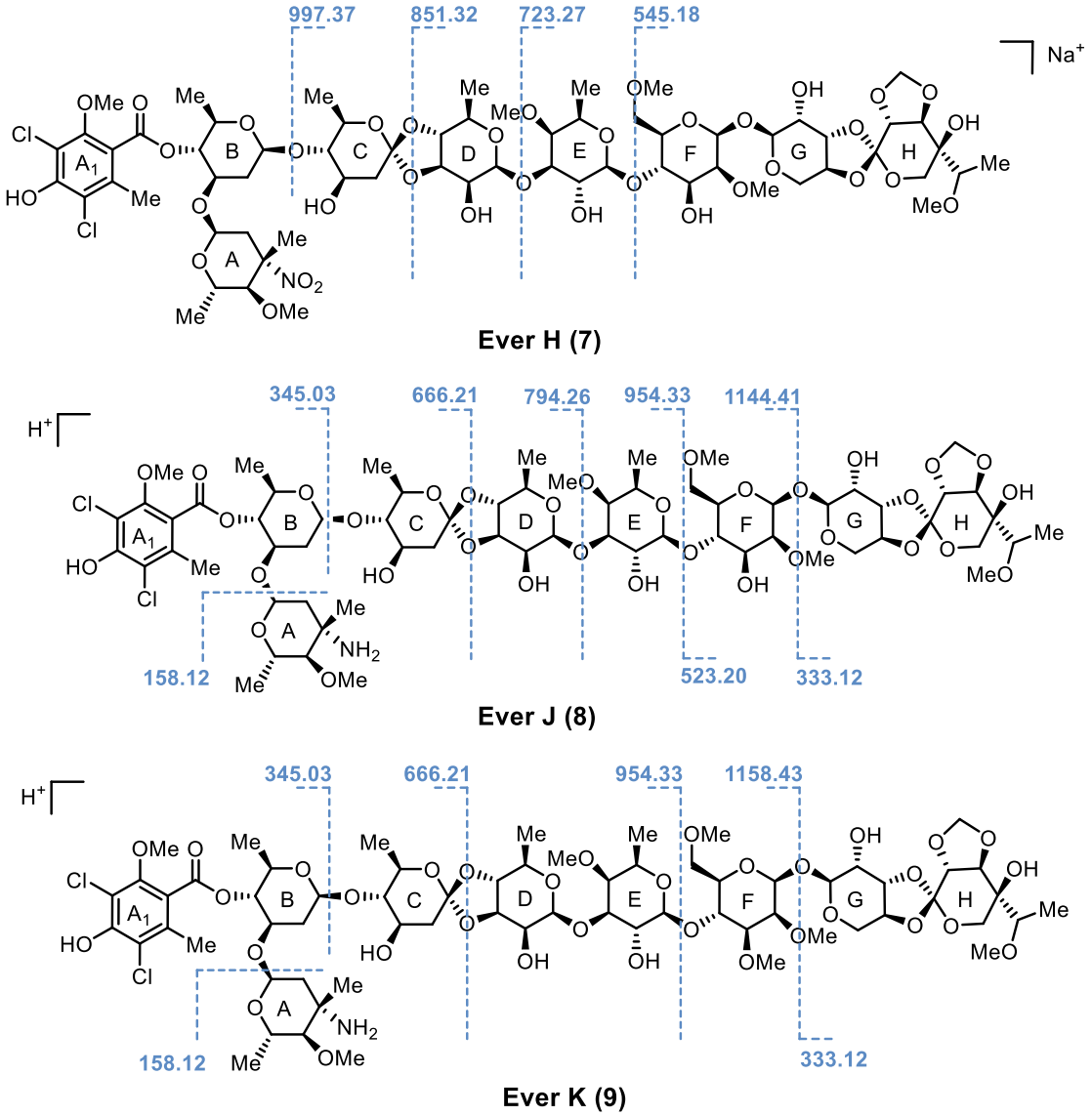

Figure 3-11. Structures of everninomicins H, J, and K as determined by NMR and/or mass spectrometric fragmentation.

spectrometric fragmentation (Figure 3-11). Structural determination of minor metabolites Ever J **(8)** and Ever K **(9)** was accomplished using high-resolution mass spectrometric fragmentation (Figure 3-11). Each of these metabolites lacked the C-3 methyl of the D-ring as well as the *O*-methyl on C-2 of the G-ring. Additionally, a hydroxyl was added to the C-2 position of the D-ring. A hydroxyl in this position has been identified in other everninomicins but was not identified in previous everninomicins produced by *M. carbonacea* var *aurantiaca* (see Chapter II). Directly downstream of *evdM3* is *evdM4* which has homology to *O*-methyltransferases. Likely, polar effects from gene replacement of *evdM3* caused loss of function of *evdM4* in turn resulting in loss of the *O*-methyl on the G-ring. Intriguingly, Ever K gained a methyl on the F-ring which has not been observed before in the everninomicins.

Genetic complementation with *evdM3* resulted in production of a metabolite that we termed Ever L **(10)** that had a mass corresponding to addition of a methyl group (Figure 3-10). Unfortunately, low production levels of Ever L precluded precise structural assignment. However,

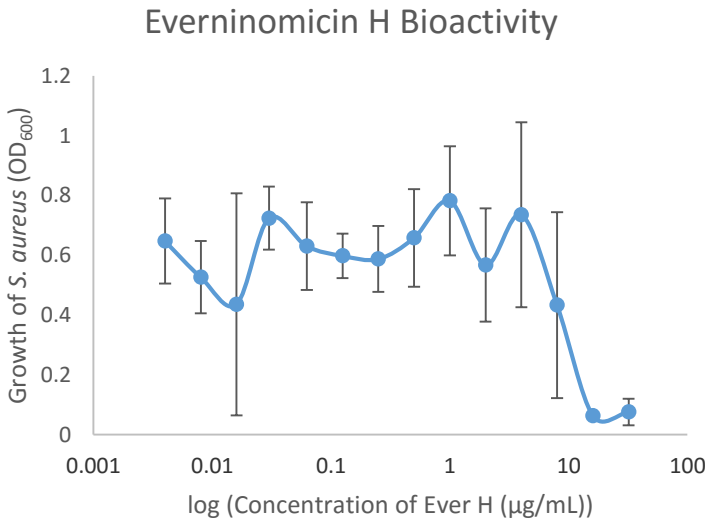

Figure 3-12. The minimal inhibitory concentration of everninomicin H was tested against *S. aureus* subsp. a*ureus Rosenbach*.

as this metabolite only appeared after complementation with the *C*-methyltransferase *evdM3*, it is likely that complementation restored the C-methyl of the D ring. These results are consistent with the predicted function of *evdM3* as a C-3 methyltransferase and with polar effects causing loss of function of *evdM4* that are not restored with genetic complementation of *evdM3*.

Excitingly, everninomicin H maintained activity against *S. aureus* subsp. *aureus Rosenbach* with an MIC of 16 µg/mL (Figure 3-12). Unfortunately, everninomicins J, K, and L were not produced in sufficient quantities to perform bioactivity assays. Although everninomcin H is less potent than everninomicin A (Ziracin™, MIC = 1 µg/mL), it is still moderately active against *S. aureus*, and can provide important information about the structure-activity relationship of the everninomicins.

Role of evdM2 in everninomicin biosynthesis

Based on translated sequence similarities, e*vdM2* encodes a sugar *O*-methyltransferase. To determine the function of this putative methyltransferase, we constructed the gene replacement *ΔevdM2::aac(3)IV*. Upon analysis of the mutant's extracts, we were unable to identify any desmethyl analogs (Figure 3-13). However we did detect the truncated everninomicin-rosaramicin conjugate **(6)**. Unfortunately, genetic complementation with *evdM2* did not restore the production of any additional metabolites. Although we are not able to assign an exact function for EvdM2, sequence similarities and the gene replacement data presented here indicate that EvdM2 installs an *O*-methyl on the eastern side of the molecule, likely the methylene of the methylenedioxy bridge.

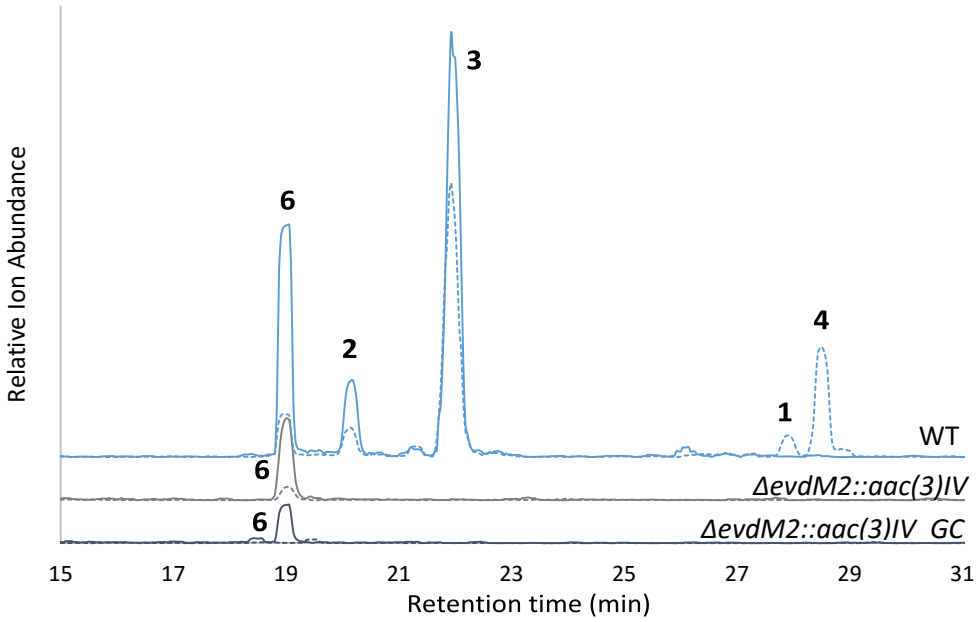

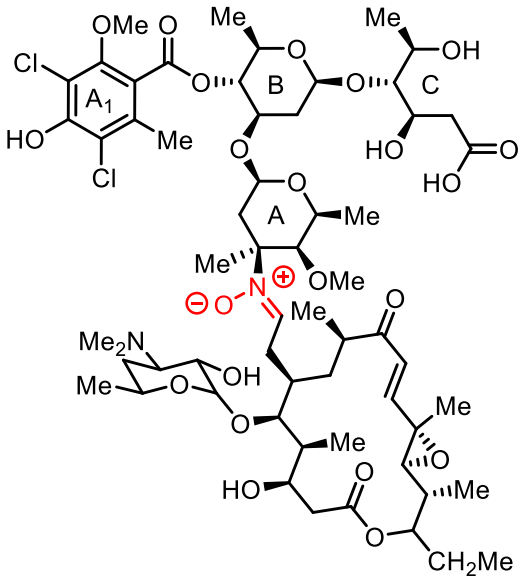

6 Truncated Everninomicin-Rosaramicin

Figure 3-13. LC/MS analysis of wild type *M. carbonacea* var *aurantiaca*, gene replacement of *evdM2* (*ΔevdM2::aac(3)IV*), and genetic complementation of *evdM3* gene replacement (*ΔevdM2::aac(3)IV_GC*) and structure of the truncated everninomicin-rosaramicin conjugate. The chromatogram shows summed ion intensities in negative mode and positive mode for everninomicins D–G and the truncated everninomicin-rosaramicin conjugate. Negative mode (dotted lines): ever D (**1**), m/z = 1,534.5 $[M-H]^-$; ever E (**2**), m/z = 1,504.5 $[M-H]^-$; ever F (**3**), m/z = 1,520.5 $[M-H]^-$; and ever G (**4**), m/z = 1,518.5 $[M-H]^-$; conjugate (**6**), m/z= 1261.5 $[M-H]^-$. Positive mode (solid lines): ever D, m/z = 1,536.5 $[M+H]^+$; ever E, m/z = 1,506.5 $[M+H]^+$; ever F, m/z = 1,522.5 $[M+H]^+$; and ever G, m/z = 1,520.5 $[M+H]^+$; conjugate 1261.5 $[M+H]^+$.

Discussion

Mutability of the evd gene cluster

Targeted gene replacement of *evdN1, evdM3,* and *evdM2* confirmed the role of the *evd* gene cluster in everninomicin biosynthesis as everninomicins D – G were not produced by these mutants. Furthermore, we generated 5 new everninomicin analogs and were able to definitively assign the role of *evdM3* as a C-3 methyltransferase responsible for methylating the C-3 position of the D ring of everninomicin. Notably, polar effects drastically effected downstream genes and resulted in accumulation of unexpected metabolites.

Analysis of the gene replacement mutants revealed that when the first gene in an operon is replaced with the cassette, disruptive polar effects cause loss of function of the entire operon. In the case of *ΔevdN1::aac(3)IV,* replacement of *evdN1,* which encodes a nitrososynthase, resulted in loss of the evernitrose entirely. As evidenced by the fact that everninomicins of various N-oxidation states are produced by the wild type strain, full oxidation of the sugar is not required for glycosylation. Thus, replacement of the nitrososynthase should have yielded the amino sugar. However, as *evdN1* is at the first gene in an operon that encodes the enzymes necessary for evernitrose formation, it is likely that polar effects from the gene replacement disrupted many downstream genes and resulted in abolished production of evernitrose.

Additionally, analysis of the *ΔevdM2::aac(3)IV* mutant revealed loss of the entire eastern portion of the molecule. This result is curious as *evdM2* is proposed to encode an O-methyltransferase, and loss of *evdM2* would be expected to result in a desmethyl compound. However, *evdM2* is also the first gene in an operon that encodes two additional methyltransferases, a glycosyltransferase, and a gene of unknown function. Replacement of

evdM2 with the cassette caused polar effects which resulted in loss of function of downstream genes leading to altered everninomicin production.

Finally, replacement of *evdM3* resulted in the production of three new metabolites, everninomicins H, J, and K. Notably, all of these metabolites are lacking the C-3 methyl of the D ring which is consistent with the proposed function of EvdM3. However, additional modifications were observed, such as hydroxylation of C-2 of the D-ring and loss of the O-methyl from C-2 of the G ring. Intriguingly, the C-3 hydroxyl of the F ring was methylated which has never before been observed in everninomicins. Inspection of the genomic surroundings of *evdM3* provided some insight into one of these unexpected changes. As *evdM3* was not the first gene in the operon, its replacement did not result in entire loss of the operon as replacement of *evdM2* or *evdN1* did. However, directly downstream of *evdM3* is another methyltransferase, *evdM4.* EvdM4 is proposed to be an O-methyltransferase but has no homology to genes in the avilamycin pathways. As the new metabolites are lacking an O-methyl on the G ring and this same position has a different decoration in the avilamycins, it is likely that polar effects resulted in the loss of function of *evdM4,* and that EvdM4 is responsible for methylation of the C-2 hydroxyl of the G ring.

Together these results provide important information about the mutability of the *evd* gene cluster. Foremost, the gene replacement method used here resulted in polar effects which drastically altered everninomicin production in some cases. Although single genes were precisely targeted, many downstream genes were affected by this change to the gene cluster. Future experiments should focus on creating deletions leaving only a small scar sequence as described

by Gust and coworkers[22] to alleviate polar effects. Despite polar effects, the *evd* gene cluster appears to be highly mutable allowing for a variety of changes at different positions.

Insights into Timing and Tolerance in Everninomicin Biosynthesis

The metabolites produced by the gene replacement mutants provided critical information about the tolerance of everninomicin biosynthetic enzymes toward unnatural substrates. Most intriguingly, despite the loss of the methyl group at C-3 of the D ring, the orthoester linkage between the C and D rings was still formed. This result is evidence that the orthoestersynthase can tolerate large changes to its substrate as the loss of a methyl group directly at the site of modification did not affect its enzymatic capabilities. Additionally, other changes to the structure, such as the loss of the O-methyl of the G ring, addition of the O-methyl on the F ring, and loss of evernitrose, were also well tolerated by the glycosyltransferases and other biosynthetic machinery as the structure was still fully assembled and elaborated.

Analysis of the structures can also provide information about timing of orthosomycin biosynthesis. Specifically, as Ever-2 is a fully elaborated heptasaccharide lacking only evernitrose, this nitrosugar must be the last sugar residue to be attached to the oligosaccharide chain. Additionally, the 1,1-linkage between rings F and G must be assembled first to provide the appropriate glycosyl acceptor for addition of subsequent sugar residues. After coupling of the F and G rings, the chain would then be assembled from this bidirectional glycosyl acceptor terminating with addition of evernitrose.

This ability to generate new everninomicin analogs by manipulation of the *evd* gene cluster will prove essential for structure-activity relationship studies. Excitingly, the biosynthetic

machinery tolerates changes to their natural substrates allowing for the generation of new congeners. Moreover, at least one of the new analogs retained activity against *S. aureus*. Using the method described here, many more everninomicin analogs can be generated which will provide a deeper understanding of the structure-activity relationship of the everninomicins.

Conclusions

The work described here provides the first functional analysis of the everninomicin gene cluster (*evd*) from *M. carbonacea* var *aurantiaca.* Replacement of three individual genes with an apramycin resistance cassette resulted in loss of production of everninomicins D-G thus confirming the role of this gene cluster in everninomicin biosynthesis. Moreover, a total of five new analogs were generated as a result of these gene replacements. Notably, at least one of the new analogs retained biological activity against *S. aureus*. These results confirm the utility of this method as a means to make novel everninomicin congeners with improved efficacy.

Acknowledgements

This work was contributed to by Emilianne K. McCranie, Kasia Derewacz, Jeffrey Spraggins, and Brian O. Bachmann. E.K.M. annotated all three orthosomycin gene clusters, constructed gene replacements, performed genetic complementation, analyzed metabolites, and performed bioactivity testing. K.D. isolated and solved the structure of everninomicin H. J.S. performed mass spectral analysis of everninomicins J, K, and L. B.O.B. supervised all experiments and analysis of data. We thank Yu Du for training in the two-step gene replacement method.

References

1. Newman, D. J. & Cragg, G. M. Natural products as sources of new drugs over the 30 years from 1981 to 2010. *J Nat Prod* **75**, 311-335 (2012).
2. Foster, D. R. & Rybak, M. J. Pharmacologic and bacteriologic properties of SCH-27899 (Ziracin), an investigational antibiotic from the everninomicin family. *Pharmacotherapy* **19**, 1111-1117 (1999).
3. Ganguly, A. K. Ziracin, a novel oligosaccharide antibiotic. *J Antibiot* **53**, 1038-1044 (2000).
4. Ganguly, A. K., McCormick, J. L., Saksena, A. K., Das, P. D. & Chan, T. Chemical Modifications and Structure Activity Studies of Ziracin and Related Everninomicin Antibiotics. *Bioorg Med Chem Lett* **9**, 1209-1214 (1999).
5. Luedemann, G. M., Ridge, G., Weinstein, M.J. Everninomicin Antibiotics and Method for the Manufacture Thereof. USA patent 3,499,078 (1970).
6. Nicolaou, K. C., Mitchell, H. J., Rodriguez, R. M., Fylaktakidou, K. C. & Suzuki, H. Total Synthesis of Everninomicin 13,384-1-Part 3: Synthesis of the DE Fragment and Completion of the Total Synthesis. *Angew Chem Int Ed Engl* **38**, 3345-3350 (1999).
7. Nicolaou, K. C., Mitchell, H.J., Suzuki, H., Rodriguez, R.M., Baudoin, O. & Fylaktakidou, K.C. Total Synthesis of Everninomicin 13,384-1-Part 1: Synthesis of the A(1)B(A)C Fragment. *Angew Chem Int Ed Engl* **38**, 3334-3339 (1999).
8. Nicolaou, K. C., Rodriguez, R. M., Fylaktakidou, K. C., Suzuki, H. & Mitchell, H. J. Total Synthesis of Everninomicin 13,384-1-Part 2: Synthesis of the FGHA(2) Fragment. *Angew Chem Int Ed Engl* **38**, 3340-3345 (1999).
9. CLSI. *Methods for Dilution Antimicrobial Susceptibility Tests for Bacteria that Grow Aerobically; Approved Standard - Ninth Edition.*, Vol. CLSI document M07-A9 (Clinical and Laboratory Standards Institute, 2012).
10. Weitnauer, G., Muhlenweg, A., Trefzer, A., Hoffmeister, G., Sussmith, R.D., Jug, G., Welzel, K., Vente, A., Girreser, U. & Bechthold, A. Biosynthesis of the orthosomycin antibiotic avilamycin A: deductions from the molecular analysis of the *avi* biosynthetic gene cluster of *Streptomyces viridochromogenes* Tu57 and production of new antibiotics. *Chem Biol* **8**, 569-581 (2001).
11. Boll, R., Hofmann, C., Heitmann, B., Hauser, G., Glaser, S., Koslowski, T., Friedrich, T. & Bechthold, A. The active conformation of avilamycin A is conferred by AviX12, a radical AdoMet enzyme. *J Biol Chem* **281**, 14756-14763 (2006).
12. Hu, Y., Al-Mestarihi, A., Grimes, C. L., Kahne, D. & Bachmann, B. O. A unifying nitrososynthase involved in nitrosugar biosynthesis. *J Am Chem Soc* **130**, 15756-15757 (2008).

13. Vey, J. L., Al-Mestarihi, A., Hu, Y., Funk, M.A., Bachmann, B.O. & Iverson, T.M. Structure and mechanism of ORF36, an amino sugar oxidizing enzyme in everninomicin biosynthesis. *Biochemistry* **49**, 9306-9317 (2010).
14. Hofmann, C., Boll, R., Heitmann, B., Hauser, G., Durr, C., Frerich, A., Weitnauer, G., Glaser, S.J. & Bechthold, A. Genes encoding enzymes responsible for biosynthesis of L-lyxose and attachment of eurekanate during avilamycin biosynthesis. *Chem Biol* **12**, 1137-1143 (2005).
15. Weitnauer, G., Gaisser, S., Kellenberger, L., Leadlay, P. F. & Bechthold, A. Analysis of a C-methyltransferase gene (aviG1) involved in avilamycin biosynthesis in Streptomyces viridochromogenes Tu57 and complementation of a Saccharopolyspora erythraea eryBIII mutant by aviG1. *Microbiology* **148**, 373-379 (2002).
16. Weitnauer, G., Hauser, G., Hofmann, C., Linder, U., Boll, R., Pelz, K., Glaser, S.J. & Bechthold, A. Novel avilamycin derivatives with improved polarity generated by targeted gene disruption. *Chem Biol* **11**, 1403-1411 (2004).
17. Treede, I., Jakobsen, L. Kirpekar, F., Vester, B., Weitnauer, G., Bechthold, A. & Douthwaite, S. The avilamycin resistance determinants AviRa and AviRb methylate 23S rRNA at the guanosine 2535 base and the uridine 2479 ribose. *Mol Microbiol* **49**, 309-318 (2003).
18. Rebets, Y., Boll, R., Horbal, L., Fedorenko, V. & Bechthold, A. Production of avilamycin A is regulated by AviC1 and AviC2, two transcriptional activators. *J Antibiot* **62**, 461-464 (2009).
19. Treede, I., Hauser, G., Muhlenweg, A., Hofmann, C., Schmidt, M., Weitnauer, G., Glaser, S. & Bechthold, A. Genes involved in formation and attachment of a two-carbon chain as a component of eurekanate, a branched-chain sugar moiety of avilamycin A. *Appl Environ Microbiol* **71**, 400-406 (2005).
20. Gust, B., Challis, G. L., Fowler, K., Kieser, T. & Chater, K. F. PCR-targeted Streptomyces gene replacement identifies a protein domain needed for biosynthesis of the sesquiterpene soil odor geosmin. *Proc Nat Acad Sci USA* **100**, 1541-1546 (2003).
21. Yu, D., Ellis, H.M., Lee, E.C., Jenkins, N.A., Copeland, N.G. & Court, D.L. An efficient recombination system for chromosome engineering in Escherichia coli. *Proc Nat Acad Sci USA* **97**, 5978-5983 (2000).
22. Gust, B., Chandra, G., Jakimowicz, D., Yuqing, T., Bruton, C.J. & Chater, K.F. Lambda red-mediated genetic manipulation of antibiotic-producing Streptomyces. *Adv Appl Microbiol* **54**, 107-128 (2004).
23. T. Kieser, M. J. B., M.J. Buttner, K.F. Chater, and D.A. Hopwood. *Practical Streptomyces Genetics*. (John Innes Foundation. , 2000).
24. Gavrish, E., Bollmann, A., Epstein, S. & Lewis, K. A trap for in situ cultivation of filamentous actinobacteria. *J Microbiol Meth* **72**, 257-262 (2008).

25. Gaisser, S., Bohm, G.A., Doumith, M., Raynal, M.C., Dhillon, N., Cortes, J. & Leadlay, P.F. Analysis of eryBI, eryBIII and eryBVII from the erythromycin biosynthetic gene cluster in Saccharopolyspora erythraea. *Mol Gen Genet* **258**, 78-88 (1998).

CHAPTER IV

ROLE OF A CONSERVED GROUP OF OXYGENASES IN THE FORMATION OF THE ORTHOESTER LINKAGES AND METHYLENEDIOXY BRIDGES OF THE ORTHOSOMYCINS

*Portions of this chapter are reproduced from "Oxidative cyclizations in orthosomycin biosynthesis expand the known chemistry of an oxygenase superfamily." Proc Nat Acad Sci USA **112**, 11547-11552 (2015) by McCulloch, K. M., McCranie, E.K., Smith, J.A., Sarwar, M., Mathieu, J.L., Gitschlag, B.L., Du, Y., Bachmann, B.O. & Iverson, T.M.*

Introduction

As the everninomicins are therapeutically promising as broad spectrum antibacterial agents, it is necessary that we understand the characteristics that contribute to their potency. We hypothesize that the orthosomycins are uniquely tailored for their bacterial targets, and particularly, we are interested in the impact of the orthoester linkages and the methylenedioxy bridge on everninomicin activity. Prior to this study, the enzymes responsible for formation of the unique oxidative features of the orthosomycins were unknown.

Orthoester linkages are a defining hallmark of the orthosomycins. However little is known about the biosynthesis of these compounds. In their original analysis of the avilamycin gene cluster, Bechthold and coworkers identified three genes, *aviO1, aviO2*, and *aviO3* which they proposed encoded oxygenases. Based on sequence similarity to known α-ketoglutarate dependent oxygenases and the presence of the HxD motif conserved among this family of oxidases, Bechthold and coworkers hypothesized that these were indeed α-ketoglutarate dependent oxidases and were responsible for formation of the orthoester linkages and

methylenedioxy bridge of avilamycin.[1] While inactivation of *aviO1* and *aviO3* resulted in abolished avilamycin production, inactivation of *aviO2* resulted in the accumulation of another metabolite. Based on their identification of this new metabolite, the researchers concluded that *aviO2* is responsible for attachment of the acetyl moiety to ring H.[2] However, as an α-ketoglutarate dependent oxidase is unlikely to catalyze acetylation and the homologous oxygenase is present in the everninomicin pathway despite the absence of an acetyl group on everninomicin congers, an alternative interpretation of the function of *aviO2* is that the oxidative ring closure is required for substrate recognition by the acetylating enzyme.

Methylenedioxy bridges are found in a variety of bacterial and plant metabolites. Methylenedioxy bridges found in plant metabolites are the result of oxidation by cytochrome P450-dependent enzymes.[3,4] Additionally, the methylenedioxy bridges of plant metabolites are associated exclusively with aromatic rings. Hygromycin A (produced by *S. hygroscopicus* but structurally unrelated to hygromycin B), dioxapyrrolomycin produced by *S. fumanus*, and xantholipin produced by *S. flavogriseus*, all contain a methylenedioxy bridge that is formed first by a SAM-dependent methylation event and subsequent oxidation.[3-6] These results suggest that likewise the methylenedioxy bridge of the orthosomycins are formed by methylation and subsequent oxidative cyclization. The oxidase from the hygromycin A pathway has been identified as a member of the metallo-dependent hydrolase superfamily.[5] However, neither a P450-dependent enzyme nor metallo-dependent hydrolase were found in any of the orthosomycin gene clusters. Therefore the methylenedioxy bridge oxidation chemistry of everninomicin represents a novel method of forming methylenedioxy bridges.

To understand the formation of the orthoester linkages and methylenedioxy bridges of the orthosomycins, we conducted phylogenetic analysis of putative oxygenases in the pathways, constructed gene replacements of oxygenases in the *evd* gene cluster, and determined crystal structures of oxygenases from each subfamily, including a costructure of one oxygenase in complex with product. Together these data provide strong evidence that this conserved family of oxygenases in the orthosomycin gene clusters is responsible for the formation of their unique oxidative features.

Methods

Phylogenetic analysis

Sequences of oxygenases from each of the known orthosomycin pathways and related oxidases were analyzed with MEGA 5 using the neighbor-joining statistical method. Test of phylogeny was the bootstrap method with 1000 replicates.

Bacterial culture conditions

E. coli strains were grown in LB broth. *M. carbonacea var aurantiaca* NRRL 2997 and replacement mutants were grown on TSB (Oxoid™ Tryptone Soy Broth) agar and in TSB liquid. Intergeneric conjugations were performed on solid AS1 media (0.1 % yeast extract, 0.5 % soluble starch, 0.02 % L-alanine, 0.02 % L-arginine, 0.05 % L-asparagine, 0.25 % NaCl, 1 % Na_2SO_4, 2 % agarose at pH 7.5, supplemented with 10 mM $MgCl_2$). Apramycin (50 μg/ml), nalidixic acid (12.5 μg/ml), chloramphenicol (30 μg/ml), and kanamycin (50 μg/ml) were used when required for selection as described below.

Construction and analysis of gene replacement mutants

The genes *evdO1*, *evdO2*, and *evdMO1* were individually deleted in *M. carbonacea* var *aurantiaca* using a modification of the PCR-targeted Streptomyces gene-replacement strategy described in detail in Chapter III. The gene replacement cassette containing the *aac(3)IV* resistance marker, *oriT*, and flippase recombinase target (FRT) regions was amplified by PCR using primers EvdO1-Red-F and EvdO1-Red-R for the *evdO1* gene replacement, EvdO2-Red-F and EvdO2-Red-R for the *evdO2* gene replacement, and EvdMO1-Red-F and EvdMO1-Red-R for the *evdMO1* gene replacement (primer sequences are found in Table 4-1). PCR products were then directly transformed via electroporation into the arabinose-induced strain *E. coli*

Primer Name	Purpose	Sequence (5'-3')
EvdO1-Red-For	*ΔevdO1::aac(3)IV*	CGGGCCCGCGACCGCTGATCAGAAGGGTGT GGACTGATGATTCCGGGGATCCGTCGACC
EvdO1-Red-Rev	*ΔevdO1::aac(3)IV*	CTGTCGCCCGGAACGCTCATCGGATGCCCCCC GAGCTCATGTAGGCTGGAGCTGCTTC
EvdO2-Red-For	*ΔevdO2::aac(3)IV*	TCGTGACTGTCGAGGTCATCCCTTGAAGGAG ACGGCATGATTCCGGGGATCCGTCGACC
EvdO2-Red-Rev	*ΔevdO2::aac(3)IV*	TGGCCTTCTTCGGGTAGGGGGGCGTGGTCGG GCCGGCTATGTAGGCTGGAGCTGCTTC
EvdMO1-Red-For	*ΔevdMO1::aac(3)IV*	TTTCCCGCGCGCACCCGAACACTAGGCTTGG AATCCATGATTCCGGGGATCCGTCGACC
EvdMO1-Red-Rev	*ΔevdMO1::aac(3)IV*	GTGGGGTCGCCGCAGGCGGCATCCGCGTCCG GCCGGTCATGTAGGCTGGAGCTGCTTC
AprUp	Confirm Gene Replacements	ATTCCGGGGATCCGTCGACC
AprDn	Confirm Gene Replacements	TGTAGGCTGGAGCTGCTTC
NeoUp	Confirm Gene Replacements	TGAATGAACTGCAGGACGAG
NeoDn	Confirm Gene Replacements	AATATCACGGGTAGCCAA
EvdO1-Southern-For	EvdO1 Southern Probe	TCAGTCCACACCCTTCTGAT
EvdO1-Southern-Rev	EvdO1 Southern Probe	GGCCTGTACCTGATGACGAG
EvdO2-Southern-For	EvdO2 Southern Probe	TGCTGCACTGTCGTTCCTAC
EvdO2-Southern-Rev	EvdO2 Southern Probe	ATACCAGCGCTTTCACGAGT
EvdMO1-Southern-For	EvdMO1 Southern Probe	GTATGGCTCACTGCCTGGTC
EvdMO1-Southern-Rev	EvdOM1 Southern Probe	GGTGCACGATCGGATGAT
Apr-Southern-For	Apramycin Southern Probe	ACCGACTGGACCTTCCTTCT
Apr-Southern-Rev	Apramycin Southern Probe	TCGCTATAATGACCCCGAAG
EvdMO1-GC-For	EvdMO1 Genetic Complementation	CATATGATGGACCGTAGGGAGATTCA
EvMO1-GC-Rev	EvdMO1 Genetic Complementation	GATATCTCAGGACGGGAGGCTCG

Table 4-1. Sequences of primers used in this study.

BW25113/pIJ790 containing cosmid CA in which gene replacement of *evdO1*, *evdO2*, or *evdMO1* was enabled via λ Red-mediated homologous recombination. The resultant cosmids were transformed via electroporation into the non-methylating *E. coli* strain ET12567 containing plasmid pUZ8002, which contains the genes necessary for conjugal transfer of the cosmid. The gene replacements in *E. coli* were maintained at 37 °C in liquid LB medium containing kanamycin, apramycin, and chloramphenicol.

Construction of gene replacements in M. carbonacea was performed as described in Chapter III using the genetic manipulation methods described in Chapter II. After 7-9 days of incubation at 30 °C, membranes were removed and colonies were streaked onto TSB plates containing apramycin. Double-crossover mutants were identified by PCR amplification of kanamycin and apramycin resistance genes using primers Apr-For and Apr-Rev for amplifying the apramycin resistance gene and Neo-For and Neo-Rev for amplifying the kanamycin resistance gene (sequences of primers found in table 4-1). Double-crossover mutants in *M. carbonacea* were confirmed by Southern hybridization. Gene specific probes were designed upstream of the genes of interest (primer sequences can be found in table 4-1). The *evdO1* probe (785 bp) was amplified using primers EvdO1- Southern-For and EvdO1-Southern-Rev. The *evdO2* probe (719 bp) was amplified using primers EvdO2-Southern-For and EvdO2-Southern-Rev. The *evdMO1* probe (798 bp) was amplified using primers EvdMO1-Southern-For and EvdMO1-Southern-Rev. An apramycin cassette probe was designed that hybridized to the apramycin resistance gene. The apramycin probe (884 bp) was amplified using primers: Apr-Southern-For and Apr-Southern-Rev. All probes were labeled with digoxigenin (DIG) using DIG High Prime DNA Labeling and Detection Starter Kit II (catalog no. 11585614910; Roche). Hybridization and detection were performed

using the aforementioned DIG Starter Kit. Everninomicins produced by the mutant strains were produced and analyzed via HPLC/MS as described in Chapters II and III.

Genetic Complementation of Oxygenase Replacements

Genetic complementation was performed as described in Chapter III. For complementation of *ΔevdO1::aac(3)IV*, an additional plasmid was ordered from Mutagenex that included *evdO1* cloned into the EcoRV and EcoRI sites of pSET152ermE to generate pSET152ermE+evdO1. For complementation of *ΔevdOM1::aac(3)IV*, *evdMO1* was amplified by PCR using primers EvdMO1-GC-For and EvdMO1-GC-Rev (sequences can be found in table 4-1). The PCR product was subsequently cloned into the NdeI and EcoRV sites of pSET152ermE.

Protein Expression and Purification

All genes were synthesized (Mr. Gene for EvdO1 and EvdO2, Genscript for AviO1, GeneArt for HygX) and subcloned into either pET28a(+) (EvdO1, EvdO2, HygX) or pET23 (AviO1). The resulting vector transformed into *E. coli* BL21(DE3). Cultures were grown at 37 °C in LB (40 µg/mL kanamycin) with shaking to an OD_{600} of 0.4, when the temperature was lowered to 18 °C. Protein expression was induced 45 min later at an OD_{600} of 0.6–0.9 by the addition of 0.5 mM IPTG. The cultures continued to shake at low temperature for 16 h and then were harvested by centrifugation at 5,000 × g for 15 min and stored at −20 °C. Cell pellets were thawed and resuspended in 15 mL of lysis buffer (50 mM NaH_2PO_4, 300 mM NaCl, 10 mM imidazole; pH 8.0) per liter of culture and supplemented with one Complete EDTA-free protease inhibitor mixture tablet (Roche Applied Science). The sample was lysed by sonication. After cell lysis, all purification

steps were performed at 4 °C. Crude lysate was clarified by centrifugation at 40,000 × g for 1 h. The supernatant was passed over a Ni-NTA column (Qiagen) equilibrated with lysis buffer. The column was then washed with lysis buffer containing 20 mM imidazole. Protein was eluted using lysis buffer with 250 mM imidazole and immediately diluted 1:1 with lysis buffer. The sample was dialyzed into storage buffer (25 mM Tris, 75 mM NaCl at pH 7.4). To incorporate Fe^{2+}, HygX was first incubated with 0.5 mM EDTA for 1 h to remove any Ni^{2+} and then dialyzed extensively against PBS. The sample was then buffer-exchanged to 50 mM Mops (pH 7.0) using a PD-10 column (GE Healthcare Life Sciences). $(NH_4)_2Fe(SO_4)_2$ was added to a final concentration of 1 mM and allowed to incubate for 30 min. The sample was then run over the PD-10 column to remove excess iron. HygX-Fe was concentrated to 12 mg/mL, flash frozen, and stored at −80 °C. The histidine tag was removed from EvdO2 and AviO1 before crystallization. Thrombin (20 U) was added and incubated overnight at 4 °C to remove the N-terminal hexahistidine tag. Cleaved proteins were passed over a Ni-NTA column to separate unprocessed sample, and the flow-through was collected. Samples were further purified through size-exclusion chromatography on a Superdex 200 10/300 GL column equilibrated in storage buffer. Fractions were analyzed using SDS/PAGE, pooled, and concentrated to 18 mg/mL (EvdO1), 6 mg/mL (EvdO2), 16 mg/mL (AviO1), or 16 mg/mL (HygX). Proteins were flash-frozen and stored at −80 °C in aliquots.

Tryptophan Fluorescence Quenching Assay

The K_d of hygromycin B binding to HygX was determined by monitoring the quenching of intrinsic fluorescence from the single tryptophan residue of HygX upon hygromycin B binding. Using a Cary Eclipse Varian fluorescence spectrometer, sample fluorescence was measured at 20

°C with both emission and excitation slits set at 10 nm and detector voltage set to 800 V. The emission wavelength was set to 280 nm, and spectra collected were from 300 to 400 nm, with 350 nm used for calculating binding affinity. Each sample contained 990 µL of 0.5 µM HygX in 25 mM Tris (pH 7.4), 75 mM NaCl, 0.05 mM AKG, and 0.05 mM $NiCl_2$, which was then mixed with 10 µL of hygromycin B (diluted in the above buffer) of varying concentrations. Spectra were measured in triplicate, and the experiment repeated three times. Because hygromycin B at higher concentrations has background fluorescence between 300 and 400 nm, the experiment was repeated using only buffer and subtracted from the measurement taken with HygX present. Change in fluorescence resulting from changing hygromycin B concentration was plotted against hygromycin B concentration and fit to a single binding-site model using Kaleidagraph Version 4.0.

Crystallization

Crystals were grown using the hanging-drop vapor diffusion method at room temperature in 3-µL drops containing an equal ratio of protein to reservoir solution. Crystals of EvdO1 (18 mg/mL in storage buffer plus 0.4 mM $NiCl_2$) appeared after 3 d with a reservoir solution of 100 mM sodium citrate tribasic (pH 5.1) and 13% (wt/wt) PEG8000. EvdO2 (6 mg/mL in storage buffer) crystallized in 100 mM imidazole (pH 8.0), 38% (wt/wt) PEG8000, and 250 mM NaCl. The EvdO2-AKG cocrystals used fully formed EvdO2 crystals soaked with freshly prepared 200 mM AKG in 100 mM imidazole (pH 8.0). AviO1 (16 mg/mL in storage buffer) crystallized in 100 mM CAPS (pH 10.5), 1.2 M NaH_2PO_4, 0.8 M K_2HPO_4, and 200 mM Li_2SO_4. HygX (16 mg/mL in storage buffer) crystallized from 100 mM Bis-Tris (pH 6.8), 100 mM MgCl2, and 12% (wt/wt) PEG8000. HygX-AKG crystals were grown by incubating HygX (16 mg/mL in storage buffer) with 3 mM AKG

for 30 min before setting up drops; crystallization conditions consisted of 50 mM CsCl, 100 mM Mes (pH 6.5), and 30% (wt/wt) Jeffamine M-600. HygX–AKG–hygromycin B crystals were grown from HygX (16 mg/mL in storage buffer plus 1 mM $NiCl_2$, 3 mM AKG, and 5 mM hygromycin B) using a reservoir containing 100 mM Mes (pH 6.3) and 18% (wt/wt) PEG20000. HygX-Fe crystallized in 0.6 M succinic acid (pH ~7). All crystals except those grown from Jeffamine M-600 were cryoprotected by creating an artificial mother liquor of the reservoir solution containing a cryoprotectant and soaking the crystals for one minute before cryocooling by plunging into liquid nitrogen. For EvdO1 and AviO1, the crystallization conditions were supplemented by 20% of a 50/50 (vol/vol) glycerol/ethylene glycol mix. For EvdO2 and HygX, the crystallization conditions were supplemented 17% (vol/vol) ethylene glycol.

Crystallographic Data Collection, Processing, Structure Determination, and Refinement

Diffraction data were collected on the LS-CAT beamlines of the Advanced Photon Source (Argonne, IL) on Mar300 CCD detectors. All data were processed and scaled using the HKL2000 suite of programs[7]. Structures of EvdO1, AviO1, and HygX were determined through single wavelength anomalous diffraction (SAD)-phasing from anomalous signal from bound nickel ions using data collected in wedges at 1.484 Å. This wavelength was experimentally determined using X-ray fluorescence scans around the Fe and Ni K-edges using an XFlash 1001 SD detector (Bruker-AXS). The HygX-Fe^{2+} dataset was collected at 1.739 Å, a wavelength identified through X-ray fluorescence scans as maximizing the anomalous signal from Fe^{2+}. Nickel-binding sites were determined using the program HKL2MAP and SHELXC/D/E[8,9] and input into the AutoSol routine of PHENIX for phasing and density modification.[10] EvdO2 was determined using molecular

replacement with PHASER.[11,12] To develop the search model for EvdO2, human phytanoyl-CoA dioxygenase phyhd1 (PDB code 3OBZ) was structurally aligned with human phytanoyl-CoA (PDB code 2A1X), and all nonconserved secondary structure, ligands and water molecules were removed. Costructures of EvdO2 with AKG and HygX with hygromycin B were determined by isomorphous replacement from the unliganded structure. All structures were improved using AutoBuild of PHENIX.[11,13] Model building was performed in COOT[14] with composite omit maps calculated in CNS.[15] Refinement was performed using phenix.refine.[16] The costructure of HygX–AKG–hygromycin B contains significant disorder at the N termini in two of the four protomers. Omit maps and additional refinement with strict restraints were used to minimize model bias during refinement of this structure. Importantly, clear electron density of a quality expected for a 1.6-Å resolution structure are observed for two chains and these were the chains used for computational docking controls and all figures.

Results

Analysis of Oxygenases from Orthosomycin Clusters

Using translated sequence similarities, we have identified 13 open reading frames from five orthosomycin gene clusters that putatively encode non-heme iron, α-ketoglutarate dependent oxygenases among five orthosomycin gene clusters. The number of putative oxygenases directly correlates with how many anticipated oxidative cyclizations are required for orthoester linkage and methylenedioxy bridge formation in each orthosomycin. The everninomicin and avilamycin gene clusters each contain three of these oxygenases which correspond to the two orthoester linkages and the methylenedioxy bridge found in each

molecule. Conversely, only one of these putative oxygenases was found in the biosynthetic cluster for hygromycin B which only contains one orthoester linkage. Furthermore, these are the only enzymes within each gene cluster that appear to have sufficient catalytic capacity for these oxidations.

Phylogenetic analysis of the thirteen orthosomycin-associated oxygenases revealed that they form a distinct subfamily of non-heme iron, α-ketoglutarate dependent oxygenases most closely related to the phytanoyl-CoA 2-hydroxylase (PhyH) subfamily (Figure 4-1). The PhyH subfamily encodes enzymes with varying enzymatic capabilities including halogenations, dioxygenations, and hydroxylations.[17-20] The orthosomycin-associated oxygenase subfamily can be further separated into subgroups. Three subgroups contain one oxygenase from each of the

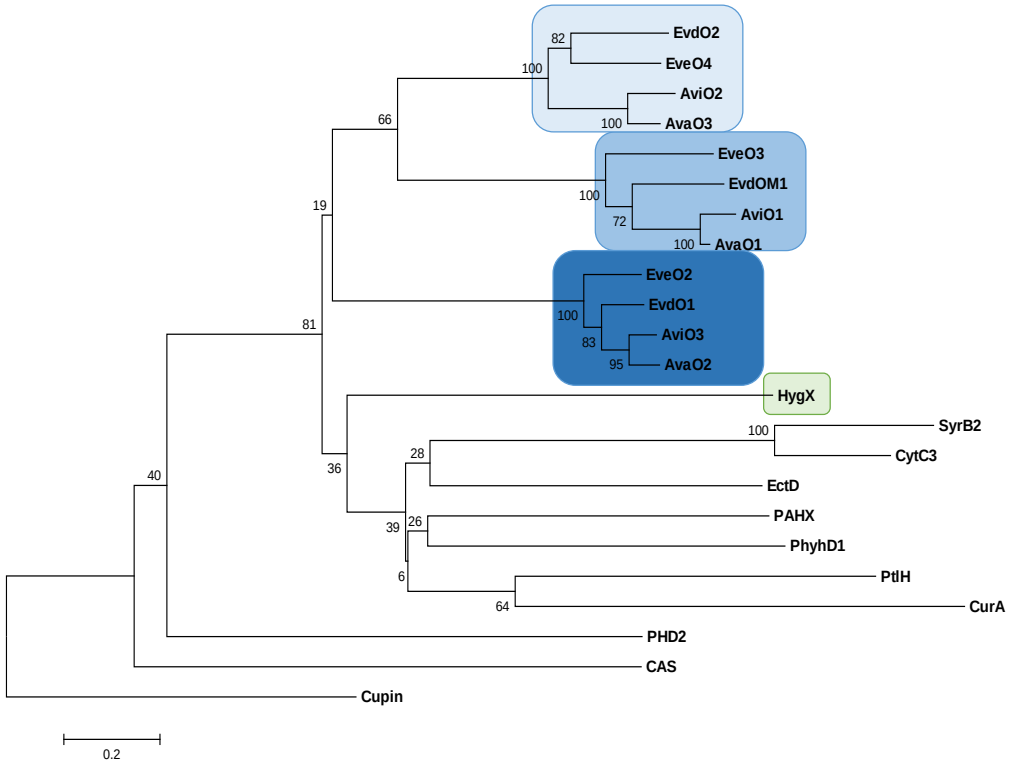

Figure 4-1. Phylogenetic analysis of orthosomycin-associated oxygenases. Analysis was conducted using MEGA 5 as described in the methods section. Class I orthosomycin-associated oxygenases formed three distinct group with each group containing one oxygenase from each pathway. The Class II-associated oxygenase, HygX, did not cluster with the others oxygenases. Adapted from *Proc Nat Acad Sci USA* **112**, 11547-11552 (2015).[25]

avilamycin and everninomicin gene clusters. The fourth subgroup contains only HygX from the hygromycin gene cluster. Sequence identity between enzymes of different subgroups is 22-43% which is consistent with a related mechanism but different substrates. Enzymes belonging to the same subgroup have much higher sequence identities of 65-93%. This high sequence identity suggests that oxygenases within subgroups catalyze the same reaction on closely related substrates. Sequence identities can be found in Table 4-2.

Oxygenase Requirement for Everninomicin Biosynthesis

In order to determine the role of the putative oxygenases in orthosomycin biosynthesis, we created gene replacements of *evdO1*, *evdO2,* and *evdMO1* from the everninomicin pathway in *M. carbonacea* var *aurantiaca*. Targeted gene replacements of *evdO1, evdO2,* and *evMO1* were

	EvdO1	**EveO2**	**AvaO2**	**AviO3**	**EvdO2**	**EveO3**	**AvaO3**	**AviO2**	**EvdMO1**	**EveO1**	**AviO1**	**AvaO1**	**HygX**
EvdO1	---	70	73	73	26	24	24	23	26	30	28	28	24
EveO2	70	---	73	75	23	26	23	22	24	27	30	30	24
AvaO2	73	73	---	89	26	23	25	25	24	25	29	29	25
AviO3	73	75	89	---	24	35	43	27	23	25	29	30	23
EvdO2	26	23	26	24	---	71	66	66	29	30	29	30	36
EveO3	24	26	23	35	71	---	69	69	31	29	31	30	29
AvaO3	24	23	25	43	66	69	---	88	30	30	31	30	28
AviO2	23	22	25	27	66	69	88	---	32	36	32	32	28
EvdMO1	26	24	24	23	29	31	30	32	---	73	74	72	29
EveO3	30	27	25	25	30	29	30	36	73	---	66	65	28
AviO1	28	30	29	29	29	31	31	32	74	66	---	93	32
AvaO1	28	30	29	30	30	30	30	32	72	65	93	---	35
HygX	24	24	25	23	36	29	28	28	29	28	32	35	---

Table 4-2. Comparison of sequence identities (% identity) among the 13 orthosomycin-associated oxygenases. Using BLAST analysis, sequence identities for all possible pairs of oxygenases were calculated. Everninomicin- and avilamycin-associated oxygenases form three distinct groups with sequence identities of greater than 65%. Sequence identities among groups drops to less than 43%. HygX does not group with the class I orthosomycin-associated oxygenases. Adapted from *Proc Nat Acad Sci USA* **112**, 11547-11552 (2015).[25]

accomplished using a two-step PCR targeting strategy described in Chapter III. To select for double crossover mutants, exconjugants that were apramycin resistant and kanamycin sensitive were chosen for further analysis. These mutant strains were then analyzed via PCR amplification of the apramycin and kanamycin resistance genes to verify the double-crossover. Using this method of verification, *evdO1, evdO2*, and *evdMO1* appeared to have been successfully disrupted in *M. carbonacea* var *aurantiaca*.

However, as PCR cannot verify the position of the crossover, we employed Southern blot analysis to confirm the replacement mutants (Figure 4-2). Digoxigenin (DIG) probes were designed upstream of each putative gene replacement. Genomic DNA from wildtype and each mutant strain was isolated and digested with appropriate endonucleases to give predictably sized fragments. Blots were analyzed for specific shifts of probe-labeled fragments for wildtype *M. carbonacea* and each mutant strain. Gene replacements were confirmed for *evdO1* and *evdMO1* predictable band shifts were observed. However, although PCR analysis suggested that *evdO2* had been successfully replaced, Southern blot analysis revealed that replacement of *evdO2* in fact was not successful as the predicted band shifts were not observed. Likely the apramycin cassette was integrated into a different region of the genome. Further efforts to generate an *evdO2* replacement were unsuccessful. This results underscores the importance of thoroughly analyzing each mutant strain by not only PCR but also Southern blot analysis.

To assess the effect of the oxygenase gene replacements on everninomicin production, tandem liquid chromatography mass spectral (LC/MS) analysis of the crude extracts of mutant strains was employed. Analysis of LC/MS data revealed abolished production of everninomicins D-G in both *evdO1* and *evdMO1* gene replacement strains (Fig 4-3). Consistent with the Southern

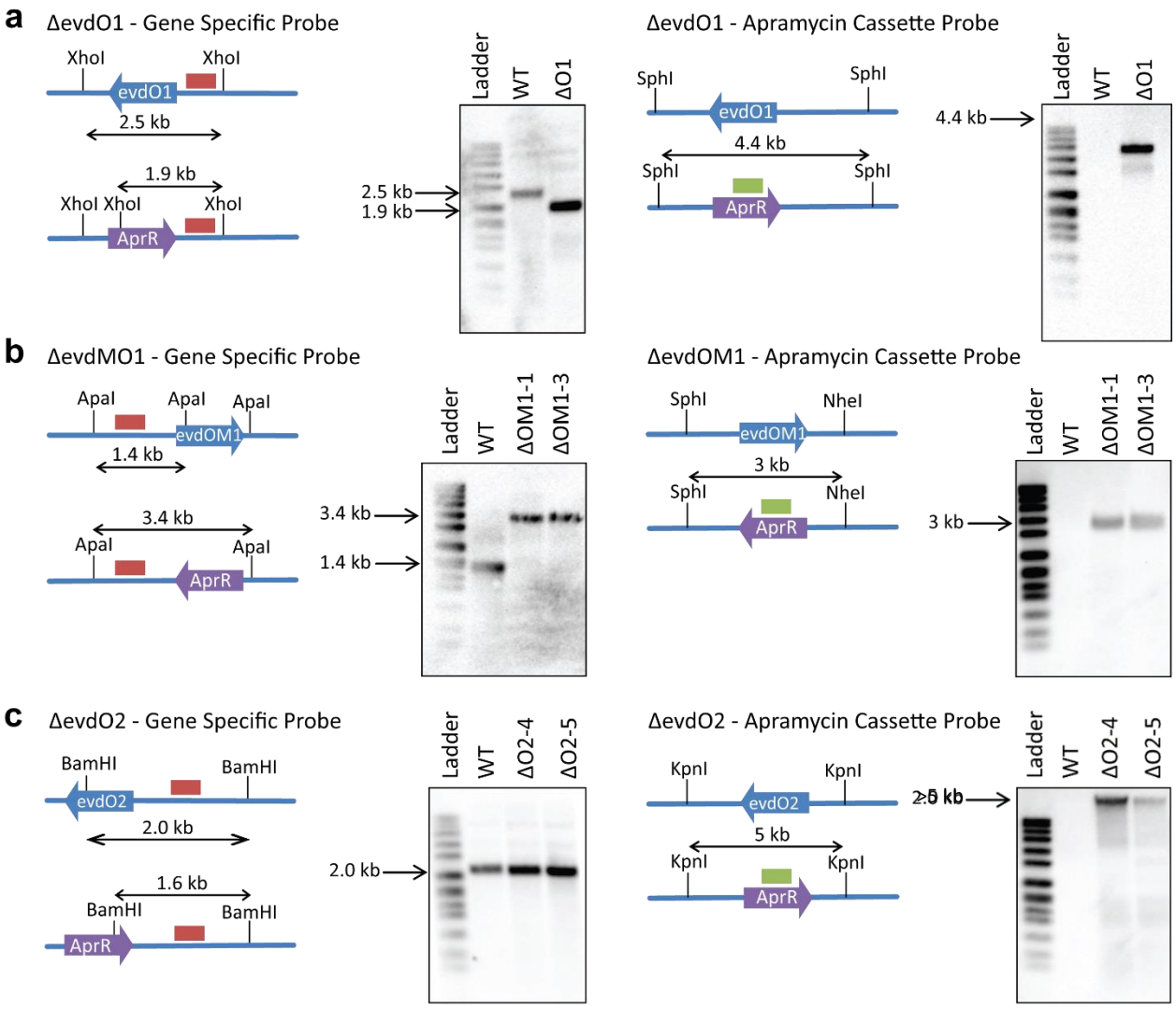

Figure 4-2. Southern hybridization of targeted deletion mutants verifying a double crossover event. (A) Southern blot analysis of *ΔevdO1::aac(3)IV*. Diagrams depict the relative shifts expected for replacement of *evdO1* with the apramycin cassette. Blots show predicted shifts were observed experimentally, thus confirming the double crossover. (B) Southern blot analysis of *ΔevdMO1::aac(3)IV*. Diagrams depict the relative shifts expected for replacement of *evdMO1* with the apramycin cassette. Blots show predicted shifts were observed experimentally, thus confirming the double crossover. (C) Southern blot analysis of *ΔevdO2::aac(3)IV*. Diagrams depict the relative shifts for replacement of *evdO2* with the apramycin cassette. Blots do not have predicted shifts showing that the gene replacement was not successful. Ladder is DNA molecular weight marker VII, DIG-labeled (product no. 11669940910; Roche Life Sciences). WT is wild-type *M. carbonacea* var *aurantiaca.* ApaI, KpnI, NheI, XhoI, SphI, and BamHI are restriction endonucleases used to cleave the genomic DNA into predictably sized fragments. Blots show predicted shifts were observed experimentally, thus confirming the double crossover. Adapted from *Proc Nat Acad Sci USA* **112**, 11547-11552 (2015).[25]

blot analysis of the *evdO2* mutant strains, everninomicin production was not affected in any of these mutants. These results confirm that *evdO1* and *evdMO1* are indeed involved in everninomicin biosynthesis and constitutes the first confirmation of the everninomicin gene cluster in *M. carbonacea* var *aurantiaca*.

Genetic Complementation of ΔevdO1::aac(3)IV and ΔevdMO1::aac(3)IV strains

To determine if polar effects were influencing everninomicin production in the gene replacements, *ΔevdO1::aac(3)IV* and *ΔevdMO1::aac(3)IV* were genetically complemented to generate strains: *ΔevdO1::aac(3)IV_GC* and *ΔevdMO1::aac(3)IV_GC*. In the case of *ΔevdMO1::aac(3)IV_GC*, everninomicin production was not restored by genetic complementation (Figure 4-3). This result was consistent with polar effects causing disruption of other critical genes in the gene cluster leading to abolished production. However in the case of *ΔevdO1::aac(3)IV_GC*, while genetic complementation did not restore production of everninomicins D-G, intriguingly we saw production of the truncated everninomicin-rosaramicin conjugate (Figure4-3). Although this conjugate is a degradation product of a larger metabolite, the C-1 position of ring C is consistent with the oxidation state of an orthoester linkage. Given that this conjugate was not observed in *ΔevdO1::aac(3)IV,* this data is highly suggestive that *evdO1* is responsible for forming the orthoester linkage between the C and D rings.

Structural Characterization of Orthosomycin-Associated Oxygenases

To further understand the role of these oxygenases in orthosomycin biosynthesis, we determined crystal structures for a representative oxygenase from each of the phylogenetic subgroups (AviO1, EvdO1, EvdO2, and HygX, Figure 4-4). Each enzyme adopted a double stranded

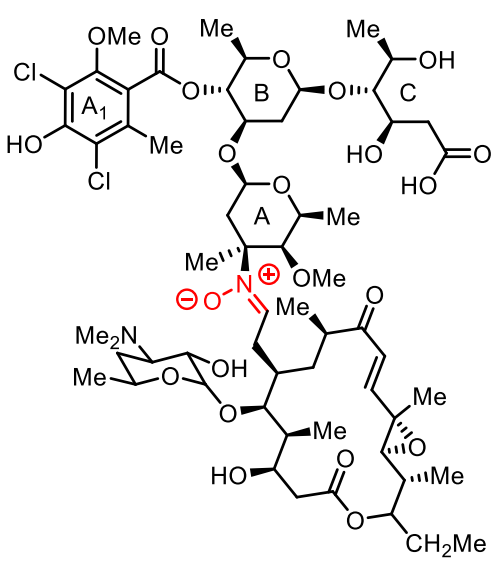

1 Truncated Everninomicin-Rosaramicin Conjugate

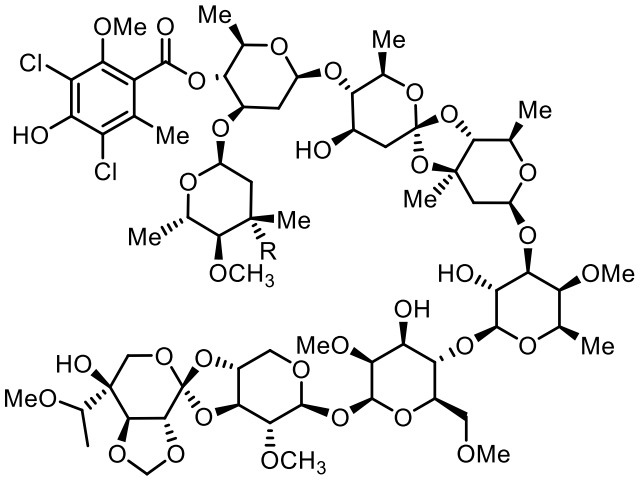

2 Ever E R = NH_2
3 Ever F R = NHOH
4 Ever D R = NO_2
5 Ever G R = NO

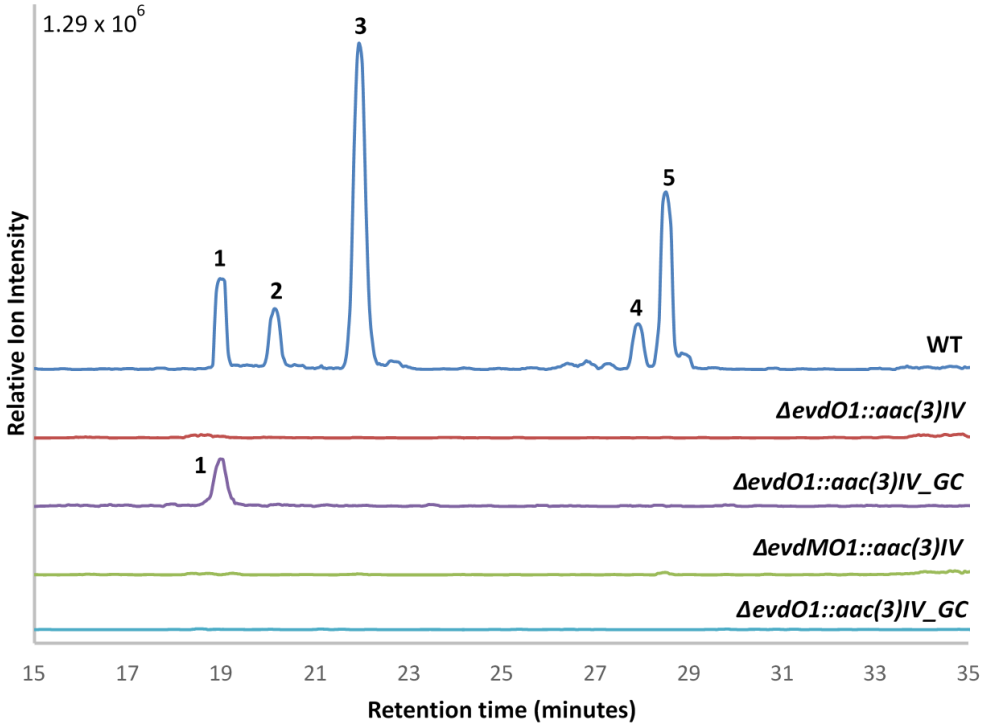

Figure 4-3. LC/MS of wild-type and deletion strains of *M. carbonacea* var. *aurantiaca* crude extracts. The chromatogram shows summed ion intensities in negative mode for everninomicins D–G and the truncated everninomicin-rosaramicin conjugate: D, m/z = 1,534.5 $[M-H]^-$; E, m/z = 1,504.5 $[M-H]^-$; F, m/z = 1,520.5 $[M-H]^-$; and G, m/z = 1,518.5 $[M-H]^-$; conjugate 1261.5 $[M-H]^-$. Adapted from *Proc Nat Acad Sci USA* **112**, 11547-11552 (2015).[25]

β-helix motif with the active site housing a metallocenter between β-sheets containing antiparallel β-strands. Although the fold was conserved among these enzymes, the oligomerization state varied, with AviO1 and EvdO2 as monomers, EvdO1 as a dimer, and HygX as a tetramer. Consistent with our sequence analysis, structural similarity searches revealed that the orthosomycin-associated oxygenases are related to the PhyH subfamily of non-heme iron, α-ketoglutarate dependent oxygenases.

Previous research has suggested that loop insertions between the β-strands of the double stranded β-helix of non-heme iron, α-ketoglutarate dependent oxygenases control substrate specificity. Indeed, all of the oxygenases characterized here contain loop inserts to form large

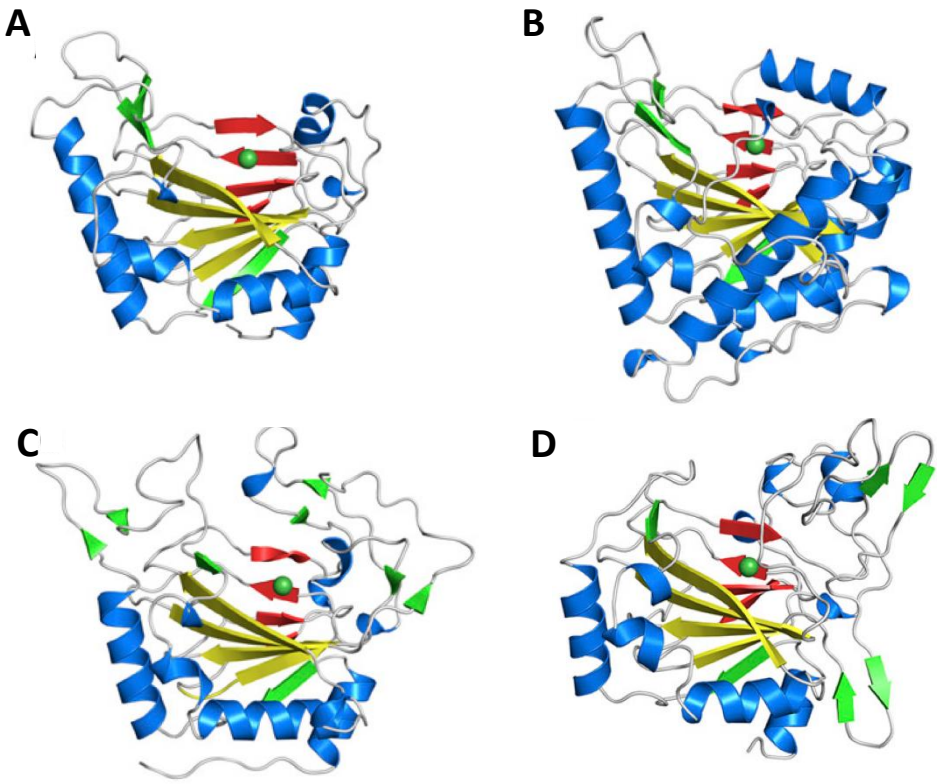

Figure 4-4. Orthosomycin-associated oxygenase structures. Cartoon representations of AviO1 (A), EvdO1 (B), EvdO2 (C), and HygX in the same orientations. The major sheet is colored yellow, the minor sheet is red, and nickel ions are green spheres. Figures courtesy of Dr. Kathryn M. McCulloch. Adapted from *Proc Nat Acad Sci USA* **112**, 11547-11552 (2015).[25]

binding clefts. Notably, all loop insertions have high crystallographic temperature factors which are commonly interpreted as a metric of flexibility. This flexibility is suggestive of substrate binding loops that change conformation upon substrate binding. Consistent with this proposal, upon α-ketoglutarate binding to HygX, comparison of the loops of the four protomers showed that the loops moved nearly 20 Å to promote active site closure.

In the majority of non-heme iron, α-ketoglutarate dependent oxygenases, iron coordination in the active site involves two histidines and one acidic residue to form a conserved H-X-D/E…H motif known as the facial triad.[21-23] Although the crystal structures described here contained catalytically inactive Ni^{2+} rather than Fe^{2+} in the active site, we have verified that Ni^{2+} retained the octahedral coordination geometry typical of Fe^{2+} coordination in the orthosomycin-associated oxygenases. Whereas, AviO1, EvdO1, and EvdO2 retained the canonical facial triad, HygX contained a variation where the acidic residue was substituted with a glycine and a glutamic acid located four residues before the distal histidine completes the metal coordination sphere to form a novel H-X-G…E-X_3-H motif. As expected, costructures of the oxygenases with α-

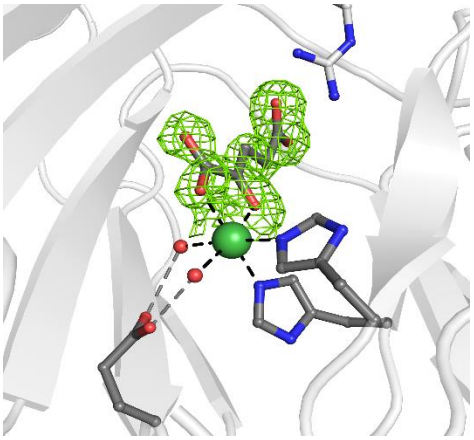

Figure 4-5. Active site of HygX in complex with α-ketoglutarate and Ni^{2+} showing the non-canonical facial triad. Figure courtesy of Dr. Kathryn M. McCulloch. Adapted from *Proc Nat Acad Sci USA* **112**, 11547-11552 (2015).[25]

ketoglutarate or succinate revealed that α-ketoglutarate binds directly to the metal with the 2-keto group *trans* to the acidic ligand (Figure 4-5).

Unfortunately, the substrates for the orthosomycin-associated oxygenases are not known and synthesis of a library of possible substrates is impractical. However, as enzymes have affinity for their products, we measured binding of hygromycin B to HygX using tryptophan fluorescence quenching (Figure 4-6A; K_d = 3.4 ± 0.5 μM). This low-micromolar affinity is consistent with affinities observed between enzymes and their products and suggests that HygX catalyzes the last step in hygromycin B biosynthesis. Subsequently, we determined the costructure of HygX with α-ketoglutarate and hygromycin B to 1.6-Å resolution (Figure 4-6B). Unambiguous electron density for hygromycin B showed one of the bridging oxygens of the orthoester approaching the metal center. The binding was highly specific with the position stabilized by 10 direct and 5 water-mediated interactions. Hygromycin B was oriented with the anomeric carbon of destomic acid

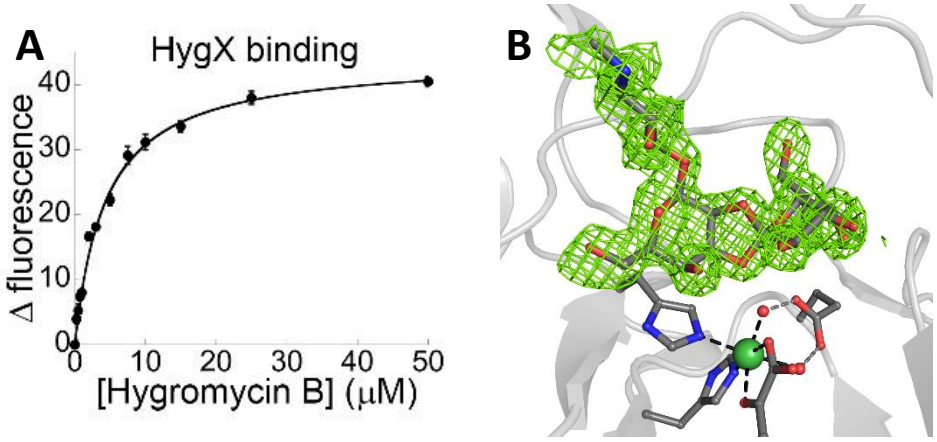

Figure 4-6. (A) Tryptophan fluorescence assay showed hygromycin B binding to HygX. K_d = 3.4 ± 0.5 μM. (B) Structure of hygromycin B in complex with HygX. Figures courtesy of Dr. Kathryn M. McCulloch. Adapted from *Proc Nat Acad Sci USA* **112**, 11547-11552 (2015).[25]

5.2 Å from the metal, close enough for oxygenation of the anomeric carbon. Interestingly, structural comparison of the HygX-hygromycin B costructure with EvdO1, EvdO2, and AviO1 structures shows that the hygromycin B ligand geometry would result in a steric clash if HygX retained the canonical facial triad. Because EvdO1, EvdO2, and AviO1 likely catalyze the same chemical reaction as HygX, the facial triad was most likely modified for substrate accommodation. The fact that HygX was able to bind hygromycin B in a chemically productive orientation for oxygenation is highly suggestive that this family of enzymes forms the orthoester linkages of the orthosomycins.

Discussion

Role of non-heme iron, α-ketoglutarate oxygenases in orthosomycin biosynthesis

Targeted gene replacements of two oxygenases from the everninomicin pathway in *M. carbonacea* var *aurantiaca* resulted in loss of everninomicin production and confirmed the requirement of this family of oxygenases for orthosomycin biosynthesis. Crystal structures of enzymes from each of the four phylogenetic subgroups confirmed our preliminary classification as non-heme iron, α-ketoglutarate oxygenases. Finally, co-structures of hygromycin B bound to HygX showed that hygromycin B binds in a chemically productive orientation with the orthoester linkage centered above the metal center. The lack of suitable substrates to determine co-structures and perform *in vitro* biochemical assays precludes identification of the exact substrate of each enzyme. However, reasonable sequence similarities between HygX and each of the remaining 12 oxygenases in the everninomicin and avilamycin pathways are consistent with each

member of this family catalyzing carbohydrate-associated ring closures. The results presented here provide evidence that the sub-family of non-heme iron, α-ketoglutarate oxygenases identified initially by comparative genomic analysis are responsible for formation of key oxidative features of the orthosomycins.

Substrate Identity and Selectivity

Although the exact substrate for each oxygenase is unknown, the crystal structures and genetic complementation experiments provided important information on substrate identity. Inspection of the hygromycin B-HygX co-structure revealed that HygX was able to bind the fully elaborated hygromycin B trisaccharide. These data suggest that the substrate for HygX is the fully decorated three-ringed compound only lacking the orthoester linkage and narrows the possibilities for HygX substrates to the two anomers at C1 of destomic acid. However, the complexity of chemical synthesis of hygromycin B rendered generation of either these anomers challenging and precluded *in vivo* biochemical assays.

Additionally, genetic complementation of *ΔevdO1::aac(3)IV* provided insights into the identity of the EvdO1 substrate. While gene replacement of *evdO1* resulted in abolished everninomicin production, complementation with the *evdO1* gene under the control of the constitutively active *ermE** promoter resulted in accumulation of the truncated everninomicin-rosaramicin conjugate (Figure 4-3, compound 1). This conjugate, although a degradation product of a larger compound, was oxidized at the C-1 position of the C ring. This conjugate was also found in wild type *M. carbonacea* var *aurantiaca* and was the result of hydrolysis of the orthoester linkage between the C and D rings (Figure 2-4). This result was unsurprising as previous research has shown that the orthoester linkages are extremely labile, particularly the

linkage between the C and D rings.[24] As the oxidized conjugate was restored only by complementation with the *evdO1* gene, this result is strongly suggestive that EvdO1 forms the orthoester linkage between the C and D rings.

Assignment of function to EvdO2 and EvdMO1 is more tenuous. Disruption of the EvdO2 homolog, AviO2, in the avilamycin pathway resulted in a new metabolite which was interpreted as the loss of an acetyl group.[2] However, as the homologous oxygenase is present in the everninomicin gene clusters, no acetyl group is present in everninomicin congeners, and a non-heme iron, α-ketoglutarate oxygenase is unlikely to catalyze acetylation, an alternative interpretation is that AviO2 catalyzes orthoester linkage formation between the G and H rings or methylenedioxy bridge formation before acetylation and that oxidation is required for recognition by the acetylating enzyme. As computational modeling studies suggested that the EvdO2 can reasonably orient the G and H rings,[25] we tentatively propose that EvdO2 forms the orthoester between the G and H rings. The final oxygenase EvdMO1 would then be expected to catalyze formation of the methylenedioxy bridge. However, further experimentation is needed to confirm the exact function of each oxygenase.

Preliminary Reaction Scheme and Possible Mechanisms

All characterized non-heme iron, α-ketoglutarate dependent oxygenases have conserved aspects to their reaction cycle. These enzymes function *via* two sequential half reactions that require sequential binding of three substrates: α-ketoglutarate, prime substrate, and oxygen.[26-29] In the first half reaction, α-ketoglutarate binds to the iron center and is converted into succinate and CO_2 by oxidative decarboxylation. This process generates a highly reactive Fe(IV)=O oxidizing intermediate. In the second half reaction, the Fe(IV)=O center abstracts hydrogen as a

radical from prime substrate which is then converted to product and the iron center is reduced back to Fe(II). While the first half reaction is the same in all characterized non-heme iron, α-ketoglutarate dependent oxygenases, the variance in the fate of the carbon-centered radical leads to a wide variety of functions for this class of enzymes.

Numerous schemes for prime substrate catalysis are observed in the superfamily including halogenations, hydroxylations, and oxidative cyclizations. The most relevant to orthoester linkage and methylenedioxy bridge formation is oxidative cyclization by clavaminate synthase. Clavaminate synthase operates first by hydrogen atom abstraction from prime substrate followed by ring closure.[30] In the costructure of proclavaminic acid-clavaminate synthase, the carbon that undergoes hydrogen atom abstraction is oriented 5.4 Å from the metal center.[31,32] Comparatively, the anomeric carbon of the destomic acid moiety of hygromycin B is 5.2 Å in the hygromycin B-HygX costructure. As this anomeric carbon is in a productive conformation, we propose that this carbon is the site of hydrogen atom abstraction although other possible sites such as the hydroxyl group cannot be excluded.[33]

Following hydrogen atom abstraction, there are several mechanistic possibilities[25,33-36], and analogous mechanisms can be used to explain both orthoester linkage and methylenedioxy bridge formation. One possibility is the transfer of a second electron to the Fe(III)-OH intermediate after generation of the carbon-centered radical. This transfer would generate an oxonium ion that could then be trapped by the vicinal hydroxyl group (Figure 4-7A). This mechanism has been proposed for the cyclization performed by clavaminate synthase.[35] We also cannot exclude the possibility of cryptic hydroxylation or halogenation. Installation of either a halide or hydroxyl group could be eliminated to generate an oxonium intermediate which would

then undergo nucleophilic attack by the vicinal oxygen (Figure 4-7B). The intermediates generated by a cryptic hydroxylation followed by oxonium ion formation would be similar to those in the acid-catalyzed rearrangement of the orthoester.[24] Finally, generation of a ketene acetal intermediate by either hydroxylation and elimination or direct desaturation is possible as this intermediate used in the synthesis of the C and D fragment (Figure 4-7C).[37,38]

Conclusions

Through genomic analysis, gene replacements, and structural characterization, we provide strong evidence that the subfamily of non-heme iron, α-ketoglutarate oxygenases form the orthoester linkages and methylenedioxy bridges of the orthosomycins. Specifically, gene replacements of two oxygenases in the everninomicin pathway confirmed the role of these enzymes in orthosomycin biosynthesis. Additionally, the costructure of hygromycin B bound to

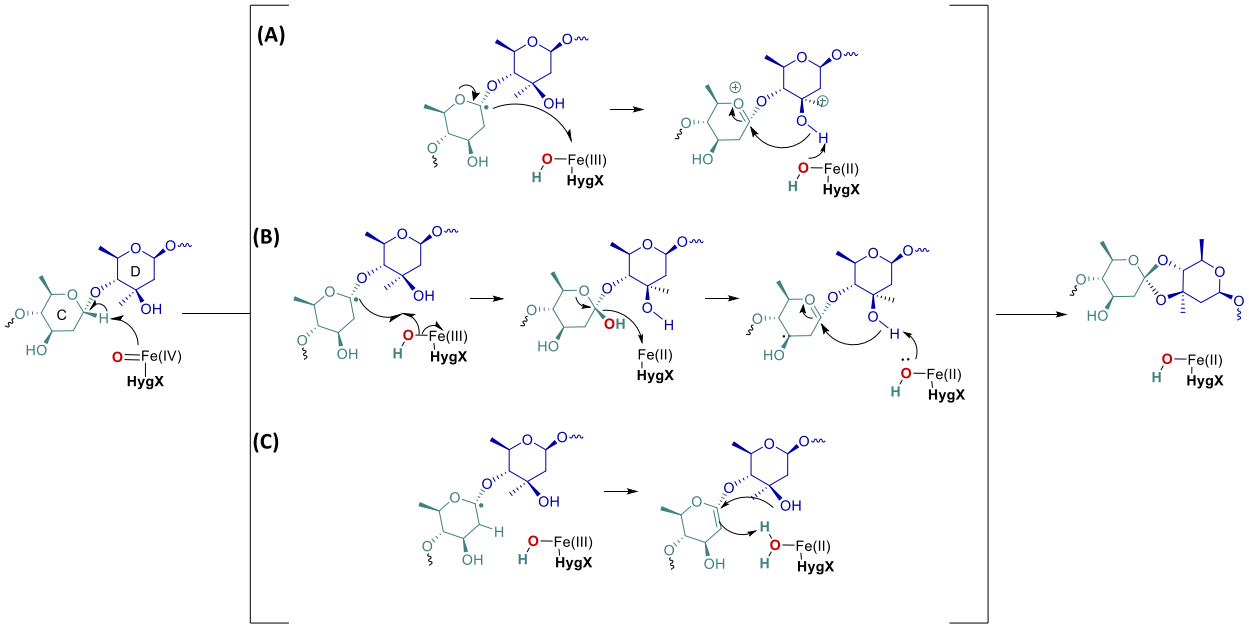

Figure 4-7. Possible mechanisms for orthoester linkage or methylenedioxy bridge formation (A) oxonium ion formation via transfer of a second electron; (B) cryptic hydroxylation leading to oxonium ion formation; (C) generation of a ketene acetal intermediate.

HygX gave insight into the identity of substrates as HygX was able to bind the fully elaborated structure with hygromycin B in a chemically productive orientation. Based on the high sequence identities and structural similarities that distinguish this subfamily of oxygenases from other non-heme iron, α-ketoglutarate oxygenases, our data support a role for this subfamily in the production of key features of orthosomycin antibiotics.

Acknowledgements

This work was contributed to by Emilianne K. McCranie, Kathryn M. McCulloch, Janette L. Matheiu, Bryan L. Gitschlag, Yu Du, Tina M. Iverson, and Brian O. Bachmann. E.K.M. performed the phylogenetic analysis, created gene replacements, designed and performed genetic complementation, and analyzed metabolites produced by wild type and mutant strains. Y.D. cloned proteins. K.M.M., J.L.M., and B.L.G. purified proteins and determined crystal structures. K.M.M. performed tryptophan fluorescence assays. B.O.B., T.M.I, K.M.M., and E.K.M. analyzed data. B.O.B and T.M.I supervised experiments. We thank R. McNees, B. Covington, and K. Derewacz for assistance with analysis of mutant extracts.

Portions of this chapter are reproduced from "Oxidative cyclizations in orthosomycin biosynthesis expand the known chemistry of an oxygenase superfamily." *Proc Nat Acad Sci USA* **112**, 11547-11552 (2015) by McCulloch, K. M., McCranie, E.K., Smith, J.A., Sarwar, M., Mathieu, J.L., Gitschlag, B.L., Du, Y., Bachmann, B.O. & Iverson, T.M.

References

1. Weitnauer, G., Muhlenweg, A., Trefzer, A., Hoffmeister, D., Sussmith, R.D. Jung, G., Welzel, K., Vente, A., Girreser, U. & Bechthold, A. Biosynthesis of the orthosomycin antibiotic avilamycin A: deductions from the molecular analysis of the *avi* biosynthetic gene cluster of *Streptomyces viridochromogenes* Tu57 and production of new antibiotics. *Chem Biol* **8**, 569-581 (2001).
2. Treede, I., Hauser, G., Muhlenweg, A., Hofmann, C., Schmidt, M., Weitnauer, G., Glaser, S. & Bechthold, A. Genes involved in formation and attachment of a two-carbon chain as a component of eurekanate, a branched-chain sugar moiety of avilamycin A. *Appl Environ Microbiol* **71**, 400-406 (2005).
3. Bauer, W. & Zenk, M. H. Formation of both methylenedioxy groups in the alkaloid (S)-stylopine is catalyzed by cytochrom P450 enzymes. *Tetrahedron Lett* **30**, 5257-5260 (1989).
4. Diaz Chavez, M. L., Rolf, M., Gesell, A. & Kutchan, T. M. Characterization of two methylenedioxy bridge-forming cytochrome P450-dependent enzymes of alkaloid formation in the Mexican prickly poppy Argemone mexicana. *Arch Biochem Biophys* **507**, 186-193 (2011).
5. Palaniappan, N., Dhote, V., Ayers, S., Starosta, A.L., Wilson, D.N. & Reynolds, K.A. Biosynthesis of the aminocyclitol subunit of hygromycin A in Streptomyces hygroscopicus NRRL 2388. *Chem Biol* **16**, 1180-1189 (2009).
6. Weitnauer, G., Hauser, G., Hofmann, C., Linder, U., Boll, R., Pelz, K., Glaser, S.J. & Bechthold, A. Novel avilamycin derivatives with improved polarity generated by targeted gene disruption. *Chem Biol* **11**, 1403-1411 (2004).
7. Otwinowski, Z. & Minor, W. Processing of X-ray diffraction data collected in oscillation mode. *Methods Enzymol* **276**, 307-326 (1997).
8. Sheldrick, G.M. Experimental phasing with SHELXC/D/E: Combining chain tracing with density modification. *Acta Crystallogr D Biol Crystallogr* **66** (Pt 4), 479-485 (2010).
9. Pape, T & Sschneider, T.R. HKL2MAP: A graphical user interface for macromolecular phasing with SHELX programs. *J Appl Cryst* **37**(5), 843-844 (2004).
10. Twewilliger, T.C., Adams, P.D., Read, R.J., McCoy, A.J., Moriarty, N.W., Grosse-Kunstleve, R.W., Afonine, P.V., Zwart, P.H. & Hung, L.W. Decision-making in structure solution using Bayesian estimates of map quality: The PHENIX AutoSol wizard. *Acta Crystallogr D Biol Crystallogr* **65** (Pt 6), 582-601 (2009).
11. Adams, P.D., Afonine, P.V., Bunkoczi, G., Chen, V.B., Davis, I.W., Echols, N., Headd, J.J., Hung, L.W., Kapral, G.J., Grosse-Kunstleve, R.W., McCoy, A.J., Moriarty, N.W., Oeffner, R., Read, R.J., Richardson, D.C., Richardson, J.S., Terwilliger, T.C. & Zwart, P.H. PHENIX: A comprehensive Python-based system for macromolecular structure solution. *Acta Crystallogr D Biol Crystallogr* **66** (Pt 2), 213-221 (2010).

12. McCoy, A.J., Grosse-Kunstleve, R.W., Adams, P.D., Winn, M.D., Storoni, L.C. & Read, R.J. *Phaser* crystallographic software. *J Appl Cryst* **40** (Pt 4), 658-674 (2007).
13. Terwilliger, T.C., Gross-Kunstleve, R.W., Afonine, P.V., Moriarty, N.W., Zwart, P.H., Hung, L.W., Read, R.J. & Adams, P.D. Iterative model building, structure refinement and density modification with the PHENIX AutoBuild wizard. *Acta Crystallogr D Biol Crystallogr* **64** (Pt 1), 61-69 (2008).
14. Emsley, P., Lohkamp, B., Scott, W.G., & Cowtan, K. Features and development of Coot. *Acta Crystallogr D Biol Crystallogr* **66** (Pt 4), 486-501 (2010).
15. Brunger, A.T. Version 1.2 of Crystallography and NMR system. *Nat Protoc* **2**(11), 2728-2733 (2007).
16. Afonine, P.V., Grosse-Kunstleve, R.W., Echols, N., Headd, J.J., Moriarty, N.W., Mustyakimov, M., Terwilliger, T.C., Urzhumtsev, A., Zwart, P.H. & Adams, P.D. Towards automated crystallographic structure refinement with *phenix.refine*. *Acta Crystallogr D Biol Crystallogr* **68** (Pt 4), 352-367 (2012).
17. Reuter, K., Pittelkow, M., Bursy, J., Heine, A., Craan, T. & Bremer, E. Synthesis of 5-hydroxyectoine from ectoine: crystal structure of the non-heme iron(II) and 2-oxoglutarate-dependent dioxygenase EctD. *PloS One* **5**, e10647, (2010).
18. Khare, D., Wang, B., Gu, L., Razelun, J., Sherman, D.H., Gerwick, W.H., Hakansson, K. & Smith, J.L. Conformational switch triggered by alpha-ketoglutarate in a halogenase of curacin A biosynthesis. *Proc Nat Acad Sci USA* **107**, 14099-14104 (2010).
19. You, Z., Omura, S., Ikeda, H., Cane, D. E. & Jogl, G. Crystal structure of the non-heme iron dioxygenase PtlH in pentalenolactone biosynthesis. *J Biol Chem* **282**, 36552-36560 (2007).
20. McDonough, M. A., Kavanagh, K.L., Butler, D., Searls, T., Oppermann, U. & Schofield, C.J. Structure of human phytanoyl-CoA 2-hydroxylase identifies molecular mechanisms of Refsum disease. *J Biol Chem* **280**, 41101-41110 (2005).
21. Hegg, E. L. & Que, L., Jr. The 2-His-1-carboxylate facial triad--an emerging structural motif in mononuclear non-heme iron(II) enzymes. *Eur J Biochem FEBS* **250**, 625-629 (1997).
22. Sato, N., Uragami, Y., Nishizaki, T., Takahashi, Y., Sazaki, G., Sugimoto, K., Nonaka, T., Masai, E., Fukuda, M. & Senda, T. Crystal structures of the reaction intermediate and its homologue of an extradiol-cleaving catecholic dioxygenase. *J Mol Biol* **321**, 621-636 (2002).
23. Arciero, D. M. & Lipscomb, J. D. Binding of 17O-labeled substrate and inhibitors to protocatechuate 4,5-dioxygenase-nitrosyl complex. Evidence for direct substrate binding to the active site Fe2+ of extradiol dioxygenases. *J Biol Chem* **261**, 2170-2178 (1986).
24. Ganguly, A. K., McCormick, J. L., Chan, T.-M., Saksena, A. K. & Das, P. R. Determination of the absolute stereochemistry at the C16 orthoester of everninomicin antibiotic: a novel acid-catalyzed isomerization of orthoesters. *Tetrahedron Lett* **38**, 7989-7992 (1997).
25. McCulloch, K. M., McCranie, E.K., Smith, K.A., Sarwar, M., Mathieu, J.L., Gitschlag, B.L., Du, Y., Bachmann, B.O. & Iverson, T.M. Oxidative cyclizations in orthosomycin biosynthesis

expand the known chemistry of an oxygenase superfamily. *Proc Nat Acad Sci USA* **112**, 11547-11552 (2015).

26. Price, J. C., Barr, E. W., Glass, T. E., Krebs, C. & Bollinger, J. M., Jr. Evidence for hydrogen abstraction from C1 of taurine by the high-spin Fe(IV) intermediate detected during oxygen activation by taurine:alpha-ketoglutarate dioxygenase (TauD). *J Am Chem Soc* **125**, 13008-13009 (2003).
27. Price, J. C., Barr, E. W., Tirupati, B., Bollinger, J. M., Jr. & Krebs, C. The first direct characterization of a high-valent iron intermediate in the reaction of an alpha-ketoglutarate-dependent dioxygenase: a high-spin FeIV complex in taurine/alpha-ketoglutarate dioxygenase (TauD) from Escherichia coli. *Biochemistry* **42**, 7497-7508 (2003).
28. Proshlyakov, D. A., Henshaw, T. F., Monterosso, G. R., Ryle, M. J. & Hausinger, R. P. Direct detection of oxygen intermediates in the non-heme Fe enzyme taurine/alpha-ketoglutarate dioxygenase. *J Am Chem Soc* **126**, 1022-1023 (2004).
29. Riggs-Gelasco, P. J., Price, J.C., Guyer, R.B., Brehm, J.H., Barr, E.W., Bollinger, J.M., Jr. & Krebs, C. EXAFS spectroscopic evidence for an Fe=O unit in the Fe(IV) intermediate observed during oxygen activation by taurine:alpha-ketoglutarate dioxygenase. *J Am Chem Soc* **126**, 8108-8109 (2004).
30. Iwata-Reuyl, D., Basak, A. & Townsend, C. A. β-Secondary Kinetic Isotope Effects in the Clavaminate Synthase-Catalyzed Oxidative Cyclization of Proclavaminic Acid and in Related Azetidinone Model Reactions. *J Am Chem Soc* **121**, 11356-11368 (1999).
31. Zhang, Z., Ren, J., Stammers, D.K., Baldwin, J.E., Harlos, K. & Schofield, C.J. Structural origins of the selectivity of the trifunctional oxygenase clavaminic acid synthase. *Nat Struct Biol* **7**, 127-133 (2000).
32. Borowski, T., de Marothy, S., Broclawik, E., Schofield, C. J. & Siegbahn, P. E. Mechanism for cyclization reaction by clavaminic acid synthase. Insights from modeling studies. *Biochemistry* **46**, 3682-3691 (2007).
33. Boal, A. K., Bollinger, J. M., Jr. & Chang, W. C. Assembly of the unusual oxacycles in the orthosomycin antibiotics. *Proc Nat Acad Sci USA* **112**, 11989-11990 (2015).
34. Roach, P. L., Clifton, I.J., Hensgens, C.M., Shibata, N., Schofield, C.J., Hajdu, J. & Baldwin, J.E. Structure of isopenicillin N synthase complexed with substrate and the mechanism of penicillin formation. *Nature* **387**, 827-830 (1997).
35. Zhang, Z., Ren, J. Harlos, K., McKinnon, C.H., Clifton, I.J. & Schofield, C.J. Crystal structure of a clavaminate synthase-Fe(II)-2-oxoglutarate-substrate-NO complex: evidence for metal centered rearrangements. *FEBS Lett* **517**, 7-12 (2002).
36. Wong, S. D., Srnec, M., Matthews, M.L., Liu, L.V., Kwak, Y., Park, K., Bell, C.B., Alp, E.E., Zhao, J., Yoda, Y., Kitao, S., Seto, M., Krebs, C., Bollinger, J.M., Jr. & Solomon, E.I. Elucidation of the Fe(IV)=O intermediate in the catalytic cycle of the halogenase SyrB2. *Nature* **499**, 320-323 (2013).

37. Beau, J.-M., Jaurand, G., Esnault, J. & Sinaÿ, P. Synthesis of the disaccharide C-D fragment found in everninomicin-C and -D, avalamycin-A and -C and curamycin-A: stereochemistry at the spiro-ortholactone center. *Tetrahedron Lett* **28**, 1105-1108 (1987).
38. Nicolaou, K. C., Rodriguez, R.M., Fylaktakidou, K.C., Suzuki, H. & Micthell, H.J. Total Synthesis of Everninomicin 13,384-1-Part 2: Synthesis of the FGHA(2) Fragment. *Angew Chem Int Ed Engl* **38**(22): 3340-334 (1999).

CHAPTER V

DISSERTATION SYNOPSIS AND FUTURE DIRECTIONS

Synopsis

Oligosaccharides are an underexplored class of bacterial secondary metabolites with interesting scaffolds. Though the number of known bioactive oligosaccharides is small, they possess potent activity against an array of biological targets including bacterial ribosomes and human hydrolases. One member of this class, acarbose, is used as a treatment for type II diabetes.[1,2] Despite their clinical importance, the biosynthesis of oligosaccharide natural products is only marginally understood. A deeper understanding of how bacteria synthesize these compounds is important for engineering efforts as well as the discovery of additional bioactive oligosaccharides.

Of particular interest are the highly decorated orthosomycins which possess potent antibacterial activity against a variety of Gram-negative and Gram-positive bacteria. One member of this class, everninomicin A, advanced to phase III clinical trials for treatment of methicillin-resistant *Staphylococcus aureus*. Despite their potential clinical significance, little is known about the biosynthesis of the orthosomycins. In this work, we investigated the biosynthesis of this family of antibiotics and developed new everninomicin analogs to better understand their structure-activity relationship for the development of an antibiotic with improved activity and pharmacological properties.

In order to investigate orthosomycin biosynthesis effectively and efficiently, methods for genetic manipulation of the everninomicin producer and for facile analysis of new everninomicin

analogs were developed. The everninomicin producer, *Micromonospora carbonacea* var *aurantiaca*, does not sporulate and must be transformed by conjugation with a donor *Escherichia coli*. Conventional conjugation protocols rely on the use of the antibiotic nalidixic acid to kill the donor *E. coli.*[3] Unfortunately, *M. carbonacea* is sensitive to nalidixic and an antibiotic-free method of selection was developed using a membrane/washer assembly. The mycelia of *M. carbonacea* are able to penetrate the membrane allowing for clean selection of exconjugants.[4] Additionally, a suitable genetic complementation vector system was developed for use in this strain to confirm gene replacement studies.

Before this report, the variety of everninomicins produced by *M. carbonacea* var *aurantiaca* was unknown. Low production levels hindered initial studies. Therefore, production parameters were altered which led to a 47-fold increase in everninomicin production. This drastic increase in production levels allowed us to report for the first time the variety of everninomicins produced by *M. carbonacea* var *aurantiaca*. Using mass spectrometric fragmentation, we were able to "sequence" the everninomicin congeners and locate changes to individual sugar residues.[5] Intriguingly, we also discovered an unusual compound that is a conjugate of everninomicin F and rosaramicin, a macrolide also produced by *M. carbonacea*.[6] Evaluation of the antibacterial activity of these conjugates revealed that they retained potent activity against *Staphylococcus aureus.* A knowledge of the variety of everninomicins produced by this strain is necessary for the evaluation of new analogs.

As little is known about orthosomycin biosynthesis, we used translated sequence similarities to assign the functions of each open reading frame in three orthosomycin gene clusters. Using the methods discussed above, we then provided the first experimental

confirmation of the everninomicin gene cluster in *M. carbonacea* var *aurantiaca*. The roles of a nitrososynthase, *C*-methyltransferase, and *O*-methyltransferase were investigated through individual targeted gene replacements. Excitingly, the gene replacements resulted in the identification of four new everninomicin analogs.

Replacement of *evdM3* not only confirmed the role of EvdM3 as a *C*-methyltransferase responsible for methylating the C-3 position of the D ring but also resulted in accumulation of three new metabolites, termed everninomicins H, J, and K. Excitingly, everninomicin H was still active against *S. aureus* although it was less potent than everninomicin A (Ziracin™).[7] Targeted gene replacement of *evdN1* which encodes the nitrososynthase resulted in accumulation of everninomicin-2, a fully decorated heptasaccharide only lacking evernitrose. Everninomicin-2 has previously been reported and retains potent activity against *S. aureus*.[8] Although the replacements were targeted and precise as evidenced by Southern blot analysis, polar effects from insertion of the apramycin resistance cassette in place of the genes of interest resulted in unexpected modifications such as loss of evernitrose. However, in the case of the *ΔevdM3::aac(3)IV* mutant, these polar effects allowed us to tentatively assign the function of EvdM4 as an *O*-methyltransferase responsible for the 2-methoxy of ring G. Likewise, the accumulation of the truncated everninomicin-rosaramicin conjugate in the *ΔevdM2::aac(3)IV* mutant suggested that EvdM2 is responsible for methylating a residue on the right side of the molecule, likely the methylenedioxy bridge prior to oxidative cyclization. Together these results provided critical information about the mutability of the gene cluster and timing of everninomicin biosynthesis.

Further investigations focused on the unique oxidative features of the orthosomycins

including their hallmark orthoester linkage.[9] Comparative genomic analysis identified a group of non-heme iron, α-ketoglutarate oxygenases likely responsible for formation of the orthoester linkages and methylenedioxy bridge. Further, comparison of these oxygenases from four class I orthosomycin pathways revealed that this group could be further subdivided with each subgroup containing one oxygenase from each pathway. Targeted replacement of two of these oxygenases in the everninomicin pathway of *M. carbonacea* var *aurantiaca* demonstrated the necessity of these enzymes. Complementation of *ΔevdO1::aac(3)IV* with the *evdO1* resulted in restoration of the truncated everninomicin-rosaramicin conjugate strongly suggesting that EvdO1 is responsible for forming the orthoester linkage between rings C and D.

Structural characterization of four oxygenases, one from each of the phylogenetic subgroups, revealed that each adopted a fold common to non-heme iron, α-ketoglutarate oxygenases although one oxygenase, HygX, contained a modified facial triad in the active site. Excitingly, the structure of hygromycin B bound to HygX was solved and revealed that hygromycin B bound in a chemically productive conformation with the anomeric carbon of destomic acid only 5.2 Å from the metal center. Additionally, the ability of HygX to bind fully elaborated hygromycin B suggests that the orthoester linkage is the last step in its biosynthesis.[9]

Through the work described, here we have made significant contributions to the understanding of orthosomycin biosynthesis. Initial method development allowed for efficient manipulation of the biosynthetic pathway and analysis of everninomicins and also resulted in the first experimental confirmation of the everninomicin biosynthetic pathway in *M. carbonacea* var *aurantiaca.* Phylogenetic analysis, gene replacements, and structural characterization identified a family of oxygenases responsible for formation of the orthosomycins' hallmark feature, the

orthoester linkage. Finally, we generated five new everninomicin analogs that inform the structure-activity relationship of the everninomicins. Notably, all of the analogs tested retained activity against *S. aureus*. This work lays the groundwork for further exploration of orthosomycin biosynthesis and generation of additional analogs toward the goal of developing improved everninomicin with improved pharmacology and potent activity against bacterial infections.

Future directions

The work described here provides a starting point for understanding orthosomycin biosynthesis and the structure-activity relationship of the everninomicins; however there is still much to be learned and many directions to explore. Future work should focus on harnessing the methods developed here to further understand orthosomycin biosynthesis and to generate additional everninomicin analogs so that the structure-activity relationship of the everninomicins can be thoroughly assessed.

First, further experimentation is needed to elucidate the exact mechanism of orthoester linkage formation by the group of α-ketoglutarate dependent oxygenases we identified. In Chapter IV, we proposed three possible mechanisms although we were unable to confirm which, if any, of these mechanisms is responsible for the oxidative cyclization. Initial activity assays using each of the everninomicin oxygenases from *M. carbonacea* var *aurantiaca* and putative disaccharide substrates synthesized by the Bennett Group at Tufts University (Figure 5-1) did not reveal activity although a variety of conditions were tried. It is possible that the appropriate reaction conditions were not used or that the enzymes require larger substrates for appropriate recognition. Notably, based on the results of the C-methyltransferase replacement reported in

Chapter III, the methyl of the D-ring is not necessary for oxidative closure of the orthoester linkages between rings C and D. Therefore, to simplify synthesis, the C-3 methyl of the D-ring may be omitted in the construction of future substrates. Additionally, it is possible that the oxygenases employ a cryptic halogenation step. Future experimentation should take this possibility into consideration, and the assay should be conducted under halogenase like conditions. When an appropriate substrate is identified, kinetic isotope effect studies should be employed to determine the site of hydrogen atom abstraction. Additionally, any intermediates that may be forming, such as an oxonium ion or a hydroxylated intermediate, should be trapped and thoroughly characterized.

During the search for metabolites produced by the *ΔevdO1::aac(3)IV* and *ΔevdMO1::aac(3)IV*, we identified a subset of masses present in the wild type and mutant strains using molecular networking.[10] These compounds are presumed to be intermediates as they cluster between the everninomicins and the truncated everninomicin-rosaramicin conjugate (see Figure 5-1). In the future, these compounds should be isolated and characterized as they likely would provide important information about timing of biosynthesis of everninomicin in *M. carbonacea* var *aurantiaca.* Methods for using molecular networking effectively in this context should be further developed to look for even more everninomicin analogs and/or biosynthetic intermediates which will shed light on important yet unknown aspects of orthosomycin biosynthesis such as the timing of glycosylations and tailoring modifications.

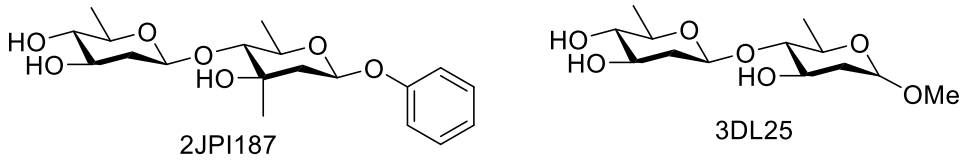

Figure 5-1. Putative disaccharide substrates tested for activity with the everninomicin oxygenases (EvdO1, EvdO2, EvdMO1). These substrates were synthesized by the Bennett Group at Tufts University.

A recent collaboration has been developed with the Wilson Group at the University of Munich to assess the structure-activity relationship of the everninomicins. The Wilson Group has developed a cryo-electron microscopy method to determine the structure of the ribosome in complex with everninomicin A. Additionally, they have established translational assays that provided specific information on everninomicin's mode of action.[11] By collaborating with the Wilson group, we will learn detailed information about the binding and activity of our newly generated analogs which will inform generation of new analogs.

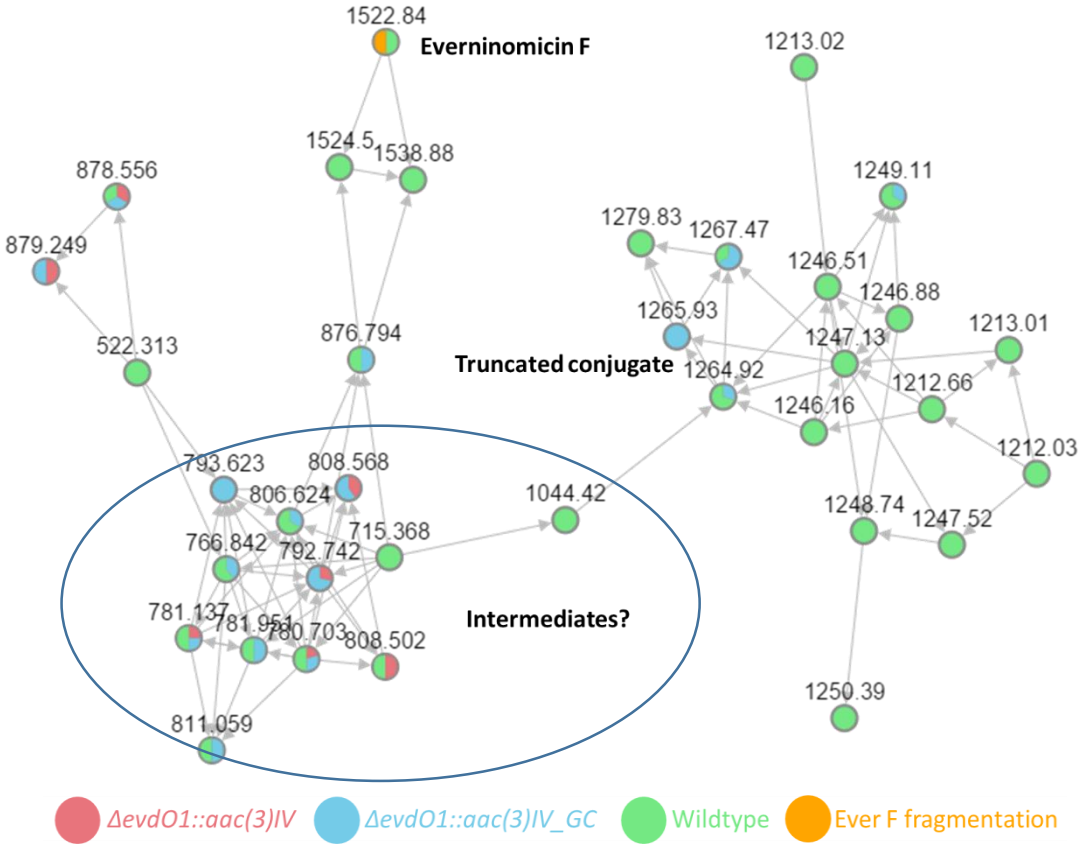

Figure 5-2. Molecular networking revealed a cluster of possible everninomicin biosynthetic intermediates. Networking was conducted using data-dependent analysis of crude extracts of wild type and mutant strains as specific fragmentation of everninomicin F. Future work will focus on identifying these possible intermediates.

Although we have successfully generated four new everninomicin analogs which will contribute to an understanding of structure activity relationships, there is a need for more analogs created through both mutasynthesis and semi-synthesis. Our work shows that we can successfully replace a methyltransferase from the everninomicin cluster with a copy located elsewhere in the genome, i.e. genetic complementation of *evdM3*. Future work should focus on genetically complementing with an engineered "methyltransferase" that is capable of different alkylations. Previous work has shown that these SAM methyltransferases can be modified to accept SAM analogs.[12,13] Our collaboration with the Wilson group will provide valuable information about structure activity relationships and will inform which modifications would be most advantageous. Through these modifications we will be able to generate truly non-natural everninomicin analogs.

An additional way to create everninomicin analogs is to harness the reactivity of the amino and the hydroxyl amino functionalities of everninomicin E and F respectively. Through the discovery of the everninomicin rosaramicin conjugate, we know that the hydroxyl amino of everninomicin F readily reacts with aldehydes to form a stable conjugate. We can use this reactivity to modify the nitrosugar and potentially add large groups to modify pharmacological properties as well as binding. Additionally, other groups have used methoxyamine appendages to add a variety of sugar residues through neoglycorandomization. This approach has successfully been used to modulate the potency of other natural products.[14-17] Future work should take advantage of this unique chemical handle to generate new analogs.

Although efficient methods for targeted gene replacement of target genes in the *evd* gene cluster were developed, polar effects caused by insertion of the apramycin resistance cassette

impaired our ability to definitively assess the role of genes in the everninomicin gene cluster. Future work should focus on creating gene replacements that avoid these deleterious polar effects. Previous work by Gust and coworkers used a flip recombinase to remove the majority of the apramycin cassette leaving only a small scar sequence.[18] However, the cassette is generally "flipped" out in *E. coli* as genetic manipulation of *E. coli* is much simpler than that of the producing organism. Unfortunately, removing the cassette in *E. coli* also removes the origin of transfer necessary for the conjugal transfer of the disrupted cosmid. To avoid this limitation, a new apramycin cassette should be created which contains the origin of transfer (oriT) outside of the flip recombinase targets. Although this will make the scar sequence slightly larger it will allow for the use of the efficient conjugation methods developed in this work. If polar effects persist, the entire disrupted operon should be genetically complemented to alleviate the effects.

Finally, the activity of the everninomicin-rosaramicin conjugate should be further explored. As this conjugate is composed of two very different scaffolds both of which are known to target the ribosome,[19,20] it will be interesting to learn if one or both compounds are contributing to its potency. If everninomicin is still able to bind to the ribosome and inhibit formation of the 70S initiation complex,[11] this would suggest that the nitrosugar is a good place for further modification of everninomicins including conjugates with other macrolide antibiotics. Furthermore, if both compounds are responsible for the activity and they target different ribosomal sites, this conjugate could extremely effective in combatting bacterial infections as the organism would have to develop resistance to both components at different ribosomal sites.

In conclusion, this work has provided the basis for further understanding of orthosomycin biosynthesis and generation of novel analogs. Identification of biosynthetic intermediates and

creation of gene replacements without deleterious polar effects will provide critical information about orthosomycin biosynthesis. Further work will focus on creating additional analogs to understand which features of everninomicin are necessary for activity and which can be modified to improve its pharmacological properties. This work will advance our understanding of oligosaccharide biosynthesis and will provide a new tool for combatting dangerous bacterial infections.

Acknowledgements

We thank the Bennett Group at Tufts University for synthesizing the disaccharides for activity assays and for discussions about possible substrates.

References

1. Wehmeier, U. F. & Piepersberg, W. Biotechnology and molecular biology of the alpha-glucosidase inhibitor acarbose. *Appl Microbiol Biotechnnol* **63**, 613-625 (2004).
2. Rockser, Y. & Wehmeier, U. F. The gac-gene cluster for the production of acarbose from Streptomyces glaucescens GLA.O: identification, isolation and characterization. *J Biotechnol* **140**, 114-123 (2009).
3. Bierman, M., Logan, R., O'Brien, K., Seno, E.T., Rao, R.N. & Schoner, B.E. Plasmid Cloning Vectors for the Conjugal Transfer of DNA from Escherichia-Coli to Streptomyces Spp. *Gene* **116**, 43-49 (1992).
4. Gavrish, E., Bollmann, A., Epstein, S. & Lewis, K. A trap for in situ cultivation of filamentous actinobacteria. *J Microbiol Meth* **72**, 257-262 (2008).
5. Chen, G., Pramanik, B. N., Bartner, P. L., Saksena, A. K. & Gross, M. L. Multiple-Stage Mass Spectrometric Analysis of Complex Oligosaccharide Antibiotics (Everninomicins) in a Quadrupole Ion Trap. *J Am Soc Mass Spectrom* **13**, 1313-1321 (2002).
6. Farnet, C. M., Staffa, A., Yang, X. Genes and proteins for the biosynthesis of rosaramicin, Google Patents (2003).
7. Urban, C., Mariano, N., Mosinka-Snipas, K., Wadee, C., Chahrour, T. & Rahal, J.J. Comparative in-vitro activity of SCH 27899, a novel everninomicin, and vancomycin. *J Antimicrob Chemother* **37**, 361-364 (1996).

8. Ganguly, A. K., Szmulewicz, S., Sarre, O. Z. & Girijavallabhan, V. M. Structure of everninomicin-2. *J Chem Soc Chem Comm,* 609-611 (1976).
9. McCulloch, K. M., McCranie, E.K., Smith, J.A., Mathieu, J.L., Gitschlag, B.L., Du, Y., Bachmann, B.O. & Iverson, T.M. Oxidative cyclizations in orthosomycin biosynthesis expand the known chemistry of an oxygenase superfamily. *Proc Nat Acad Sci USA* **112**, 11547-11552 (2015).
10. Duncan, K. R., Crusemann, M., Lechner, A., Sarkar, A., Li, J., Ziemert, N., Wang, M., Bandeira, N., Moore, B.S., Dorrestein, P.C. & Jensen, P.R. Molecular networking and pattern-based genome mining improves discovery of biosynthetic gene clusters and their products from Salinispora species. *Chem Biol* **22**, 460-471 (2015).
11. Mikolajka, A., Liu, H., Chen Y., Starosta, A.L., Marquez, V., Ivanova, M., Cooperman, B.S. & Wilson, D.N. Differential effects of thiopeptide and orthosomycin antibiotics on translational GTPases. *Chem Biol* **18**, 589-600 (2011).
12. Islam, K., Bothwell, I., Chen, Y., Sengelaub, C., Wang. R., Deng, H. & Luo, M. Bioorthogonal profiling of protein methylation using azido derivative of S-adenosyl-L-methionine. *J Am Chem Soc* **134**, 5909-5915 (2012).
13. Zhang, C. S., Weller, R. L., Thorson, J. S. & Rajski, S. R. Natural product diversification using a non-natural cofactor analogue of S-adenosyl-L-methionine. *J Am Chem Soc* **128**, 2760-2761 (2006).
14. Langenhan, J. M., Peters, N. R., Guzei, I. A., Hoffmann, F. M. & Thorson, J. S. Enhancing the anticancer properties of cardiac glycosides by neoglycorandomization. *Proc Nat Acad Sci USA* **102**, 12305-12310 (2005).
15. Ahmed, A., Peters, N.R., Fitzgerald, M.K., Watson, J.A., Hoffman, F.M. & Thorson, J.S. Colchicine Glycorandomization Influences Cytotoxicity and Mechanism of Action. *J Am Chem Soc* **128**, 14224-14225 (2006).
16. Griffith, B. R*.,* Byron, R., Krepel, C., Fu, X., Blanchard, S., Ahmend, A., Edmiston, C.E. & Thorson, J.S. Model for Antibiotic Optimization via Neoglycosylation: Synthesis of Liponeoglycopeptides Active against VRE. *J Am Chem Soc* **129**, 8150-8155 (2007).
17. Langenhan, J. M., Engle, J.M., Slevin, L.K., Fay, L.R., Lucker, R.W., Smith, K.R. & Endo, M.M. Modifying the glycosidic linkage in digitoxin analogs provides selective cytotoxins. *Bioorg Med Chem Lett* **18**, 670-673 (2008).
18. Gust, B., Challis, G. L., Fowler, K., Kieser, T. & Chater, K. F. PCR-targeted Streptomyces gene replacement identifies a protein domain needed for biosynthesis of the sesquiterpene soil odor geosmin. *Proc Nat Acad Sci USA* **100**, 1541-1546 (2003).
19. Champney, W. S. T., C. L. Evernimicin (SCH27899) Inhibits both Translation and 50S Ribosomal Subunit Formation in Staphylococcus aureus Cells. *Antimicrob Agents Chemother* **44**, 1413-1417 (2000).

20. Siegrist, S., Lagouardat, J., Moreau, N. & Le Goffic, F. Mechanism of Action of a 16-Membered Macrolide. *Eur J Biochem* **115**, 323-327 (1981).

Appendix A.

NMR Spectra

Table of Contents

Figure A-1. ^{1}H proton NMR of truncated everninomicin-rosaramicin conjugate in CD_4OD.

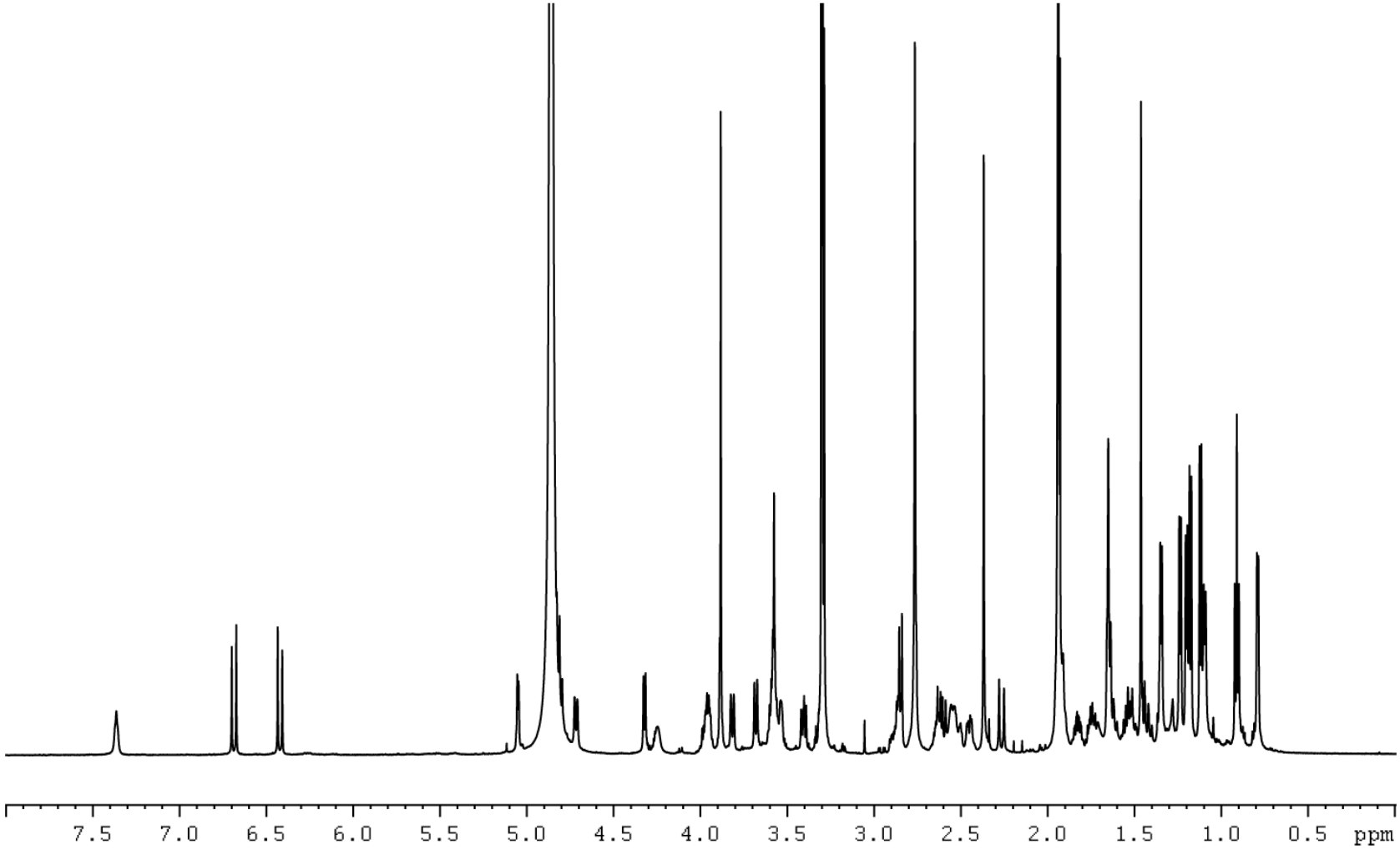

Figure A-2. ^{13}C carbon NMR of truncated everninomicin-rosaramicin conjugate in CD_4OD.

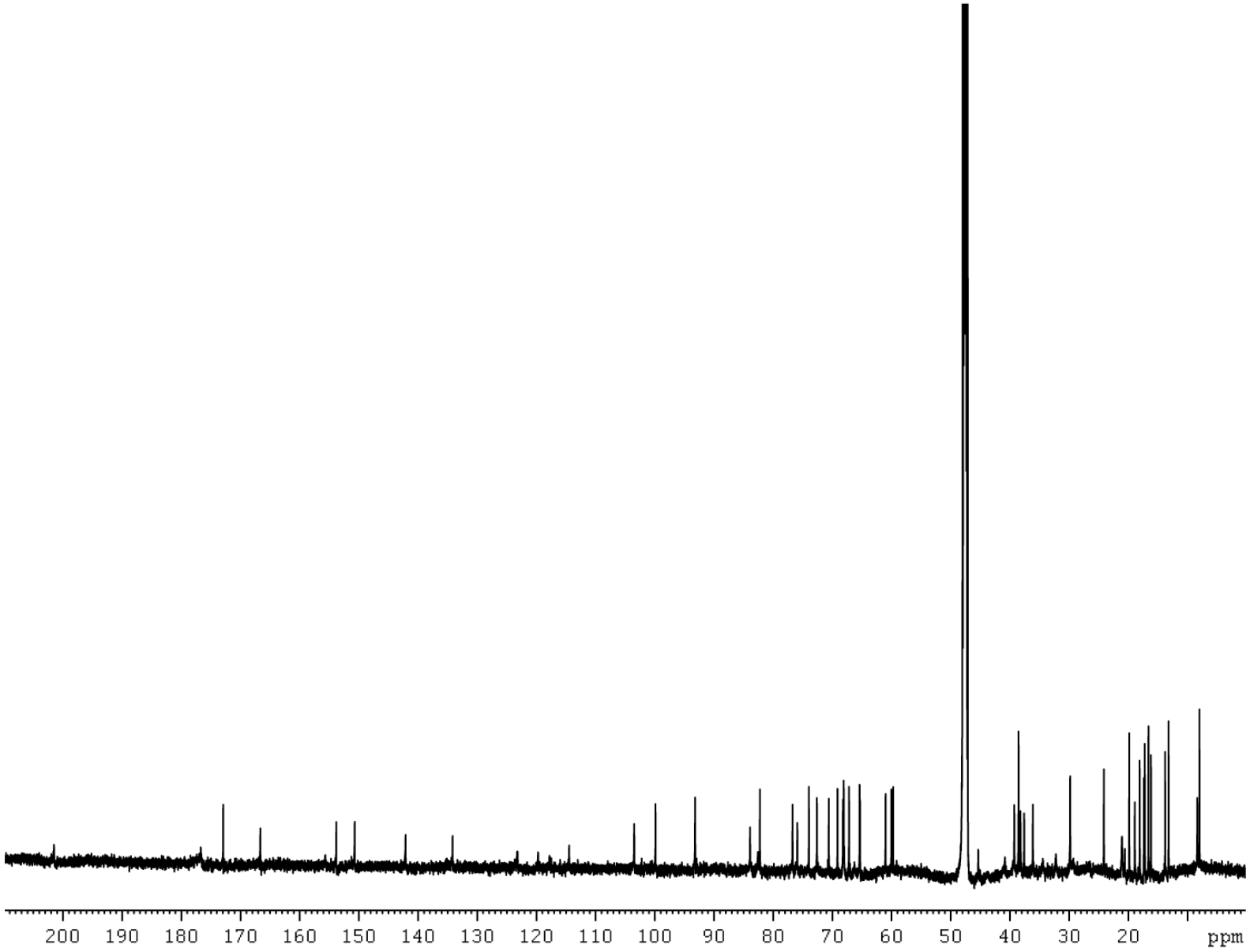

Figure A-3. COSY NMR of truncated everninomicin-rosaramicin conjugate in CD_4OD.

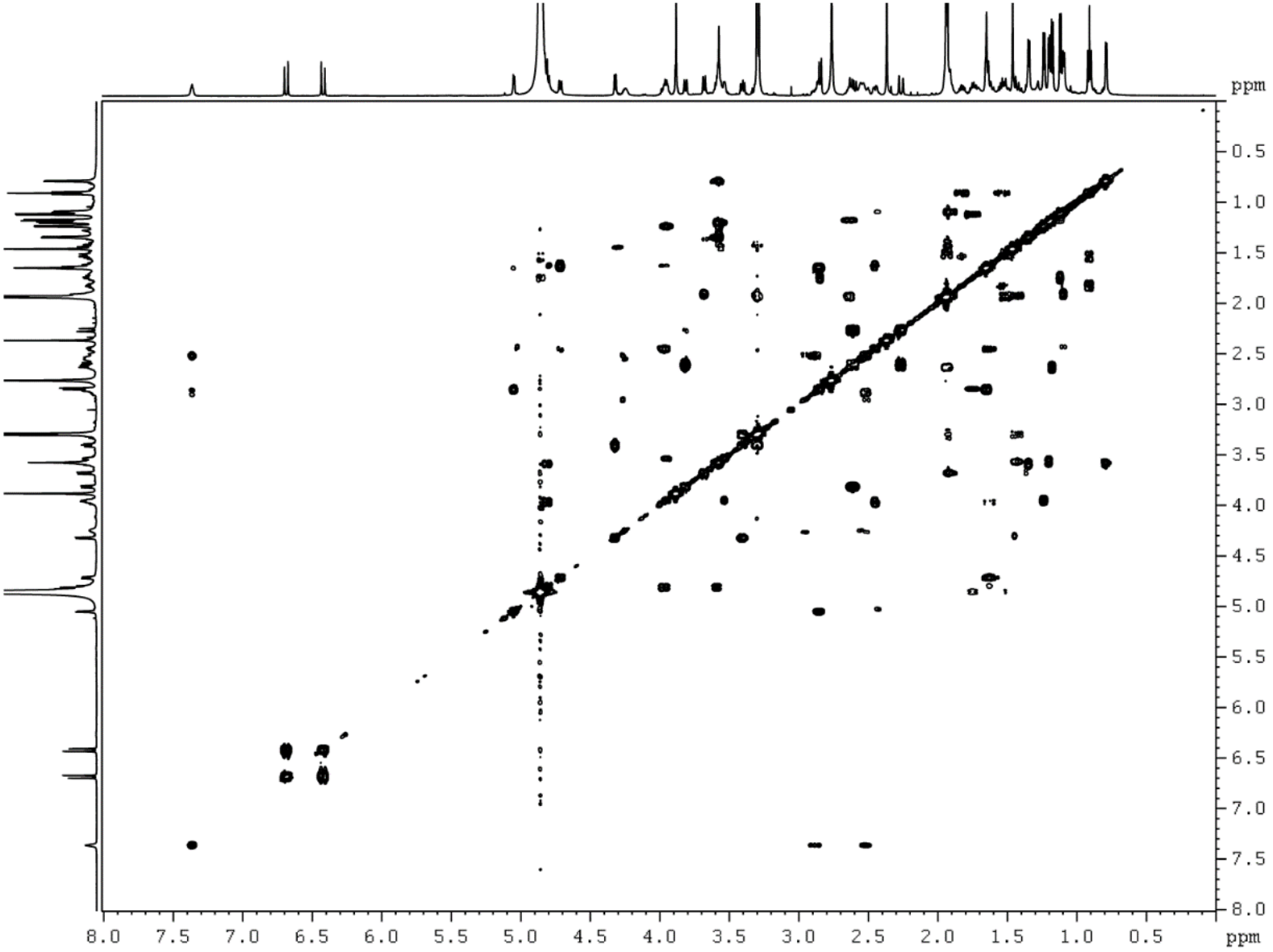

Figure A-4. HSQC NMR of truncated everninomicin-rosaramicin conjugate in CD_4OD.

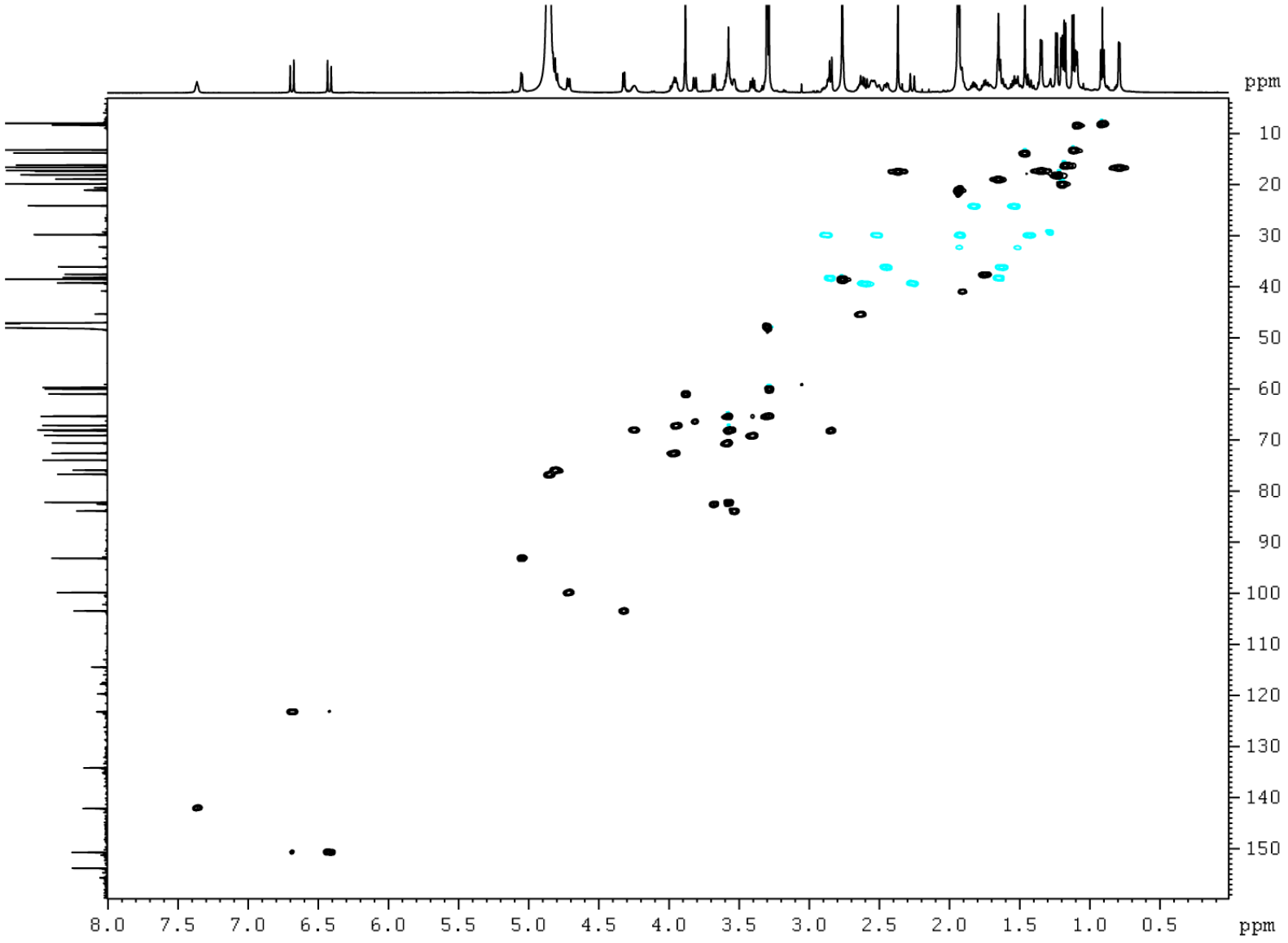

Figure A-5. HMBC NMR of truncated everninomicin-rosaramicin conjugate in CD_4OD.

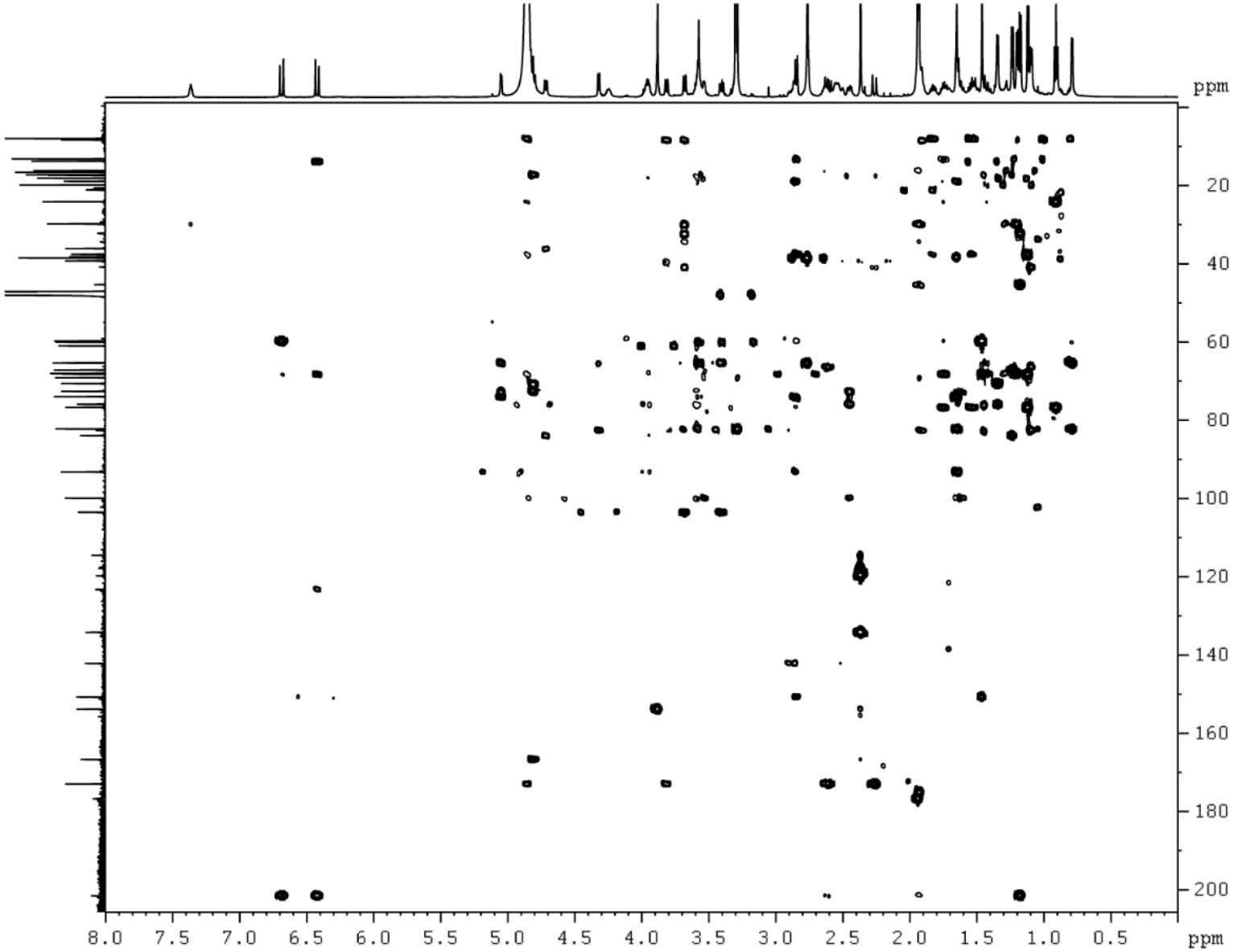

Figure A-6. TOCSY NMR of truncated everninomicin-rosaramicin conjugate in CD_4OD.

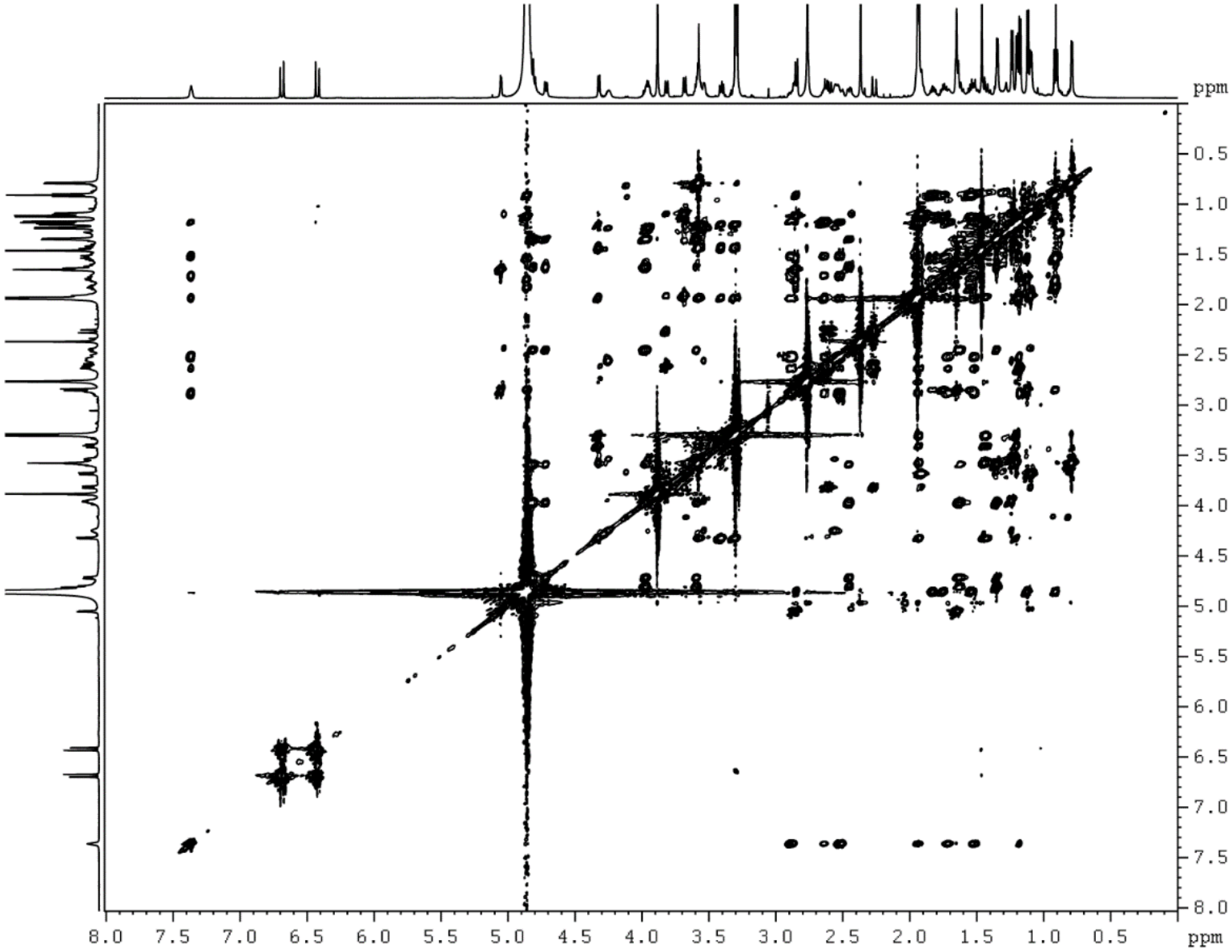

Figure A-7. NOESY NMR of truncated everninomicin-rosaramicin conjugate in CD_4OD.

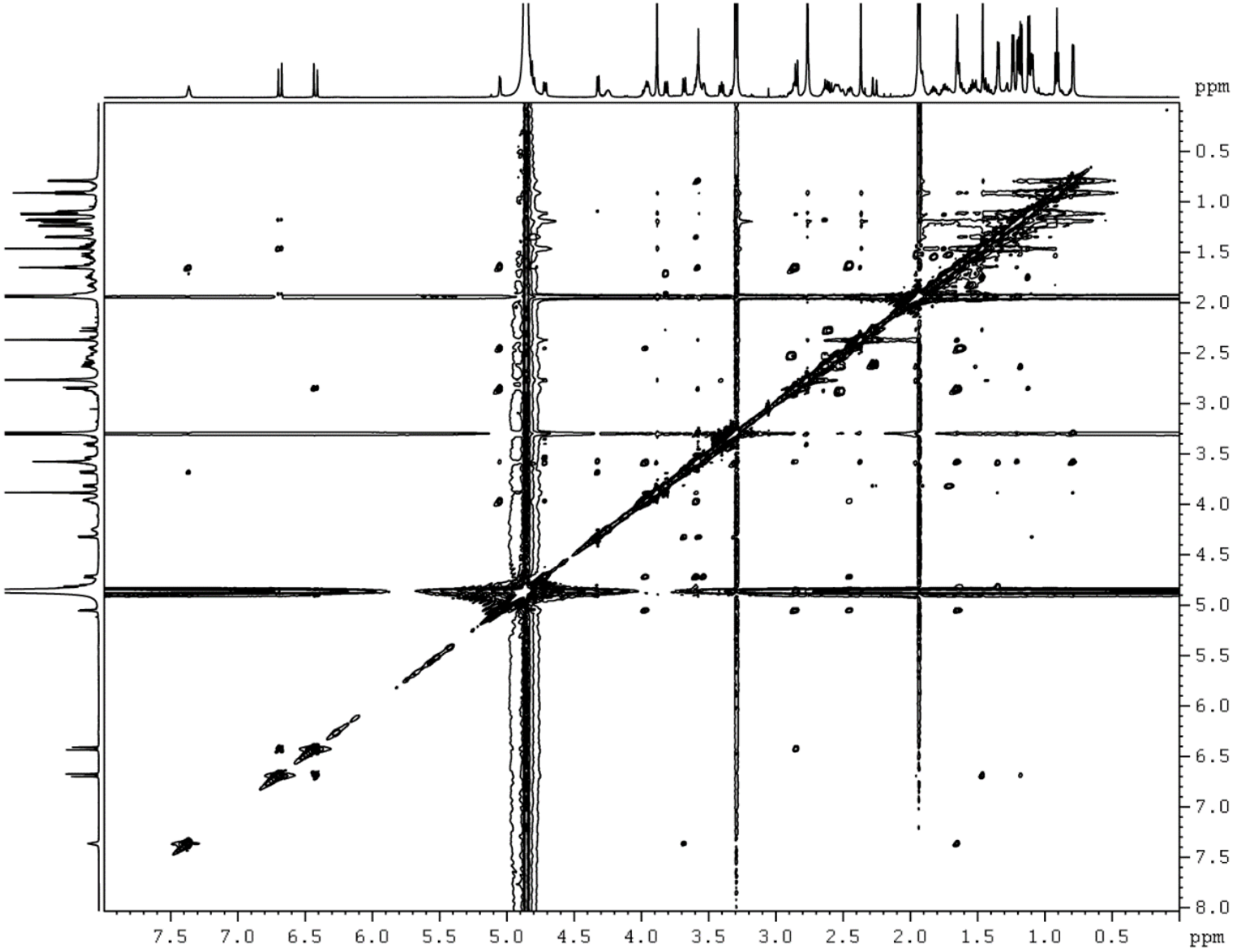

Figure A-8. ^{1}H proton NMR of everninomicin-rosaramicin conjugate in CD_4OD.

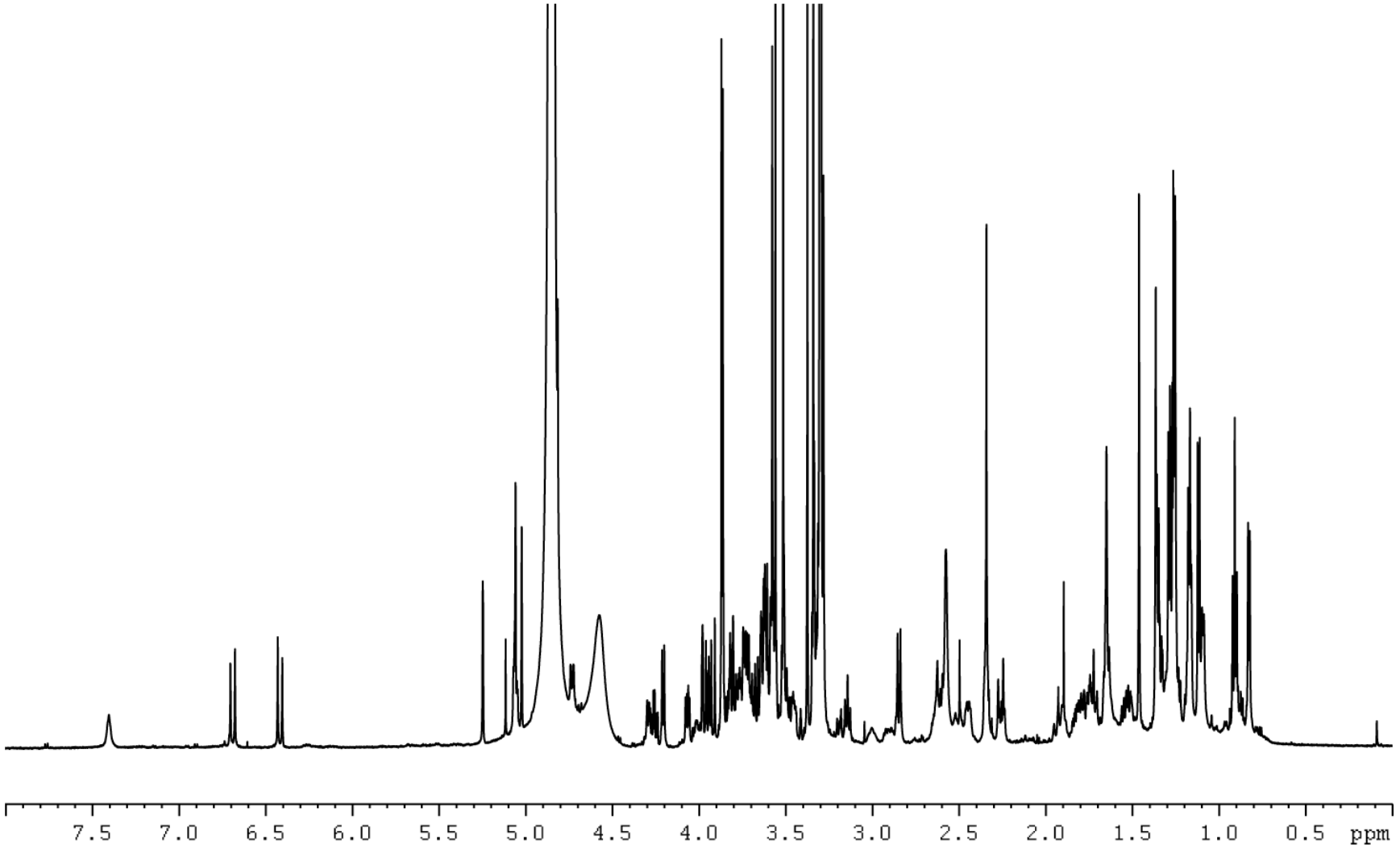

Figure A-9. COSY NMR of everninomicin-rosaramicin conjugate in CD_4OD.

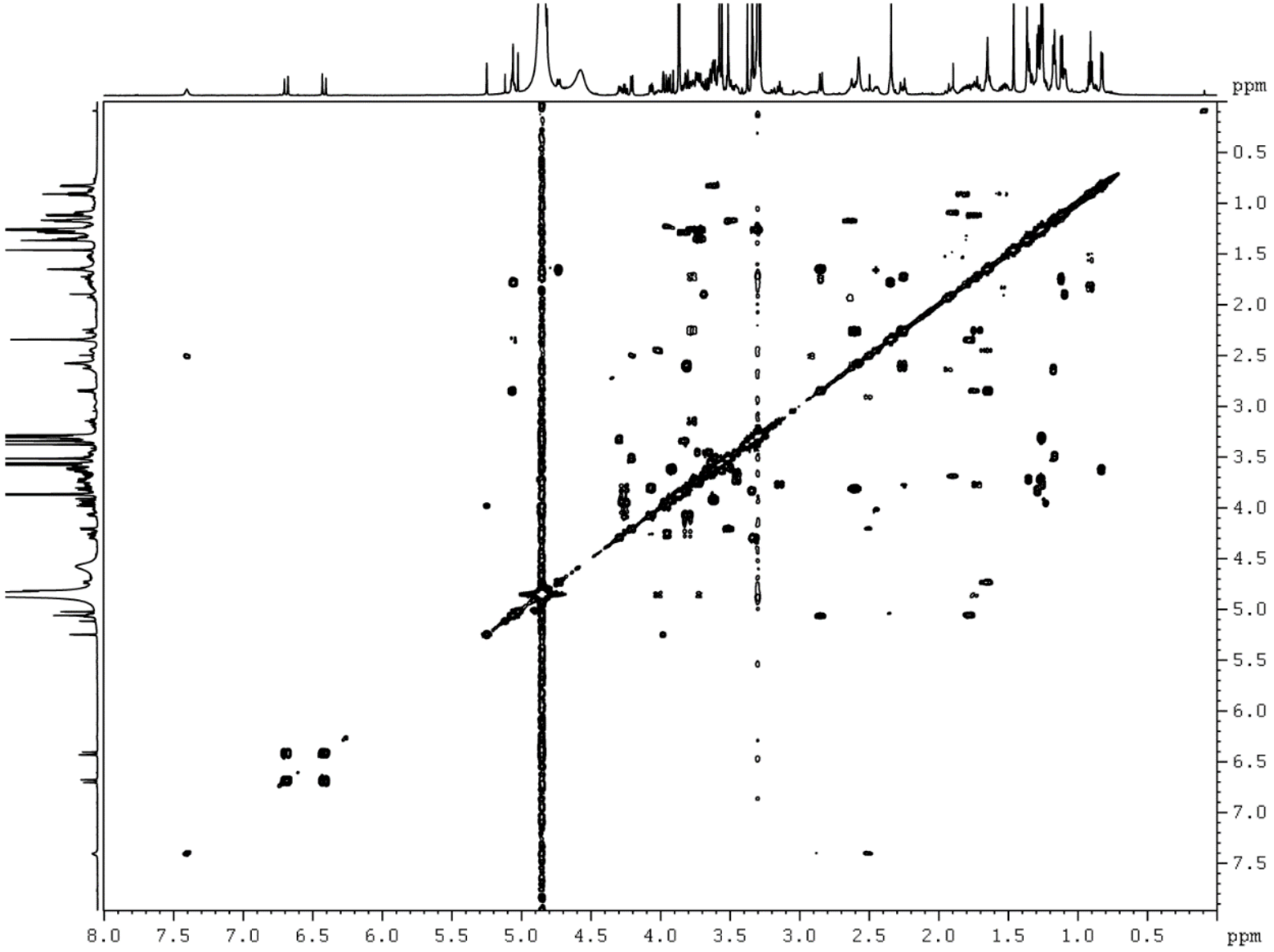

Figure A-10. HSQC NMR of everninomicin-rosaramicin conjugate in CD_4OD.

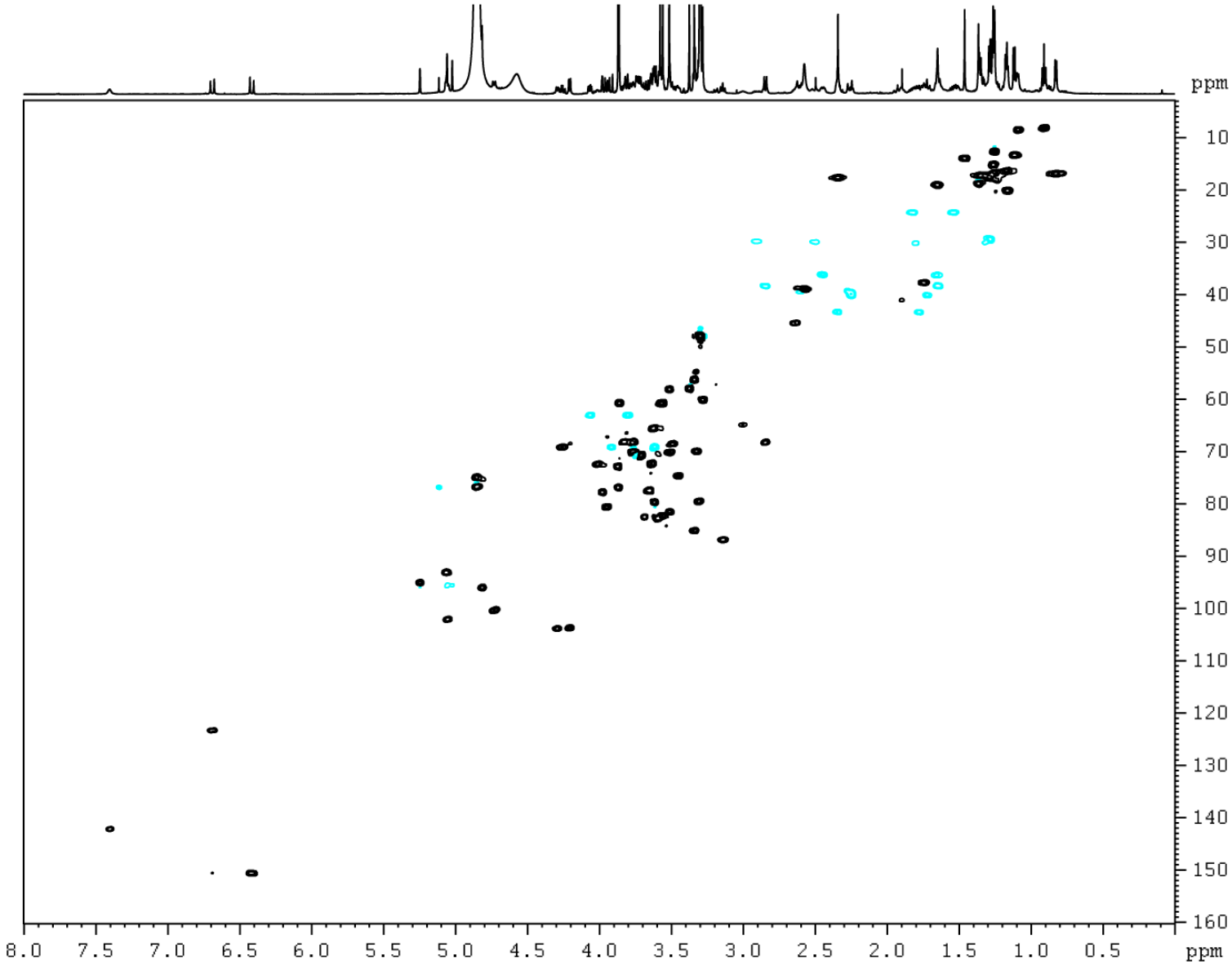

Figure A-11. HMBC NMR of everninomicin-rosaramicin conjugate in CD_4OD.

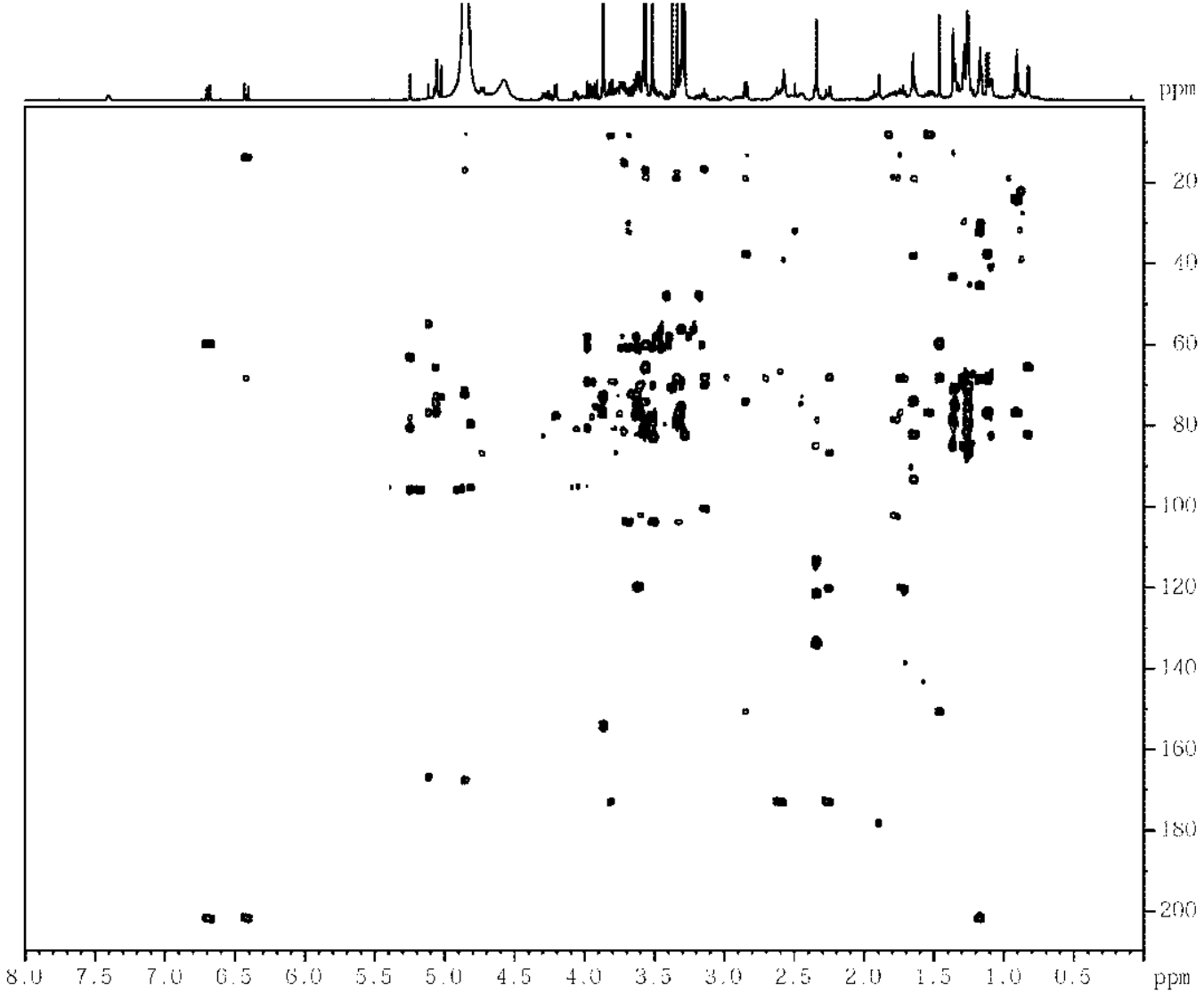

Figure A-12. ^{1}H proton NMR of Ever H in CD_4OD.

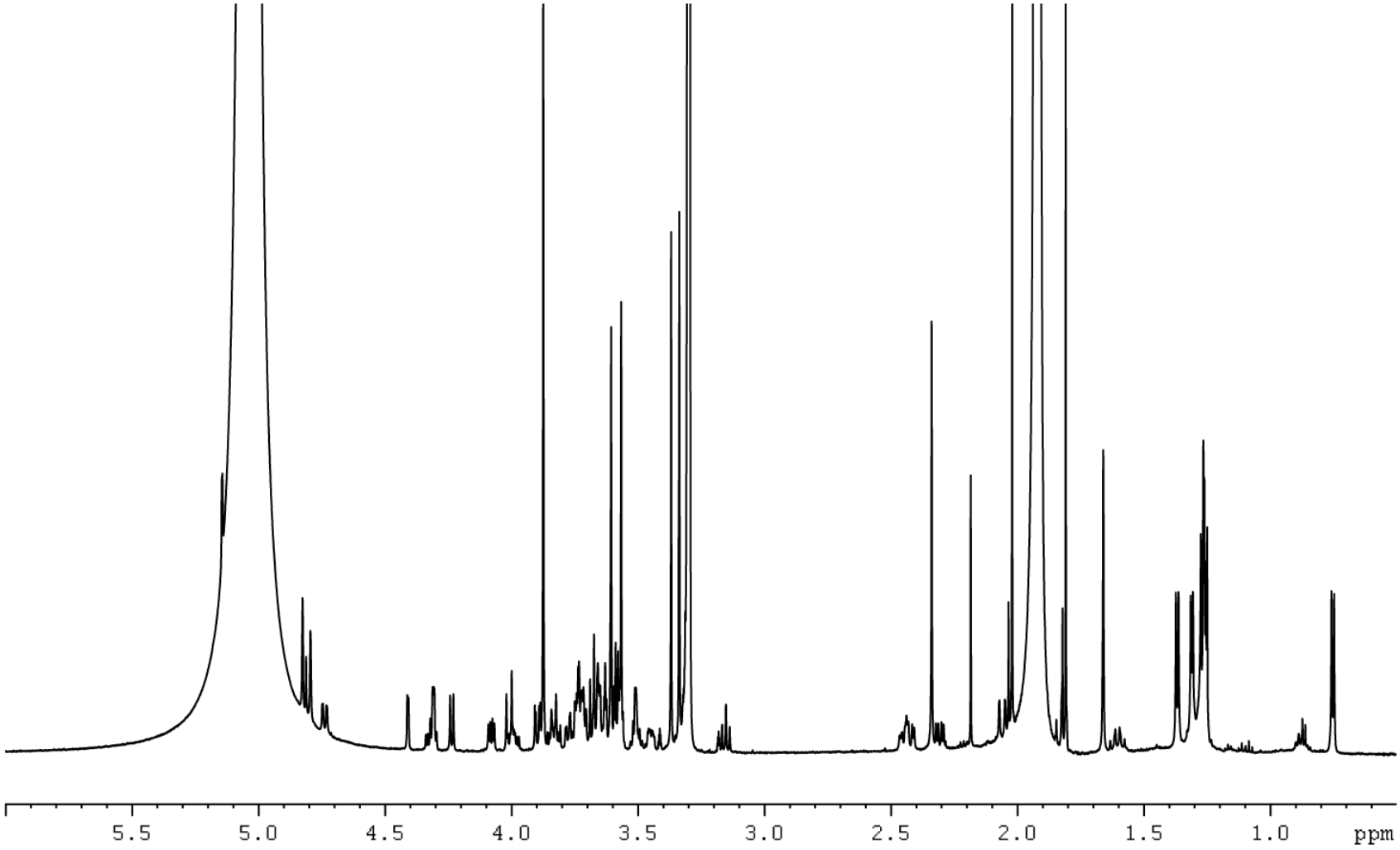

Figure A-13. ^{13}C carbon NMR of Ever H in CD_4OD.

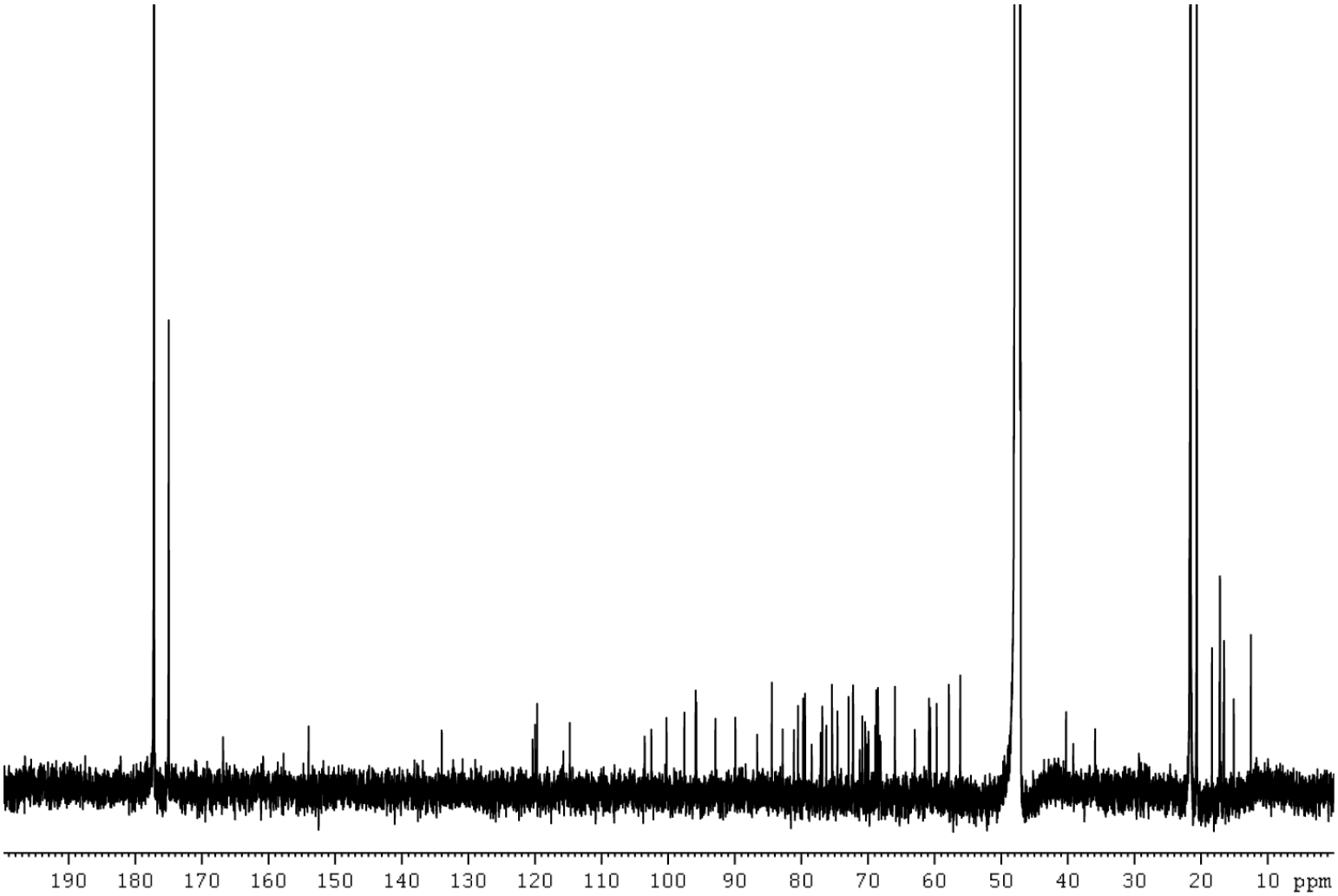

Figure A-14. COSY NMR of Ever H in CD_4OD.

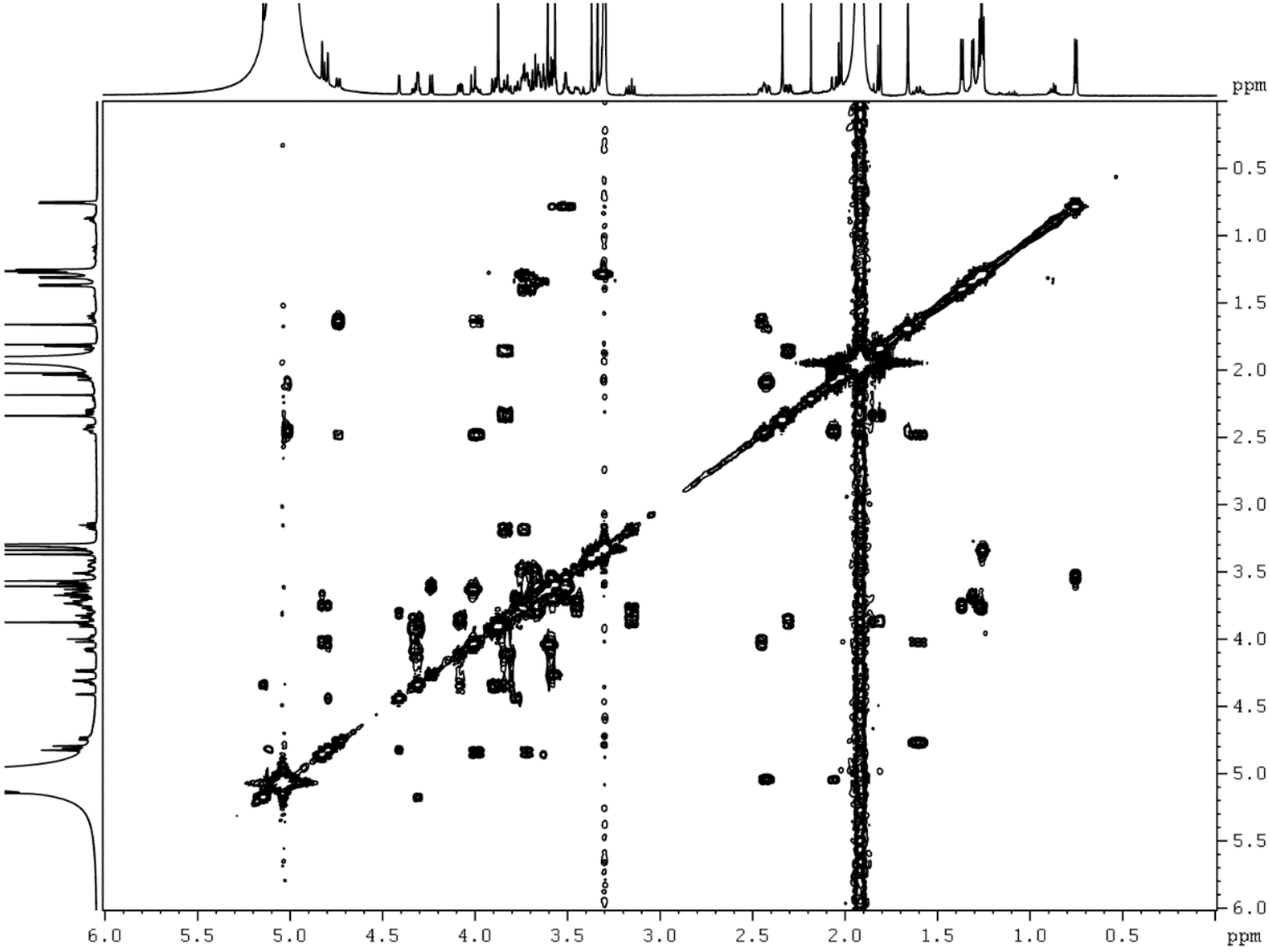

Figure A-15. HSQC NMR of Ever H in CD_4OD.

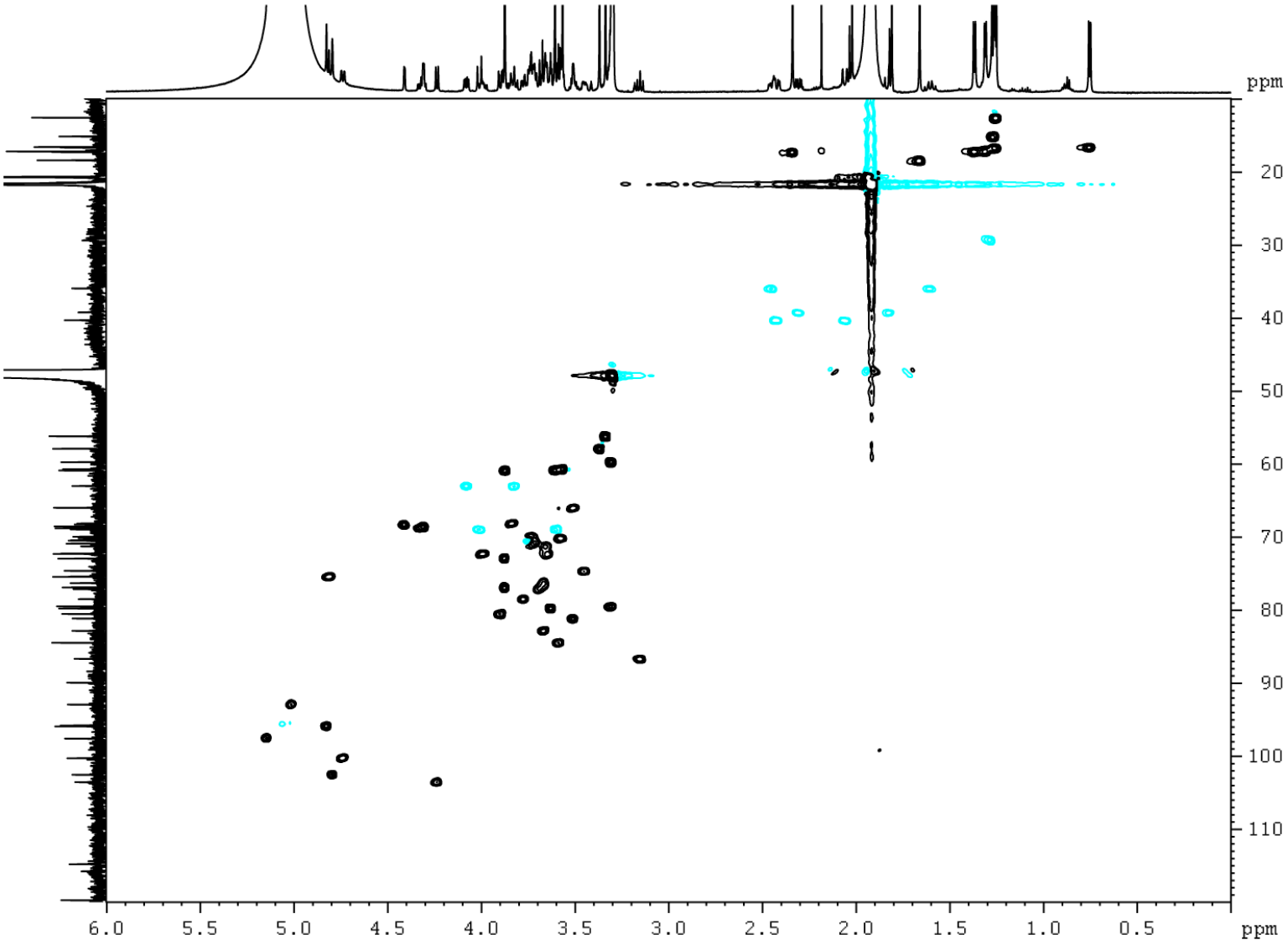

Figure A-16. HMBC NMR of Ever H in CD_4OD.

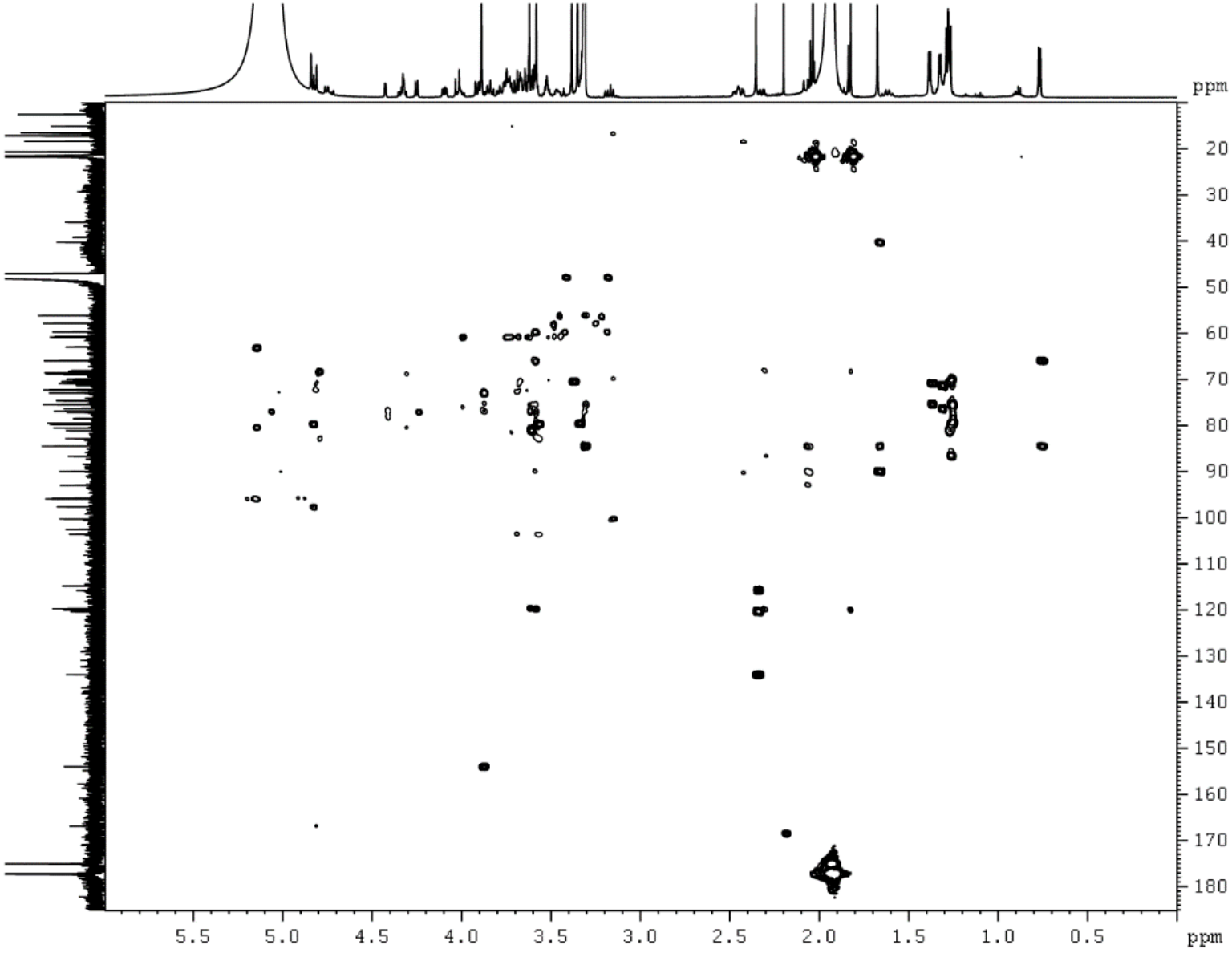

Figure A-17. TOCSY NMR of Ever H in CD_4OD.

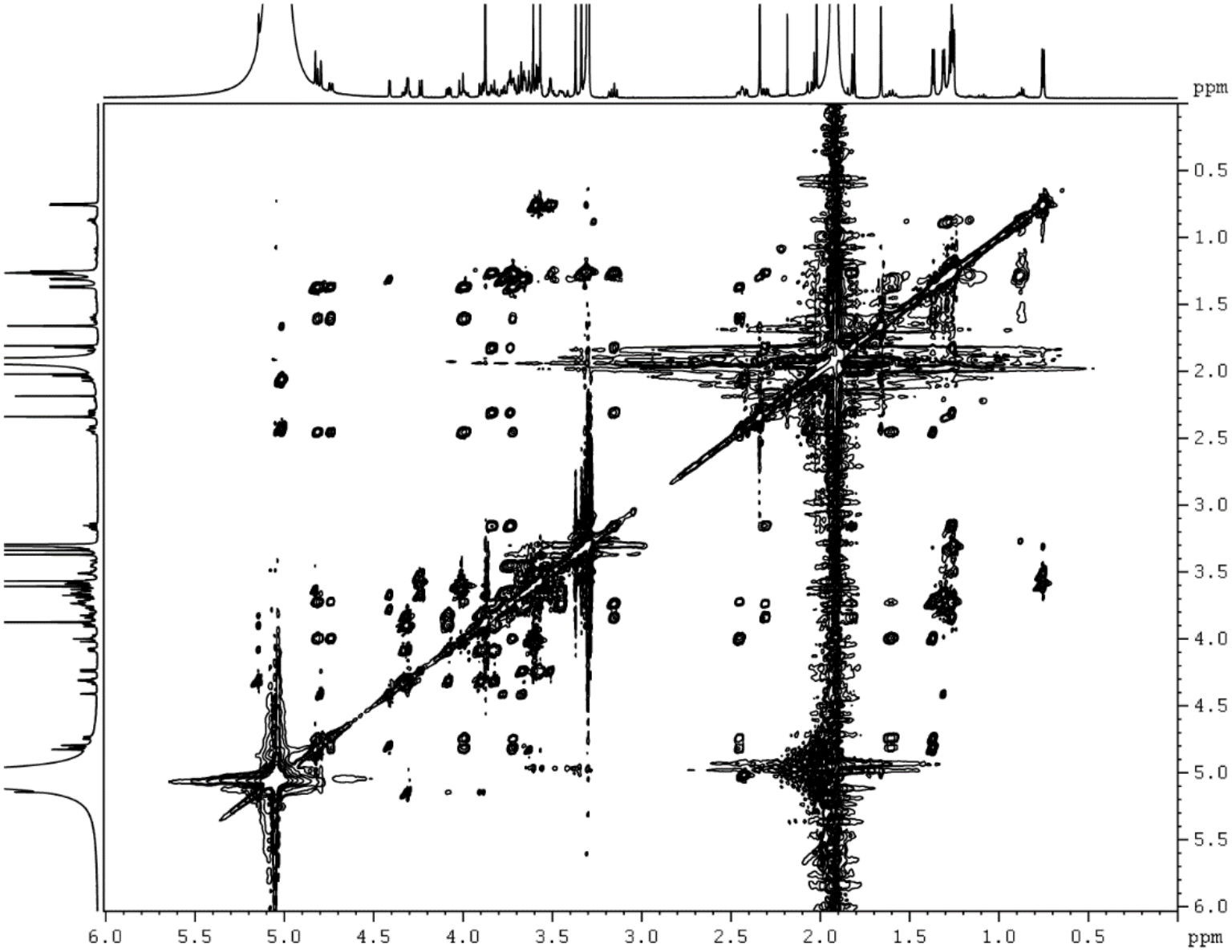

Table A-1. Truncated everninomicin-rosaramicin conjugate NMR data.

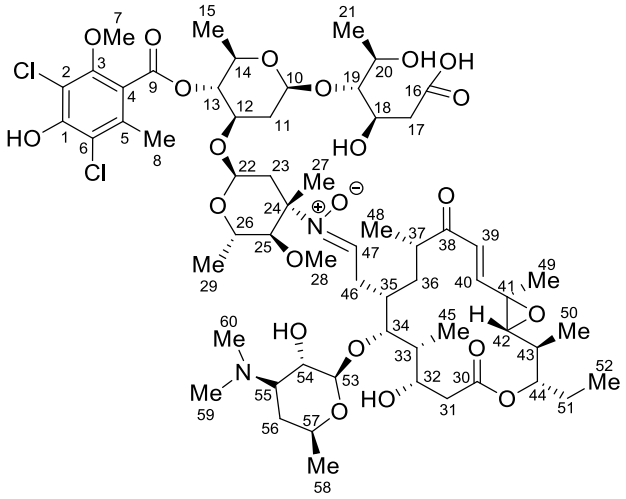

Pos.	^{13}C	^{1}H	HMBC	NOESY
1	155.7			
2	114.6			
3	153.9			
4	117.8			
5	134.2			
6	119.7			
7	61.1	3.88, 3H, s	3	
8	17.4	2.36, 3H, s	2, 3, 4, 5, 6	
9	166.7			
10	100.0	4.72, 1H, dd (9.4, 10.8 Hz)	11, 19	11, 12, 14, 19
11	36.1	1.63, 1H, m	10, 12	
		2.45, 1H, ddd (3.8, 5.3, 11 Hz)	10, 12, 13	10, 12, 22
12	72.7	3.97, 1H, overlap	13, 22	10, 11, 14, 22
13	75.9	4.81, 1H, overlap	9, 12, 13, 14, 15	
14	70.7	3.59, 1H, overlap	10, 13, 15	10, 12, 15
15	17.3	1.35, 3H, d (6.4 Hz)	13, 14	
16	176.8			
17	39.3	2.56, 2H, broad	16, 18	
18	68.0	4.25, 1H, broad		19
19	84.0	3.53, 1H, overlap	10	10
20	67.2	3.95, 1H, overlap		19
21	18.2	1.23, 3H, d (6.3 Hz)	19, 20	
22	93.2	5.05, 1H, d (4.8 Hz)	12, 24, 26	11, 12, 23
23	38.3	1.65, 1H, dd (1.9, 2.8 Hz)	22, 24, 27	
		2.86, 1H, overlap	22, 24, 27	
24	73.9			
25	82.3	3.58, 1H, overlap	26, 28	29
26	65.4	3.59, 1H, overlap	25	27
27	18.9	1.65, 3H, s	22, 23, 24, 25	22, 23, 26, 47
28	60.1	3.28, 3H, s	25	29
29	16.7	0.79, 3H, d (5 Hz)	25, 26	
30	172.9			
31	39.4	2.25, 1H, d (16.8 Hz)	30, 33	
		2.60, 1H overlap	30, 32	
32	66.3	3.83, 1H, broad (10.2 Hz)	30, 31, 45	31, 34, 35
33	40.8	1.91, 1H, overlap	34, 35	
34	82.5	3.67, 1H, broad (10 Hz)	33, 35, 36, 45, 46, 53	32, 35, 47, 53
35	34.6	1.71, 1H, m		
36	32.3	1.51, 1H, overlap	37, 40	
		1.93, 1H	37, 46, 48	

Pos.	^{13}C	^{1}H	HMBC	NOESY
37	45.4	2.64, 1H, overlap	38	
38	201.4			
39	123.2	6.68, 1H, d (15.7 Hz)	38, 41	48, 49
40	150.6	6.45, 1H, d (15.7 Hz)	38, 39, 42, 49	42
41	59.6			
42	68.2	2.84, 1H, d (9.6 Hz)	40, 41, 43, 50	
43	37.6	1.74, 1H, m	42, 44, 50	
44	76.8	4.86, 1H, overlap	30, 43, 51, 52	
45	8.5	1.09, 3H, d (6.5 Hz)	32, 33, 34	
46	30.0	2.51, 1H, overlap		
		2.88, 1H, overlap	47	
47	142.1	7.36, 1H, broad	46	27, 34
48	16.3	1.17, 3H, d (7 Hz)	36, 37, 38	
49	13.9	1.46, 3H,s	40, 41, 42	39, 43
50	13.2	1.12, 3H, d (6.7 Hz)	42, 43, 44	
51	24.2	1.54, 1H, overlap	43, 44, 52	
		1.83, 1H, m	43, 52	
52	8.05	0.91, 3H, t (7.3 Hz)	44, 51	
53	103.5	4.32, 1H, d (7.2 Hz)	34, 55	34, 57
54	69.1	3.41, 1H, dd (7.2, 10.5 Hz)	53, 55	59 or 60
55	65.3	3.30, 1H, overlap	54	57
56	29.8	1.43, 1H, overlap	57, 58	
		1.92, 1H		
57	68.1	3.57, 1H, overlap	59, 61	53
58	19.9	1.19, 3H, d (6.2 Hz)	56, 57	
59	38.7	2.77, 3H, s	55, 60	
60	38.7	2.77, 3H, s	55, 59	

Table A-2. Everninomicin-rosaramicin conjugate (**9**) NMR data.

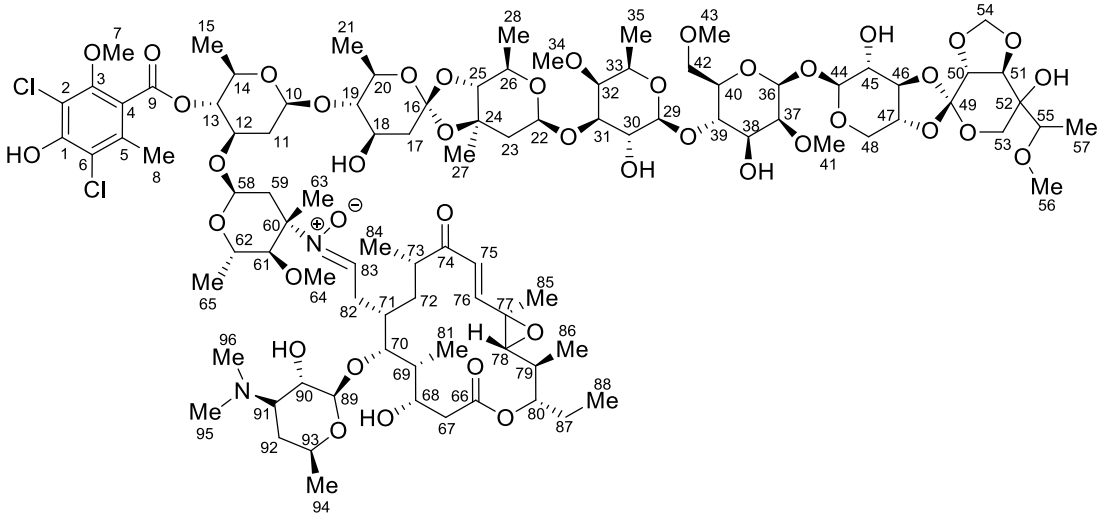

Pos.	^{13}C	^{1}H	HMBC
1	?		
2	113.3		
3	154.0		
4	?		
5	133.7		
6	121.1		
7	60.7	3.87, 3H, s	3
8	17.5	2.34, 3H, s	4, 5, 6
9	166.8		
10	100.3	4.73, 1H, dd (9.4, 10.8 Hz)	11, 19
11	36.2	1.66, 1H, m	10, 12
		2.45, 1H, m	10, 12
12	72.3	4.01, 1H, m	11, 13, 14
13	74.9	4.85, 1H, overlap	9, 12, 14
14	70.8	3.71, 1H, overlap	13, 15
15	17.2	1.35, 3H, overlap	14
16	120.2		
17	39.9	1.73, 1H,	16
		2.25, 1H	16, 18, 19
18	68.1	3.77, 1H, overlap	17, 19
19	86.8	3.14, 1H, dd (8.9, 9.2 Hz)	10, 18, 20, 21
20	70.0	3.77, 1H, overlap	19, 21
21	16.5	1.26, 3H, overlap	19, 20
22	102.0	5.05, 1H, overlap	23, 31
23	43.2	1.78, 1H, dd (1.9, 2.8 Hz)	24
		2.35, 1H, overlap	22, 24
24	78.7		
25	85.0	3.34, 1H, overlap	
26	68.1	3.83, 1H, overlap	28
27	18.7	1.36, 3H, s	23, 24, 25
28	17.4	1.29, 3H, d (6.5 Hz)	25, 26
29	103.9	4.21, 1H, d (7.7 Hz)	30, 39
30	70.1	3.51, 1H, overlap	
31	82.7	3.59, 1H, overlap	32
32	81.4	3.51, 1H, broad (10.2 Hz)	
33	70.5	3.71, 1H, overlap	35
34	60.7	3.57, 3H, s	32
35	15.1	1.26, 3H, overlap	33
36	95.9	4.82, 1H, overlap	44

Pos.	^{13}C	^{1}H	HMBC
37	79.6	41	
38	?		
39	77.7	3.98, 1H, overlap	29
40	?		
41	58.1	3.51, 3H, s	37
42	70.5	3.75, 2H, overlap	
43	57.9	3.38, 3H, s	42
44	94.9	5.25, 1H, d (1.4 Hz)	36, 45
45	72.5	3.97, 1H, overlap	46
46	80.6	3.95, 1H,dd (2.5, 10.1 Hz)	
47	69.1	4.26, 1H, ddd (4.4, 10, 15 Hz)	
48	62.9	3.80, 1H, overlap	46, 47
		4.07, 1H, dd (4.7, 9.9 Hz)	46
49	119.7		
50	72.8	3.87, 1H, overlap	
51	76.8	3.87, 1H, overlap	
52	75.3		
53	69.1	3.62, 1H, overlap	49, 51, 52
		3.92, 1H, d (12.2 Hz)	
54	95.4	5.02, 1H, s	50
		5.06, 1H, s	
55	79.5	3.31, 1H, d (6.2 Hz)	56
56	56.3	3.34, 3H, s	55
57	12.5	1.25, 3H, overlap	52, 55
58	93.1	5.06, 1H, overlap	12, 59
59	38.3	1.64, 1H, overlap	60
		2.85, 1H, overlap	60, 63
60	73.9		
61	82.3	3.57, 1H, overlap	60, 64
62	65.5	3.63, 1H, overlap	61, 65
63	19.1	1.65, 3H, s	59, 60, 61
64	60.1	3.28, 3H, s	61
65	16.8	0.82, 3H, d (6 Hz)	61, 62
66	172.9		
67	39.5	2.27, 1H, overlap	66
		2.61, 1H, overlap	66
68	66.5	3.81, 1H, overlap	
69	40.9	1.91, 1H, overlap	
70	82.3	3.69, 1H, overlap	89
71	34.6	1.72. 1H, overlap	
72	32.1	1.50, 1H, overlap	
		1.93, 1H, overlap	
73	45.4	2.64, 1H, overlap	84
74	201.6		
75	123.3	6.69, 1H, d (16 Hz)	74, 76
76	150.6	6.42, 1H, d (16 Hz)	75, 77
77	59.8		
78	68.2	2.85, 1H, overlap	76, 79
79	37.6	1.75, 1H, overlap	86
80	76.7	4.85, 1H, overlap	79, 87
81	8.4	1.09, 3H, d (6.6 Hz)	
82	29.8	2.50, 1H, overlap	
		2.91, 1H, m	
83	142.2	7.40, 1H, broad	
84	16.3	1.17, 3H, overlap	72, 73, 74
85	13.9	1.46, 3H, overlap	76, 77, 78
86	13.2	1.11, 3H, d (6.8 Hz)	78, 79, 80
87	24.2	1.54, 1H, m	80
		1.82, 1H, overlap	
88	8.1	0.91, 3H, t (7.4 Hz)	80, 87
89	103.8	4.30, 1H, d (7.1 Hz)	70
90	69.9	3.32, 1H, overlap	
91	64.9	3.00, 1H, m	95, 96
92	30.0	1.32. 1H, overlap	
		1.81, 1H, overlap	
93	68.5	3.49. 1H, overlap	94
94	20.1	1.16, 3H, overlap	93
95	38.9	2.58, 3H, s	91
96	38.9	2.62, 3H, s	91

Table A-3. Everninomicin H NMR Data.

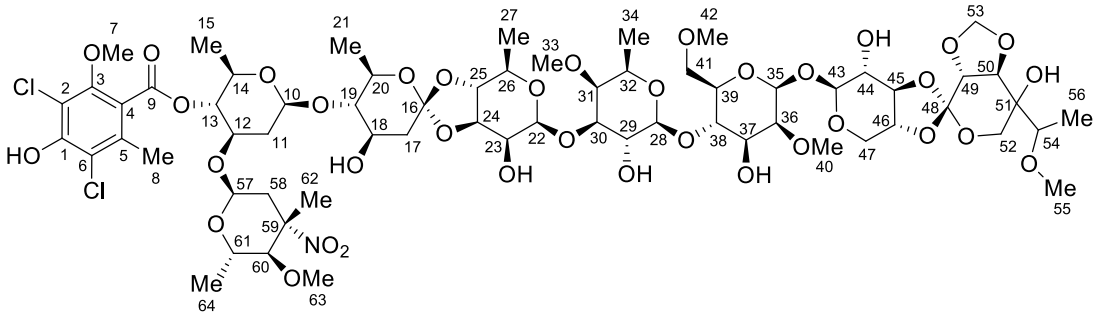

Pos.	^{13}C	^{1}H	HMBC
1	?		
2	114.8		
3	154.1		
4	115.8		
5	134.2		
6	120.2		
7	60.8	3.88, 3H, s	3
8	17.4	2.34, 3H, s	4, 5, 6
9	166.8		
10	100.2	4.75, 1H, dd (4.7, 10 Hz)	19
11	36.0	1.61, 1H, m	
		2.46, 1H, m	10, 12, 13
12	72.3	3.99, 1H, overlap	13
13	75.4	4.81, 1H, overlap	9, 12, 14
14	70.8	3.72, 1H, m	
15	17.3	1.38, 3H, d (6.4 Hz)	13, 14
16	119.9		
17	39.4	1.84, 1H, dd (9.7, 12.7 Hz)	16, 18
		2.33, 1H, dd (5, 12.7 Hz)	
18	68.1	3.84, 1H, overlap	
19	86.7	3.17, 1H, t (9 Hz)	10, 18, 20, 21
20	69.9	3.73, 1H, m	
21	16.7	1.26, 3H, overlap	19, 20
22	102.5	4.80, 1H, overlap	23, 30
23	68.3	4.41, 1H, dd (1.9, 2.8 Hz)	22, 24, 25
24	78.3	3.78, 1H, overlap	25
25	76.3	3.69, 1H, overlap	
26	71.3	3.66, 1H, m	
27	17.3	1.31, 3H, d (5.5 Hz)	25, 26
28	103.5	4.24, 1H, d (7.8 Hz)	38
29	70.13	3.57, 1H, overlap	28, 30
30	82.8	3.67, 1H, overlap	22, 32
31	81.2	3.51, 1H, overlap	29, 30, 33
32	70.7	3.72, 1H, m	31
33	60.7	3.61, 3H, s	31
34	15.2	1.27, 3H, overlap	31, 32
35	95.8	4.83, 1H, overlap	36, 43
36	79.8	3.63, 1H, overlap	37, 40
37	72.3	3.65, 1H, overlap	
38	77.0	3.69, 1H, overlap	28, 37, 39
39	74.6	3.45, 1H, m	
40	60.7	3.56, 3H, s	36
41	70.5	3.75, 2H, overlap	
42	57.9	3.37, 3H, s	41
43	97.5	5.15, 1H, overlap	35, 44, 47
44	68.6	4.31, 1H, overlap	45, 46
45	80.5	3.89, 1H, dd (2.7, 10.3 Hz)	
46	68.8	4.34, 1H, overlap	

Pos.	^{13}C	^{1}H	HMBC
47	63.0	3.82, 1H, overlap	
		4.08, 1H, dd (4.5, 9.7 Hz)	43, 45, 46
48	119.8		
49	72.8	3.88, 1H, overlap	50
50	77.0	3.87, 1H, overlap	49
51	75.7		
52	68.9	3.61, 1H, overlap	48, 50, 51
		4.01, 1H, d (12.3 Hz)	51
53	95.3	5.02, 1H, overlap	49
		5.06, 1H, overlap	50
54	79.5	3.31, 1H, m	50, 51, 52, 55
55	56.1	3.33, 1H, s	54
56	12.6	1.25, 3H, overlap	51, 54
57	92.8	5.03, 1H, dd	59, 61
58	40.2	2.08, 1H, dd (1, 13 Hz)	57, 59, 60
		2.44, 1H, dd (5, 13.5 Hz)	59, 62
59	89.9		
60	84.4	3.60, 1H, overlap	59, 61, 63
61	65.9	3.51, 1H, m	
62	18.4	1.68, 3H, s	58, 59, 60
63	59.7	3.30, 3H, s	60
64	16.5	0.77, 3H, d (6 Hz)	60, 61

Appendix B.

Mass Spectra

Table of Contents

Figure B-1. Mass spectra of everninomicins D (A), E (B), F (C), and G (D). Adapted from *Proc Nat Acad Sci USA* **112**, 11547-11552 (2015).

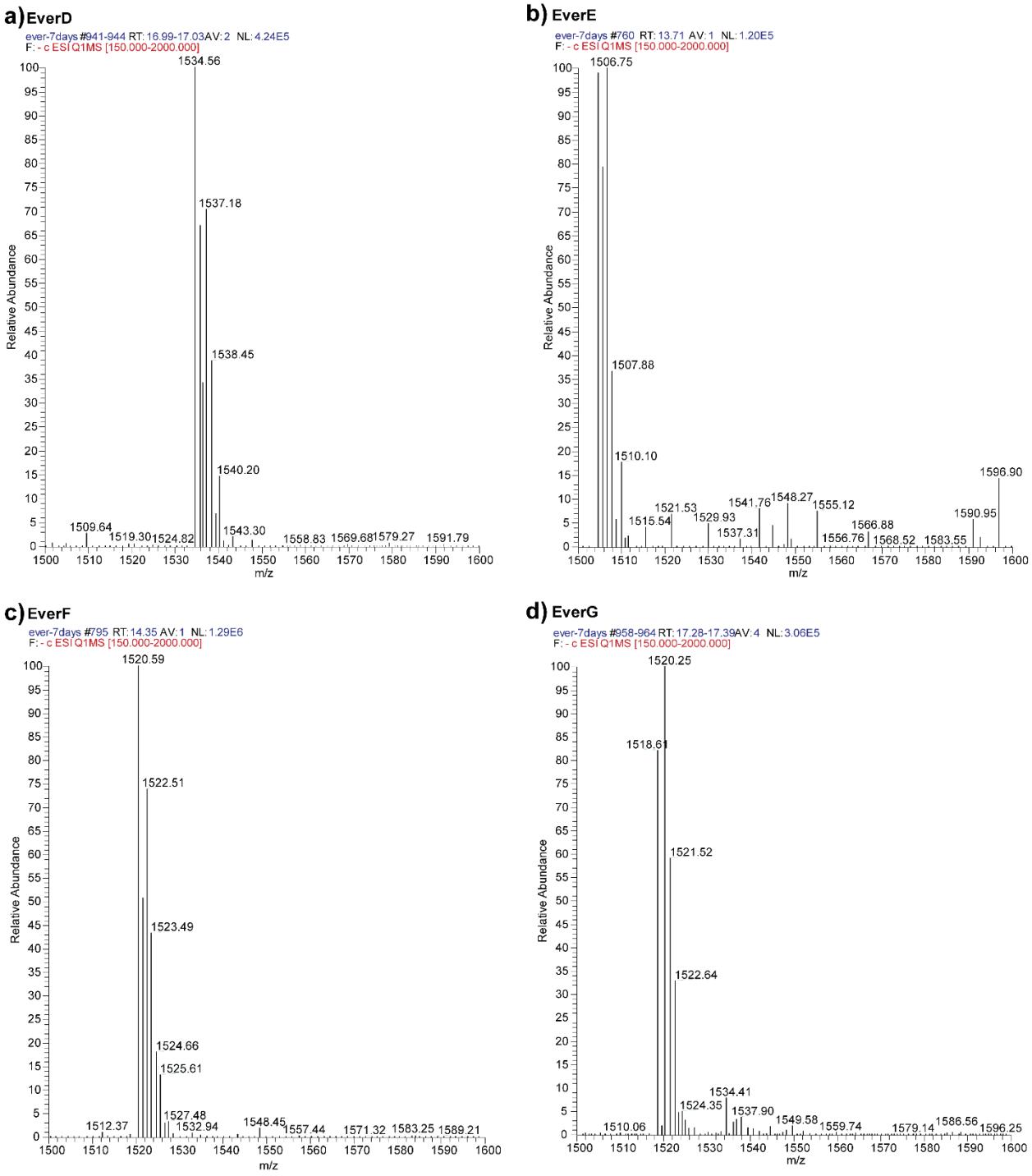

Figure B-2. Everninomicin E mass spectrometric fragmentation data. (A) Mass spectrometric fragmentation pattern for ever E. Dashed lines indicate positions of cleavage during fragmentation experiments. (B) Spectrum for fragmentation of ever E (m/z =1506.567 $[M+H]^+$). Adapted from *Proc Nat Acad Sci USA* **112**, 11547-11552 (2015).[25]

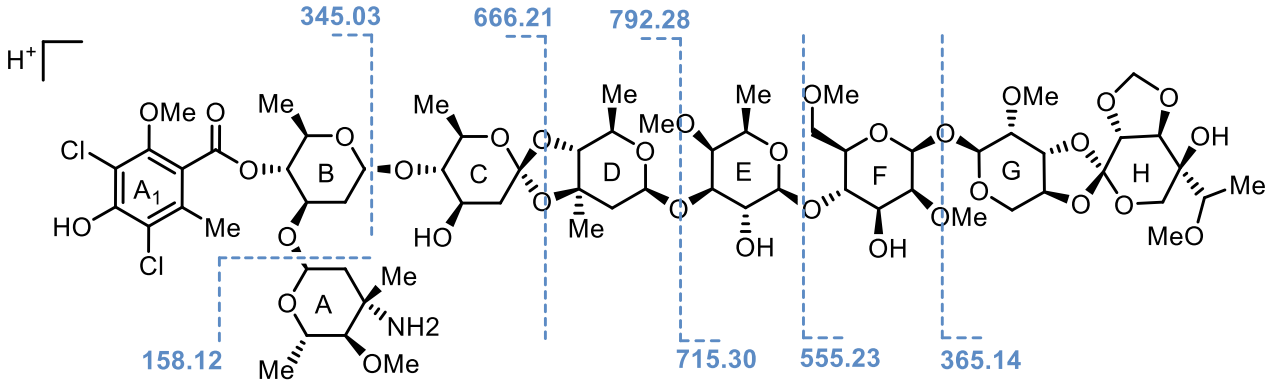

Ever E

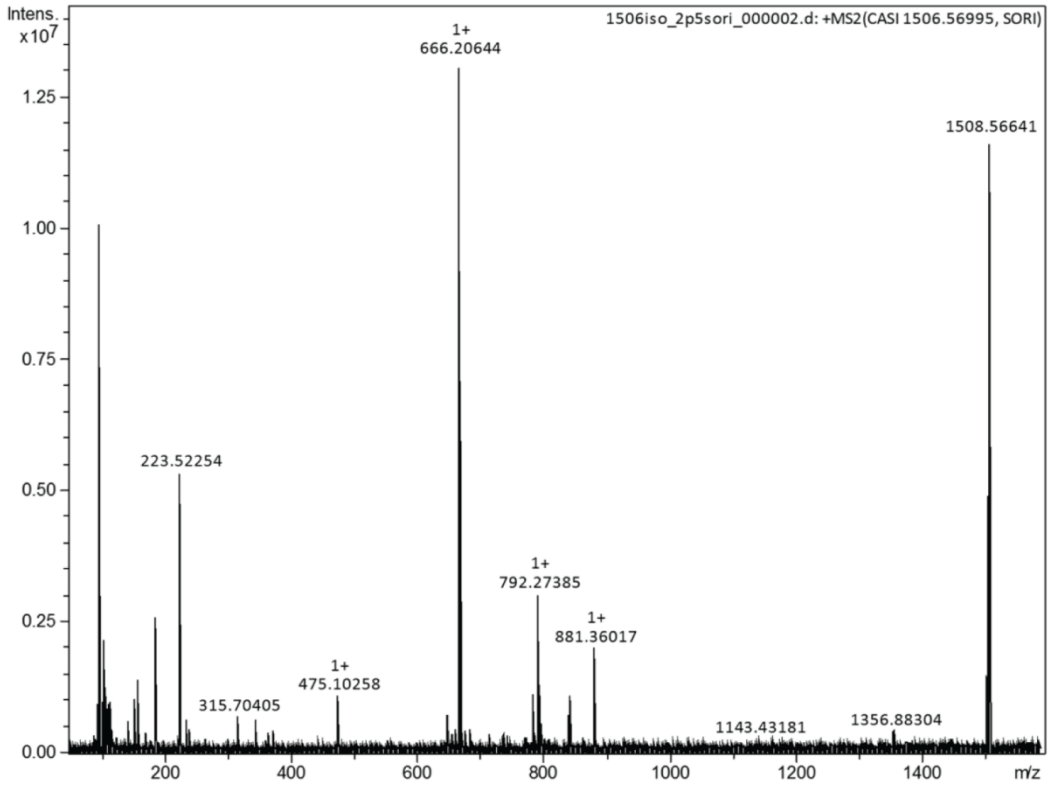

Figure B-3. Everninomicin F mass spectrometric fragmentation data. (A) Mass spectrometric fragmentation pattern for ever F. Dashed lines indicate positions of cleavage during fragmentation experiments. (B) Spectra for fragmentation of ever F (m/z =1522.5 $[M+H]^+$) continued on next page. Adapted from *Proc Nat Acad Sci USA* **112**, 11547-11552 (2015).[25]

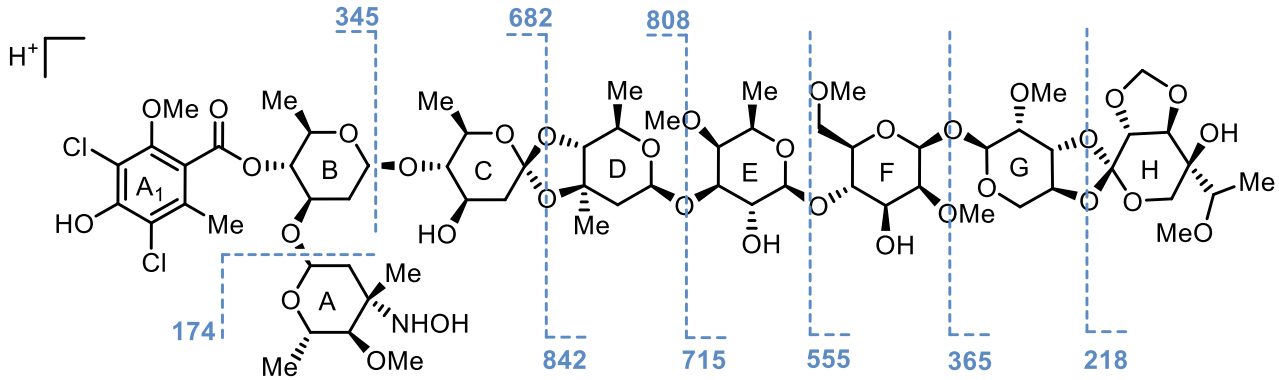

Ever F

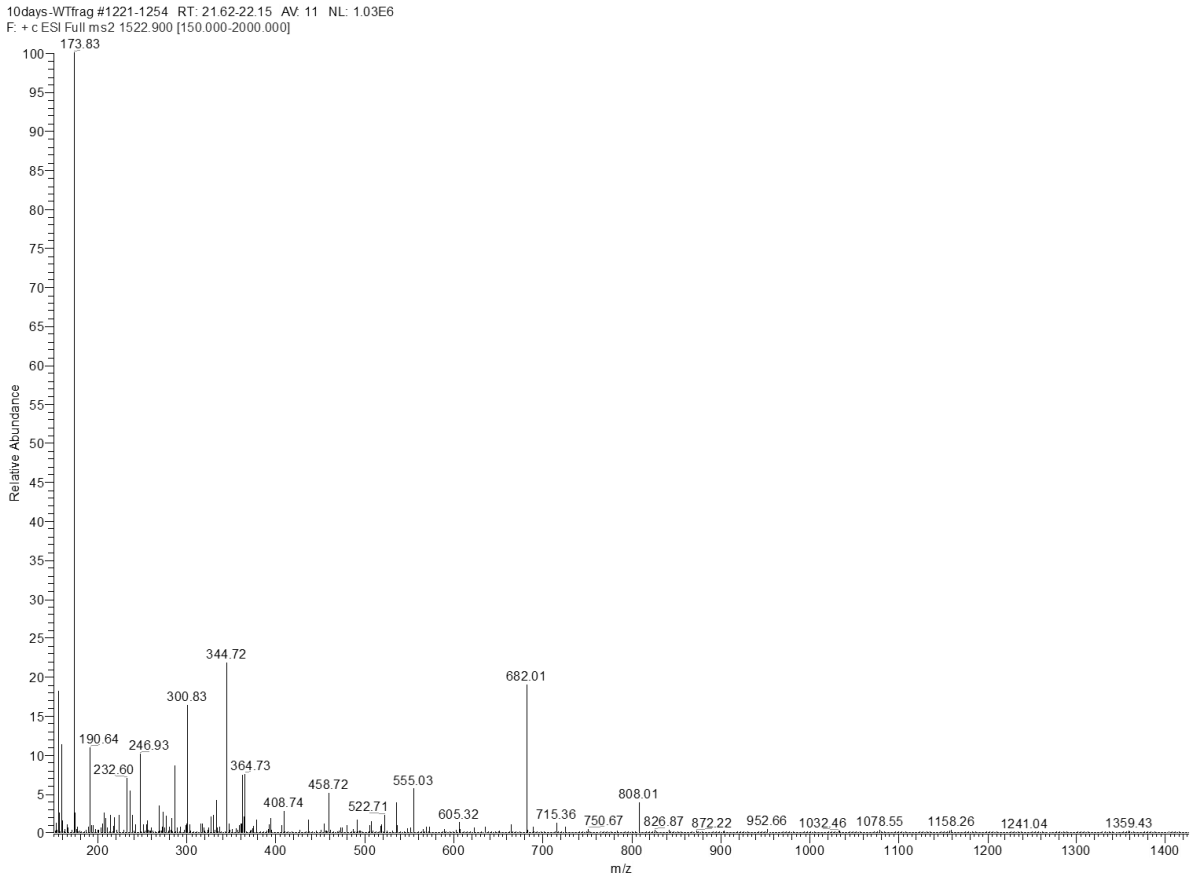

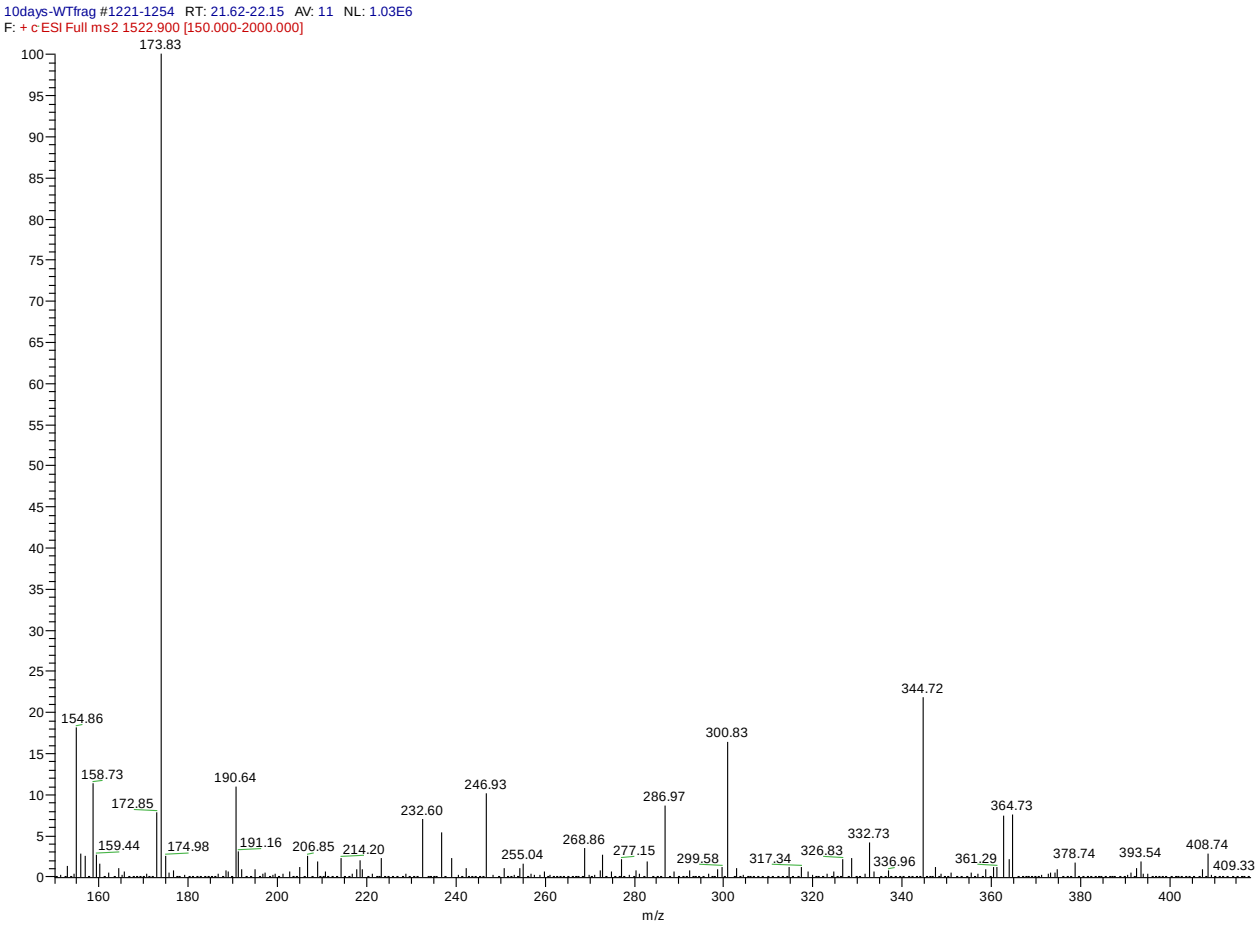
10days-WTfrag #1221-1254 RT: 21.62-22.15 AV: 11 NL: 1.03E6
F: + c ESI Full ms2 1522.900 [150.000-2000.000]
173.83
154.86
158.73
172.85
159.44
174.98
190.64
191.16
206.85
214.20
232.60
246.93
255.04
268.86
277.15
286.97
299.58
300.83
317.34
326.83
332.73
336.96
344.72
361.29
364.73
378.74
393.54
408.74
409.33
m/z

Figure B-4. Everninomicin-2 mass spectrometric fragmentation data. (A) Mass spectrometric fragmentation pattern for ever-2. Dashed lines indicate positions of cleavage during fragmentation experiments. (B) Spectrum for fragmentation of ever H (m/z =1349.5 $[M+H]^+$).

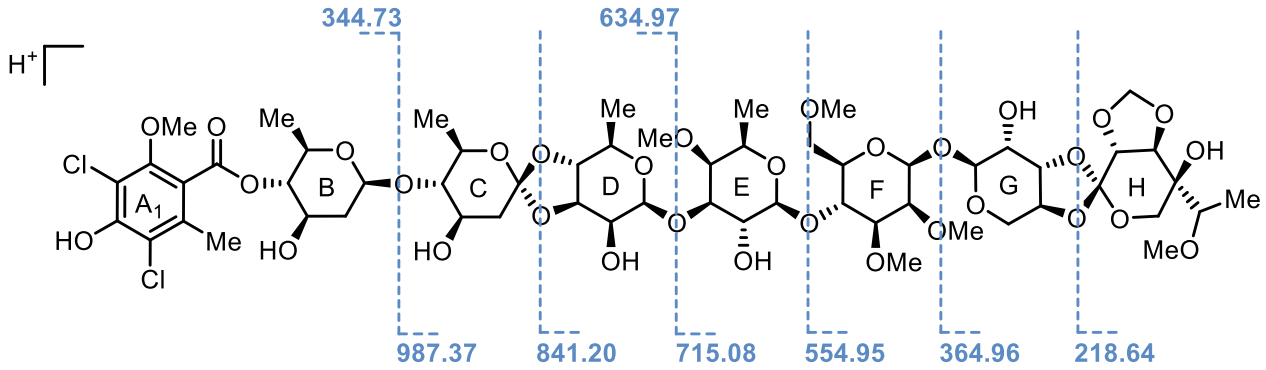

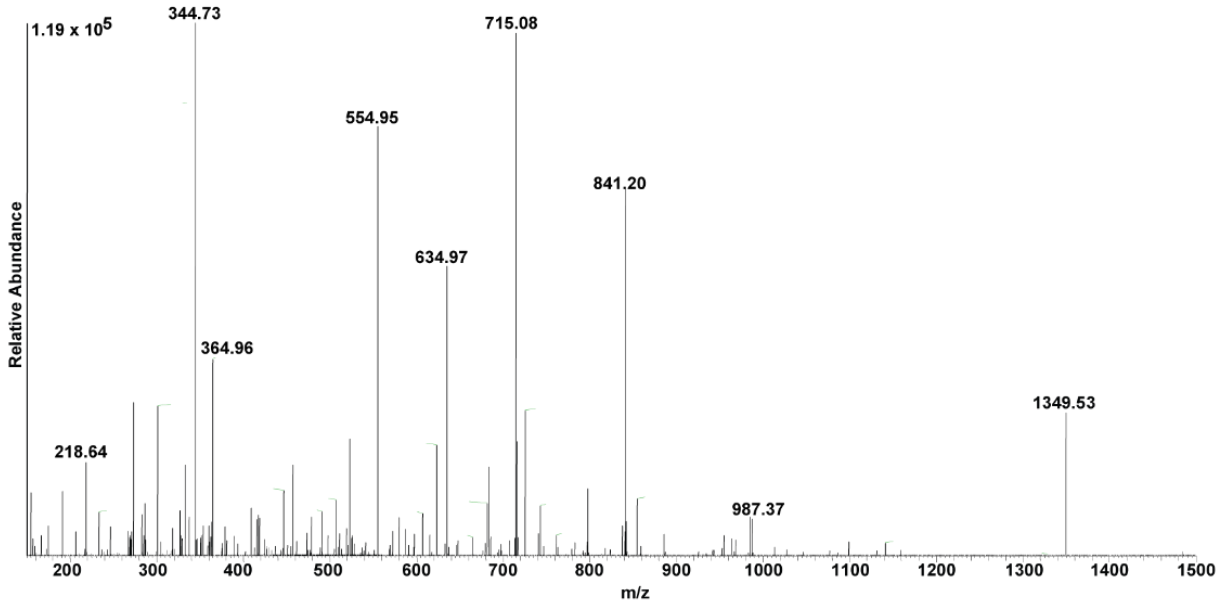

Figure B-5. Everninomicin H mass spectrometric fragmentation data. (A) Mass spectrometric fragmentation pattern for Ever H. Dashed lines indicate positions of cleavage during fragmentation experiments. (B) Spectrum for fragmentation of ever H (m/z = 1546.5 $[M+Na]^+$).

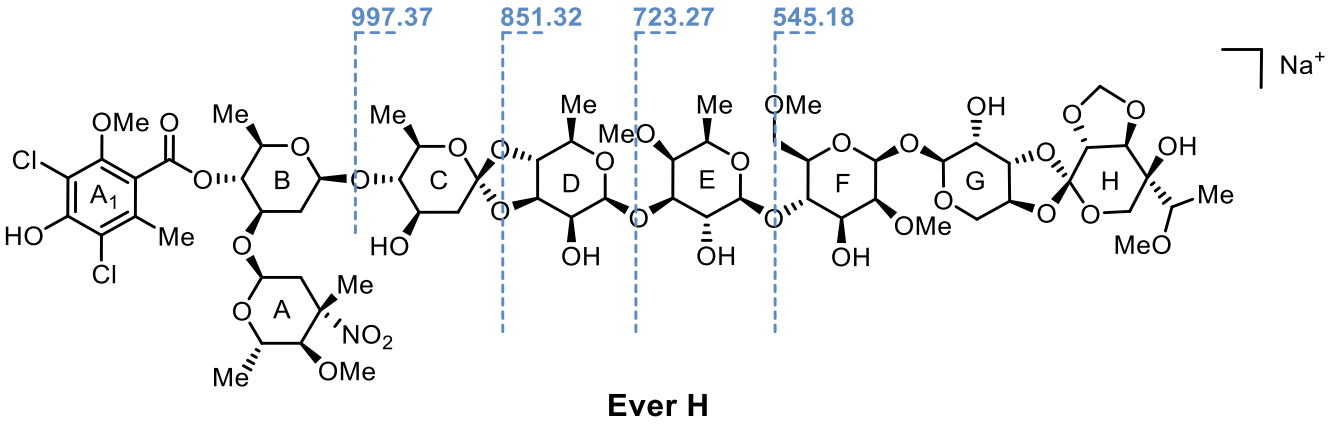

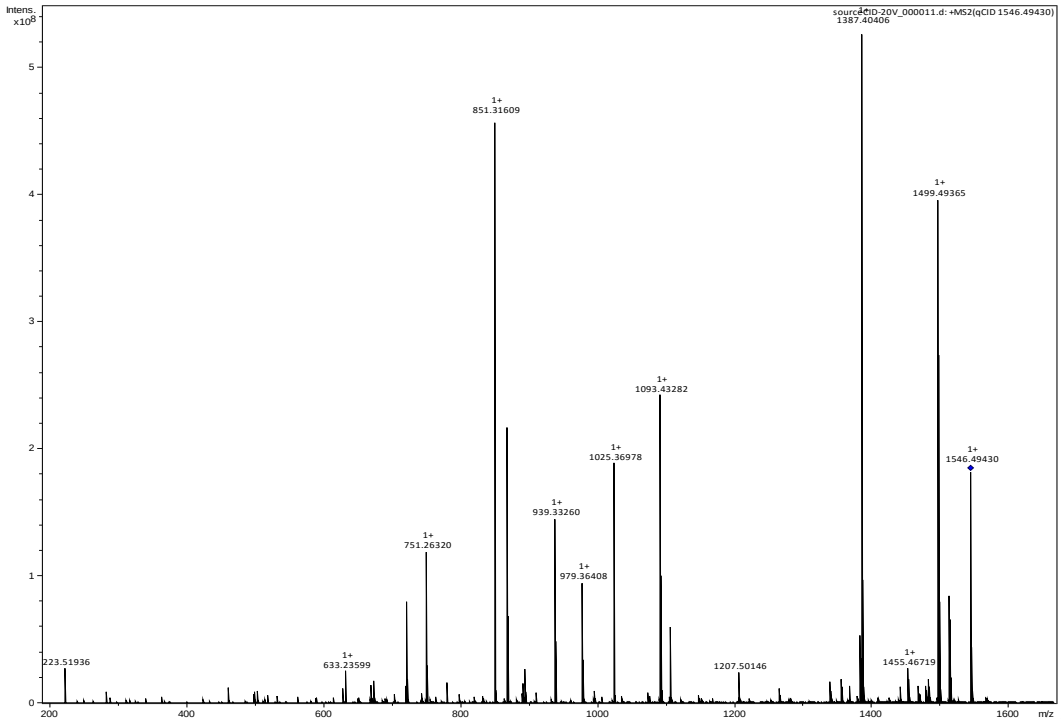

Figure B-6. Everninomicin J mass spectrometric fragmentation data. (A) Mass spectrometric fragmentation pattern for Ever J. Dashed lines indicate positions of cleavage during fragmentation experiments. (B) Spectrum for fragmentation of ever J (m/z = 1494.5 $[M+H]^+$).

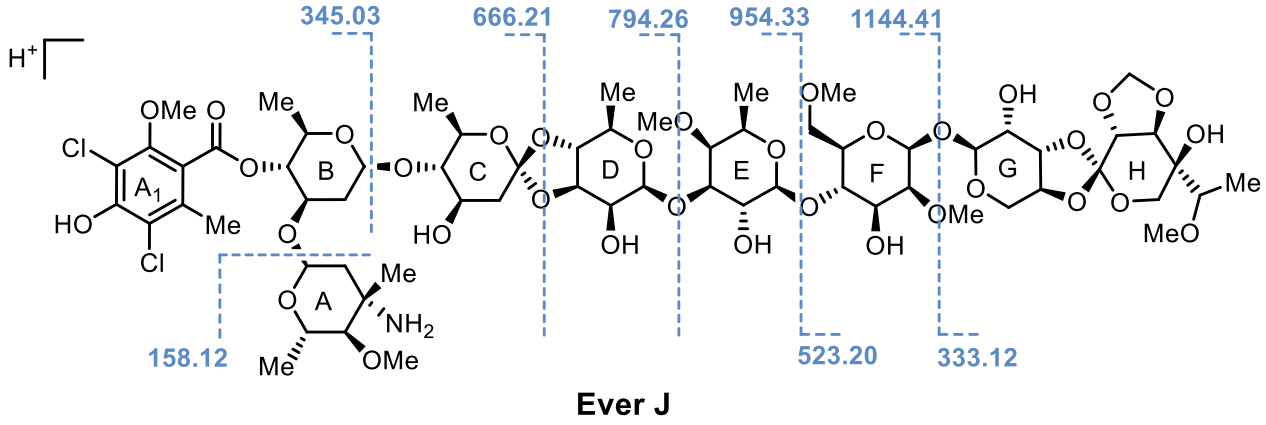

Ever J

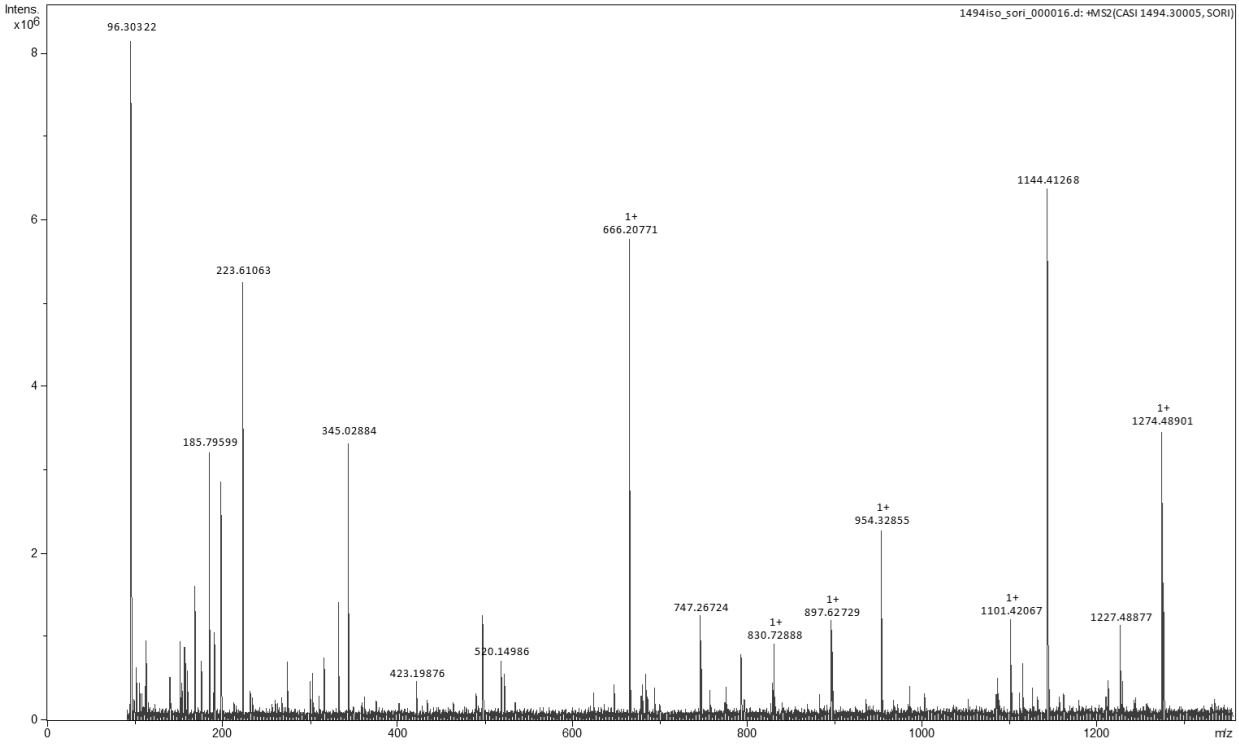

Figure B-7. Everninomicin K mass spectrometric fragmentation data. A) Mass spectrometric fragmentation pattern for Ever K. Dashed lines indicate positions of cleavage during fragmentation experiments. (B) Spectrum for fragmentation of ever K (m/z = 1508.5 $[M+H]^+$).

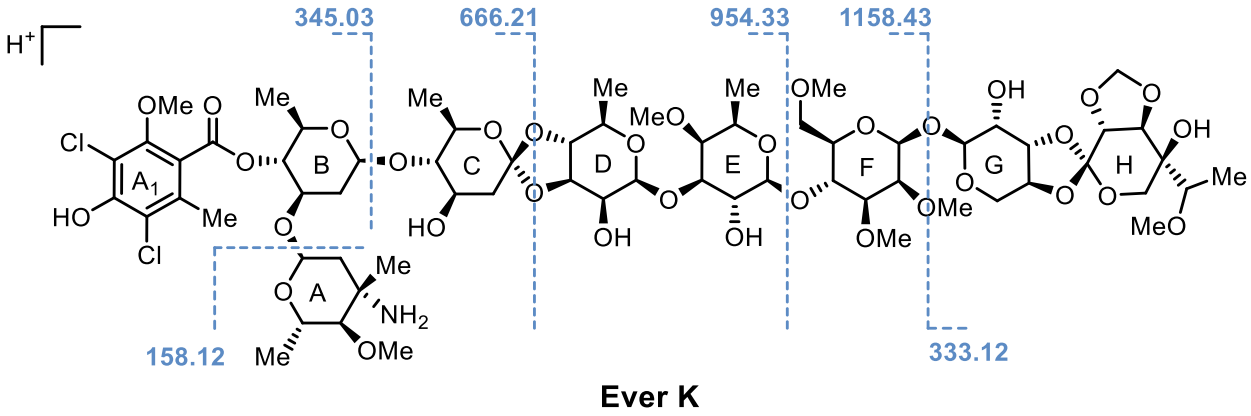

Ever K

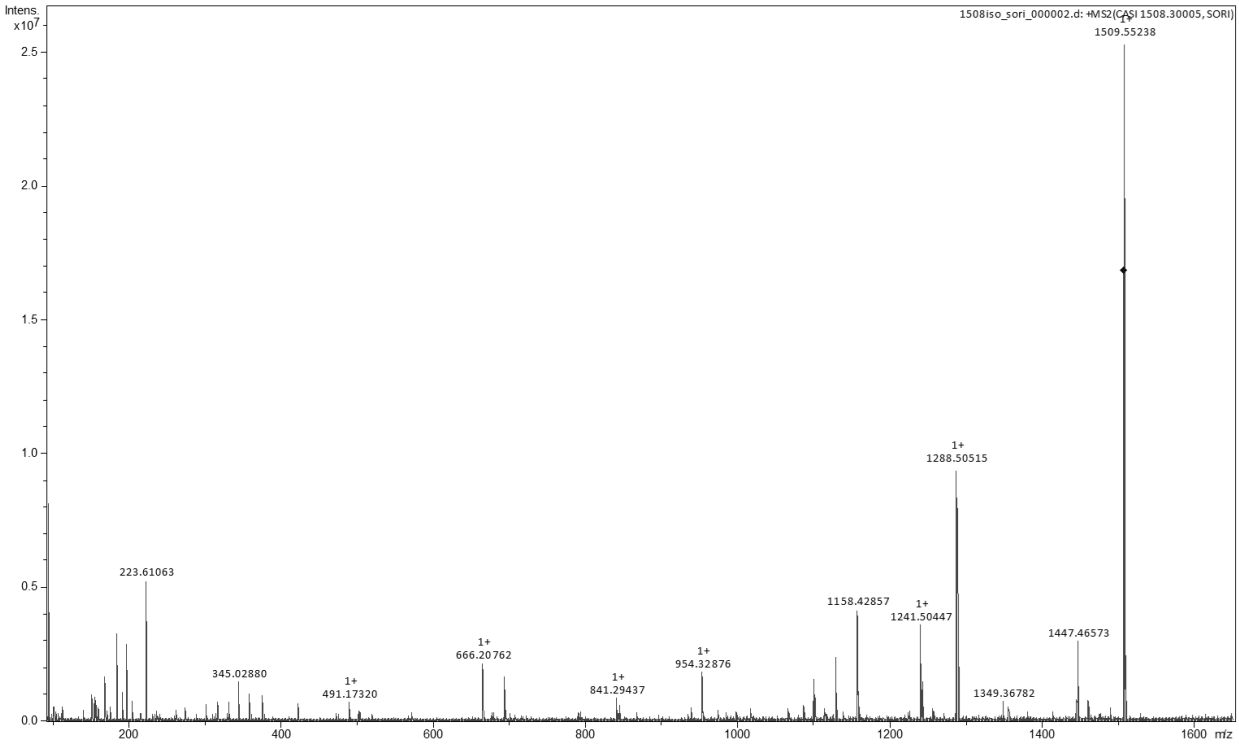

Figure B-8. Mass spectra of everninomicin L. Theoretical mass for Everninomicin L ($C_{65}H_{97}Cl_2NO_{36}$) is 1536.50946. Experimental mass was determined to be 1536.50870. The mass accuracy is 0.5 ppm.